DOSE-RESPONSE ANALYSIS OF HYPOTHALAMIC-PITUITARY-THYROID (HPT) AXIS PERTURBATIONS IN THE ADULT RAT USING STATISTICAL METHODS FOR THE BINARY MIXTURE OF PCB126 AND PERCHLORATE AND COMPUTATIONAL MODELING FOR IODIDE DEFICIENCY AND PERCHLORATE

by

EVA DANEKE MCLANAHAN

(Under the Direction of Jeffrey W. Fisher)

ABSTRACT

Some environmental chemicals affect endocrine function and may alter hormone systems at low doses. The hypothalamic-pituitary-thyroid (HPT) axis controls many physiologic functions, including metabolism, growth, development, and reproduction. Two studies were conducted to evaluate the low dose effects of ammonium perchlorate (ClO_4^-) on the HPT axis of adult male rats pretreated with 3,3',4,4'5,-pentachlorobiphenyl (PCB126). Both compounds are widespread environmental contaminants and have well characterized primary modes of action for disruption of the HPT axis. Results indicated that for rats pretreated with PCB126 and then placed on drinking water containing ClO_4^- the effects on the HPT axis endpoints examined were less than additive, and PCB126 appeared to mask the effects of ClO_4^-. The TSH stimulated thyroid created a condition where the effect of ClO_4^- on inhibition of thyroidal iodide uptake was diminished. In addition, no synergistic or greater than additive responses were observed when animals were dosed at concentrations at or near the no-observed-effect-level (NOEL).

A biologically based dose-response (BBDR) model of the adult male rat HPT axis was also constructed. The model for the adult male rat includes sub-models for dietary iodide, thyroid stimulating hormone (TSH), as well as thyroid hormones, thyroxine (T_4) and 3,5,3'-triiodothyronine (T_3). First, the individual sub-models were developed independently of one another using radiolabeled tracer studies to estimate various model parameters. Then, the models were combined to form one endogenous model that includes (1)feedback of T_4 on TSH production, (2)stimulation of T_4/T_3 production and thyroidal iodide uptake by TSH, and (3)the use of thyroidal iodide in hormone production. Model application included prediction of perturbations in the thyroid axis that result in iodide deficient conditions, as well as linking the BBDR-HPT axis model with a physiologically based pharmacokinetic (PBPK) model for ClO_4^- by the primary mode of action, competitive competition of thyroidal iodide uptake. Model exercises revealed the distinct possibility of an additional mode of action for ClO_4^- perturbation of the system. These models demonstrate the ability of the BBDR-HPT axis model to be integrated with other PBPK models for thyroid toxic compounds to predict changes based on the mode of action of the compound.

INDEX WORDS: PCB126, Perchlorate, Thyroid, Rat, BBDR Model, Iodide, Thyroid hormones, HPT Axis

DOSE-RESPONSE ANALYSIS OF HYPOTHALAMIC-PITUITARY-THYROID (HPT) AXIS PERTURBATIONS IN THE ADULT RAT USING STATISTICAL METHODS FOR THE BINARY MIXTURE OF PCB126 AND PERCHLORATE AND COMPUTATIONAL MODELING FOR IODIDE DEFICIENCY AND PERCHLORATE

by

EVA DANEKE MCLANAHAN

BSEH, The University of Georgia, 2003

A Dissertation Submitted to the Graduate Faculty of The University of Georgia in Partial Fulfillment of the Requirements for the Degree

DOCTOR OF PHILOSOPHY

ATHENS, GEORGIA

2007

DOSE-RESPONSE ANALYSIS OF HYPOTHALAMIC-PITUITARY-THYROID (HPT) AXIS PERTURBATIONS IN THE ADULT RAT USING STATISTICAL METHODS FOR THE BINARY MIXTURE OF PCB126 AND PERCHLORATE AND COMPUTATIONAL MODELING FOR IODIDE DEFICIENCY AND PERCHLORATE

by

EVA DANEKE MCLANAHAN

Major Professor: Jeffrey W. Fisher

Committee: Marsha C. Black
James V. Bruckner
Deborah A. Keys
David R. Mattie

Electronic Version Approved:

Maureen Grasso
Dean of the Graduate School
The University of Georgia
December 2007

DEDICATION

This work is dedicated to my inspiration and first mentor in the field of toxicology, "Rambo" Randy Manning. I admire him for his integrity, dedication, and wealth of knowledge. He has truly been a phenomenal role model and cherished friend.

I also dedicate this work to my husband, Paul, whose immeasurable patience and understanding is invaluable. I am eternally grateful for his unwavering faith in me and willingness to make many sacrifices, thereby providing the means for me to complete my degree. In addition, my four-legged friends provided comfort, love, and always brightened my day. Coltrane was a steadfast companion, greeting me no matter what time I arrived home and always willing to listen. And dear little Charlie (🐾 GDF, 5496), her excitement for life, passion for adventure, and unconditional love enriched my life like never before.

ACKNOWLEDGMENTS

"The future belongs to those who believe in the beauty of their dreams."

- Eleanor Roosevelt

All my life I have been fortunate to have a strong foundation of support provided by my friends and family. My parents have always encouraged me to pursue my dreams and persevere to accomplish my goals, and for that I express my utmost appreciation. I am grateful for the love, encouragement, and patience provided by my immediate and extended family, as well as all my friends throughout this endeavor.

Numerous people have assisted with the completion of this research, and I am very appreciative of all their contributions to make this work a success. Researchers at AFRL/HEPB, USEPA/NHEERL, Boston Medical Center, and UGA laboratories of Drs. James V. Bruckner and Duncan C. Ferguson provided analytical assistance. Special thanks to Srinivasa Muralidhara (SM) for his patience and hours of training and laboratory assistance. My sincere gratitude goes to my graduate committee members, Drs. Marsha C. Black, James V. Bruckner, Deborah A. Keys, and David R. Mattie, who guided me, believed in me, and held me to the high standards necessary to succeed as a scientist.

I am indebted to my advisor and friend, Dr. Jeffrey W. Fisher, who was always available to provide academic and emotional support. He instilled his faith in me and had confidence in my ability to accomplish the exciting, yet extremely challenging, and monumental task of modeling the thyroid axis. However, I could not have completed the research without the many hours he spent collaborating and reviewing my project. Thank you.

Finally, the financial support for this research was provided in many forms. Primary funding for this work was provided by the Agency for Toxic Substances and Disease Registry (ATSDR) (U61/ATU472105) and the United States Environmental Protection Agency (U.S. EPA) Science to Achieve Results (STAR) grant (RD83213401-0). I was fortunate to have been the recipient of two Fellowships, including a National Science Foundation GK-12 Graduate Teaching Fellowship (DGE0229577) and an U.S. EPA STAR Fellowship (FP916793). Special thanks to Dr. David A. Knauft (PI – DGE0229577) for three busy years, a plethora of learning, and an unforgettable excursion to Costa Rica.

TABLE OF CONTENTS

Page

LIST OF TABLES

Page

LIST OF FIGURES

Page

CHAPTER 1

INTRODUCTION

Many environmental chemicals have been shown to affect the hypothalamic-pituitary-thyroid (HPT) axis of vertebrates and invertebrates. Two widespread environmental chemicals, 3,3',4,4',5-pentachlorobiphenyl (PCB126) and perchlorate (ClO_4^-), were evaluated based on their primary, well-defined modes of action to disrupt the HPT axis in rodents. Laboratory studies with the adult rat were conducted to gain insights into the kinetics of these chemicals and their ability to disrupt homeostasis. In many cases rodent toxicity data are used to extrapolate to humans and make predictions of human health effects. One method of extrapolating the kinetics and potential effects of chemicals on laboratory animals is through the use of mathematical modeling, such as physiologically based pharmacokinetic (PBPK) or biologically based dose-response (BBDR) modeling. This dissertation includes the statistical analyses of the effects of ClO_4^- on adult male rats pretreated with PCB126 and the development of BBDR models of the HPT axis in the adult rat that predict perturbations resulting from iodide deficient conditions and ClO_4^- exposures.

Purpose of Study

The purpose of this study was to evaluate the hypothalamic-pituitary-thyroid (HPT) axis dose dependent effects of ClO_4^- on adult male rats pretreated with varying doses of PCB126, using knowledge of their primary modes of action. Two studies were conducted to determine the dose-response characteristics for binary mixtures of ClO_4^- and PCB126. Adult rats were

pretreated with a wide range of single oral bolus doses of PCB126 and then placed on drinking water containing ClO_4^-, also over a range of concentrations known to cause mininmal to no effect on the HPT axis. This exposure scenario allowed for: 1) the evaluation of ClO_4^- effects on the HPT axis in rats that were in various hypothyroid states when ClO_4^- treatment was initiated, 2) the evaluation of the dose-response characteristics for a binary mixture of chemicals that act on the HPT axis by two different modes of action, and 3) the collection of kinetic data sets for future development of a BBDR model to describe the interactions of a binary mixture on the HPT axis.

Finally, the ultimate goal was to develop a biologically based dose-response (BBDR) model of the adult rat HPT axis (BBDR-HPT axis model) that could be linked to physiologically based pharmacokinetic (PBPK) models of thyroid active compounds to predict perturbations in the thyroid system. However, because ClO_4^- (a thyroid active chemical) is thought to cause an iodide deficient condition in the thyroid by competitive inhibition of iodide uptake, it was necessary first to mathematically describe the changes induced by iodide deficiency using literature derived datasets. Next, a PBPK model for ClO_4^- was constructed and linked to the BBDR-HPT axis model to predict perturbations in serum thyroid hormone concentrations. The BBDR-HPT axis model was developed with the idea that it can be integrated with PBPK models for additional thyroid active chemicals to predict disturbances from exposure alone (e.g. PCB126) or in combination (e.g. PCB126 and ClO_4^-). Furthermore, the BBDR-HPT axis model, presented in Chapter 4, will be used as the foundation for expansion and description of the maturing and developing HPT axis in rodents and humans.

Scope of Dissertation

This dissertation includes a brief literature review (Chapter 2) of approaches and models developed previously for the HPT axis. Due to the clinical significance of the HPT axis, many models have been created, although none have included dietary iodide, an indispensable element for thyroid hormone production. The approaches, successes, and problems associated with the models are discussed. Research published on the HPT axis effects that resul from chemical mixtures are also reviewed.

Following the literature review, Chapter 3 describes the experiments and conclusions of the laboratory studies to determine binary mixture effects of PCB126 and ClO_4^- on the adult male rat HPT axis. This chapter was published in Toxicological Sciences (McLanahan *et al.*, 2007). Portions of Chapter 3 were presented at several national scientific meetings, including poster presentations at the Society of Toxicology Contemporary Concepts in Toxicology special meeting (February 2005; Atlanta, GA), Society of Toxicology annual conference (March 2005; New Orleans, LA), and an invited oral presentation at the Toxicology and Risk Assessment Conference (April 2006; Cincinatti, OH). Chapter 4 reports the development of a BBDR-HPT axis model for the adult rat and application to iodide deficient conditions and was submitted to Toxicological Sciences (McLanahan *et al.*, submitted October 2, 2007). A portion of Chapter 4 was presented in poster format at the U.S. EPA Graduate Fellowship Conference (September 2006; Washington, D.C.) and the Society of Toxicology annual conference (March 2007; Charlotte, NC). In Chapter 5, the BBDR-HPT axis model presented in Chapter 4 is combined with a PBPK model for ClO_4^- to simulate the ClO_4^- induced perturbations on serum thyroid hormones and will be submitted to Environmental Health Perspectives. The final chapter,

Chapter 6, summarizes the conclusions and importance of this research project and future work that will benefit from, and build upon the BBDR-HPT axis model developed.

Two invited book chapters are in progress based on the research reported in this dissertation and are co-authored with Dr. Jeffrey W. Fisher. A chapter in "Principle and Practice of Mixtures Toxicology" (M. Mumtaz, ed.) focusing on the effects of chemical mixtures on the HPT axis and a case study of the research in Chapter 3. Also, a chapter on HPT axis mathematical models in "Quantitative Modeling in Toxicology" (K. Krishnan and M.E. Andersen, eds.) is under development based upon the research presented in Chapters 4 and 5.

CHAPTER 2

LITERATURE REVIEW

Many clinical and research endocrinologists have reviewed the details of the thyroid axis over the past several decades (Bianco *et al.*, 2002; Boas *et al.*, 2006; Carrasco *et al.*, 1993; Dohan *et al.*, 2003; Hennemann *et al.*, 2001; Morley, 1981; Vassart *et al.*, 1992, Yen *et al.*, 2001; and Zoeller *et al.*, 2007). However, no reviews focus on the mathematical models of the thyroid axis or how mixtures of compounds affect the homeostasis and control mechanisms of the thyroid axis. Therefore, the aim of this literature review is to evaluate models of the hypothalamic-pituitary-thyroid (HPT) axis that have been developed, as well as several studies on how chemical mixtures disrupt the HPT axis.

Modeling of the HPT Axis

In the past, multiple mathematical descriptions of HPT axis components have been reported. However, to date, the most common approaches used to describe production, distribution, metabolism, and elimination of thyroid hormones involve multiexponential, multicompartmental, and noncompartmental analyses. DiStefano and Landaw (1984) presented a review and explanation of these types of models.

Briefly, multiexponential models are often described as models of data and are composed of polynomial functions and sums-of-exponential functions, which do not require hypotheses about the physiological processes. These models have been used and developed for many areas of science (e.g. classical pharmacokinetics and engineering); however, without including

mechanisms or physiology in the mathematical descriptions, they cannot be used reliably for extrapolation or predictive purposes.

Multicompartmental models and noncompartmental models are models of systems and often have two or more compartments interconnected, to describe an exchange of material. Exchange may occur by movement across a barrier (e.g. membrane transport) or undergoing metabolic transformation. Multicompartmental models involve mass balance and rates of transfer from one compartment (pool) to another. Physiologically based pharmacokinetic (PBPK) models involve mass balance and transfer of masses from one compartment to another. PBPK models often have physiologically analogous compartments, while the pools in classical pharmacokinetic (PK) multicompartmental models are equivalent distribution volumes, although sometimes they can be assigned physiological identity. Noncompartmental models are often used to estimate steady-state whole organism parameters including volume of distribution (V_D), plasma clearance rate (PCR), and whole-body mean residence time (MRT). Noncompartmental models are useful when measurements are made in a single pool and only one endogenous or exogenous source feeds the pool, but is not desired to describe data collected from systems where there is more than on source (e.g. endocrine systems including the thyroid) (DiStefano, 1982).

Landmark classical PK multicompartmental models for the thyroid hormones (thyroxine, T_4; and 3,5,3'-triiodothyronine,T_3) and their derivatives (3,3',5'-triiodothyronine, rT_3; 3,3'-diiodothyronine, 3,3'-T_2; 3',5'-diiodothyronine, 3',5'-T_2; and 3'-monoiodothyronine, T_1) have been developed for the rodent by DiStefano and colleagues (DiStefano *et al.*, 1982; DiStefano and Feng, 1988). In general, these models were based upon radiolabeled injections of the compounds and consisted of three or more compartments (plasma, fast, and slow pools). The PK

models developed by DiStefano and colleagues, employing multiexponential and multicompartmental techniques, were used to estimate kinetic parameters of thyroid hormone production, transport, and metabolism. The models were capable of reproducing kinetics of the iv doses of radiolabeled T_3 and T_4 but have little utility for exploration of perturbations on the axis due to exposure to thyroid active compounds. These models provided quantitative insights into the HPT axis, but are not models for endogenous forms of thyroid hormones and are therefore of limited usefulness for toxicological research.

Li (1995) and colleagues also employed a PK compartmental approach to model the dynamic and pulsatile nature of the human thyroid axis, including estimates for thyroid releasing hormone (TRH), thyroid stimulating hormone (TSH), T_4, and T_3. This model is different from previously developed models in that it described the pulsatile secretions of hormones, as well as feedback (e.g. TRH stimulation of TSH production and free T_3 and T_4 inhibition of TSH production), and serum binding of hormones in plasma and tissues. Unfortunately the model presented by Li *et al.* (1995) employs an approach that resulted in 54 unknown coefficients, which results in significant uncertainty and the inability to associate the coefficients with biological processes. However, comparing coefficients for a few selected parameters associated with the feedback control of the hormones, the authors suggest that the feedback effects of thyroid hormones on the hypothalamus (control of TRH secretion) are much smaller than effects on the pituitary (control of TSH secretion). Furthermore, the authors also suggest that thyroid hormone negative feedback control on TSH secretion has a significant impact when TRH concentrations are low, and this influence disappears when TRH concentration is high, resulting in a condition of maximal secretion of TSH where thyroid hormones have little influence on TSH secretion in humans. The utility of this model is to explore the magnitude and frequency of

the pulsatile nature of the HPT axis. This model cannot be readily incorporated or linked with PBPK models for compounds that disrupt the HPT axis because of the theoretical basis of the model (lacking data for model validation).

In 1996, Kohn *et al.* developed a physiological dosimetric model of the distribution of 2,3,7,8-tetrachlorodibenzo-p-dioxin (TCDD) in the rodent that also included a HPT axis sub-model. The very complex model presented for thyroid hormone regulation was comprised of five compartments (liver, thyroid, pituitary, rapidly perfused tissues, and blood), including the description of TSH stimulation of T_4 and T_3 production in the thyroid and regulation of TSH production by hypothalamic peptides (somatostatin, SS; and thyroid releasing hormone, TRH). However, the model did not describe the primary negative feedback loop of the HPT axis, inhibition of TSH secretion by T_4. This feedback was implicitly described by T_4 inhibiting the synthesis and secretion of the hypothalamic peptides that, in turn, regulated TSH secretion. Regardless, the TCDD model integrated with the HPT axis model was utilized to predict decreases in serum T_4, via a TCDD-dependent increase in phase II conjugation of T_4, and alterations in serum T_3 and TSH after 31 weeks of biweekly oral dosing of TCDD (Kohn *et al.*, 1996).

In 2002, Dietrich *et al.*, applied an engineering approach to describe the T_4/TSH negative feedback loop in humans and the pulsatile nature of TSH secretion. Four approaches were evaluated for their ability to describe the pulsatile nature of TSH secretion by the pituitary. One of the four models was able to replicate the fractal (complex, repetitive mathematical description) behavior of TSH oscillations seen in the empirical data observed in human subjects. Using these models the authors were able to provide insight into the mechanism of TSH release, suggesting that the regulation of TSH release is more complex than a simple non-competitive

inhibition of TRH mediated activation of TSH release (Dietrich *et al.*, 2002). In addition, authors suggest that TSH may also play a role in an ultra-short feedback loop upon its own release from the pituitary gland (Dietrich *et al.*, 2002).

More recently, Mukhopadhyay and Bhattacharyya (2006) implemented discrete time delays for hormone transport and feedback mechanisms in order to describe the pulsatile nature of TSH secretion in humans. This simple mathematical representation described the T_4/TSH negative feedback based upon serum T_4 concentration, and assumed that secreted TSH activated an *enzyme* in the thyroid to produce T_4. This model has limited applications, but did provide some insights into the thyroid axis malfunction causing periodic catatonic schizophrenia, which is thought to be associated with the periodic variations in TSH.

In addition to the aforementioned models, PBPK models for radiolabeled iodide in rodent and human have been developed for different life stages (Merrill *et al.*, 2003, 2005; Clewell *et al.*, 2003a, 2003b). These were based on ^{125}I or ^{131}I kinetic studies and did not include dietary iodine (^{127}I) or thyroid hormones.

Although several types of kinetic models, as reviewed above, have been constructed to describe the thyroid axis, to date none have taken into account dietary iodide, TSH, T_4, and T_3. Therefore, one goal of this research was to develop a biologically based dose-response (BBDR) model of the adult male rat HPT axis, which includes the utilization of dietary iodide in the thyroid gland for thyroid hormone production.

Mixtures Studies of Thyroid Active Chemicals

Challenges exist to improve chemical risk assessment practices, particularly with the reliance of human health risk assessments on laboratory animal toxicology studies. Many individual chemicals are known to disturb the hypothalamic-pituitary-thyroid (HPT) axis in

rodents by fairly well understood mechanisms of action (Capen, 2001). Numerous studies on the effects of individual chemicals on the HPT axis have been reported. However, few HPT axis toxicity studies have been designed to evaluate the interactions that may occur from chemical mixtures. Assessing toxic effects of chemical mixtures is important because humans are exposed to mixtures of chemicals, not individual chemicals.

Perchlorate (ClO_4^-), a thyroid active chemical and an environmental contaminant, has received much attention over the last decade because of its prevalence in water systems (Motzer, 2001). The primary well-defined mode of action for ClO_4^- disruption of the thyroid axis is by blocking thyroidal uptake of iodide (Wolff, 1998). The ClO_4^- inhibition of thyroidal iodide uptake can result in a disease state called hypothyroidism, characterized by low circulating levels of T_4 and increased levels of TSH. Recently, research efforts have been expanded to better understand the contributions of other common pollutants that share a similar mode of action as perchlorate on the thyroid gland, namely nitrate and thiocyanate (Braverman *et al.*, 2005 and Tonacchera *et al.*, 2004). Nitrate is found in food and water and thiocyanate in food and tobacco products. These authors report 'response' additivity based on the affinity (Km) of the anion for the sodium-iodide symporter (NIS) protein using a non-linear Michaelis Menten equation to describe competitive inhibition of thyroidal uptake of radiolabeled iodide (Tonacchera *et al.*, 2004).

A few binary mixture studies have been conducted in rats that include perchlorate as one of the compounds. Khan *et al.* (2005) reported synergistic interactions occurred when rats ingested the binary combination of ammonium perchlorate (NH_4ClO_4) and sodium chlorate ($NaClO_3$) in drinking water for 7 days, as evidenced by greater decreases in serum T_4 levels than seen with the individual chemicals. Interestingly, Khan *et al.* (2005) also noted that male Fischer

rats appear less sensitive than male Sprague-Dawley rats to NH_4ClO_4 induced alterations in the HPT axis. In a more recent study, perchlorate was administered alone or in combination with ethanol to female Myers' rats to examine the effects on plasma thyroid hormones and brain catecholamine concentrations (James-Walke *et al.*, 2006). However, perchlorate doses administered (300 µg/L and 3000 µg/L; yielding average intake of 0.06 and 0.6 mg/kg bw) for 21 days were not high enough to alone result in statistically significant effects on serum T_4 and T_3 concentrations. Furthermore, when these doses of perchlorate were administered with 10% ethanol, no further reductions in total serum T_4 or T_3 were observed (James-Walke *et al.*, 2006).

In complex mixture studies with a different class of chemicals, namely organochlorines, Desaulniers *et al.* (2003) and Crofton *et al.* (2005) administered rats cocktails of mixtures containing polychlorinated biphenyls (PCBs), polychlorinated dibenzo-p-dioxins (PCDDs), and polychlorinated dibenzofurans (PCDFs) and evaluated serum thyroxine (T_4) concentrations. A primary mechanism of action by which these chemicals act on the HPT axis is through activation of the aryl hydrocarbon receptor (AhR), resulting in enhanced hepatic metabolism and clearance of T_4, although several other mechanisms are possible (Crofton *et al.*, 2005).

Additive decreases in serum T_4 concentrations were observed by Desaulniers *et al.* (2003) after administration of mixtures of either 6 PCDDs, 3 non-*ortho*-PCBs, or 7 PCDFs to prepubertal female Sprague-Dawley rats. Crofton *et al.* (2005) evaluated serum T_4 levels after four consecutive days of oral gavage dosing with a mixture of eighteen polyhalogenated aromatic hydrocarbons, including PCB126. There was no deviation from additivity at the lowest mixture dose, but a greater-than-additive decrease in serum T_4 was observed at the three highest mixture doses.

Many studies have been conducted to determine the effect of complex mixtures of thyroid active compounds; however, only the few mentioned above were conducted such that the contribution of each component of the mixture could be ascertained. For example, Zhou *et al.* (2002) evaluated the effect of a complex mixture of polybrominated diphenyl ethers on the thyroid axis; however, the contribution of each component of the mixture was not analyzed, so determination of the mixture effect relative to the individual compounds was not available. It is important to determine the ability of complex mixtures to affect the HPT axis, but also equally important is to determine the contributions of the mixture components in order to determine if the mixture behaves in a less than additive, additive, or greater than additive fashion.

References

Bianco, A.C., Salvatore, D., Gereben, B., Berry, M.J., and Larsen, P.R. (2002). Biochemistry, Cellular and Molecular Biology, and Physiological Roles of the Iodothyronine Selenodeiodinases. *Endocrinol. Rev.* **23,** 38-89.

Boas, M., Feldt-Rasmussen, U., Skakkebaek, N.E., Main, K.M. (2006). Environmental Chemicals and Thyroid Function. *Eur J Endocrinol.* **154,** 599-611.

Braverman, L.E., He, X., Pino, S., Cross, M., Magnani, B., Lamm, S.H., Kruse, M.B., Engel, A., Crump, K.S., and Gibbs, J.P. (2005). The effect of perchlorate, thiocyanate, and nitrate on thyroid function in workers exposed to perchlorate long-term. *J. Clin. Endocrinol. Metab.* **90,** 700-706.

Capen, CC. (2001). Toxic Responses of the Endocrine System. In *Casarett and Doull's Toxicology, the Basic Science of Poisons,* 6th ed., Klaassen, C.D. (ed.), McGraw-Hill, New York.

Carrasco, N. (1993). Iodide Transport in the Thyroid Gland. **1154,** 65-82.

Clewell, R.A., Merrill, E.A., Yu, K.O., Mahle, D.A., Sterner, T.R., Fisher, J.W., and Gearhart, J.M. (2003a). Predicting Neonatal Perchlorate Dose and Inhibition of Iodide Uptake in the Rat during Lactation Using Physiologically-Based Pharmacokinetic Modeling. *Toxicol. Sci.* **74,** 416-436.

Clewell, R.A., Merrill, E.A., Yu, K.O., Mahle, D.A., Sterner, T.R., Mattie, D.R., Robinson, P. and Fisher, J.W. (2003b). Predicting Fetal Perchlorate Dose and Inhibition of Iodide Kinetics during Gestation: A Physiologically-Based Pharmacokinetic Analysis of Perchlorate and Iodide Kinetics in the Rat. *Toxicol. Sci.* **73,** 235-255.

Crofton, K.M., Craft, E.S., Hedge, J.M., Gennings, C., Simmons, J.E., Carchman, R.A., Carter, Jr., W.H., and DeVito, M.J. Thyroid-Hormone-Disrupting Chemicals: Evidence for Dose-Dependent Additivity or Synergism. *Environ. Health. Perspect.* **2005,** *113,* 1549-1554.

Desaulniers, D. Leingartner, K., Musicki, B., Yagminas, A., Xiao, G.-H., Cole, J., Marro, L., Charbonneau, M., and Tsang, B.K. Effects of Postnatal Exposure to Mixtures of Non-ortho-PCBs, PCDDs, and PCDFs in Prepubertal Female Rats. *Toxicol. Sci.* **2003,** *75,* 468-480.

Dietrich, J.W., Tesche, A., Pickardt, C.R., and Mitzdorf, U. (2002). Fractal Properties of Thyrotropic Feedback Control: Implications of a Nonlinear Model Compared with Empirical Data. In: *Cybernetics and Systems 2002.* R. trappl (Hrsg). Vienna.

DiStefano III, J.J., Jang, M., Malone, T.K., and Broutman, M. (1982). Comprehensive Kinetics of Triiodothyronine Production, Distribution, and Metabolism in Blood and Tissue Pools of the Rat Using Optimized Blood-Sampling Protocols. *Endocrinol.* **110,** 198-213.

DiStefano III., J.J., and Feng, D. (1988). Comparative Aspects of the Distribution, Metabolism, and Excretion of Six Iodothyronines in the Rat. *Endocrinol.***123,** 2514-2525.

DiStefano III., J.J. and Landaw, E.M. (1984). Multiexponential, multicompartmental, and noncompartmental modeling. I. Methodological limitations and physiological interpretations. *Am. J. Physiol.* **246,** R651-654.

Dohan, O., de la Vieja, A., Paroder, V., Riedel, C., Artani, M., Reed, M., Christopher, C.S., and Carrasco, N. (2003). The Sodium/Iodide Symporter (NIS): Characterization, Regulation, and Medical Significance. *Endocr. Rev.* **24,** 48-77.

Hennemann, G., Docter, R., Friesema, E.C.H., De Jong, M., Krenning, E.P., and Visser, T.J. (2001). Plasma Membrane Transport of Thyroid Hormones and Its Role in Thyroid Hormone Metabolism and Bioavailability. *Endocr. Rev.* **22,** 451-476.

James-Walke, N.L., Williams, H.L., Taylor, D.A., and McMillen, B.A. (2006). The Effect of Oral Consumption of Perchlorate, Alone and in Combination with Ethanol, on Plasma Thyroid Hormone and Brain Catecholamine Concentrations in the Rat. *Basic Clin. Pharmacol. Toxicol.* **99,** 340-345.

Khan, M.A., Fenton, S.E., Swank, A.E., Hester, S.D., Williams, A., and Wolf, D.C. (2005). A Mixture of Ammonium Perchlorate and Sodium Chlorate Enhances Alterations of the Pituitary-Thyroid Axis Caused by the Individual Chemicals in Adult Male F344 Rats. *Toxicol. Pathol.* **33,** 776-783.

Kohn, M.C., Sewall, C.H., Lucier, G.W., and Porteier, C.J. (1996). A Mechanistic Model of Effects of Dioxin on Thyroid Hormones in the Rat. *Toxicol. Appl. Pharmacol.* **165,** 29-48.

Li, G., Liu, B., and Liu, Y. (1995). A dynamical model of the pulsatile secretion of the hypothalamo-pituitary-thyroid axis. *Biosystems.* **35,** 83-92.

Merrill, E.A., Clewell, R.A., Gearhard, J.M., Robinson, P.J., Sterner, T.R., Yu, K.O., Mattie, D.R., and Fisher J.W. (2003). PBPK Predictions of Perchlorate Distribution and Its Effect on Thyroid Uptake of Radioiodide in the Male Rat. *Toxicol. Sci.* **73,** 256-269.

Merrill, E.A., Clewell, R.A., Sterner, T.R., and Fisher, J.W. (2005). PBPK Model for Radioactive Iodide and Perchlorate Kinetics and Perchlorate-Induced Inhibition of Iodide Uptake in Humans. *Toxicol. Sci.* **83,** 25-43.

Morley, J.E. (1981). Neuroendocrine control of thyrotropin secretion. *Endocr. Rev.* **2,** 396-426.

Motzer, W.E. (2001). Perchlorate: Problems, Detection, and Solutions. *Environ. Foren.* **2,** 301-311.

Mukhopadhyay, B., and Bhattacharyya, R. (2006). A Mathematical Model Describing the Thyroid-Pituitary Axis with Time Delays in Hormone Transportation. *Appl. Math.* **51,** 549-564.

Tonacchera, M., Pinchera, A., Dimida, A., Ferrarini, E., Agretti, P., Vitti, P., Santini, F., Crump, K., and Gibbs, J. (2004). Relative potencies and additivity of perchlorate, thiocyanate, nitrate, and iodide on the inhibition of radioactive iodide uptake by the human sodium iodide symporter. *Thyroid.* **14,** 1012-1019.

Vassart, G. and Dumont, J.E. (1992). The Thyrotropin Receptor and the Regulation of Thyrocyte Function and Growth. *Endocr. Rev.* **13,** 596-611.

Wolff, J. (1998). Perchlorate and the Thyroid Gland. *Pharmacol. Rev.* **50,** 89-105.

Yen, P. (2001). Physiological and Molecular Basis of Thyroid Hormone Action. *Physiol. Rev.* **81,** 1097-1142.

Zoeller, R.T., Tan, S.W., and Tyl, R.W. (2007). General Background on the Hypothalamic-Pituitary-Thyroid (HPT) Axis. *Crit. Rev. Toxicol.* **37,** 11-53.

Zhou, T., Taylor, M.M., DeVito, M.J., and Crofton, K.M. (2002). Developmental exposure to brominated diphenyl ethers results in thyroid hormone disruption. *Toxicol. Sci.* **66,** 105-116.

CHAPTER 3

LOW-DOSE EFFECTS OF AMMONIUM PERCHLORATE ON THE HYPOTHALAMIC-PITUITARY-THYROID (HPT) AXIS OF ADULT MALE RATS PRETREATED WITH PCB126[1]

[1] McLanahan, E.D., Campbell, Jr., J.L., Ferguson, D.C., Harmon, B., Hedge, J.M., Crofton, K.M., Mattie, D.R., Braverman, L., Keys, D.A., Mumtaz, M., and J.W. Fisher. 2007. *Toxicological Sciences*. 97:308-317.
Reprinted here with permission of the publisher.

Abstract

The objective of this research was to characterize the disturbances in the hypothalamic-pituitary-thyroid (HPT) axis resulting from exposure to a binary mixture, 3,3',4,4',5-pentachlorobphenyl (PCB126) and perchlorate (ClO_4^-), known to cause hypothyroidism by different modes of action. Two studies were conducted to determine the HPT axis effects of ClO_4^- on adult male Sprague-Dawley rats pretreated with PCB126. In Dosing Study I, rats were administered a single oral dose of PCB126 (0, 7.5, or 75 μg/kg) on Day 0 and nine days later ClO_4^- (0, 0.01, 0.1, or 1 mg/kg-day) was added to the drinking water until euthanasia on Day 22. Significant dose-dependent trends were found for all thyroid function indices measured following ClO_4^- in drinking water for 14 days. 75 μg PCB126/kg resulted in a significant increase in hepatic T_4-glucuronide (T_4-G) formation, causing a decline in serum T_4 and fT_4, and resulting in increased serum TSH. Serum TSH was also increased in animals that received 7.5 μg PCB126/kg; no other HPT axis alterations were found in these animals. When pretreated with PCB126 the ClO_4^- dose trends disappeared, suggesting a less than additive effect on the HPT axis. In Dosing Study II, animals were given lower doses of PCB126 (0, 0.075, 0.75, or 7.5 μg/kg) on Day 0, and followed with ClO_4^- (0 or 0.01 mg/kg-day) in drinking water beginning on Day 1 and continuing for several days to explore transient HPT axis effects. No statistical effects were seen for PCB126 or ClO_4^- alone, and no perturbations were found when administered sequentially in Dosing Study II. In conclusion, these studies demonstrate that HPT axis disturbances following exposure to ClO_4^- are less than additive when pretreated with relatively high doses of PCB126. At relatively low doses, at or near the NOEL for PCB126 and ClO_4^-, no interactions between the chemicals occur.

Key Words: PCB126, perchlorate, rat, thyroid, T_4, TSH, UDPGT

Introduction

Several important scientific challenges exist to improve chemical risk assessment practices, particularly with the reliance of human health risk assessments on laboratory animal toxicology studies. For example, most toxicology studies are conducted with a single chemical; however, humans are exposed to complex mixtures of chemicals. Environmental exposures to chemicals are typically much lower than the doses administered to laboratory animals. For toxicants that indirectly disturb endocrine system homeostasis, the interpretation of laboratory animal findings is confounded by significant species differences in endocrine physiology, such as the hypothalamic-pituitary-thyroid (HPT) axis (Capen, 1996).

To begin to understand some of the scientific challenges for mixtures toxicology and endocrine disrupting chemicals, we designed studies to evaluate HPT disturbances in rats administered low to moderate binary doses of two thyroid active chemicals that induce hypothyroidism by dissimilar mechanisms. Perchlorate (ClO_4^-) and 3,3',4,4',5-pentachlorobiphenyl (PCB126) were selected because of their widespread distribution in the environment (ATSDR, 2000; NRC, 2005; and NTP, 2006), detection in human tissues (CDC, 2005 and Blount *et al.*, 2006), and their well characterized mode of action on the HPT axis in rats (Craft *et al.*, 2002; Fisher *et al.*, 2006; NRC, 2005; and Yu *et al.*, 2002). PCB126 is a potent coplanar (non-*ortho*) dioxin-like PCB congener with a toxic equivalency factor of 0.1 (Safe, 1994) and generally exists with mixtures of multiple PCB congeners in the environment. PCBs are no longer used by industry, but are ubiquitous in the environment with detectable concentrations found across all media, including air, soil, water, sediment, and biota (NTP, 2006). The primary mode of action for PCB126 mediated disruption of the HPT axis is through increased phase II metabolism of the thyroid hormone, thyroxine (T_4). PCB126 binds to and

activates hepatic aryl hydrocarbon receptors (AhR). AhR activation results in the upregulation of several hepatic enzymes, including uridine diphosphate glucuronyl transferases (UDPGTs). An increase in phase II conjugation of T_4 (formation of T_4-glucuronide, T_4-G) results in increased biliary excretion of T_4-G (Craft *et al.*, 2002) and decreased circulating T_4, leading to hypothyroidism. Dose-response characteristics for PCB126 and HPT disturbances in the rat were recently characterized in our laboratory (Fisher *et al*., 2006).

Perchlorate has been the subject of several toxicology studies targeting the HPT axis in wildlife, laboratory animals and humans because of its presence in water and food supplies (NRC, 2005). The ammonium perchlorate (AP) salt is used as an oxidizer in pyrotechnics, solid rocket fuels, and air bags. AP is highly water soluble and dissociates in water forming the perchlorate anion (Motzer, 2001). Apparently perchlorate is also formed naturally (Dasgupta *et al*., 2005). Perchlorate acts on the HPT axis by competing for thyroidal uptake of dietary iodide (I^-), resulting in a decline in available iodide for synthesis of the thyroid hormones (Wolff, 1998 and Yu *et al.*, 2002) and the onset of hypothyroidism. A specialized transporter protein, referred to as the sodium/iodide symporter (NIS), located on the basolateral side of the follicular cell actively transports iodide and possibly perchlorate from the blood supply into the thyroid gland. Competitive inhibition of thyroidal uptake of radiolabeled iodide by perchlorate in the adult rat has been carefully characterized, along with the subsequent perturbations in serum thyroid hormones and thyroid stimulating hormone (TSH) (Yu *et al*., 2002).

Very few studies with mixtures of either PCBs or anions have been conducted to ascertain mixture composition contributions to disruption of the HPT axis in the rat. In one study, Crofton *et al.* (2005) evaluated serum T_4 levels after four consecutive days of oral gavage dosing with a mixture of eighteen polyhalogenated aromatic hydrocarbons, including PCB126.

There was no deviation from additivity at the lowest mixture dose, but a greater-than-additive decrease in serum T_4 was observed at the three highest mixture doses. Khan *et al.* (2005) reported that synergistic interactions occurred when rats ingested binary combinations of perchlorate and chlorate in drinking water for 7 days, as evidenced by greater decreases in serum T_4 levels. Interestingly, Khan *et al.* (2005) also noted that male Fischer rats appear less sensitive than male Sprague-Dawley rats to ClO_4^- induced alterations in the HPT axis. *In vitro* competitive inhibition studies using FTRL-5 and COS NIS-6 cells have been undertaken with several anions to estimate the affinity of anions for the NIS protein (Van Sande *et al.*, 2003).

In the present study, we evaluated the combined effects of two chemicals, both of which induce hypothyroidism by different mechanisms in the rat. Rats were pretreated with a single oral bolus dose of a potent and persistent thyroid active chemical (PCB126) that is cleared slowly from the body. Dose- and time-dependent perturbations of the HPT axis are well characterized for PCB126. At a specified time after dosing, the PCB126 pretreated rats were given drinking water containing a second thyroid active chemical, ClO_4^-, for different periods of time. Dose- and time-dependent perturbations of ClO_4^- on the HPT axis have also been characterized. Our working hypothesis was that for rats in which serum TSH was elevated by pretreatment with PCB126, the blocking effects of ClO_4^- on thyroidal uptake of iodide would be diminished, resulting in less than additive perturbations in the HPT axis. TSH stimulates the production of the NIS protein, which results in increased thyroidal uptake of iodide (Eng *et al.*, 2001) and the formation and secretion of thyroid hormones. If increases in TSH associated with PCB126 leads to increases in the NIS protein, perchlorate may be less effective at blocking the thyroidal uptake of iodide.

Materials and Methods

Dose Selection and Design

To study the interactions of PCB126 and ClO_4^-, doses of each chemical were selected that are known to cause moderate disturbances in the HPT axis and those that are thought to cause minimal or no disturbances in the HPT axis in the adult male rat. PCB126 dose selection (single oral bolus administration of 7.5 and 75 μg/kg) was based on previous research in our laboratory with single oral bolus doses of PCB126 and resulting perturbations in the HPT axis of the male Sprague-Dawley rat (Fisher *et al*., 2006). Rats were given ClO_4^- in drinking water for two weeks at dose rates of 0.01, 0.1, and 1.0 mg/kg-day; the two highest doses (0.1 and 1.0 mg/kg-day) were previously reported to cause moderate disturbances of the HPT axis (Yu *et al*., 2002).

Dosing Study I. The average weight on Day 0 for 128 Sprague-Dawley rats used in this study was 216 ± 11 g. This study was divided into two groups (Table 3.1) with group 1 dosed one day prior to group 2. On Day 0 a portion of the rats were administered single oral bolus doses of PCB126 dissolved in corn oil (7.5 or 75 μg/kg) or corn oil alone (controls), while others remained on house supplied water. On Day 9 after dosing with PCB126, rats were administered ClO_4^- (0, 0.01, 0.10, or 1.00 mg/kg-day) in their drinking water for an additional 14 days. Rats were euthanized on Day 22 between 7 and 10 A.M. and tissues collected for analysis (*See Methods: Tissue collection and preparation)*.

Dosing Study II. The purpose of this study was to examine the interactions of lower doses of PCB126 with perchlorate. The time on treatment for Dosing Study II was shortened to five days or less after administration of a single oral gavage, lower dose of PCB126 (0, 0.075, 0.75, or 7.5 μg PCB126/kg) on Day 0 to capture the transient perturbations in the HPT axis. The average weight on Day 0 for 192 adult male Sprague-Dawley rats used in this study was 250 g ±

16 g. One day following PCB126 dosing, rats were administered ClO_4^- in drinking water to obtain doses of 0 or 0.01 mg/kg-day. A portion of the rats received only PCB126 and were euthanized and tissues collected 12 hr, 1 day, 2 days, and 5 days post dosing. In addition to PCB126, a subset of rats also received ClO_4^- in drinking water that began one day post PCB126 dose, and these animals were euthanized 2 days and 5 days post PCB126 dosing, respectively (Table 3.2).

Chemicals and Reagents

PCB126 (100 µg/mL in isooctane) was obtained from Accustandard Corporation (New Haven, CT). Dosing solutions (target doses 0.0, 0.075, 0.75, 7.5, and 75 µg/kg) were prepared as detailed in Fisher *et al.* (2006) having final concentrations of 0, 0.02, 0.2, 1.2, and 12.0 µg PCB126/ml corn oil, respectively. Ammonium perchlorate salt (99.8% pure) was obtained from Aldrich (Milwaukee, WI). Final ClO_4^- drinking water concentrations for target doses of 0, 0.01, 0.1, and 1.0 mg/kg-day were 0, 0.09, 0.9, and 9.0 mg/L.

Animals

Adult male Sprague-Dawley (SD) rats were obtained from Charles River Laboratories (Wilmington, MA) weighing 161-180g on arrival. Rats were housed individually in a "shoe-box" style cage at an accredited American Association for Accreditation of Laboratory Animal Care (AAALAC) facility with humidity/climate-control and a 12-h light/dark cycle. Rats were fed Purina PMI Certified Rodent Chow #5001 and provided water (with or without perchlorate) *ad libitum*. Rats were allowed to acclimate for one week prior to dosing. The studies were conducted in accordance with the National Institutes of Health (NIH) guidelines for the care and use of laboratory animals. Body weights and food and water consumption were determined at the time of dosing, every three days during the study, and at euthanasia.

Tissue Collection and Preparation

Rats were euthanized by CO_2 asphyxiation and exsanguinated from the inferior vena cava as described in Fisher *et al.* (2006). Whole blood was collected in serum separator tubes, allowed to clot, centrifuged, and the serum removed. Serum aliquots were stored at -80ºC until analysis of TSH and thyroid hormones. Livers were excised, weighed, and divided for analysis. Five grams of the liver were used to make microsomes for UDPGT activity (Fisher *et al.*, 2006). Liver microsomes were also stored at -80ºC until analysis. Thyroids were excised free of fat and connective tissue and weights recorded. Both thyroid lobes from Dosing Study I animals and one lobe from animals in Dosing Study II were placed in 10% formalin for histomorphometric determination of the colloid/follicular volume ratio. The other lobe in Dosing Study II was frozen at -80ºC until analysis of iodide content.

Hepatic Enzyme Analysis

Thyroxine-glucuronide (T_4-G) formation rates catalyzed by uridine diphosphate glucuronyl transferases (UDPGTs) and glucuronic acid were determined for all doses and dose combinations based on the method of Visser *et al.* (1993) as modified by Zhou *et al*. (2001). The calculated activity of hepatic UDPGTs was reported as pM T_4-G formed/mg protein/min. The minimal UDPGT activity detection using T_4 as the substrate was 0.05 pM T_4-G/mg protein/min. Hepatic microsomal protein was determined using the Folin phenol reagent method published by Lowry *et al*. (1951).

Serum Hormone and TSH Analyses

Serum aliquots of 0.5 mL were stored at -80ºC until analysis, which occurred less than four months post collection. A previously unfrozen serum aliquot was used for each assay. Serum free T_4 (fT_4) concentrations were measured by equilibrium dialysis using a radioisotopic

assay kit (No. 40-2210, Nichols Institute Diagnostics, San Juan Capistrano, CA). Serum total T_4 was determined by radioimmunoassay as in Fisher *et al*. (2006) using T_4-15 antisera obtained from Endocrine Sciences (Calabasas, CA). Serum TSH was measured using a purchased (commercially available) rat TSH radioimmunoassay kit (MPBiomedicals #07C-90102, Orangeburg, NY).

The intra-assay coefficients of variation were 4.8%, 9.4%, and 6.0% for Dosing Study I measurements of fT_4, T_4, and TSH, respectively. For Dosing Study II, the intra-assay coefficients of variation were 19.4%, 7.7%, and 14.6%.

Thyroid Histopathology and Iodide Content

Thyroid glands were collected and prepared for histomorphometric analysis with a hematoxylin and eosin stain (Fisher *et al*., 2006). Two sections, for each lobe of the thyroid when available, were examined microscopically and two photographs of each section were taken for digital analysis of area ratios. Images with average area of 0.55 mm^2 were analyzed using the computer software Image-Pro Plus (MediaCybernetics, Silver Spring, MD). Follicular epithelial cell area was contrasted with colloid area (black versus white, respectively) and the total black versus white area was computationally determined. These values were then used to determine the colloid volume to epithelial follicular cell volume (C/EFC) ratios. An average of four ratios (4 images) was determined for each animal.

In Dosing Study I, both lobes of the thyroid from each animal were used for histomorphometric analysis; however, in Dosing Study II, one lobe from each thyroid, alternating right and left, was reserved for iodide analysis. Total thyroidal endogenous iodide content (^{127}I) was determined using the method of Benotti *et al.* (1965) for a portion of Dosing Study II animals.

Statistical analyses

All statistical analyses were performed using the statistical software package SAS (Statistical Analysis System) V8.2 (SAS Institute Inc., Cary, NC). Dosing Study I data were transformed by taking the square root prior to analysis. Analysis of variance (ANOVA) was used to determine if there were differences between the measurements taken on the two days of collection for controls or animals treated with only perchlorate. No statistical differences ($p \leq 0.05$) were determined between days of euthanasia for the control or ClO_4^- only dose groups. Therefore, results from these rats were grouped together, which resulted in a total of 16 rats in the control and ClO_4^- only dose groups for Dosing Study I.

Subsequently, the transformed data were evaluated by ANOVA to determine treatment related effects (PCB126 or ClO_4^-) and followed by Tukey's multiple comparison (MC) test ($p \leq 0.05$) to compare treatment means (individual compounds and mixtures) to control means. In addition, Tukey's MC test was used for comparison of the mixture means to the responses of the individual chemicals. ANOVA followed by Tukey's MC test, was also utilized for analysis of Dosing Study II data. Data presented are expressed as percent of control (100%) ± SEM.

The Tukey-Ciminera-Heyse (TCH) trend test (Tukey *et al*., 1985) was used, in addition to ANOVA and Tukey's MC test, in order to detect nonzero trends in response to the test compounds. The TCH test was conducted sequentially, using contrast coefficients calculated using SAS v8.2 and equations and methods described by Antonello *et al*. (1993), to determine the no-statistical-significance-of-trend (NOSTASOT) dose. For Dosing Study I, contrast coefficients were calculated for ClO_4^- doses (0, 0.01, 0.10, and 1.0 mg/kg-day), and the TCH test was used to determine ClO_4^- trends at different dose concentrations of PCB126 (0, 7.5, and 75 μg/kg) pretreatment for each variable. The contrast coefficients for Dosing Study II were

calculated for PCB126 doses (0, 0.075, 0.75, and 7.5 µg/kg) and used to determine PCB126 trends at each time point, with (2 and 5 day) and without ClO_4^- (0.5, 1, 2, and 5 day). A significant non-zero trend was identified when $p \leq 0.05$. The NOSTASOT dose was determined when $p > 0.05$.

Results

Dosing Study I

Body and organ weights. There were no significant differences in cumulative mean body weight gain over the 22 day study period after either a single oral bolus dose of PCB126 (7.5 or 75 µg/kg), 14 day exposure to ClO_4^- in drinking water (0.01, 0.10, or 1.00 mg/kg-day), or a combination of the two after a nine day pretreatment period with PCB126. The average weight gain for all animals was 120 ± 24 g. In addition, food and water consumption were not altered during the course of the study with daily intakes averaging 24.9 ± 1.0 g and 38.9 ± 2.2 mL, respectively. Rats administered 75 µg PCB126/kg had a significant increase of 18% in mean liver to body weight ratio (Table 3.3). No treatment related differences in thyroid weights were found (data not shown).

Individual chemical treatment. Administration of 7.5 and 75 µg PCB126/kg resulted in a dose-dependent increase in the rate of hepatic T_4-glucuronide (T_4-G) formation, although only the 75 µg PCB126/kg dose group was significantly elevated by 166% above control (Figure 1). Seventy-five but not 7.5 µg PCB126/kg resulted in a significant decrease in serum T_4 (49%) and fT_4 (51%) concentrations compared to controls at 22 days post treatment. Elevated serum TSH concentrations were detected for both PCB126 dose groups (Figure 1). However, the 7.5 µg/kg

dose group TSH concentrations were slightly higher than the 75 µg/kg dose group concentrations, although not statistically different from one another.

When the TCH trend test was employed to evaluate trends in the data across the three ClO_4^- dose groups, dose-dependent trends were detected for all thyroid function indices measured. A dose-dependent increase in mean serum TSH concentrations was observed in rats that received 0.01, 0.1, or 1.0 mg/kg-day of ClO_4^- in drinking water for 14 days (Figure 1). The NOSTASOT dose, or lowest dose of ClO_4^- that did not cause a statistical alteration in serum TSH, was 0.01 mg/kg-day. An increasing trend was also determined for rate of T_4-G formation, while a decreasing trend was seen in serum T_4 and fT_4 concentrations with a NOSTASOT dose of 0.10 mg ClO_4^-/kg-day for these indices (Figure 1). Histopathology analysis of thyroids from animals that received either PCB126 or ClO_4^- did not result in any statistical differences from control. The mean colloid:epithelial follicular cell (C/EFC) ratio for vehicle control animals that received no test compounds was 1.19 ± 0.25 (see supplemental data).

Binary mixture treatment. No dose-dependent trends were detected for the effect of ClO_4^- on the rate of T_4-G formation when animals were pretreated with 7.5 or 75 µg PCB126/kg. Thus, PCB126 masked the effect of exposure to ClO_4^- for 14 days in drinking water on the rate of T_4-G formation (Figure 1). Results from Tukey's MC test also support this finding, since no statistical differences between the co-exposed animals and animals that received only PCB126 were seen.

PCB126 also masked the effect of ClO_4^- on serum fT_4, T_4, and TSH measured after a nine day pretreatment period with either 7.5 or 75 µg PCB126/kg and followed with exposure to ClO_4^- in drinking water for 14 days (0.01, 0.1, or 1.0 mg/kg-day). As previously stated, ClO_4^- dose-dependent trends were observed for changes in serum T_4, fT_4, and TSH concentrations

when ClO_4^- was administered alone for 14 days in drinking water; however, no ClO_4^- trends were found when it was administered to rats that were pretreated with PCB126.

No changes in the volume of colloid or follicular cells (C/EFC ratio) were seen in animals that received both PCB126 and ClO_4^-; similar C/EFC ratios were determined for animals that received only one test compound (see supplemental data).

In summary the binary mixture of 7.5 or 75 μg PCB126/kg and either 0.01, 0.1, or 1.0 mg ClO_4^-/kg-day resulted in the disappearance of the ClO_4^- dose-dependent HPT axis effects (Figure 1) indicating a less than additive response for the binary mixture.

Dosing Study II

Dosing Study II provided information on binary mixtures for lower doses of PCB126 determined in this study to be at or near NOSTASOT doses for PCB126, combined with a NOSTASOT ClO_4^- dose of 0.01 mg/kg-day determined in Dosing Study I. To carry out these studies in the same fashion as Dosing Study I, shorter treatment periods were selected as described in the Methods.

Body and organ weights. No significant difference in body weight gain was observed over the 5 day period after a single oral gavage dose of 0.075, 0.75, or 7.5 μg PCB126/kg. Also, no significant changes were found in liver or thyroid weights (data not shown). Food consumption was not monitored in this study because no differences were found at the higher doses in Dosing Study I. Water consumption was monitored to calculate ClO_4^- intake. The average daily intake of water was 41.5 ± 6.6 mL.

Individual chemical treatment. A dose-dependent increase in rate of T_4-G formation was observed for animals treated with PCB126 at 2 and 5 days post-dosing (Figure 2). The rate of T_4-G formation peaked at day 2 and began to return to control values by day 5 (see supplemental

data). The NOSTASOT dose for increase in rate of T_4-G formation was found to be the lowest dose of PCB126 (0.075 µg/kg) administered.

Interestingly, these low doses of PCB126 resulted in a dose-dependent decrease in serum fT_4 at 12 and 24 hours post dosing with NOSTASOT doses of <0.075 and 0.75, respectively (see supplemental data). No trend or statistically significant differences from controls were detected at later time points of 2 or 5 days after dosing (Figure 2). No PCB126 dose-dependent trends were determined for serum T_4 (Figure 2). An increasing trend in serum TSH due to PCB126 exposure (NOSTASOT dose of 0.75 µg PCB126/kg) was found at 12 hours post-dosing (see supplemental data), but no trends were evident at later time points.

There were no statistical differences (Tukey's MC test) in the rate of T_4-G formation or serum T_4, fT_4, or TSH concentrations in rats administered 0.01 mg ClO_4^-/kg-day for one or four days (Figure 2).

Binary mixture treatment. For the binary mixture in Dosing Study II, animals were pretreated with PCB126 (0.075, 0.75, or 7.5 µg/kg) for one day and exposed to 0.01 mg ClO_4^- /kg-day in drinking water for one or four days. The TCH trend test failed to find any significant PCB126 dose trends in the co-exposure data for Dosing Study II (Figure 2). The serum TSH concentrations were not statistically different from control values (Tukey's MC test) and the TCH test did not detect a trend across PCB126 doses.

No statistical significant differences in thyroid morphology were observed in these animals (see supplemental data). Total thyroidal iodide content was not significantly altered by treatment. Stable iodide (^{127}I) content ranged from 10-15 µg per thyroid gland (Figure 3).

Discussion

The objective of these experiments was to characterize the low-dose interactions between two thyroid active compounds, 3,3',4,4',5-pentachlorbiphenyl (PCB126) and perchlorate (ClO_4^-), which act via different modes of action to disturb the hypothalamic-pituitary-thyroid (HPT) axis. PCB126 is thought to act primarily by binding to the Ah-receptor (AhR) to induce hepatic UDPGT enzymes which increase the metabolism of T_4; ClO_4^- acts by inhibiting iodide uptake into the thyroid gland, resulting in decreased thyroid hormone production. The studies were designed to evaluate HPT axis disturbances caused by low doses of ClO_4^- on rats with modest preexisting disturbances in the HPT axis as a result of PCB126. The serum half-life ($t_{1/2}$) of PCB126 in rats is approximately 17 days (Yoshimura *et al.*, 1985), while the plasma $t_{1/2}$ of intravenously administered $^{36}ClO_4^-$ is 7.3 hours (Yu *et al*., 2002). The long $t_{1/2}$ of PCB126 allowed for administration of a single dose of PCB126 several days before treatment with ClO_4^- was initiated. This experimental design may mimic human exposures to these chemicals. PCB126 human exposure occurs from contaminated diet and its $t_{1/2}$ is approximately 4.5 years (Ogura, 2004), while ClO_4^- exposure occurs primarily from ingestion of water and food with a $t_{1/2}$ of 6-8 hours (NRC, 2005).

Generally speaking, the dose-response characteristics of PCB126 on the HPT axis were similar to those obtained previously at higher doses (Fisher *et al*., 2006). That is, serum TSH concentrations were elevated, serum thyroid hormones were either unchanged or decreased and hepatic T_4-G production rates were increased. Interestingly, in this study, serum TSH concentrations in animals dosed with 7.5 µg/kg were similar to the 75 µg/kg dose group. Fisher *et al*. (2006) reported that 75 µg/kg of PCB126 resulted in elevated serum TSH concentrations greater than the 275 µg/kg dose group. Other PCB126 studies report variable findings for

treatment related changes in serum TSH concentrations (Martin, 2002 and NTP, 2006) suggesting that PCB126 may be disturbing the HPT axis by more than one mechanism of action. Further evidence for this suggestion comes from the present study. Serum fT_4 concentrations declined by 12 hrs after dosing with PCB126, but a corresponding increase in hepatic T_4-G formation was not observed (see supplemental data). Similar findings have been reported for other PCBs in which declines in serum T_4 were not accompanied by UDPGT induction (Hansen, 1998 and Li and Hansen, 1996). This may suggest PCB126 disturbs the thyroid axis by another mechanism that has yet to be elucidated.

After fourteen days of ClO_4^- treatment in drinking water, serum thyroid hormone concentrations were similar to control values across the dose groups that received only ClO_4^-, suggesting that the modest thyroid upregulation by TSH provided adequate compensation for thyroidal iodide uptake and thyroid hormone synthesis. The possible induction of hepatic T_4-G formation by ClO_4^- deserves further study, since rate of T_4-G formation has not been reported previously for ClO_4^- treated animals. In the present study, the no-statistical-significance-of-trend (NOSTASOT) dose, also considered to be the no-observed-effect-level (NOEL), for alterations in serum TSH was 0.01 mg ClO_4^-/kg-day. The alterations in serum T_4, fT_4, and TSH for rats exposed to ClO_4^- alone in Dosing Study I agree with previously published data for the 0.10 and 1.00 mg/kg-day exposures (Yu *et al.*, 2002). The determination of 0.01 mg ClO_4^-/kg-day as a no-statistical-significance-of-trend (NOSTASOT) dose based on serum TSH extended the dose-response curve for ClO_4^- established in Yu *et al.* (2002) into the low-dose region.

The binary mixtures data collected from Dosing Study I support our hypothesis that ClO_4^- is less effective as a thyroid axis disruptor in rats pretreated with PCB126. In the data from animals co-exposed with the high PCB126 (75 μg/kg) dose from Dosing Study I, it is evident

that PCB126 dominated the HPT axis responses in these co-exposed animals. Serum total and free T_4 in animals co-administered 75 μg PCB126/kg and 1.0 mg ClO_4^-/kg-day were significantly below control values by about 40%, which corresponded to the decrease seen in PCB126 (75 μg/kg) only animals (50%). At this highest dose of ClO_4^- (1.0 mg/kg-day) administered in Dosing Study I, a dose-dependent decrease in serum total and free T_4 (8% and 13%, respectively) and subsequent increase in TSH of 100% was found. This suggests that the upregulation and stimulation of the thyroid by TSH at this dose of ClO_4^- was not sufficient to maintain normal thyroidal iodide levels for hormone production. However, in animals pretreated with 75 μg PCB126/kg prior to administration of the high dose of ClO_4^- (1.0 mg/kg-day), ClO_4^- was unable to exacerbate the hypothyroid condition further. That is, there was no further decrease in serum total or free T_4, and no ClO_4^- dose related statistical trend in serum TSH was found in animals pretreated with PCB126.

Additionally, it is speculated that due to prior exposure to PCB126, the degree to which ClO_4^- is able to block thyroidal iodide uptake (and subsequently disturb the HPT axis) is diminished in the presence of elevated TSH, which is known to stimulate NIS protein expression and activity (Dohan *et al.*, 2003). PCB126 appeared to mask the effect of ClO_4^- in these animals, which is supported by the lack of ClO_4^- dose-response trends in the binary mixture studies conducted in Dosing Study I. Since ClO_4^- dose-response trends were found when the compound was administered alone, the disappearance of these trends in PCB126 and ClO_4^- co-exposed animals suggests that the effect is less than additive at the dose combinations tested in Dosing Study I. This is also supported by evaluating expected additive responses based on the absolute mean percent change from control (supplemental data). The response as percent of control for hepatic rate of T_4-G formation averaged 39% less than additive. On average for the

binary mixture combinations tested in Dosing Study I, TSH was 35% less than expected under the response additivity assumption for chemicals of dissimilar modes of action, and total T_4 averaged 5% less than additive. The free T_4 deviation from additivity was different for each dose of PCB126. At the low dose of PCB126 (7.5 μg/kg) animals co-exposed had mean serum free T_4 levels on average 17% greater than expected under the additivity assumption; however, animals co-exposed with 75 μg PCB126/kg had free T_4 levels 13% less than the predicted additive response. The reason for the difference at these two PCB126 doses is not known, but may be related to displacement of the hormone from carrier proteins in the blood. PCBs and their hydroxyl metabolites have been shown to displace T_4 from the serum binding protein transthyretin (TTR) in rats (Brower and van den Berg, 1986; Chauhan *et al.*, 2000; and Cheek *et al*., 1999); at low concentrations, the M-1 metabolite of PCB126 (Koga, 1990) may play a similar role to PCB metabolites already identified to have this behavior.

In animals that are hypothyroid, as indicated by elevated serum TSH and decreased serum T_4 concentrations prior to ClO_4^- exposure, the apparent dose-response curve for ClO_4^- inhibition of iodide uptake is shifted to the right. The ClO_4^- dose-response curve shift to the right in hypothyroid, or TSH stimulated animals, suggests that a higher dose of ClO_4^- is needed to result in the same degree of inhibition of iodide uptake at the NIS that is seen in TSH normal, euthyroid rats.

In Dosing Study II, the objective was to dose rats with low doses of PCB126 and monitor transient changes in the HPT axis to determine a NOEL dose for PCB126. Also, binary experiments were conducted at low doses of both PCB126 and ClO_4^- to further characterize HPT axis responses. This study resulted only in a few statistically significant trends for PCB126 up to one day post dose and no statistical differences from control for animals treated with 0.01 mg

ClO_4^-/kg-day for one or four days. A NOEL for PCB126, based on its well-defined primary mode of action of PCB126 (phase II conjugation of T_4) was found to be 0.075 µg/kg. Results from Dosing Study II demonstrate that doses of PCB126 and ClO_4^-, which do not cause alternations in the HPT axis when administered alone, will not result in HPT axis disturbances when administered sequentially. Thus, it appears no interaction (synergism or potentiation) occurs at relatively low doses between PCB126 and ClO_4^- for the thyroid axis indices measured in this study.

No statistically significant differences in thyroid morphology were determined for either study. Changes in thyroid gland have been seen in studies of the individual compounds. Fisher *et al.* (2006) found a statistically significant change in the ratio of colloid volume to epithelium volume 22 days post-dose at the highest dose of PCB126 administered (275 µg/kg). In addition, female rats exposed to 30 mg ClO_4^-/kg-day for two weeks prior to mating through lactation day 22 exhibited altered thyroid morphology, measured by colloid depletion, follicular hyperplasia and hypertrophy (York *et al.,* 2005). To a much lesser extent, animals exposed to 0. 1 and 1.0 mg ClO_4^-/kg-day for the same length of exposure exhibited some colloid depletion and follicular hyperplasia, while no colloid depletion was found in animals exposed to 0.01 mg ClO_4^-/kg-day and follicular hyperplasia was not different from controls (York *et al.,* 2005). Thus, since no differences in thyroid colloid volume and follicular epithelial cell volume ratios were found for the PCB126 and ClO_4^- experiments presented in this paper, either the treatment period was too short or the doses too low to result in structural changes within the thyroid gland itself.

One issue confronting toxicologists today is accurately extrapolating data from high-dose toxicology studies to low-dose exposures seen in the environment. In many cases, low-dose studies are needed to simulate more realistic human environmental exposures, and to provide

information to minimize uncertainty in the low-dose area of the dose-response curve. However, challenges exist when implementing studies in the laboratory to explore endocrine effects in the low-dose region. Minor changes in hormone levels that result from low-dose exposures are difficult to discern because of hormone inter-individual and intra-assay variability between laboratories. Since the statistical power to detect differences in treated groups can be affected by this variability, future experiments, with a greater number of rats and more refined assays for hormone determination, could be conducted to support the conclusion that PCB126 masked effects of ClO_4^- at these low-dose rates examined.

In conclusion, these studies demonstrate that in animals treated with relatively high doses PCB126 prior to ClO_4^- exposure, HPT axis disturbances are less than additive and the ClO_4^- dose-response curve appears shifted to the right. In addition, when animals are co-exposed with doses at or near the NOEL for each compound, no interaction between the compounds is observed for the thyroid indices measured.

The data from this study and previously published individual chemical studies will be utilized in the development of biologically-based pharmacokinetic models for the adult male rat HPT axis. These models will be used to characterize and further the understanding of dose-response relationships for exposure to mixtures of thyroid disrupting chemical mixtures. In addition, HPT axis mathematical models will help to interpret the non-linear dose response based on the primary well defined modes of action.

Acknowledgments

Primary funding for this research was kindly provided by ATSDR grant U61/ATU472105-(02, 03, 04, and 05). Additional research support was provided by the National

Health and Environmental Effects Research Laboratory, Office of Research and Development, U.S. Environmental Protection Agency and the U.S. Air Force Research Laboratory, Human Effectiveness Directorate, Biosciences and Protection Division, Applied Biotechnology Branch. E.D.M. supported through National Science Foundation Fellowship (DGE0229577) and currently EPA STAR Fellowship (FP-91679301-0). Special thanks to Dr W. Matthew Henderson, Debbie Ebalobo, and John Swint for helping with the animal studies. The views expressed in this article are those of the authors and do not represent official opinions of the Department of Defense, U.S. Environmental Protection Agency, or Agency for Toxic Substances and Disease Registry. Mention of trade names or commercial products does not constitute endorsement or recommendation for use.

References

Antonello, J.M., Clark, R.L., and Heyse, J.F. (1993). Application of the Tukey Trend Test Procedure to Assess Developmental and Reproductive Toxicity I. Measurement Data. *Fund. Appl. Toxicol.* **21,** 52-58.

ATSDR (Agency for Toxic Substances and Disease Registry). (2000). Toxicological profile for polychlorinated biphenyls (PCBs). Atlanta, GA: U.S. Department of Health and Human Services, Public Health Service.

Benotti, J., Benotti, N., Pino, S., and Gardyna, H. (1965). Determination of total iodine in urine, stool, diets, and tissue. *Clin Chem*. **11**, 932-936

Blount, B.C., Pirkle, J.L., Osterloh, J.D., Valentin-Blasini, L., and Caldwell, K.L. (2006). Urinary perchlorate and thyroid hormone levels in adolescent and adult men and women living in the United States. *Environ. Health. Perspect.* **114**, 1865-1871.

Brower, A. and van den Berg, K.J. (1986). Binding of a metabolite of 3,4,3',4'-tetrachlorobiphneyl to transthyretin reduces serum vitamin A transport by inhibiting the formation of the protein complex carrying both retinol and thyroxin. *Toxicol. Appl. Pharmacol*. **85,** 301-312.

Capen, C. C. (1996). Toxic responses of the endocrine system. In: Casarett and Doull's Toxicology: The Basic Science of Poisons (C. D. Klaassen, Ed.), pp. 617–640. McGraw-Hill, New York.

CDC (Centers for Disease Control and Prevention). 2005. National Health and Nutrition Examination Survey. Available: http://www.cdc.gov/nchs/nhanes.htm [Accessed 19 February 2007].

Chauhan, K. R., Kodavanti, P. R., and McKinney, J. D. (2000). Assessing the role of ortho-substitution on polychlorinated biphenyl binding to transthyretin, a thyroxine transport protein. *Toxicol. Appl. Pharmacol.* **162,** 10–21.

Cheek, A. O., Kow, K., Chen, J., and McLachlan, J. A. (1999). Potential mechanisms of thyroid disruption in humans: Interaction of organochlorine compounds with thyroid receptor, transthyretin, and thyroid-binding globulin. *Environ. Health Perspect.* **107,** 273–278.

Craft, E.S., DeVito, M.J. and Crofton, K.M. (2002). Comparative Responsiveness of Hypothyroxinemia and Hepatic Enzyme Induction in Long-Evans Rats Versus C57BL/6J Mice Exposed to TCDD-like and Phenobarbital -like Polychlorinated Biphneyl Congeners. *Toxicol. Sci.* **68,** 372-380.

Crofton, K.M., Craft, E.S., Hedge, J.M., Gennings, C., Simmons, J.E., Carchman, R.A., Hans Carter Jr., W., and DeVito, M.J. (2005). Thyroid-Hormone-Disrupting Chemicals:

Evidence for Dose-Dependent Additivity or Synergism. *Environ. Health. Perspect.* **113,** 1549-1554.

Dasgupta, P.K., Martinelango, P.K., Jackson, W.A., Anderson, T.A., Tian, K., Tock, R.W., and Rajagopalan, S. (2005). The Origin of Naturally Occurring Perchlorate: The Role of Atmospheric Processes. *Environ. Sci. Technol.* **39,** 1569-1575.

Dohan, O., de la Vieja, A., Paroder, V., Riedel, C., Artani, M., Reed, M., Ginter, C.S., and Carrasco, N. (2003). The Sodium/Iodide Symporter (NIS): Characterization, Regulation, and Medical Significance. *Endocr. Rev.* **24,** 48-77.

Eng, P.H.K., Cardona, G.R., Previti, M.C., Chin, W.W., and Braverman, L.E. (2001). Regulation of the sodium iodide symporter by iodide in FRTL-5 cells. *Eur. J. Endocrinol.* **144,** 139-144.

Fisher, J.W., Campbell, J., Muralidhara, S., Bruckner, J.V., Ferguson, D., Mumtaz, M., Harmon, B., Hedge, J.M., Crofton, K.M., Kim, H. and Almekinder, T.L. (2006). Effect of PCB126 on Hepatic Metabolism of Thyroxine and Perturbations in the Hypothalamic-Pituitary-Thyroid Axis in the Rat. *Toxicol. Sci*. **90,** 87-95.

Hansen, L. G. (1998). Stepping backward to improve assessment of PCB congener toxicities. *Environ. Health. Perspect.* **106** (Suppl. 1), 171-189.

Khan, M.A., Fenton, S.E., Swank, A.E., Hester, S.D., Williams, A., and Wolf, D.C. (2005). A Mixture of Ammonium Perchlorate and Sodium Chlorate Enhances Alterations of the Pituitary-Thyroid Axis Caused by the Individual Chemicals in Adult Male F344 Rats. *Toxicol. Pathol.* **33,** 776-783.

Koga, N., Beppu, M., and Yoshimura, H. (1990). Metabolism in Vivo of 3,4,5,3',4'-Pentachlorobiphenyl and Toxicological Assessment of the Metabolite in Rats. *J. Pharmacobiodyn.* **13,** 497-506.

Li, M-H. and Hansen, L.G. (1996). Enzyme induction and acute endocrine effects in prepubertal female rats receiving environmental PCB/PCDF/PCDD mixtures. *Environ. Health. Perspect.* **104,** 712-722.

Lowry, O.H., Rosebrough, N.J., Farr, A.L., and Randall, R.J. (1951). Protein Measurement with the Folin Phenol Reagent. *J. Biol. Chem.* **193**, 265-275.

Martin, L. A. (2002). Differential effects of polychlorinated biphenyl (PCB) mixtures and congeners on the disposition of thyroxine(T_4). Ph.D. Dissertation, Rutgers the State University of New Jersey, New Brunswick, NJ.

Motzer, W.E. (2001). Perchlorate: Problems, Detection, and Solutions. *Environ. Foren.* **2,** 301-311.

NRC (National Research Council). (2005). Health Implications of Perchlorate Ingestion. National Research Council of the National Academies. National Academies Press, Washington, D.C.

NTP (National Toxicology Program). (2006). NTP toxicology and carcinogenesis studies of 3,3',4,4',5-pentachlorobiphenyl (PCB126) (CAS No. 57465-28-8) in female Harlan Sprague-Dawley rats (Gavage Studies). *Nat.l Toxicol. Program Tech. Rep. Ser.* **520,** 4-246.

Ogura, I. (2004). Half-life of each dioxin and PCB congener in the human body. *Organohalogen Compounds.* **66**, 3376-3384.

Safe, SH. (1994). Polychlorinated Biphenyls (PCBs): Environmental Impact, Biochemical and Toxic Responses, and Implications for Risk Assessment. *Crit Rev Toxicol* **24**, 87-149.

Tukey, J.W., Ciminera, J.L., and Heyse, J.F. (1985). Testing the Statistical Certainty of a Response to Increasing Doses of a Drug. *Biometrics*. **41,** 295-301.

Van Sande, J., Massart, C., Beauwens, R., Schoutens, A., Costagliola, S., Dumont, J.E., and Wolff, J. (2003). Anion Selectivity by the Sodium Iodide Symporter. *Endocrinol.* **144,** 247-252.

Visser, T. J., Kaptein, E., van Toor, H., van Raaij, J. A. G. M., van den Berg, K. J., Joe, C., vanEngelen, J. G. M., and Brouwer, A. (1993). Glucuronidation of thyroid hormone in rat liver: Effects of in vivo assay conditions. *Endocrinology* **135**, 2177–2186.

Wolff, J. (1998). Perchlorate and the Thyroid Gland. *Pharmacol. Rev.* **50,** 89-105.

York, R.G., Lewis, E., Brown, W.R., Girard, M.F., Mattie, D.R., Funk, K.A., and Strawson, J.A. (2005). Refining the Effects Observed in a Developmental Neurobehavioral Study of Ammonium Perchlorate Administered Orally in Drinking Water to Rats. I. Thyroid and Reproductive Effects. *Int. J. Toxicol.* **24,** 403-418.

Yoshimura, H., Yoshihara, S., Koga, N., Nagata, K., Wada, I., Kuroki, J., and Hokama, Y. (1985). Inductive Effect on Hepatic Enzymes and Toxicity of Congeners of PCBs and PCDFs. *Environ. Health. Perspect.* **59,** 113-119.

Yu, K.O., Narayanan, L., Mattie, D.R., Godfrey, R.J., Todd, P.N., Sterner, T.R., Mahle, D.A.m Lumpkin, M.H., and Fisher, J.W. (2002). The pharmacokinetics of perchlorate and its effect on the hypothalamus-pituitary-thyroid axis in the male rat. *Toxicol Appl Pharmacol* **182,** 148-159.

Zhou, T., Ross, D. G., De Vito, M. J., and Crofton, K. M. (2001). Effects of short-term in vivo exposure to polybrominated diphenyl ethers on thyroid hormones and hepatic enzyme activities in weanling rats. *Toxicol. Sci.* **61**, 76–82.

Table 3.1. Study design and dosing schedule for Dosing Study I. Animals were dosed and euthanized in two groups, which were separated by one day, as indicated by Groups 1 and 2. A single oral gavage dose of PCB126 in corn oil was administered on Day 0. Ammonium perchlorate was added to the drinking water to obtain the target doses indicated, beginning on Day 9 and continuing until the end of study, Day 22. Eight animals (N) were used for each dose combination.

Group	PCB126 Dose (µg/kg)	Perchlorate Dose (mg/kg-day)	N
	Day 0	Day 9-22	
1	0	0	8
1	0	0.01	8
1	0	0.1	8
1	0	1.0	8
1	7.5	0	8
1	7.5	0.01	8
1	7.5	0.1	8
1	7.5	1.0	8
2	0	0	8
2	0	0.01	8
2	0	0.1	8
2	0	1.0	8
2	75	0	8
2	75	0.01	8
2	75	0.1	8
2	75	1.0	8

Table 3.2. Study design and dosing schedule for Dosing Study II. A single oral gavage dose of PCB126 in corn oil was administered on Day 0. Ammonium perchlorate was added to the drinking water to obtain the target doses indicated, beginning on Day 1 and continuing until the end of study. Eight animals (N) were used for each dose combination and time point.

PCB126 Dose (µg/kg)	Perchlorate Dose (mg/kg-day)	End of Study (Day)	N
Day 0	Day 1 – End of Study		
0	NA[a]	0.5	8
0.075	NA	0.5	8
0.75	NA	0.5	8
7.5	NA	0.5	8
0	NA	1	8
0.075	NA	1	8
0.75	NA	1	8
7.5	NA	1	8
0	0	2	8
0.075	0	2	8
0.75	0	2	8
7.5	0	2	8
0	0.01	2	8
0.075	0.01	2	8
0.75	0.01	2	8
7.5	0.01	2	8
0	0	5	8
0.075	0	5	8
0.75	0	5	8
7.5	0	5	8
0	0.01	5	8
0.075	0.01	5	8
0.75	0.01	5	8
7.5	0.01	5	8

[a] Not applicable (NA). Animals were euthanized before ClO_4^- treatment began in order to obtain transient disturbances in the HPT axis due to PCB126 alone.

Table 3.3. The liver/body weight (BW) ratios for all animals in Dosing Study I were multiplied by 100 and are shown in the Table ± SEM. Animals that received 75 µg PCB126/kg had statistically increased (18%) relative liver weight compared to controls.

Treatment Group	**N**	**Liver/BW ratio (x 100)**
Vehicle Control	16	4.08 ± 0.27
ClO_4^- 0.01 mg/kg-day	16	4.22 ± 0.39
ClO_4^- 0.10 mg/kg-day	16	4.12 ± 0.35
ClO_4^- 1.00 mg/kg-day	16	4.14 ± 0.43
PCB126 7.5 µg/kg	8	4.43 ± 0.24
PCB126 7.5 µg/kg and ClO_4^- 0.01 mg/kg-day	8	4.46 ± 0.36
PCB126 7.5 µg/kg and ClO_4^- 0.10 mg/kg-day	8	4.51 ± 0.30
PCB126 7.5 µg/kg and ClO_4^- 1.0 mg/kg-day	8	4.48 ± 0.24
PCB126 75 µg/kg	8	4.74 ± 0.36[a]
PCB126 75 µg/kg and ClO_4^- 0.01 mg/kg-day	8	4.68 ± 0.37[a]
PCB126 75 µg/kg and ClO_4^- 0.10 mg/kg-day	8	4.92 ± 0.25[a]
PCB126 75 µg/kg and ClO_4^- 1.0 mg/kg-day	8	4.90 ± 0.23[a]

[a] Significantly different from control ($p \leq 0.05$).

Figure 3.1. DOSING STUDY 1. Hepatic and thyroid axis responses (% of control) in adult rats: 22 days after a single oral bolus gavage of 7.5 or 75 µg/kg of PCB126 (**clear bar**), 14 days after ingesting of either 0.01, 0.1 or 1.0 mg/kg of ClO_4^- in drinking water (solid circle ± SEM connected by sold lines (—●—)), or co-exposed to both PCB126 and ClO_4^- (**shaded bars**) as described in Methods. Statistically significant trends associated with dose of PCB126 only is indicated with an italicized *a*, (**clear bar**), and for ClO_4^- only, with an italicized *b* , (—●—). In rats co-administered PCB126 and ClO_4^- (**shaded bars**), a pound sign (#) indicates a significant difference from corresponding rats dosed with only ClO_4^- and an asterisk (*) indicates the co-administered rats were significantly different from controls. Control (100%) indicated by dashed line (- - - -). Control mean values ± SEM (n=16) for each assay (fT_4: 2.27 ± 0.14 ng/dL, T_4: 4.58 ± 0.14 µg/dL, TSH: 4.60 ± 0.49 ng/mL, and T_4-G: 0.72 ± 0.05 pmol T_4-G formed/mg protein/min).

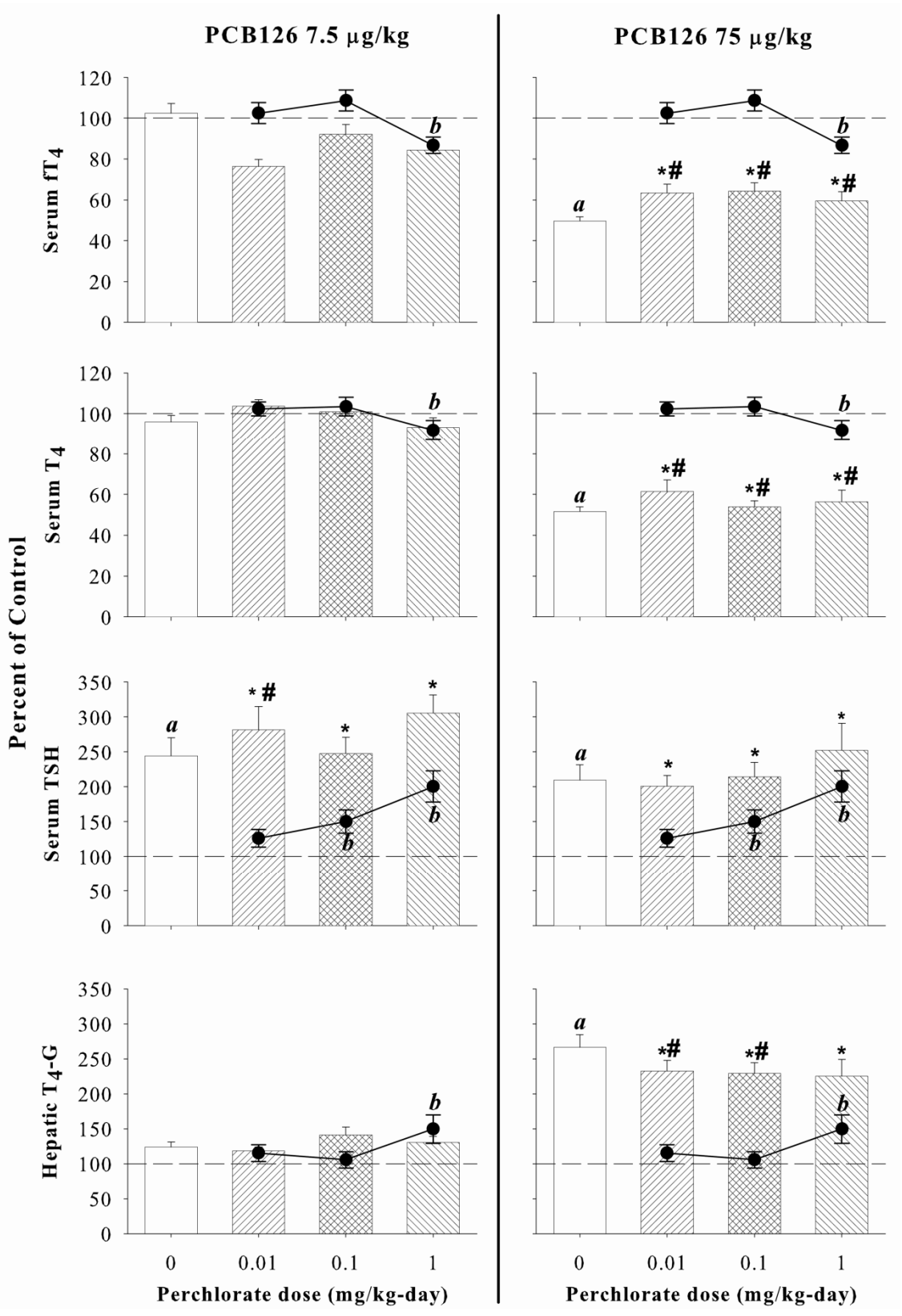
PCB126 7.5 µg/kg
PCB126 75 µg/kg
Percent of Control
Serum fT4
Serum T4
Serum TSH
Hepatic T4-G
Perchlorate dose (mg/kg-day)
Perchlorate dose (mg/kg-day)
0
0.01
0.1
1

Figure 3.1

Figure 3.2. DOSING STUDY II. Hepatic and thyroid axis response (% of control) in adult rats: Two (left column of panels) or five (right column of panels) days post PCB126 dose (0, 0.075, 0.75, or 7.5 μg/kg; solid circle ± SEM connected by solid lines (—●—)); one (left column of panels) or four (right column of panels) day exposure to ClO_4^- in drinking water (0.01 mg/kg-day; **clear bar**), or co-exposed animals (**shaded bars**) as described in Methods. Statistically significant trends associated with dose of PCB126 only are indicated with an italicized *a*, (—●—). No statistical differences from control were found for animals treated with 0.01 mg ClO_4^-/kg-day alone (**clear bar**). In rats co-administered PCB126 and ClO_4^- (**shaded bars**), a pound sign (#) indicates a significant difference from corresponding rats dosed with only ClO_4^-. No significant differences from control for co-exposed animals were detected. Control (100%) represented by dashed line (- - - -). Control mean values ± SEM (n=8) for one day ClO_4^- exposure: (fT_4: 2.46 ± 0.16 ng/dL, T_4: 4.41 ± 0.49 μg/dL, TSH: 7.80 ± 0.83 ng/mL; and T_4-G: 0.62 ± 0.04 pmol T_4-G formed/mg protein/min) and four day ClO_4^- exposure: (fT_4: 2.32 ± 0.16 ng/dL, T_4: 3.32 ± 0.26 μg/dL, TSH: 8.73 ± 0.81 ng/mL, and T_4-G: 0.72 ± 0.08 pmol T_4-G formed/mg protein/min).

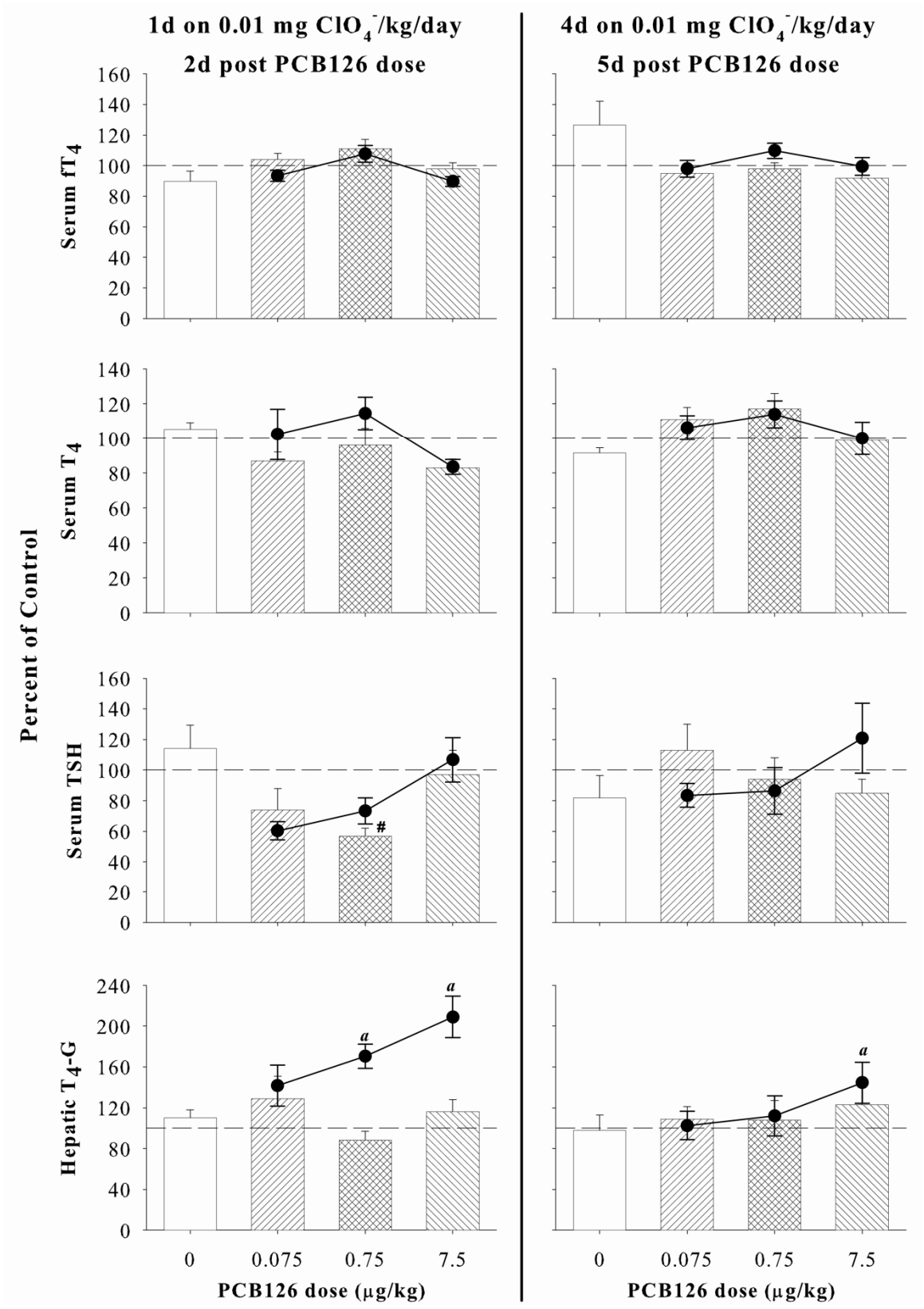
1d on 0.01 mg ClO_4^-/kg/day
2d post PCB126 dose
4d on 0.01 mg ClO_4^-/kg/day
5d post PCB126 dose
Percent of Control
Serum fT_4
Serum T_4
Serum TSH
Hepatic T_4-G
#
a
0
0.075
0.75
7.5
PCB126 dose (µg/kg)

Figure 3.2

Figure 3.3. Stable endogenous iodide (^{127}I) measured in one lobe of the thyroid from a portion of the rats in Dosing Study II. The total thyroidal iodide content (μg) was calculated using the total thyroidal weight determined. The plot shows total thyroidal ^{127}I for control rats (**clear bar**) and treated rats (**dark bars**) exposed to (1) 0.01 mg ClO_4^-/kg-day for four days, as well as co-exposed rats pretreated with PCB126 doses of (2) 0.075, (3) 0.75, and (4) 7.5 μg PCB126/kg for one day, followed by 0.01 mg ClO_4^-/kg-day drinking water exposure for four days. There were no significant differences ($p \leq 0.05$) between total thyroidal ^{127}I content in treated versus control rats.

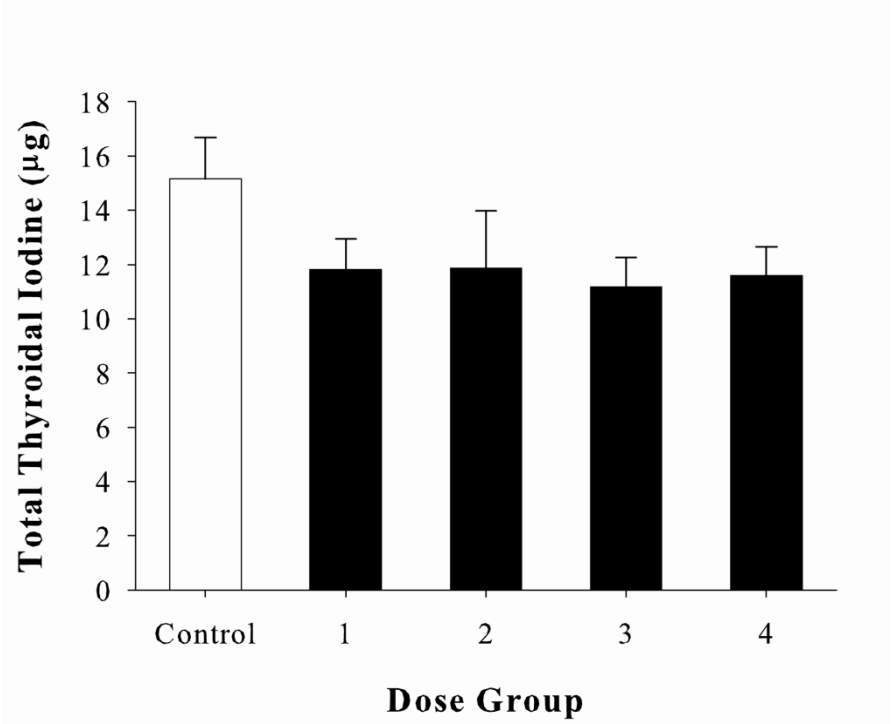
Total Thyroidal Iodine (µg)
18
16
14
12
10
8
6
4
2
0
Control
1
2
3
4
Dose Group

Figure 3.3

Supplementary Data

"Low-Dose Effects of Ammonium Perchlorate on the Hypothalamic-Pituitary-Thyroid (HPT) Axis of Adult Male Rats Pretreated with PCB126"

McLanahan, E.D., Campbell, Jr., J.L., Ferguson, D.C., Harmon, B., Hedge, J.M., Crofton, K.M., Mattie, D.R., Braverman, L., Keys, D.A., Mumtaz, M., and J.W. Fisher.

The supplementary data provided includes the results from histomorphometric analysis of the thyroid glands for all dose groups in Dosing Study I (Table 3.1S) and Dosing Study II (Tables 3.2S and 3.3S). Table 3.4S shows the HPT axis responses as percent of control for Dosing Study I for the individual compounds, the calculated additive response, the binary mixture response, and the deviation from additivity. Finally, the HPT axis responses for animals dosed with 0, 0.075, 0.75, or 7.5 μg PCB126/kg in Dosing Study II is shown in Figure 3.1S.

Table 3.1S. Thyroid Histopathology C/EFC data for Dosing Study I.

ClO_4^- dose (mg/kg-day)	PCB126 dose (µg/kg)	% Colloid and Follicular Volume Fraction ± SD Colloid Volume (C)	Follicular Volume (EFC)	Ratio C/EFC
0.0	0.0	53.85 ± 4.90	46.15 ± 4.90	1.19 ± 0.25
0.0	7.5	53.02 ± 5.58	46.98 ± 5.58	1.13 ± 0.26
0.0	75	52.66 ± 5.04	47.34 ± 5.04	1.11 ± 0.22
0.01	0.0	52.96 ± 5.10	47.04 ± 5.10	1.15 ± 0.23
0.10	0.0	51.56 ± 4.25	48.44 ± 4.25	1.08 ± 0.19
1.00	0.0	53.47 ± 4.30	46.53 ± 4.30	1.17 ± 0.21
0.01	7.5	52.64 ± 4.88	47.36 ± 4.88	1.11 ± 0.23
	75	57.53 ± 4.93	42.47 ± 4.93	1.35 ± 0.30
0.10	7.5	52.83 ± 3.34	47.17 ± 3.34	1.12 ± 0.15
	75	50.98 ± 3.96	49.02 ± 3.96	1.04 ± 0.17
1.00	7.5	50.25 ± 7.12	50.21 ± 7.12	0.99 ± 0.31
	75	49.79 ± 4.25	49.75 ± 4.25	1.01 ± 0.18

*No significant differences were detected ($p \leq 0.05$).

Table 3.2S. Thyroid Histology C/EFC data for 1 Day Perchlorate Exposure (Dosing Study II).

ClO_4^- dose (mg/kg-day)	PCB126 dose (µg/kg)	% Colloid and Follicular Volume Fraction ± SD Colloid Volume (C)	Follicular Volume (EFC)	Ratio C/EFC
0.0	0.0	57.16 ± 4.93	42.84 ± 4.93	1.33 ± 0.31
0.0	0.075	59.70 ± 9.38	40.30 ± 9.38	1.48 ± 0.62
0.0	0.75	49.73 ± 5.74	40.27 ± 5.74	1.48 ± 0.41
0.0	7.5	59.22 ± 6.18	40.78 ± 6.18	1.45 ± 0.38
0.01	0.0	56.40 ± 7.39	43.60 ± 7.39	1.29 ± 0.39
	0.075	48.77 ± 6.39	51.23 ± 63.9	0.95 ± .26
	0.75	47.34 ± 6.26	52.66 ± 6.26	0.90 ± 0.23
	7.5	43.76 ± 5.31	56.24 ± 5.31	0.78 ± 0.17

*No significantly different ratios.

Table 3.3S. Thyroid Histology C/EFC data for 4 Day Perchlorate Exposure (Dosing Study II).

ClO_4^- dose (mg/kg-day)	PCB126 dose (µg/kg)	% Colloid and Follicular Volume Fraction ± S.D. Colloid Volume (C)	Follicular Volume (EFC)	Ratio C/EFC
0.0	0.0	47.27 ± 6.75	52.73 ± 6.75	0.90 ± .26
0.0	0.075	50.25 ± 7.51	49.75 ± 7.51	1.01 ± 0.34
0.0	0.75	44.65 ± 8.17	55.35 ± 8.17	0.81 ± .31
0.0	7.5	45.18 ± 6.66	54.82 ± 6.66	0.82 ± 0.23
0.01	0.0	50.89 ± 5.92	49.11 ± 5.92	1.04 ± 0.28
	0.075	48.25 ± 5.73	51.75 ± 5.73	0.93 ± 0.23
	0.75	50.51 ± 6.21	49.49 ±6.21	1.02 ± 0.25
	7.5	47.70 ± 53.7	52.30 ± 5.37	0.91 ± 0.20

*No significantly different ratios.

Table 3.4S. DOSING STUDY I. Table displays the individual chemical responses for hepatic and thyroid function indices as percent of control. The expected response for the co-exposed animals based on the assumption of additivity is shown, as well as the actual mean percent of control for co-exposed animals. The final column shows the deviation from the additivity estimate.

			PCB126 7.5 µg/kg				PCB126 7.5 µg/kg			
	ClO_4^- Dose	ClO_4^- only response	PCB126 only response	Additive Response Predicted[1]	Co-exposed Actual Response	Deviation from Additivity[2]	PCB126 only response	Additive Response Predicted[1]	Co-exposed Actual Response	Deviation from Additivity[2]
	mg/kg-day	% Control	% Control	% Control	% Control	%	% Control	% Control	% Control	%
Free T_4										
	0.01	103		105	76	28		52	63	-11
	0.1	109	102	111	92	19	50	58	64	-6
	1	87		89	84	5		36	59	-23
Total T_4										
	0.01	102		98	104	-5		54	61	-7
	0.1	103	96	99	101	-2	52	55	54	1
	1	92		88	93	-5		44	56	-13
TSH										
	0.01	126		270	281	11		236	201	-35
	0.1	150	244	294	248	-47	209	260	214	-45
	1	200		344	305	-39		310	252	-57
T_4-G										
	0.01	115		139	118	-21		282	232	-50
	0.1	106	124	129	141	12	267	272	229	-43
	1	150		173	131	-42		316	225	-92

[1] Additive response predicted using the equation: $\%\ Control_{Additive} = (\%_{ClO4} - 100) + (\%_{PCB126} - 100) + 100$

[2] A negative (-) number indicates a less than additive response, and a positive number indicates a greater than additive response.

Figure 3.1S. Thyroid axis response up to 5 days following PCB126 oral gavage dose of either 0.075 (●), 0.75 (○), or 7.5 (▼) μg/kg. Control (0 μg/kg) indicated by dashed line (100%). A) Hepatic rate of T_4-G formation plotted as percent of control ± SEM (0.5 day: 0.85 ± 0.09; 1 day 0.75 ± 0.08; 2 day: 0.62 ± 0.04; and 5 day: 0.72 ± 0.08 pmol T_4-G formed/mg protein/min). B) Serum fT_4 concentration displayed as percent of control ± SEM (0.5 day: 3.75 ± 0.31; 1 day 2.52 ± 0.11; 2 day: 2.46 ± 0.16; and 5 day: 2.32 ± 0.16 ng/dL). C) Serum T_4 concentrations shown as percent of control ± SEM (0.5 day: 3.92 ± 0.51; 1 day 3.86 ± 0.52; 2 day: 4.41 ± 0.49; and 5 day: 3.32 ± 0.26 μg/dL). D) Serum TSH concentrations plotted as percent of control ± SEM (0.5 day: 3.07 ± 0.47; 1 day 6.53 ± 0.56; 2 day: 7.80 ± 0.83; and 5 day: 8.73 ± 0.81 ng/mL). Doses of significant trend ($p \leq 0.05$) indicated by asterisk (*).

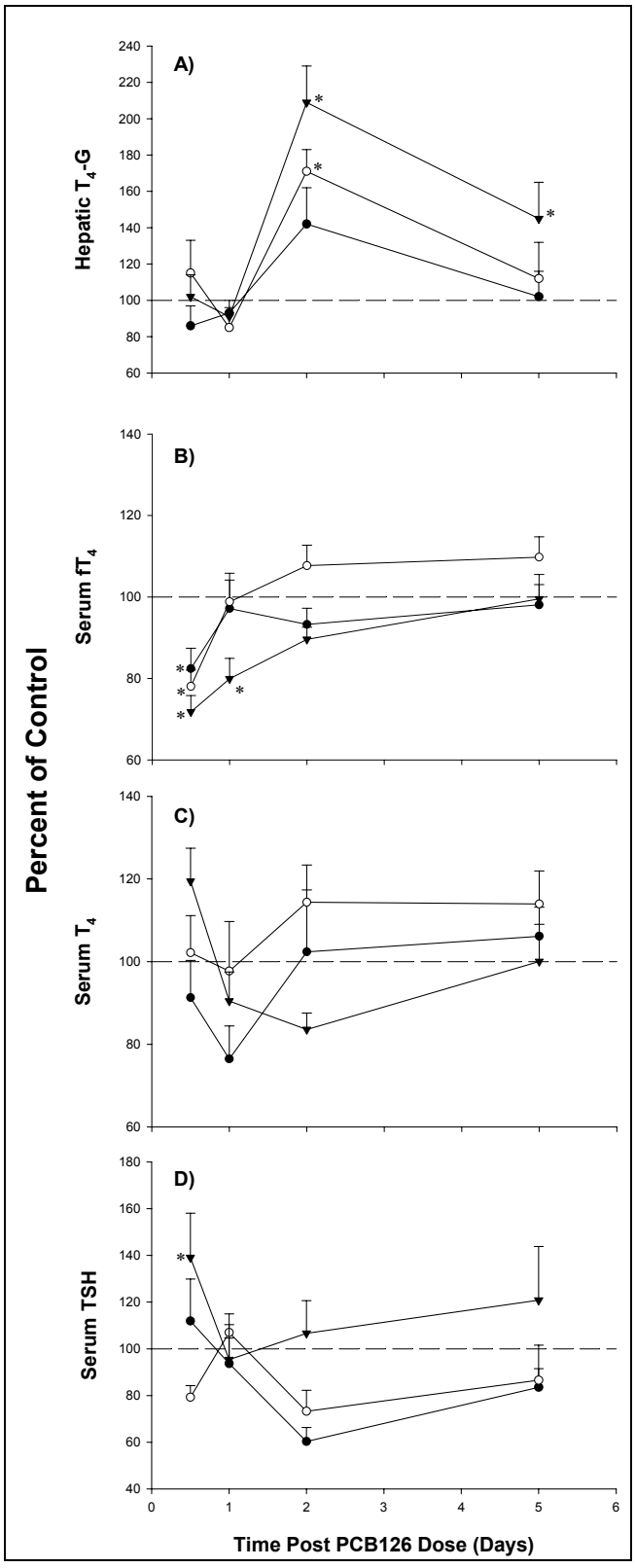
A)
B)
C)
D)
Hepatic T4-G
Serum fT4
Serum T4
Serum TSH
Percent of Control
Time Post PCB126 Dose (Days)

Figure 3.1S

CHAPTER 4

A BIOLOGICALLY BASED DOSE-RESPONSE MODEL FOR DIETARY IODIDE AND THE HYPOTHALAMIC-PITUITARY-THYROID AXIS IN THE ADULT RAT: EVALUATION OF IODIDE DEFICIENCY[2]

[2] E.D. McLanahan, M.E. Andersen, and J.W. Fisher.
Submitted to *Toxicological Sciences* on October 2, 2007.

Abstract

A biologically based dose-response (BBDR) model was developed for dietary iodide and the hypothalamic-pituitary-thyroid (HPT) axis in adult rats. This BBDR-HPT axis model includes sub-models for dietary iodide, thyroid stimulating hormone (TSH), and the thyroid hormones thyroxine (T_4) and 3,5,3'-triiodothyroine (T_3). The sub-models are linked together via key biological processes, including: 1) the influence of T_4 on TSH production (the HPT axis negative feedback loop); 2) stimulation of thyroidal T_4 and T_3 production by TSH; 3) TSH upregulation of the thyroid sodium/iodide symporter (NIS); and 4) recycling of iodide from the metabolism of thyroid hormones. The BBDR-HPT axis model was calibrated to predict steady-state concentrations of iodide, T_4, T_3, and TSH for the euthyroid rat whose dietary intake of iodide was 20 μg/day. Then the calibrated BBDR-HPT axis model was used to predict perturbations in the HPT axis caused by insufficient dietary iodide intake and simulation results were compared to experimental findings. The BBDR-HPT axis model was successful in simulating dietary iodide induced hypothyroid conditions for perturbations in serum T_4, TSH, and thyroid iodide stores for low iodide diets of 0.33 to 1.14 μg/day. Model predictions of serum T_3 concentrations were inconsistent with some reported experimental findings. BBDR-HPT axis model simulations revealed a very steep dose-response relationship between dietary intake of iodide and perturbations in the HPT axis when dietary iodide intake becomes insufficient (less than 2 μg/day) to sustain the HPT axis. This research demonstrates that biologically based models can be successfully developed to predict complex responses in endocrine systems such as the HPT axis.

Key Words: iodide, BBDR model, HPT axis, thyroxine, TSH, rat

Introduction

The hypothalamic-pituitary-thyroid (HPT) axis regulates many physiologic functions, including metabolism, growth, development, and reproduction. HPT axis homeostasis is maintained by complex feedback controls; however, this system may be altered and unable to compensate for changes resulting from exposure to thyroid active environmental contaminants or ingestion of insufficient or excessive amounts of iodide. Iodine, an essential nutrient, is a constituent required for formation of thyroid hormones and is involved in autoregulation of the thyroid gland. During critical periods of development, alterations in the thyroid axis can result in improper development with lifelong consequences. Iodine deficiency, which leads to hypothyroidism, ranks among the highest preventable causes of mental retardation and brain damage throughout the world (Delange, 2001). Insufficient iodine intake is still prevalent in almost one third of world population (Hamann *et al.*, 2006).

The process of thyroid hormone formation is highly regulated. The thyroid gland actively sequesters iodide via the sodium (Na^+)/iodide(I^-) symporter (NIS). Iodide is then available for incorporation and use in thyroid hormone production. The normal thyroid gland produces thyroxine (T_4) in greater quantities than the biologically active hormone 3,5,3'-triiodothyronine (T_3) (Greer *et al.*, 1968). Thyroid hormones are secreted from the thyroid gland into systemic circulation, where T_4 can be metabolized to T_3 in peripheral tissues by a family of enzymes called 5'-deiodinases. T_3 binds to nuclear receptors in virtually every cell of the body to regulate gene expression. When circulating blood levels of T_4 and T_3 are low, the anterior pituitary gland is stimulated to produce more thyroid stimulating hormone (TSH), a classical negative feedback loop. TSH is carried to the thyroid gland by blood, where TSH binds to receptors on the plasma membrane of thyroid follicular cells. This receptor-TSH complex

regulates second messenger cascades, which stimulates the increase in NIS expression and activity, and increased production of thyroid peroxidase (TPO) and thyroglobulin (Tg) (Kogai *et al.*, 2006). These orchestrated biochemical events ultimately allow for increased thyroidal uptake of iodide and production and secretion of T_4 and T_3.

Several investigators have quantitatively described selected aspects of the HPT axis using mathematical tools. Classical pharmacokinetic (PK) models for the thyroid hormones T_4 and T_3 have been developed for the rodent (DiStefano *et al.*, 1982; DiStefano and Feng, 1988). Three compartment (blood, fast, and slow pools) models for radiolabeled T_4 and T_3 were used to estimate thyroid hormone production rates, kinetic compartment parameters for the thyroid hormones, and their metabolic clearance rates. Li (1995) and colleagues also employed a more theoretical PK compartmental approach to simulate the dynamic and pulsatile nature of the human thyroid axis, which included serum TSH, T_4, and T_3 concentrations. In 1996, Kohn *et al.* developed a physiological dosimetric model of the distribution of 2,3,7,8-tetrachlorodibenzo-p-dioxin (TCDD) in the rodent that also incorporated a HPT axis sub-model. The HPT axis sub-model included the negative feedback loop and production and metabolism of T_4 and T_3. The TCDD model integrated with the HPT axis model was utilized to predict decreases in serum T_4, via a TCDD-dependent increase in hepatic phase II conjugation of T_4 (Kohn *et al.*, 1996).

More recently, Dietrich *et al.* (2002) used a complex engineering approach to describe biofeedback (e.g. T_4/TSH negative feedback loop in humans) and the pulsatile nature of TSH secretion. Mukhopadhyay and Bhattacharyya (2006) also employed an engineering control system approach, including time delays to describe the pulsatile nature of the human HPT axis for thyroxine and TSH feedback and plasma distribution. In addition to the aforementioned models, physiologically based pharmacokinetic (PBPK) models for radiolabeled iodide (^{125}I) in

rodent and human have been developed for different life stages (Merrill *et al.*, 2003, 2005; Clewell *et al.*, 2003a, 2003b). These were ^{125}I kinetic models and did not include dietary iodide (^{127}I) or thyroid hormones.

Although several mathematical models have been constructed to describe the thyroid axis, to date none have taken into account TSH and dietary iodide (^{127}I) linked to T_4 and T_3 formation and secretion. Therefore, the objective of this research was to develop a biologically based dose-response (BBDR) model of the adult male rat HPT axis (BBDR-HPT axis model), including description of dietary iodide and its utilization in the thyroid gland for hormone production. DeVito *et al*. (1999) concluded serum hormone levels (T_4, T_3, and TSH), along with thyroid weight and histology are the most critical endpoints for determination of xenobiotic effects on thyroid toxicity. Thus, a quantitative BBDR-HPT model was developed to include the most informative serum hormones, namely, T_4 and T_3, and the signaling molecule, TSH. Several novel features included in our model are the active transport and regulation of iodide uptake into the thyroid by the NIS, T_4/TSH negative feedback loop, extrathyroidal metabolism of T_4 to form the biologically active T_3, fecal excretion of T_4-glucuronide, and recycling of metabolically derived iodide from extrathyroidal metabolism of thyroid hormones.

Many environmental contaminants have been shown to disrupt thyroid hormone homeostasis (Brucker-Davis, 1998). The BBDR-HPT axis model reported in this paper can be integrated with PBPK models of thyroid disrupting chemicals using chemical specific mode(s) of action, to predict changes in serum T_4, T_3, and TSH and total thyroidal iodide content. However, as a first step in this direction, iodide sufficiency and insufficiency were evaluated with the BBDR-HPT axis model in the adult rat to better understand the role of dietary iodide in HPT axis homeostasis.

Materials and Methods

The BBDR-HPT axis sub-models for the adult rat were constructed using simple model structure that allowed us to focus on an empirical 'system based evaluation' of key biochemical features of the HPT axis, such as the negative feedback loop. For example, the production of thyroid hormones (Equation 15) is controlled, in part, by the model predicted serum TSH concentration, while the maximal rate of active sequestration of iodide into the thyroid (Equation 2) is also controlled by the serum TSH concentration. Other investigators have recently described endocrine systems, using serum levels of signaling molecules to control feedback loops such as the adult male rat hypothalamic-pituitary-gonadal (HPG) axis (Barton and Andersen, 1998) and the human HPG axis/menstrual cycle (Schlosser and Selgrade, 2000 and Rasgon *et al.*, 2003). Future modeling efforts focused on expanding the BBDR-HPT axis model to include other tissues of interest (e.g. brain for correlation of tissue concentrations to developmental effects) can be readily integrated into our model structure.

Models were coded using acslXtreme version 2.4.0.11 (Aegis Technologies, Huntsville, Alabama) and solved with the Gear algorithm for stiff systems. Standardized units of nanomoles (nmol), liters (L), kilograms (kg), and hours (hr) were used in the sub-models. The approach for the development of the BBDR-HPT axis model was to first create simple and independent sub-model structures for radiolabeled –iodide, -TSH, -T_4, and -T_3 using radiotracer studies reported in literature for the adult rat. This provided a number of BBDR-HPT axis model parameter values, although sometimes preliminary, and helped to evaluate the adequacy of using the proposed structure for each sub-model. Boundary conditions were implemented in the development of each radiolabeled sub-model, such that estimated model parameter values could

not result in simulation outcomes that deviated from the boundary conditions for the HPT axis reported in Table 4.1.

Literature derived datasets with endogenous information for the sub-models (iodide, TSH, T_4, and T_3) were gathered and the sub-models were linked as a system to simulate the HPT axis in the euthyroid adult rat. Key features of the BBDR-HPT axis model included the negative feedback loop, thyroid hormone production using available dietary iodide, and the metabolism of thyroid hormones with release of free iodide available for reuse in thyroid hormone production or urinary excretion. The euthyroid steady-state BBDR-HPT axis model relied on dietary iodide as the only exogenous input. Finally, the calibrated euthyroid, iodide sufficient adult rat BBDR-HPT axis model was tested for its ability to predict perturbations in the system under iodide deficient conditions.

Datasets used for Sub-Model Development

Key datasets were selected for development of the radiotracer sub-models for ^{125}I, ^{125}I-TSH, ^{131}I-T_4, and ^{125}I-T_3. Data for ^{125}I published by Yu *et al.* (2002) was selected for use in development and calibration of the iodide sub-model. Adult male Sprague-Dawley rats were administered 33μg ^{125}I/kg bw via tail vein injection and serum and thyroid concentrations were determined up to 96 hours post dose, as well as cumulative urinary ^{125}I excretion over a 24 hr period following iv dose. Concentrations of ^{125}I in plasma up to 24 hrs post dose were published in Yu *et al.* (2002); however, additional data for thyroid bound and total concentration of ^{125}I, urinary excretion, and serum concentrations 30-96 hr post dose were kindly provided by Dr. Yu (personal communication). The plasma disappearance of ^{125}I-TSH was reported in male Hebrew University rats (80-100g) for up to 2 hours post iv dose of 5 ng ^{125}I-TSH (Spira *et al.*, 1979). Schroder van der Elst *et al.* (1997) reported ^{131}I-T_4 concentrations 0.25-6 hr post iv dose in

female Wistar rats (180g) as percent of 1.7ng ^{131}I-T_4 dose in several tissues, including blood and liver. In normal adult male Sprague-Dawley rats (300-375g), DiStefano *et al.* (1993) characterized the distribution of a 0.83 ng ^{125}I-T_3 iv dose in liver and plasma up to 1.2 hr post dose.

Sub-Model Structure and Key Equations

Iodide. A simple sub-model structure was implemented to predict iodide kinetics. Iodide was described as distributing into a volume of distribution (Vd) and a thyroid gland (Figure 4.1A). Iodide is rapidly absorbed to the bloodstream from the digestive tract and quickly diffuses into extracellular spaces throughout the body. Iodide fate is largely determined by a competition between thyroidal sequestration and urinary excretion (Verger *et al.*, 2001). Urinary excretion of iodide is described as a first order clearance from the Vd. Uptake of iodide into the thyroid compartment is described assuming active uptake by the sodium(Na^+)/iodide(I^-) symporter (NIS) and diffusion (Figure 4.1A).

Iodide processing by the thyroid is multi-faceted. Free iodide enters the thyroid two ways: 1) active uptake by NIS and 2) diffusion via ion channels. NIS is a plasma membrane protein that actively transports two sodium molecules with one iodide molecule down the sodium ion gradient, which is generated by sodium-potassium ATPases (Kogai *et al.*, 2006). TSH has been shown to stimulate NIS mRNA production, NIS protein expression, and retention in the plasma membrane (Carrasco, 1993; Kogai *et al*., 2000; Levy *et al.*, 1997; Riedel *et al.*, 2001; and Sherwin and Tong, 1974). Sherwin and Tong (1994) found that TSH-induced stimulation of iodide transport increased the rate of iodide uptake and did not affect the affinity (Km_i) of iodide for the transporter. Thus, iodide uptake into the thyroid via the NIS ($dTNIS_i/dt$, nmol/hr) and TSH stimulation of the NIS iodide transport rate ($VmaxT_i^{TSH}$, nmol/hr) was described as follows:

$$\frac{dTNIS_i}{dt} = \frac{V\max T_i^{TSH} \times Cvt_i}{Km_i + Cvt_i} \quad [1]$$

$$V\max T_i^{TSH} = \frac{V\max T_i \times Ca_{TSH}}{K_{NIS}^{TSH} + Ca_{TSH}} \quad [2]$$

where Cvt_i is the free concentration of iodide in thyroid blood (nmol/L), Km_i is the affinity constant of iodide for the NIS (nmol/L), $VmaxT_i$ is the TSH stimulated maximum rate of NIS iodide uptake (nmol/hr), Ca_{TSH} is the serum concentration of TSH (nmol/L), and K^{TSH}_{NIS} is the concentration of TSH that gives rise to half-maximal rate of NIS transport of iodide (nmol/L). For the purpose of the estimating parameters using the radiolabeled iodide (^{125}I) sub-model, Ca_{TSH} was set to a value equal to the average control, euthyroid serum concentration (6.5 ng/mL or 0.232 nmol/L) from McLanahan *et al.* (2007).

Once iodide enters the thyroid by NIS active uptake or diffusion, iodide is incorporated (organified) by binding to tyrosine residues present in thyroglobulin (Tg) via a thyroid peroxidase (TPO) mechanism (Degroot and Niepomiszcze, 1977). TSH increases the expression of many genes involved in thyroid hormone synthesis, including Tg and TPO (Kogai *et al*., 2006). The rate of incorporation of iodide (dRIB/dt, nmol/hr) into thyroid hormone precursors and TSH stimulation ($VmaxB^{TSH}_i$, nmol/hr) of the organification process is simplified and described by:

$$\frac{dRIB}{dt} = \frac{V\max B_i^{TSH} \times CTF_i}{Kb_i + CTF_i} \quad [3]$$

$$V\max B_i^{TSH} = \frac{V\max B_i \times Ca_{\mathrm{TSH}}}{Kb_{\mathrm{TSH}} + Ca_{\mathrm{TSH}}} \quad [4]$$

where CTF_i (nmol/L) is the free concentration of iodide in the thyroid, Kb_i (nmol/L) is the fitted concentration of free iodide in the thyroid when binding rate is half-maximal, $VmaxB_i$ (nmol/hr)

is the TSH stimulated maximum rate of organification of iodide, and Kb_{TSH} (nmol/L) is the concentration of serum TSH that produces half-maximal organification rate of iodide. In the ^{125}I sub-model the concentration of TSH in serum (Ca_{TSH}) was also set to constant as previously described.

Loss of free iodide from the thyroid by outward diffusion was described using an estimated permeability cross-product (PAT_i) and loss of bound iodide as thyroid hormones is described in Equations 15-17. Thus, the thyroid tissue compartment for iodide was described for free ($dATF_i$/dt, nmol/hr), bound/thyroid hormone incorporated ($dATB_i$/dt, nmol/hr), and total (AT_i, nmol) iodide by the following equations:

$$\frac{dATF_i}{dt} = \frac{dTNIS_i}{dt} + PAT_i \times (Cvt_i - CTF_i) - \frac{dRIB}{dt} \qquad [5]$$

$$\frac{dATB_i}{dt} = \left[\frac{dRIB}{dt} - \left(\frac{d\mathrm{T4}_{prod}}{dt} \times \mathrm{T4}_i\mathrm{eq} \right) - \left(\frac{d\mathrm{T3}_{prod}}{dt} \times \mathrm{T3}_i\mathrm{eq} \right) \right] \qquad [6]$$

$$AT_i = \int \frac{dATF_i}{dt} + \int \frac{dATB_i}{dt} \qquad [7]$$

where $dT4_{prod}$/dt is the secretion rate of T_4 from the thyroid (nmol T_4/hr), $T4_i$eq is the molar fraction of iodide in a T_4 molecule (0.6534), $dT3_{prod}$/dt is the secretion rate of T_3 from the thyroid (nmol T_3/hr), and $T3_i$eq is the molar fraction of iodide in a T_3 molecule (0.5848).

Thyroid Stimulating Hormone (TSH). Since TSH does not distribute into tissues, a one-compartment sub-model for TSH was constructed using a Vd (Figure 4.1B). The amount of ^{125}I-TSH in the serum is determined by an iv dose to the Vd and first order clearance as shown below:

$$\frac{dAVd_{TSH}}{dt} = RIV_{TSH} - \left(kel_{TSH} \times AVd_{TSH} \right) \qquad [8]$$

where RIV_{TSH} is the ^{125}I-TSH infusion rate (nmol/hr), kel_{TSH} is the clearance rate of TSH (hr^{-1}), and AVd_{TSH} is the amount of TSH in the Vd (nmol), which is representative of the serum concentration. This model is amended in the endogenous description of TSH in the BBDR-HPT axis model to include endogenous production of TSH, by an empirical description based on serum T_4 concentrations (the T_4/TSH negative feedback loop described later, Equation 14).

Thyroxine (T_4) and 3,5,3'-Triiodothyronine (T_3). Each thyroid hormone sub-model was developed with a Vd and liver compartment (Figure 4.1C and 4.1D). Bidirectional diffusion of T_4 in the liver was included in the description of hepatic influx and efflux. T_4 has also been shown to be actively transported into the liver by a high affinity, low capacity transporter, as well as a low affinity, high capacity transporter (Krenning *et al.*, 1981). However, hepatic uptake of T_4 was simplified and described using a single Michaelis-Menten equation:

$$\frac{dLU_{T4}}{dt} = \frac{V\max_{T4}^{LU} \times \left(Cvl_{T4} \times 0.01\right)}{Km_{T4}^{LU} + \left(Cvl_{T4} \times 0.01\right)} \qquad [9]$$

where $Vmax^{LU}_{T4}$ is the maximal rate of active uptake of T_4 into the liver (nmol/hr), Km^{LU}_{T4} is the affinity constant for T_4 active transport (nmol/L), and Cvl_{T4} is the concentration of T_4 in the liver venous blood (nmol/L). Since at least ninety-nine percent of T_4 is bound to serum proteins in rodents (Mendel *et al.*, 1992), the sub-model code was modified to reflect only free serum T_4 (1% of total serum T_4) available for active transport and diffusion into the liver. Phase II metabolism of T_4 in the liver was described using Michaelis-Menten metabolism equations for glucuronidation (formation of T_4-glucuronide, T_4-G) and type I 5'-deiodination of T_4, forming T_3 and free iodide. The diffusion limited liver blood compartment for T_4 was described using the equations:

$$\frac{dALb_{T4}}{dt} = Q_L \times (Ca_{T4} - Cvl_{T4}) + PAL_{T4} \times (CL_{T4} - (Cvl_{T4} \times 0.01)) - \frac{dLU_{T4}}{dt} \qquad [10]$$

$$Cvl_{T4} = \frac{\int \frac{dALb_{T4}}{dt}}{V_{Lb} \times PL_{T4}} \quad [11]$$

where $dALb_{T4}/dt$ is the rate of change of T_4 in the liver blood (nmol/hr), Q_L is the blood flow to the liver (L/hr), Ca_{T4} is the arterial blood concentration of T_4 perfusing the liver (nmol/L), PAL_{T4} is the permeability area cross-product for liver bidirectional diffusion of T_4 (L/hr), Cvl_{T4} is the concentration of T_4 in the liver venous blood (nmol/L), V_{Lb} is the volume of liver blood (L), and PL_{T4} is the T_4 liver:blood partition coefficient (unitless).

The liver tissue compartment for T_4 was described as follows:

$$\frac{dAL_{T4}}{dt} = PAL_{T4} \times ((Cvl_{T4} \times 0.01) - CL_{T4}) + \frac{dLU_{T4}}{dt} - \frac{dDIL_{T4}}{dt} - \frac{dUGT_{T4}}{dt} \quad [12]$$

$$CL_{T4} = \frac{\int \frac{dAL_{T4}}{dt}}{V_L} \quad [13]$$

where dAL_{T4}/dt is the rate of change of T_4 in the liver tissue (nmol/hr), CL_{T4} is the concentration of T_4 in the liver (nmol/L), dLU_{T4}/dt is the rate of active uptake of T_4 into the liver from liver blood (nmol/hr, Equation 9), $dDIL_{T4}/dt$ is the rate of T_4 conversion to T_3 and free iodide by type I 5'-deiodinating enzymes (nmol/hr), $dUGT_{T4}/dt$ is the rate of formation of T_4-G formation (nmol/hr), and V_L is the volume of the liver (L). T_4 has also been shown to undergo other hepatic metabolic processes, such as sulfation (T_4-S formation), however this route accounts for a small fraction (6%) of overall T_4 metabolism (Rutgers *et al.*, 1989). Furthermore, T_4-S is rapidly deiodinated in the liver (Visser *et al.*, 1990) and so the T_4-S metabolic route was not included in this model. To account for the rest of the body metabolism of T_4 to T_3, a first order metabolism of T_4 was included as a loss from the Vd compartment.

Similar to T_4, transport of T_3 into the liver compartment was described by bidirectional diffusion and active uptake by a transporter protein (Figure 4.1C). Experimental evidence for

hepatic transporter uptake of T_3 from blood suggests that T_3 uptake is not saturable at physiological conditions (Blondeau *et al.*, 1988), thus the active uptake was described as a first-order process. Hepatic metabolism of T_3 in the liver was described as a first-order process also, with the assumption that a percentage of the metabolized T_3 is excreted in feces as T_3 conjugates (e.g. T_3-G, T_3-S, etc.). The remainder is metabolized to free iodide, assuming T_3 metabolism to T_2 is the rate limiting step in releasing free iodide. The fraction of T_3 metabolism excreted in feces (FT3feces) was fit to provide an approximation (26%) of the a priori boundary condition of 30% (DiStefano *et al.*, 1993) for percent of T_3 dose excreted in feces (Table 4.1). First-order metabolism of T_3 was included in the Vd to account for rest of body metabolism of T_3 to T_0, also assuming that T_3 to T_2 is the rate limiting step.

Linking the Sub-Models to Create a BBDR-HPT Axis Model

The sub-models described above for iodide, T_4, T_3, and TSH are linked as shown in Figure 4.2. All compartments for each sub-model were assigned steady-state derived masses at the onset of the simulations. The mass of TSH, iodide, or thyroid hormones was established by running the simulations to steady-state with a dietary iodide intake of 20 μg per day. Dietary intake of iodide was assumed to take place over a 12-hr period, with food/iodide consumption occurring during the night hours (7 pm - 7 am).

TSH is secreted by the anterior pituitary and is found in systemic circulation. Briefly, the TSH one-compartment model in the linked BBDR-HPT axis model was modified from Equation 8 to include an endogenous production term. The production of TSH is based on the primary negative feedback loop of the thyroid axis; that is adequate levels of serum thyroid hormones result in a normal secretion of TSH from the pituitary, but when serum thyroid hormone levels decrease, the feedback control is diminished and TSH production rate increases. Several

researchers have shown a negative correlation between serum T_4 and TSH concentrations (Fukuda *et al.*, 1975; Riesco *et al.*, 1977; and Pedraza *et al.*, 2006). This is a primary experimental observation reported by several laboratories and used in the development of the negative feedback loop for the BBDR-HPT axis model. Since total serum T_4 is a common measurement in most thyroid disruptor studies, as opposed to free T_4, the TSH/T_4 negative feedback loop was described using total serum T_4 as shown in Equation 14. The empirical description of TSH production is regulated by the model predicted total serum T_4 concentration (Ca_{T4}). The complete equation used to determine the amount of TSH in the Vd is as follows:

$$\frac{dAVd_{TSH}}{dt} = \underbrace{\frac{k_0^{TSH} \times \mathrm{K}_{\mathrm{T4}}^{\mathrm{inh}}}{\mathrm{K}_{\mathrm{T4}}^{\mathrm{inh}} + Ca_{\mathrm{T4}}}}_{\text{production}} - \underbrace{kel_{\mathrm{TSH}} \times Ca_{\mathrm{TSH}}}_{\text{elimination}} \qquad [14]$$

where $k_0{}^{\mathrm{TSH}}$ (nmol/hr) is the maximal production rate of TSH in the absence of T_4, $\mathrm{K}^{\mathrm{inh}}{}_{\mathrm{T4}}$ (nmol/L) is the estimated concentration of T_4 in the serum which results in half-maximal production rate of TSH, Ca_{T4} (nmol/L) is the total T_4 serum concentration, and Ca_{TSH} (nmol/L) is the TSH serum concentration calculated by dividing the integral of Equation 14 by Vd_{TSH} (L).

The rate of total thyroidal production and secretion of thyroid hormones (T_4 and T_3) is determined by a fitted rate constant ($k^{\mathrm{IB}}{}_{\mathrm{TSH}}$) times the model predicted serum concentration of TSH and concentration of available thyroidal iodide in the form of hormone precursors:

$$\frac{dTH_{prod}}{dt} = k_{TSH}^{IB} \times Ca_{TSH} \times CTB_i \qquad [15]$$

where $k^{\mathrm{IB}}{}_{\mathrm{TSH}}$ (L^2/nmol/hr) is a linear rate term, Ca_{TSH} (nmol/L) is the serum concentration of TSH, and CTB_i (nmol/L) is the concentration of bound thyroidal iodide as thyroid hormone precursors. The proportion of thyroid hormones produced as T_3 and T_4 is then described as a fraction of the total production rate, using the following equations:

$$\frac{dT3_{prod}}{dt} = FT3 \times \frac{dTH_{prod}}{dt} \quad [16]$$

$$\frac{dT4_{prod}}{dt} = \frac{dTH_{prod}}{dt} - \frac{dT3_{prod}}{dt} \quad [17]$$

where $dT3_{prod}/dt$ is the rate of thyroidal T_3 production (nmol/hr), and $dT4_{prod}/dt$ is the rate of thyroidal T_4 production (nmol/hr). The ratio of T_3/T_4 secretion increases modestly during iodide deficiency. To account for this, Equation 18 was derived from Pedraza *et al.* (2006), who collected experimental data on total thyroidal iodide stores and thyroidal T3/T4 ratios for different rates of iodide intake (Figure 4.3). FT3 (unitless) is the fraction of overall thyroid hormone production within the thyroid that is T_3 and was modeled as:

$$FT3 = 0.2652 \times AT_i^{-0.4684} \quad [18]$$

where AT_i is the total amount of iodide in the thyroid (μg), as calculated in Equation 7 and converted to μg. In iodide deficient conditions, a shift from primarily T_4 to T_3 production in the thyroid occurs (Greer *et al.*, 1968; Pedraza *et al.*, 2006). This may be due to the increase in deiodination of T_4 in the thyroid, or simply the formation of less T_4 because less iodide is needed to make T_3. However, no instances have been reported where the thyroid synthesizes only T_3 at the cost of zero T_4 production. A MIN command was implemented in acslXtreme to ensure that the exponential FT3 function (Equation 18) did not exceed 0.90.

Datasets used in Steady-State Euthyroid BBDR-HPT axis model calibration.

Serum T_4, T_3, and TSH, along with total thyroid iodide data from adult male Sprague-Dawley rats published by McLanahan *et al.* (2007) were used to calibrate the model for steady-state euthyroid conditions in the adult rat (320g). It was also important to include liver T_4 and T_3 concentrations for calibration; however, there are few datasets with tissue concentrations of thyroid hormones. Morreale de Escobar *et al.* (1994) reported concentrations of T_4 and T_3 in

several different tissues, including the liver of control, euthyroid adult female Wistar rats. This study was used in the linked BBDR-HPT axis model calibrations. Furthermore, the only study found to contain free iodide serum concentrations was Eng *et al.* (1999) in which they reported the data for euthyroid (control) adult male Sprague-Dawley rats.

Model Parameters

Model parameters were derived from the published literature whenever possible. Default assumptions for allometric scaling were employed. Thus, blood flows (Q), maximum velocities (V_{max})[3], and permeability area cross-products (PA), were multiplied by $BW^{0.75}$ and clearance rates (Cl and kel) were divided by $BW^{0.25}$. Volumes of distribution (Vd) were scaled linearly with BW.

Physiological Parameters. Growth equations developed by Mirfazaelian *et al*. (2007) were used to account for body weight changes for simulations that were longer than one month. Otherwise, the terminal body weight reported for the study was used in simulation. Blood flows and tissue volumes (V) were obtained from literature (Brown *et al.*, 1997; Malendowicz and Bednarek, 1986; McLanahan *et al.*, 2007). Physiological parameters are shown in Table 4.2.

Literature Derived Compound-Specific Parameters. When possible, compound-specific parameters for each sub-model were derived from literature. Parameters for iodide, T_4, T_3, and TSH are shown in Table 4.3. Liver partition coefficients for T_4 (PL_{T4}, 1.27) and T_3 (PL_{T3}, 4.47) were determined from steady state serum and liver concentrations reported by Escobar-Morreale *et al.* (1996) for female euthyroid, control rats. These values are similar to the values used by Kohn *et al.* (1996) for T_4 and T_3 liver partition coefficients (1.632 and 2.22, respectively) that

[3] An evaluation of literature for total thyroid iodide (^{127}I) concentrations for the range of body weights simulated in this study (120-500g) showed slight change in total amount of thyroidal ^{127}I. The model parameter maintaining the stores in the thyroid is $VmaxBc_i$ (Vmax for iodide incorporation into thyroid hormone precursors). Thus, to empirically describe total thyroid ^{127}I concentrations, the value of $VmaxBc_i$ is divided by $BW^{0.75}$.

were estimated from K_{ow} values and the use of various regression equations. No partition coefficients were explicitly incorporated into the endogenous iodide sub-model. Implicitly, the tissue/blood values could be considered to have a value of 1.0. Organification (binding of iodide in the thyroid) of iodide to form thyroid hormone precursors accounted for the large NIS-dependent ratio of iodide in the thyroid compared to serum levels.

The volume of distribution (Vd) for T_4, T_3, and TSH were obtained from literature, as shown in Table 4.3, and the volume of the liver was subtracted from the Vd for T_4 and T_3 (Table 4.3). The Vd for T_4 (15.6 L/kg) was obtained from the thyroid hormone model developed by Kohn *et al.* (1996), while the Vd for T_3 of 18.6 L/kg was estimated and used by DiStefano *et al.* (1986) in a simple compartmental model for T_3. A TSH Vd (5.54 L/kg) was used as reported by Connors *et al.* (1984). These authors intravenously dosed female Sprague-Dawley rats (170-220g) with ^{125}I-TSH.

Clearance terms to account for metabolism in the Vd for TSH, T_4, and T_3 were calculated from literature values using the relationship

$$k_{el} = \frac{\ln 2}{t_{1/2}} \qquad [19]$$

where $t_{1/2}$ is the serum half-life of the compound (hr) reported as 0.3667 hr for ^{125}I-TSH (Lemarchand-Beraud and Berthier, 1981), and 6 and 12hr for T_3 and T_4, respectively (Abrams and Larsen, 1973).

Affinity constants, Km(s), for metabolism and active transport of iodide and T_4 were obtained from the literature (Table 4.3). The affinity constant for thyroid iodide transport by the NIS (Km_i) of 3.1×10^4 nmol/L was the average value reported by Gluzman and Niepomniszcze (1983), using radiolabeled iodide and euthyroid human and porcine thyroid cells. The affinity constant for active uptake of T_4 into the liver (Km^{LU}_{T4}) of 650 nmol/L was reported by Blondeau

et al. (1988) using rat hepatocytes. Michaelis-Menten saturable metabolism of T_4 in the liver was described for the phase II glucuronidation and deiodination pathways. The saturable metabolism of T_4, by type I 5'-deiodination, was described assuming that one molecule of T_3 and iodide are formed for each molecule of T_4 metabolized. Phase II metabolism of T_4 (T_4-glucurnoide formation, T_4-G) occurs by a reaction catalyzed by uridine diphosphate glucuronyl transferases (UDPGTs). The Km value for the type I 5'-deiodinase metabolism of T_4 (Km^{DI}_{T4}, 2300 nmol/L) was obtained from Leonard and Visser (1986) from *in vitro* metabolic studies, and Km for the formation of T_4-G (Km^{UGT}_{T4}, 1×10^5 nmol/L) was taken from Visser *et al.* (1993) *in vitro* studies in Wistar rat liver microsomes. For each of these saturable metabolic processes the Km values were derived from the literature and Vmax values were optimized to fit serum kinetics of T_4 that resulted in values that were close to the boundary conditions for fraction of T_4 metabolized to T_3 and fraction of T_4 excreted in feces (Table 4.1).

When sub-models were combined for the BBDR-HPT axis model, endogenous production of TSH was described as shown in Equation 14. The maximal rate of TSH production (k_0^{TSH}) was set to the value (6 nmol/hr) of TSH secretion reported by Connors *et al.* (1984) 14 days after thyroidectomy in adult female Sprague-Dawley rats (Table 4.3).

Parameter optimization. Model parameters not available in literature were first optimized to fit each radiotracer dataset (^{125}I, ^{131}I-T_4, and ^{125}I-T_3), then when the models were linked to form the BBDR-HPT axis model parameters were re-optimized to fit euthyroid, steady-state, iodide sufficient (20 μg iodide/day) conditions. Optimization of model parameters was performed using acslXtreme Parameter Estimation version 2.4.0.11 (Aegis Technologies, Huntsville, Alabama).

Two parameters that were determined from visual fits were kept constant throughout model optimization, including the volume of distribution of iodide (Vdc_i, 0.5 L/kg BW) and the linear rate term for thyroid hormone production (k^{IB}_{TSH}, 5×10^{-7} L^2/nmol/hr). Setting these model parameters to a constant value was determined necessary in order for the optimization to successfully converge upon a maximum log-likelihood function.

A global optimization of model parameters for the BBDR-HPT axis model was performed as well. During this optimization, all estimated model parameters were optimized to steady-state, euthyroid, iodide-sufficient (20 μgI/day) measurements that included serum and liver T_4 and T_3, serum TSH, serum free iodide, and total thyroidal iodide. Boundary conditions (Table 4.1) were also included in the optimization process.

Sensitivity Analysis

An analysis of model parameter sensitivity under steady-state conditions was determined for predicted serum concentrations of T_4, T_3, and TSH and total thyroidal iodide content. Normalized sensitivity coefficients (NSC) were calculated that represent a fractional change in output corresponding to a fractional change in the parameter as described previously (Clewell *et al.*, 2000; Merrill *et al.*, 2003; and Tornero-Velez and Rappaport, 2001). Model parameters were increased by 1% and the model executed using iodide sufficient (20 μg/day) and iodide deficient (1 μg/day) intakes. The NSCs were calculated using the equation

$$\text{Normalized Sensitivity Coefficient} = \frac{(A-B)/B}{(C-D)/D} \qquad [20]$$

where A equals the model response (serum T_4, T_3, TSH, or total thyroid iodide) with a 1% increase in parameter value, B is response with original parameter value, C is parameter value increased by 1%, and D is original parameter value.

Application of BBDR Model to Iodide Deficiency

Studies that provided a time- course for iodide deficiency (ID) induced HPT axis alterations (Riesco *et al.*, 1977; Okamura *et al.*, 1981a; and Okamura *et al.*, 1981b) and one study evaluating recovery from ID (Fukuda *et al.*, 1975) were available in published literature. These papers contained the most complete experimental datasets which included iodide content of the diet, serum T_4, T_3, TSH, thyroid iodide. Many other studies prior to 1970 have been conducted; however, they were considered incomplete for modeling purposes.

Average daily iodide intake was calculated by multiplying food consumption (20 g/day assumed when not reported for the study) by the iodide content in the diet (μg/g). To compare across studies we have reported the intakes as μg iodide per day. The iodide deficiency datasets simulated using our BBDR-HPT axis model are briefly described below.

Riesco *et al.* (1977) provided adult male Holtzman Sprague-Dawley (120g) rats a low iodide diet (LID) resulting in intake of 0.3-0.4 μg I/day for a short term ID study. They determined serum T_4, T_3, TSH and total thyroid iodide after 0, 2, 4, 6, 8, 11, 15, and 26 days of feeding the LID. An average intake of 0.35 μg I/day was used in model simulation.

A longer time course for HPT response of rats maintained on a LID was reported by Okamura *et al.* (1981a). Adult male Simonsen Albino and Holtzman Sprague-Dawley rats were divided by strain and provided a LID of 0.3-0.36 μg I/day (15-18 μg I/kg chow). Average intake of 0.33 μg I/day was used in model simulation. Measurements of serum T_4, T_3, TSH and total thyroid iodide were obtained after 0, 14, 28, 56, and 84 days of feeding the LID. Simonsen Albino rats appeared to display a greater sensitivity or degree of HPT axis response to the LID than the Holtzman Sprague-Dawley rats.

Another study by Okamura and workers (1981b) examined the opposing effects of iodide and nutritional deficiency, by administering two different LID diets (ICN Remington and Teklad Remington). For modeling purposes, the nutritionally deficient ICN Remington diet was not considered. Adult male Holtzman Sprague-Dawley rats (139g) were administered the Teklad Remington (57ng I/g or 1.14μg I/day, nutritionally adequate) diet beginning on day 0 were killed following 19, 33, 63, and 96 days of treatment. Measurements of serum T_4, T_3, TSH, and total thyroid iodide were obtained. However, for some unknown reason the serum TSH concentrations reported in this study were much greater than other studies and no measurements for baseline TSH at day 0 were provided. For these reasons, a fold change was not calculated for comparison to our model nor was the data compared to model simulations.

Fukuda *et al.* (1975) evaluated the recovery of the HPT axis in rats that were placed on an ID diet and then followed with iodide supplementation. Adult male Sprague-Dawley rats (400-500g) were placed on a LID of 0.6 μg I/day (30μg I/kg chow) for seven months, and then to study the recovery phase they were provided iodide supplementation in drinking water. Iodide supplementation provided an additional intake of 2 or 8 μg I/day for four days, yielding an average total intake during the supplementation or refeeding period of 2.6 or 8.6μg I/day. Serial blood samples were taken and measurements of serum T_4 and TSH were obtained 0, 1, 2, 3, 6 and 9 days during supplementation. Due to a wide range in serum TSH concentrations at the onset of iodide supplementation, as well as serum T_4 concentrations reported as non-detectable, the data model simulations and data were expressed as percent of baseline at the onset of the recovery phase.

Results

Radiotracer Sub-Model Development

The unlinked radiotracer sub-models (Figure 4.1) for each component of the BBDR-HPT axis model were optimized and used to predict published kinetic datasets described in previously. The use and development of these models provided support and validation of the model structure to be linked to form the complete BBDR-HPT axis model. The sub-models used physiological parameters shown in Table 4.2 and compound-specific parameters (supplementary data) for each sub-model that were optimized by fitting to their respective kinetic datasets (Figure 4.4).

Iodide. Model simulations of administered radiolabeled iodide (^{125}I) in the adult rat (Yu *et al.*, 2002 and Dr. Yu personal communication) are shown in Figures 4.4A and 4.4B. To obtain optimized parameter values for these kinetic datasets, the concentration of TSH was held at a constant euthyroid value (0.232 nmol/L). The volume of distribution (Vdc_i, 0.5L/kg BW) was visually fit to the serum time-course kinetics of an iv dose of 33 μg ^{125}I/kg reported by Yu *et al.* (2002) (Figure 4.4A). Additionally, the first-order urinary clearance rate ($ClUc_i$) of 0.02 hr^{-1} was set during parameter optimization of thyroid iodide constants in order to provide a fit to the total amount of ^{125}I excreted in urine over a 24-hr period (Figure 4.4A).

The estimated parameter values for Equations 2-4 for iodide processing in the thyroid were simultaneously optimized to total and bound thyroid ^{125}I concentrations obtained (Dr. Yu, personal communication). Specifically, the Vmax of NIS thyroidal iodide uptake ($VmaxTc_i$, 1119.4 nmol/hr) and TSH concentration that produced a half-maximal uptake rate of iodide at the NIS (K^{NIS}_{TSH}, 1.15 nmol/L), maximal rate of iodide incorporation into thyroid hormone precursors ($VmaxBc_i$, 2243.6 nmol/hr), and concentration of free thyroid iodide (Kb_i, 221.1 nmol/L) that results in half-maximal $VmaxBc_i$ were optimized. The permeability area cross-

product for bidirectional diffusion of iodide into and out of the thyroid gland ($PATc_i$) was insensitive to predicting the total and bound thyroidal iodide stores, thus the value of 0.0001 L/hr reported by Merrill *et al.* (2003) was retained. The simple iodide model structure and optimized parameters provide model simulations of the Yu *et al.* (2002 and personal communication) ^{125}I iv dosing study that adequately predicted total serum ^{125}I concentration (Figure 4.4A), cumulative amount of ^{125}I excreted in urine (Figure 4.4A), and the bound and total thyroidal ^{125}I concentrations (Figure 4.4B).

3,5,3'-Triiodothyronine (T_3). The radiolabeled T_3 (^{125}I-T_3) sub-model structure was developed and first optimized using ^{125}I-T_3 kinetics following an iv dose of 0.83ng (DiStefano *et al.,* 1993). The uptake of ^{125}I-T_3 into the liver after iv administration of 0.83 ng of ^{125}I-T_3 (DiStefano *et al.*, 1993) in adult male Sprague-Dawley rats could not be described assuming blood-flow limited kinetics (simulations not shown). Thus, a first order active uptake term was implemented along with simple bidirectional diffusion to describe the ^{125}I-T_3 liver kinetics. The first order uptake rate (k^{LU}_{T3}, 1.5 hr^{-1}) and diffusion constant ($PALc_{T3}$, 0.0683 L/hr) were simultaneously optimized to the ^{125}I-T_3 liver kinetic dataset of DiStefano *et al.* (1993) (Figure 4.4C). In addition, first order rate of T_3 metabolism in the liver ($kmetLc_{T3}$, 1.15 nmol/hr) was optimized to the same dataset and fraction of this metabolism of T_3 (FT3feces, 0.30 unitless) resulting in an estimated fecal elimination using 30% of ^{125}I-T_3 dose excreted in feces as a guideline (Table 4.1). The rate of clearance of ^{125}I-T_3 from the serum was slightly under predicted, while the fitted uptake and clearance in the liver was adequately characterized by the sub-model simulation (Figure 4.4C).

Thyroxine (T_4). T_4 model parameters not available in literature ($Vmaxc^{LU}_{T4}$, $Vmaxc^{UGT}_{T4}$, $Vmaxc^{DI}_{T4}$, and $PALc_{T4}$) were first estimated by simultaneous optimization of these

parameter values with ^{131}I-T_4 kinetic data reported in the adult female Wistar rat by Schroder van der Elst *et al.* (1997) using Equations 9-13. Rats were administered an iv dose of 1.7 ng ^{131}I-T_4 and the distribution was characterized up to 6 hrs after dosing, in blood, liver, and other tissues. The Vmax values for liver uptake ($Vmaxc^{LU}_{T4}$, 10552 nmol/hr), type I 5'-deiodination ($Vmaxc^{DI}_{T4}$, 15.1 nmol/hr), T_4-G formation ($Vmax^{UGT}_{T4}$, 1080.32 nmol/hr), and the permeability area cross-product for diffusion of T_4 into the liver ($PALc_{T4}$, 0.0488 L/hr) were obtained by optimization of serum and liver T_4 kinetics after an iv dose. In addition, these metabolic Vmax ($Vmaxc^{DI}_{T4}$ and $Vmax^{UGT}_{T4}$) parameters were optimized such that the percent of ^{131}I-T_4 metabolized was similar to reported values in the literature (Table 4.1). In this case, the sub-model predicted percent of metabolized ^{131}I-T_4 as 40% for T_4 conversion to T_3 and 24% for T_4 excreted in feces as T_4-G. The T_4 sub-model reproduced the serum and liver ^{131}I-T_4 time-course with slight over prediction of serum and liver concentrations reported as percent dose (Figure 4.4D).

Thyroid Stimulating Hormone (TSH). Spira *et al.* (1979) administered 5ng ^{125}I-TSH via tail vein injection to adult male Hebrew University rats 5 days post thyroidectomy and determined serum concentrations 0.033 to 2hr post dose. This time course was simulated using the literature derived Vd_{TSH} (Connors *et al*., 1984) value of 5.54 L/kg and an elimination constant, $kelc_{TSH}$ (Lemarchand-Beraud and Berthier, 1986) equal to 1.8899 hr^{-1}. The sub-model for ^{125}I-TSH was able to adequately predict serum ^{125}I-TSH up to 2hr post dose (Figure 4.4E).

Dietary Iodide BBDR-HPT Axis Model – Model Calibration and Simulation of Steady-State Euthyroid, Iodide Sufficient Conditions. Many toxicology studies using rats in the laboratory are conducted in iodide sufficient conditions. Common laboratory diets contain 0.8 mg/kg iodide (e.g. LabDiet 5001 and 5008) and thus iodide intake averages 15-20 μg iodide per

day for the normal lab rat assuming 20-25g chow intake per day. Thus, the iodide sufficient model compound-specific parameter optimizations (Table 4.3) and simulations (Figure 4.5) were determined for the common intake for laboratory rats of 20μg I/day.

When the radiotracer sub-models were linked to create the BBDR-HPT axis model by including the production of thyroid hormones (Equations 15-18), metabolism of thyroid hormones, recycling of freed iodide, and the T_4/TSH negative feedback loop (Equation 14), as shown in Figure 4.2, an adequate description of the euthyroid, steady-state iodide sufficient (20μg I/day) condition was not readily achieved. For example, predictions of serum iodide were too low, liver concentrations of T_3 and T_4 were too high, and serum T_4 concentrations were too high, which resulted in under-predicted serum TSH concentrations (simulations not shown). Therefore, the sub-model parameter values obtained to predict serum clearance kinetics of trace amounts of radiolabeled iodide, T_4, T_3, and TSH (supplemental data) were adjusted. This was not completely unexpected for describing endogenous masses of thyroid hormones, dietary iodide, and TSH. Thus, a global optimization of model parameters for the BBDR-HPT axis model was performed and final model parameters are shown in Table 4.3.

Using the BBDR-HPT axis model, the optimized urinary clearance constant ($Cluc_i$) was decreased to 0.0046 hr^{-1} from 0.02hr^{-1} to predict the free plasma iodide levels (Figure 4.5A) reported by Eng *et al.* (1999). The maximum rate of thyroidal uptake of iodide by the NIS ($VmaxTc_I$) was increased to a value of 5738.267 nmol/hr compared to a radiotracer derived value of 1119.4 nmol/hr. While the optimized maximum rate of incorporation of iodide into thyroid stores or binding as thyroid hormone precursors ($VmaxBc_i$) was decreased from a radiotracer derived value of 2243.6 to 1005.9 nmol/hr. Figure 4.5A shows the simulated and measured total amount of iodide in the thyroid (McLanahan *et al.*, 2007).

The maximum rate of active uptake of T_4 into the liver ($Vmaxc^{LU}_{T4}$) decreased in the global optimization of the BBDR-HPT axis model to a value of 4384.73 nmol/hr compared to a radiotracer value of 10552 nmol/hr. The maximum rate of T_4 glucuronidation ($Vmaxc^{UGT}_{T4}$) increased from a radiotracer value of 1080.32 to 3435.89 nmol/hr. The calibrated steady-state euthyroid, iodide sufficient model predictions for a 320g rat are shown in Figure 4.5. Total thyroid and free serum iodide (Figure 4.5A), serum TSH (Figure 4.5B), serum and liver T_4 (Figure 4.5C), and serum and liver T_3 (Figure 4.5D) model predictions fall within the range for normal rats reported in literature.

Iodide Deficiency HPT Axis Simulations

Using the BBDR-HPT axis model parameter values, globally optimized for euthyroid iodide sufficient steady-state conditions, the ability of the model to predict temporal changes in serum thyroid hormones (T_4 and T_3), TSH, and total thyroidal iodide was tested for iodide deficient conditions.

HPT axis disturbances from an iodide deficient diet of 0.35 μg I/day for 26 days (Riesco *et al.*, 1977) is depicted in Figure 4.6 for adult male Holtzman-Sprague Dawley (HSD) rats. Serum T_4 concentrations gradually decreased in parallel fashion with thyroidal iodide stores, while only a slight change occurred in serum T_3 concentrations. Serum TSH concentrations increased over 10-fold during the study period. After 15 days of administration of the LID, the thyroidal iodide stores were severely depleted. The BBDR-HPT axis model predictions of serum thyroid hormones were in agreement with observed values. The predicted thyroidal iodide stores were slightly underpredicted initially and near the end of the study. Serum TSH increases were predicted during the first 11 days and then moderately over predicted by day 15. In severe iodide deficient conditions, when thyroidal iodide stores were predicted to be below 1 μg, oscillations in

serum TSH and T_4 and thyroidal iodide occurred because of assumptions about dietary intake of iodide.

Next, the capability of the BBDR-HPT axis model to predict changes during administration of 0.33 μg I/day administered for 84 days to adult male Simonsen Albino (SA) and HSD rats (Okamura *et al.*, 1981a) was tested (Figure 4.7). The SA strain (Figure 4.7A) exhibited a greater sensitivity, shown by the rapid increase in TSH compared to the HSD strain (Figure 4.7B). The BBDR-HPT axis model predicted the change in TSH better for the SA rats than the HSD rats. Serum T_3 concentrations were predicted to be lower than suggested by the data.

BBDR-HPT axis model simulations for a LID of 1.14 μg I/day administered to adult male HSD (Okamura *et al.*, 1981b) are depicted in Figure 4.8. The initial decrease in thyroidal iodide stores and the apparent recovery after 60 days suggests adaptive response(s), such as the negative feedback loop. The BBDR-HPT axis model predictions also suggest this as evidenced by an increase in predicted thyroidal iodide stores and little decline in serum thyroid hormones after 25 days. At a dietary intake of 1 μg/day, this strain of adult rat has some ability to compensate for low iodide intake. Predictions of serum T_3 were slightly under-predicted.

Finally, the BBDR-HPT axis model was used to simulate recovery of the HPT axis in rats rendered iodide deficient for seven months with an average daily iodide intake of 0.6 μg/day (Figure 4.9). On Day 0 of the recovery phase, the rats were supplemented with iodide in drinking water to provide total intake of either 2.6 or 8.6 μg I/day. Serial blood samples were obtained for measurement of serum T_4 and TSH (Fukuda *et al.*, 1975) for 9 days of recovery. The BBDR-HPT axis model slightly over-predicted day 1 increases in serum T_4 following iodide

supplementation for both doses, while the remaining predicted serum T_4 and TSH concentrations agreed with observations.

Sensitivity Analysis

The sensitivity analysis of the BBDR-HPT axis model was carried out assuming steady-state serum concentrations of T_4, T_3, and TSH, and total thyroid iodide content for an iodide sufficient (IS) intake of 20 μg I/day and iodide deficient (ID) intake of 1 μg I/day. None of the parameters are associated with normalized sensitivity coefficients (NSCs) greater than 1.0, suggesting that there is minimal amplification of error from the inputs to the model outputs (Clewell *et al.*, 2000). Figure 4.10 shows the NSCs for the model parameters that resulted in an NSC of 0.90 or greater for at least one model output (serum T_4, T_3 and TSH or total thyroidal iodide). Total amount of thyroidal iodide predictions were most affected by a 1% change in the volume of the thyroid (NSC = 0.99) under IS conditions and a NSC of 0.98 under ID conditions. A one percent change in the thyroid hormone production constant (k^{IB}_{TSH}) also reflected similar sensitivity of the total amount of iodide in the thyroid with NSCs of -0.95 and -0.96 under IS and ID conditions, respectively.

Discussion

The intent was to develop a first generation biologically based dose-response (BBDR) model for the hypothalamic-pituitary-thyroid (HPT) axis in the adult rat to describe the negative feedback loop parsimoniously using serum thyroxine (T_4) and thyroid stimulating hormone (TSH) levels to control the TSH mediated thyroidal uptake of dietary iodide, and the production and secretion of thyroid hormones. The use of 'macroscopic' kinetic properties of the HPT axis and simple model parameters that represent composite and complex 'microscopic' biochemical

reactions appear to successfully describe many datasets from several laboratories. We first described the HPT axis under steady-state, euthyroid conditions using simple model structures and equations. The dominant negative feedback control of T_4 on TSH was described (Equation 14), along with the stimulation of TSH on thyroidal iodide uptake (Equations 1-2) and subsequent thyroid hormone production (Equation 15) using simple and empirical relationships of critical events of the HPT axis. As mentioned in results, a few of the BBDR-HPT axis predictions deviated from observations for rats fed low iodine diets (LID). It is unclear if strain differences or assay methods played a role in the reported literature results.

Adult rats excrete approximately 95% of a daily iodide sufficient intake (normal laboratory intake of 20 μg I/day), according to our model simulations. Urinary iodide levels arise from metabolism of thyroid hormones, as well as excess iodide provided in the diet. The normal adult rat stores 10-15 μg iodide (McLanahan *et al.*, 2007) and model predictions estimate that rats utilize about 1.4 μg I/day in thyroid hormone production under normal, euthyroid conditions. Furthermore, under iodide sufficient conditions our model predicts that 85% of the daily T_3 production is derived from T_4 metabolism, with the remaining (15%) produced in the thyroid. This is in agreement with others who suggest that at least 80% of the daily T_3 production occurs as a result of T_4 metabolism in a euthyroid system (Burger, 1986).

Many current studies that employ updated and revised thyroid hormone assay techniques to examine HPT axis effects resulting from iodide deficiency only report data for single time points, and do not evaluate the time component of HPT axis perturbations (Pedraza *et al.*, 2006; Hotz *et al.*, 1997). Only a handful of kinetic studies examining multiple indices of thyroid function in relationship to iodide intake have been reported (Okamura *et al.*, 1981a, 1981b;

Riesco *et al.*, 1976, 1977). Our model was developed for *iodine sufficient* (euthyroid) and *iodine deficient* (hypothyroid) conditions, both which were effectively described.

Using optimized model parameters for the euthyroid, iodide sufficient model, the BBDR-HPT axis model was tested for its ability to predict changes in serum T_4, T_3, TSH, and total thyroid iodide during administration of LIDs. The model predicted the temporal response for decreases in serum T_4 and increases in serum TSH resulting from the lack of available iodide for thyroid hormone production in an acceptable manner with some exceptions. Across all studies, the predictions of serum T_3 may be less consistent with the experimental data compared to other predicted endpoints. Interestingly, the percent of daily T_3 production in the thyroid increases significantly under iodide deficient conditions (Abrams and Larsen, 1973 and Greer *et al.*, 1968), which is in agreement with our model. The percent of overall T_3 production in the thyroid is predicted to increase from 15% (iodide sufficient 20 μg I/day intake) to 25% as iodide intake rate decreases to 1μg/day and 45% at an iodide intake rate of 0.35 μg/day.

Model predictions during steady-state iodide deficiency of 1 μg I/day suggest that the percent of daily iodide intake excreted in urine decreases to about 65% and only 0.67 μg of iodide is utilized in daily thyroid hormone production. Thyroid iodide stores are severely depleted to about 20% (2.8 μg) of euthyroid, iodide sufficient values, resulting in a decrease of over 50% in serum T_4 concentrations.

Ultimately, the BBDR-HPT axis model was used to generate a dose-response plot for iodide intake and resulting serum T_4 and TSH concentrations (Figure 4.11). Using this model we confirm a sharp decline in serum T_4 such that the TSH stimulation of thyroid axis is unable to compensate for the lack of available iodide for thyroid hormone production. Others have

reported that laboratory rats require an iodide intake greater than 2 μg I/day to maintain euthyroid status (Pedraza *et al.*, 2006).

Challenges and Limitations

As with every mathematical model, the utility and limitations of this BBDR-HPT axis model require discussion. Discovering details that pertain to how the HPT axis works is an active area of research. For example, our model does not describe events at the molecular level, or all metabolites of thyroid hormones (reverse T_3, T_2, T_1, or thyroid hormone conjugates other than T_4-glucuronide). Attempting to describe detailed biological process in a modeling framework would require focused laboratory studies and, in our opinion, widespread use of improved analytical tools for measuring thyroid hormones and TSH. Our model does not include physiological changes that occur during a long-term iodide deficient condition, resulting in a hypothyroid disease state. Structural changes in the thyroid (Colzani *et al.*, 1999), increases in thyroid blood flow (Michalkiewicz *et al.*, 1989), and altered biological activity of thyroid hormone metabolizing enzymes (Janssen *et al.*, 1994; Pedraza *et al.*, 2006; Obregon, *et al.*, 2005) are examples of HPT axis alterations that are not accounted for in this model and may have affected the ability of our model to reproduce serum T_3 data.

The reported literature for the adult rat and HPT axis function varies dramatically. For example, reported TSH values for adult male Sprague-Dawley rats range from 4.6 ± 0.49 ng/mL to 8.73 ± 0.81 ng/mL (McLanahan *et al.*, 2007), approximately 15 to 20 ng/mL (Siglin *et al.*, 2000), 327 ± 174 ng/mL (Okamura *et al.*, 1981a), to a high of 440 ± 220 ng/mL (Lemarchand-Beraud and Berthier, 1981). Several factors may contribute to this variability including, time of sampling, weight of animal, and radioimmunoassay (RIA) analytical method and standards

employed. Thus, in reporting our model results we reported TSH as fold change to normalize and compare model simulations with more datasets.

Most of the ID studies occurred prior to 1990 and many methods for analysis of thyroid hormones, TSH, and iodide have evolved since their publication. However, the biggest concern when analyzing data from ID studies is the actual iodine concentration in the diet and the amount that the rat consumes. This amount can vary significantly between batches of rodent chow and can produce varying results as demonstrated by Naeije *et al.* (1978). Unfortunately the actual iodine concentration in rodent chow is not always measured by laboratories conducting ID studies, but rather the value reported by the manufacturer is included in the manuscript.

Other challenges were encountered during model development, including the inability of several parameters, which were optimized in the radiotracer sub-models to fit data points following iv doses of each compound, to reproduce steady-state, euthyroid iodide sufficient datasets. When the model parameters were re-optimized in the dietary iodide BBDR-HPT axis model, five parameters ($Cluc_i$, $VmaxTc_i$, $VmaxBc_i$, $Vmaxc^{UGT}{}_{T4}$, and $Vmaxc^{LU}{}_{T4}$) differed from radiotracer parameters by more than one fold. This suggests that radiotracer kinetics for the HPT axis may not adequately represent mass transfer kinetics of the endogenous substances.

Future Directions

The development of this model was initiated with the ultimate goal of integrating it with physiologically based pharmacokinetic (PBPK) models for thyroid toxicants. Thyroid toxicants are defined as compounds which alter serum thyroid hormone and TSH concentrations (Zoeller and Tan, 2007); and the BBDR-HPT axis model presented here is able to predict serum changes under iodine deficient conditions. In order to better understand the thyroid axis and temporal responses mathematically, it was necessary to first test the model under these iodine deficient

conditions. Some environmentally relevant compounds, such as perchlorate and thiocyanate, inhibit NIS thyroid iodide uptake and may result in conditions that 'mimic' iodide deficiency, a decline in available iodide for thyroid hormone synthesis (Wolff, 1998). As the field evolves and more data become available, this first-generation BBDR-HPT axis model can be expanded to contain other tissues of interest (e.g. brain and heart) and other thyroid axis compensatory mechanisms (e.g. changes in 5'-deiodinase activity). This model can also be expanded to relate dose-response and HPT axis status to frank toxicity or neurodevelopmental effects. However, the dietary iodide BBDR-HPT axis model presented here, which integrates a variety of physiologic processes, will be used to predict complex, non-linear dose responses resulting from exposure to thyroid toxic chemicals (e.g. PCB126 and perchlorate from McLanahan *et al.* (2007)), alone and in combination.

Funding

United States Environmental Protection Agency Science to Achieve Results research grant (RD83213401-0); United States Environmental Protection Agency Science to Achieve Results Fellowship (FP-91679301-0 to E.D.M).

Acknowledgments

The authors extend special thanks to Dr. Kyung O. Yu for providing experimental datasets for use in radioiodide model development. Sincere thanks to Dr. Jerry L. Campbell, Jr. for model review. The views expressed in this manuscript are those of the authors and do not represent official opinions of the United States Environmental Protection Agency. Mention of trade names or commercial products does not constitute endorsement or recommendation for use.

References

Abrams, G.M. and Larsen, P.R. (1973). Triiodothyronine and Thyroxine in the Serum and Thyroid Gland of Iodine-Deficient Rats. *J. Clin. Invest.* **52,** 2522-2531.

Barton, H.A. and Andersen, M.E. (1998). A Model for Pharmacokinetics and Physiological Feedback among Hormones of the Testicular-Pituitary Axis in Adult Male Rats: A Framework for Evaluating Effects of Endocrine Active Compounds. *Toxicol. Sci.* **45,** 174-187.

Blondeau, J., Osty, J., and Fracon, J. (1988). Characterization of the Thyroid Hormone Transport System of Isolated Hepatocytes. *J. Biol. Chem.* **263,** 2685-2692.

Brown, R., Delp, M., Lindstedt, S., Rhombert, L., and Belies, R. (1997). Physiological Parameter Values for Physiologically Based Pharmacokinetic Models. *Toxicol. Ind. Health.* **13,** 407-484.

Brucker-Davis, F. (1998). Effects of environmental synthetic chemicals on thyroid function. *Thyroid.* **8**, 827-856.

Burger, A. (1986). Nondeiodinative Pathways of Thyroid Hormone Metabolism. In Thyroid Hormone Metabolism (G. Hennemann, Ed.), pp 255-276. Marcel Dekker, Inc., New York.

Carrasco, N. (1993). Iodide transport in the thyroid gland. *Biochimica et Biophysica Acta*. **1154,** 65-82.

Clewell III, H.J., Gentry, P.R., Covington, T.R., and Gearhart, J.M. (2000). Development of a Physiologically Based Pharmacokinetic Model of Trichloroethylene and Its Metabolites for Use in Risk Assessment. *Environ. Health Perspect.* **108(Suppl),** 283-305.

Clewell, R.A., Merrill, E.A., Yu, K.O., Mahle, D.A., Sterner, T.R., Fisher, J.W., and Gearhart, J. M. (2003a). Predicting Neonatal Perchlorate Dose and Inhibition of Iodide Uptake in the Rat during Lactation Using Physiologically-Based Pharmacokinetic Modeling. *Toxicol. Sci.* **74,** 416-436.

Clewell, R.A., Merrill, E.A., Yu, K.O., Mahle, D.A., Sterner, T.R., Mattie, D., Robinson, P., and Fisher, J.W. (2003b). Predicting Fetal Perchlorate Dose and Inhibition of Iodide Kinetics during Gestation: A Physiologically-Based Pharmacokinetic Analysis of Perchlorate and Iodide Kinetics in the Rat. *Toxicol. Sci.* **73,** 235-255.

Colzani, R.M., Alex, S., Fang, S-L., Stone, S., and Braverman, L.E. (1999). Effects of iodine repletion on thyroid morphology in iodine and/or selenium deficient rat term fetuses, pups, and mothers. *Biochimie*. **81,** 485-491.

Connors J.M., DeVito, W.J, and Hedge, G.A. (1984). The Effects of the Duration of Severe Hypothyroidism and Aging on the Metabolic Clearance Rate of Thyrotropin (TSH) and the Pituitary TSH Response to TSH-Releasing Hormone. *Endocrinol.* **114,** 1930-1937.

Degroot, L.J. and Niepomiszcze, H. (1977). Biosynthesis of Thyroid Hormone: Basic and Clinical Aspects. *Metabolism.* **26,** 665-718.

Delange, F. (2001). Iodine deficiency as a cause of brain damage. *Postgrad. Med. J.* **77,** 217-220.

DeVito, M., Biegel, L., Brouwer, A., Brown, S., Brucker-Davis, F., Cheek, A. O., Christensen, R., Colborn, T., Cooke, P., Crissman, J., Crofton, K., Doerge, D., Gray, E., Hauser, P., Hurley, P., Kohn, M., Lazar, J., McMaster, S., McClain, M., McConnell, E., Meier, C., Miller, R., Tietge, J., and Tyl, R. (1999). Screening methods for thyroid hormone disruptors. *Environ Health Perspect*. **107**, 407-415.

Dietrich, J.W., Tesche, A., Pickardt, C.R., and Mitzdorf, U. (2002). Fractal Properties of the Thyrotropic Feedback Control: Implications of a Nonlinear Model Compared with Empirical Data. In: *Cybernetics and Systems 2002*. R. Trappl (Hrsg). Vienna.

DiStefano III, J.J. (1986). Modeling Approaches and Models of the Distribution and Disposal of Thyroid Hormones. In Thyroid Hormone Metabolism (G. Hennemann, Ed.), pp 39-76. Marcel Dekker, Inc., New York.

DiStefano III, J.J. and Feng, D.(1988). Comparative Aspects of the Distribution, Metabolism, and Excretion of Six Iodothyronines in the Rat. *Endocrinol.* **123,** 2514-2525.

DiStefano III, J.J., and Sapin, V. (1987). Fecal and Urinary Excretion of Six Iodothyronines in the Rat. *Endocrinol.* **121,** 1742-1750.

DiStefano III, J.J., Malone, T., and Jang, M. (1982). Comprehensive Kinetics of Thyroxine Distribution and Metabolism in Blood and Tissue Pools of the Rat from only Six Blood Samples: Dominance of Large, Slowly Exchanging Tissue Pools. *Endocrinol.* **111,** 108-117.

DiStefano III, J.J., Nguyen, T.T., and Yen, Y. (1993). Transfer Kinetics of 3,5,3'-Triiodothyronine and Thyroxine from Rat Blood to Large and Small Intestines, Liver, and Kidneys *in Vivo*. *Endocrinol*. **132,** 1735-1744.

Eng, P.H.K., Cardona, G.R., Fang, S., Previti, M., Alex, S., Carrasco, N., Chin, W.W., and Braverman, L.E. (1999). Escape from the Acute Wolff-Chaikoff Effect Is Associated with a Decrease in Thyroid Sodium/Iodide Symporter Messenger Ribonucleic Acid and Protein. *Endocrinol.* **140,** 3404-3410.

Escobar-Morreale, H.F., Escobar del Rey, F., Obregon, M.J., and Morreale de Escobar, G. (1996). Only the Combined Treatment with Thyroxine and Triiodothyronine Ensures Euthyroidism in All Tissues of the Thyroidectomized Rat. *Endocrinol.* **137,** 2490-2502.

Fukuda, H., Yasuda, N., Greer, M.A., Kutas, M., and Greer, S.E. (1975). Changes in Plasma Thyroxine, Triiodothyronine, and TSH During Adaptation to Iodine Deficiency in the Rat. *Endocrinol.* **97,** 307-314.

Gluzman, B.E. and Niepomniszcze, H. (1983). Kinetics of iodide trapping mechanism in normal and pathological human thyroid slices. *Acta Endocrinol.* **103,** 34-39.

Greer, M.A., Grimm, Y., and Studer, H. (1968). Qualitative Changes in the Secretion of Thyroid Hormones Induced by Iodine Deficiency. *Endocrinol.* **83,** 1193-1198.

Hamann, I., Seidlova-Wuttke, D., Wuttke, W., and Kohrle, J. (2006). Effects of isoflavonoids and other plant-derived compounds on the hypothalamus-pituitary-thyroid hormone axis. *Maturitas*. **55S,** S14-S25.

Hotz, C.S., Fitzpatrick, D.W., Trick, K.D., and L'Abbe, M.R. (1997). Dietary Iodine and Selenium Interact To Affect Thyroid Hormone Metabolism of Rats. *J. Nutr.* **127,** 1214-1218.

Janssen, K., van der Heide, D., Visser, T.J., Kaptein, E., and Beynen, A.C. (1994). Thyroid Function and Deiodinase Activities in Rats with Marginal Iodine Deficiency. *Biol. Trace. Elem. Res.* **40,** 237-246.

Kogai, T., Curcio, F., Hyman, S., Cornford, E.M., Brent, G.A., and Hershman, J.M. (2000). Induction of follicle formation in long-term cultured normal human thyroid cells treated with thyrotropin stimulates iodide uptake but not sodium/iodide symporter messenger RNA and protein expression. *J. Endocrinol.* **167,** 125-135.

Kogai, T., Taki, K., and Brent, G.A. (2006). Enhancement of sodium/iodide symporter expression in thyroid and breast cancer cells. *Endocrine-Related Cancer.* **13,** 797-826.

Kohn M.C., Sewall, C.H., Lucier, G.W., and Portier, C.J. (1996). A Mechanistic Model of Effects of Dioxin on Thyroid Hormones in the Rat. *Toxicol. Appl. Pharmacol.* **165,** 29-48.

Krenning, E., Docter, R., Bernard, B., Visser, T., and Hennemann, G. (1981). Characteristics of Active Transport of Thyroid Hormone into Rat Hepatocytes. *Biochimica et Biophysica Acta.* **676,** 314-320.

Lemarchand-Beraud T., and Berthier, C. (1981). Effects of graded doses of triiodothyronine on TSH synthesis and secretion rates in hypothyroid rats. *Acta. Endocrinol.* **97,** 74-84.

Leonard, J.L. and Visser, T.J. (1986). Biochemistry of Deiodination. In Thyroid Hormone Metabolism (G. Hennemann, Ed.), pp 189-229. Marcel Dekker, Inc., New York.

Levy, O., Dai, G., Riedel, C., Ginter, C.S., Paul, E.M., Lebowitz, A.N., and Carrasco, N. (1997). Characterization of the Thyroid Na+/I- Symporter with an Anti-COOH Terminus Antibody. *Proc. Natl. Acad. Sci. USA.* **94,** 5568-5573.

Li, G., Liu, B., and Liu, Y. (1995). A dynamical model of the pulsatile secretion of the hypothalamic-pituitary-thyroid axis. *Biosystems.* **35,** 83-92.

Malendowicz, L.K, and Bednarek, J. (1986). Sex Dimorphism in the Thyroid Gland IV. Cytologic Aspects of Sex Dimorphism in the Rat Thyroid Gland. *Acta. Anat.* **127,** 115-118.

McLanahan, E.D., Campbell Jr., J.L., Ferguson, D.C., Harmon, B., Hedge, J.M., Crofton, K.M., Mattie, D.R., Braverman, L., Keys, D.A., Mumtaz, M., and Fisher, J.W. (2007). Low-

Dose Effects of Ammonium Perchlorate on the Hypothalamic-Pituitary-Thyroid (HPT) Axis of Adult Male Rats Pretreated with PCB126. *Toxicol. Sci.* **97,** 308-317.

Mendel, C.M., Cavalieri, R.R., Kohrle, J. (1992). Thyroxine (T_4) Transport and Distribution in Rats Treated with EMD 21388, a Synthetic Flavonoid That Displaces T_4 from Transthyretin. *Endocrinol.* **130,** 1525-1532.

Merrill, E.A., Clewell, R.A., Gearhart, J.M., Robinson, P.J., Sterner, T.R., Yu, K.O, Mattie, D.R., and Fisher, J.W. (2003). PBPK Predictions of Perchlorate Distribution and Its Effect on Thyroid Uptake of Radioiodide in the Male Rat. *Toxicol. Sci.* **73,** 256-269.

Merrill, E.A., Clewell, R.A., Sterner, T.R., and Fisher, J.W. (2005). PBPK Model for Radioactive Iodide and Perchlorate Kinetics and Perchlorate-Induced Inhibition of Iodide Uptake in Humans. *Toxicol. Sci.* **83,** 25-43.

Michalkiewicz, M., Huffman, L.J., Connors, J.M., and Hedge, G.A. (1989). Alterations in Thyroid Blood Flow Induced by Varying Levels of Iodine Intake in the Rat. *Endocrinol.* **125,** 54-60.

Mirfazaelian, A., Kim, K., Lee, S., Kim, H.J., Bruckner, J.V., and Fisher J.W. (2007). Organ Growth Functions in Maturing Male Sprague-Dawley Rats. *J. Toxicol. Environ. Health A.* **70,** 429-438.

Morreale de Escobar, G., Calvo, R., Escobar del Rey, F., and Obregon, M.J. (1994). Thyroid Hormones in Tissues from Fetal an Adult Rats. *Endocrinol.***134,** 2410-2415.

Mukhopadhyay, B., and Bhattacharyya, R. (2006). A Mathematical Model Describing the Thyroid-Pituitary Axis with Time Delays in Hormone Transportation. *Appl. Math.* **51,** 549-564.

Naeije, R., Vanhaelst, L., and Golstein, J. (1978). Pituitary-Thyroid Axis During Short Term, Mild and Severe, Iodine Depletion in the Rat. *Horm. Metab. Res.* **10,** 521-525.

Nguyen, T.T., DiStefano III, J.J., Yamada, H., and Yen, Y.M. (1993). Steady state organ distribution and metabolism of thyroxine and 3,5,3'-triiodothyronine in intestines, liver, kidneys, blood, and residual carcass of the rat in vivo. *Endocrinol.* **133,** 2973-2983.

Obregon, M., Escobar del Rey, F., and Morreale de Escobar, G. (2005). The Effects of Iodine Deficiency on Thyroid Hormone Deiodination. *Thyroid.* **15,** 917-929.

Okamura, K., Taurog, A., and Krulich, L. (1981a). Strain Differences among Rats in Response to Remington Iodine-Deficient Diets. *Endocrinol.* **109,** 458-463.

Okamura, K., Taurog, A., and Krulich, L. (1981b). Elevation of Serum 3,5,3'-Triiodothyronine and Thyroxine Levels in Rats Fed Remington Diets; Opposing Effects of Nutritional Deficiency and Iodine Deficiency. *Endocrinol*. **108,** 1247-1256.

Pedraza, P.E., Obregon, M., Escobar-Morreale, H.F., Escobar del Rey, F., and Morreale de Escobar, G. (2006). Mechanisms of Adaptation to Iodine Deficiency in Rats: Thyroid Status Is Tissue Specific. Its Relevance for Man. *Endocrinol.* **147,** 2098-2108.

Rasgon, N.L., Pumphrey, L., Prolo, P., Elman, S., Negrao, A.B., Licinio, J., and Garfinkel, A. (2003). Emergent Oscillations in Mathematical Model of the Human Menstrual Cycle. *CNS Spectr.* **8,** 805-814.

Riedel, C., Levy, O., and Carrasco, N. (2001). Post-transcriptional Regulation of the Sodium/Iodide Symporter by Thyrotropin. *J. Biol. Chem.* **276,** 21458-21463.

Riesco, G., Taurog, A., and Larsen, P.R. (1976). Variations in the Response of the Thyroid Gland of the Rat to Different Low-Iodine Diets: Correlation with Iodine Content of Diet. *Endocrinol.* **99,** 270-280.

Riesco, G., Taurog, A., Larsen, P.R., and Krulich, L. (1977). Acute and Chronic Responses to Iodine Deficiency in Rats. *Endocrinol.* **100,** 303-313.

Rutgers, M., Pigmans, I.G., Bonthuis, F., Docter, R., and Visser, T.J. (1989). Effects of propylthiouracil on the biliary clearance of thyroxine (T_4) in rats: decreased excretion of 3,5,3'-triiodothyronine glucuronide and increased excretion of 3,3',5'-triiodothyronine glucuronide and T_4 sulfate. *Endocrinol.* **125,** 2175-2186.

Schlosser, P.M. and Selgrade, J.F. (2000). A Model of Gonadotropin Regulation during the Menstrual Cycle in Women: Qualitative Features. *Environ. Health Perspect.* **108,** 873-881.

Schroder-van der Elst, J.P., van der Heide, D., Rokos, H., Kohrle, J., and Morreale de Escobar, G. (1997). Different Tissue Distribution, Elimination, and Kinetics of Thyroxine and Its Conformational Analog, the Synthetic Flavonoid EMD 49209 in the Rat. *Endocrinol.* **138,** 79-84.

Sherwin, J.R., and Tong, W. (1974). The Actions of Iodide and TSH on Thyroid Cells Showing a Dual Control System for the Iodide Pump. *Endocrinol.* **94,** 1465-1474.

Siglin, J.C., Mattie, D.R., Dodd, D.E., Hildebrandt, P.K., and Baker, W.H. (2000). A 90-Day Drinking Water Toxicity Study in Rats of the Environmental Contaminant Ammonium Perchlorate. *Toxicol. Sci.* **57,** 61-74.

Spira, O., Birkenfeld, A., Gross, J., and Gordon, A. (1979). TSH Synthesis and Release in the Thyroidectomized Rat: a) Effect of Short- and Long-Term Hypothyroidism. *Acta Endocrinol.* **92,** 489-501.

Tornero-Velez, R. and Rappaport, S.M. (2001). Physiological Modeling of the Relative Contributions of Styrene-7,9-oxide Derived from Direct Inhalation and from Styrene Metabolism to the Systemic Dose in Humans. *Toxicol. Sci.* **64,** 151-161.

Verger, P., Aurengo, A., Geoffroy, B., and Le Guen, B. (2001). Iodine Kinetics and Effectiveness of Stable Iodine Prophylaxis After Intake of Radioactive Iodine: A Review. *Thyroid.* **11,** 353-360.

Visser, T.J., Kaptein, E., van Toor, H., van Raaij, J.A.G.M., van den Berg, K.J., Joe, C.T.T., van Engelen, J.G.M., and Brouwer, A. (1993). Glucuronidation of Thyroid Hormone in Rat Liver: Effects of *in Vivo* Treatment with Microsomal Enzyme Inducers and *in Vitro* Assay Conditions. *Endocrinol.* **133,** 2177-2186.

Visser, T.J., van Buuren, J.C.J., Rutgers, M., Rooda, S.J.E., and de Herder, W.W. (1990). The Role of Sulfation in Thyroid Hormone Metabolism. *Trends Endorcinol. Metab.* **1,** 211-218.

Wolff, J. (1998). Perchlorate and the Thyroid Gland. *Pharmacol. Rev.* **50,** 89-105.

Yu, K.O., Narayanan, L., Mattie, D.R., Godfrey, R.J., Todd, P.N., Sterner, T.R., Mahle, D.A., Lumpkin, M.H., and Fisher, J.W. (2002). The pharmacokinetics of perchlorate and its effect on the hypothalamus-pituitary-thyroid axis in the male rat. *Toxicol. Appl. Pharmacol.* **182,** 148-159.

Zoeller, R.T. and Tan, S.W. (2007). Implications of Research on Assays to Characterize Thyroid Toxicants. *Crit. Rev. Toxicol.* **37,** 195-210.

Table 4.1. Model Boundaries for Parameter Estimation

Boundary Condition	Literature Values	Radiotracer Model Predicted
T_4 metabolized to T_3 (%)	14-27% [a]	40%
T_4 excreted in feces (T_4-G) (%)	10-38% [b,c]	24%
T_3 excreted in feces (%)	4.9-54.9% [c,d]	26%

[a] DiStefano *et al.*, 1982
[b] Nguyen *et al.*, 1993
[c] DiStefano *et al.*, 1987
[d] DiStefano *et al.*, 1993

Table 4.2. Physiological Parameters for the Adult Rat

Parameter	Value	Source
Tissue volumes		
Body weight, BW (kg)	0.350	McLanahan *et al.*, 2007
Liver, VLc (% BW)	3.66	Brown *et al.*, 1997
Liver blood, VLBc (% VL)	21	Brown *et al.*, 1997
Thyroid, VTc (% BW)	0.005	McLanahan *et al.*, 2007
Thyroid blood, VTBc (% VT)	15.7	Malendowicz and Bednarek, 1986
Blood flows		
Cardiac output, QCc (L/hr/kg$^{0.075}$)	14.0	Brown *et al.*, 1997
Liver, QLc (% QC)	17.4	Brown *et al.*, 1997
Thyroid, QTc (% QC)	1.6 [a]	Brown *et al.*, 1997

[a] Human value.

Table 4.3. Compound-Specific Parameters

Parameter	Value	Source
Volume of distribution (% BW)		
Iodide, Vdc_i	50-VT	Visual Fit
TSH, Vdc_{TSH}	5.54	Connors *et al.*, 1984
T_4, Vdc_{T4}	15.6-VL	Kohn *et al.*, 1996
T_3, Vdc_{T3}	18.6-VL	DiStefano, 1986
Partition coefficients (unitless)		
T_4 – Liver:blood, PL_{T4}	1.27	Escobar-Morreale *et al.*, 1996
T_3 – Liver:blood, PL_{T3}	4.47	Escobar-Morreale *et al.*, 1996
Permeability area cross-products (L/hr/kg$^{0.75}$)		
T_4 – Liver blood to liver tissue, $PALc_{T4}$	0.0423	Optimized
T_3 – Liver blood to liver tissue, $PALc_{T3}$	0.1699	Optimized
Iodide – Thyroid blood to thyroid tissue, $PATc_i$	0.0001	Merrill *et al.*, 2003
Affinity constants (nmol/L)		
Iodide – Thyroid NIS, Km_i	31519	Merrill *et al.*, 2003; Gluzman and Niepomniszcze, 1983
TSH – Thyroid NIS, K^{NIS}_{TSH}	0.949	Optimized
Iodide – Iodide organification in thyroid, Kb_i	244.59	Optimized
TSH – Iodide organification in thyroid, Kb_{TSH}	733.98	Optimized
T_4 – Liver Type I 5'-deiodinase, Km^{DI}_{T4}	2300	Leonard and Visser, 1986
T_4 – Liver glucuronidation, Km^{UGT}_{T4}	1×10^5	Visser *et al.*, 1993
T_4 – Liver uptake, Km^{LU}_{T4}	650	Blondeau *et al.*, 1988
Maximum velocities (nmol/hr/kg$^{0.75}$)		
Iodide – Thyroid NIS, $VmaxTc_i$	5738.267	Optimized
Iodide – Iodide organification in thyroid, $VmaxBc_i$	1005.9[a]	Optimized
T_4 – Liver Type I 5'-deiodinase, $Vmaxc^{DI}_{T4}$	19.89	Optimized
T_4 – Liver glucuronidation, $Vmaxc^{UGT}_{T4}$	3435.89	Optimized
T_4 – Liver uptake, $Vmaxc^{LU}_{T4}$	4384.73	Optimized
T_3 – 1st order Liver uptake, k^{LU}_{T3} (1/hr)	1.25	Optimized
Clearance values		
Iodide – Urinary excretion, $ClUc_i$ (L/hr/kg$^{0.25}$)	0.0046	Optimized
TSH – Vd clearance, $kelc_{TSH}$ (/hr/kg$^{0.25}$)	1.8899	Lemarchand-Beraud and Berthier, 1981
T_4 – Vd metabolism, $kelc_{T4}$ (/hr/kg$^{0.25}$)	0.05[b]	Abrams and Larsen, 1973
T_3 – Vd metabolism, $kelc_{T3}$ (/hr/kg$^{0.25}$)	0.12[b]	Abrams and Larsen, 1973
T_3 – Liver metabolism, $kmetLc_{T3}$ (/hr/kg$^{0.25}$)	3.65	Optimized
T_3 – fraction of liver T_3 metabolism excreted in feces, FT3feces (unitless)	0.30	Visually Fit
TSH / Thyroid hormone production parameters		
Thyroid hormone production constant, k^{IB}_{TSH} (L^2/nmol/hr)	5×10^{-7}	Visually Fit
Maximum rate of TSH production in the absence of T_4, k_0^{TSH} (nmol/hr/kg$^{0.75}$)	6	Connors *et al.*, 1984
T_4 concentration for half-maximal TSH production, $K_{inh\ T4}$ (nmol/L)	0.2	Optimized

[a] Scaled by dividing by BW$^{0.75}$. See footnote in *Materials and Methods*.
[b] Calculated from serum half-life using kel=ln2/$t_{1/2}$

Figure 4.1. Sub-model structure for radiotracer compounds used in model development and preliminary estimation of kinetic parameters. (A) ^{125}Iodide sub-model for an iv dose to Vd, 1st order urinary elimination, and distribution to thyroid. Thyroid described with active uptake (bold arrow) and bidirectional diffusion. Bound ^{125}I in thyroid is used in thyroid hormone production. (B) ^{125}I-TSH sub-model described for an iv dose to Vd and 1st order elimination. (C) ^{125}I-T_3 model described for an iv dose and 1st order clearance from Vd and distribution to the liver where it is transported via active uptake or diffusion. Liver clearance is described with one rate partitioned as 30% eliminated through feces and the remaining metabolized to free iodide. (D) ^{131}I-T_4 sub-model for an iv dose to the Vd, 1st order clearance from Vd and distribution to the liver where it is also taken up via active transport or passive difussion. T_4 in the liver is metabolized via Type I 5'-deiodnation and formation of T_4-glucuronide (T_4-G).

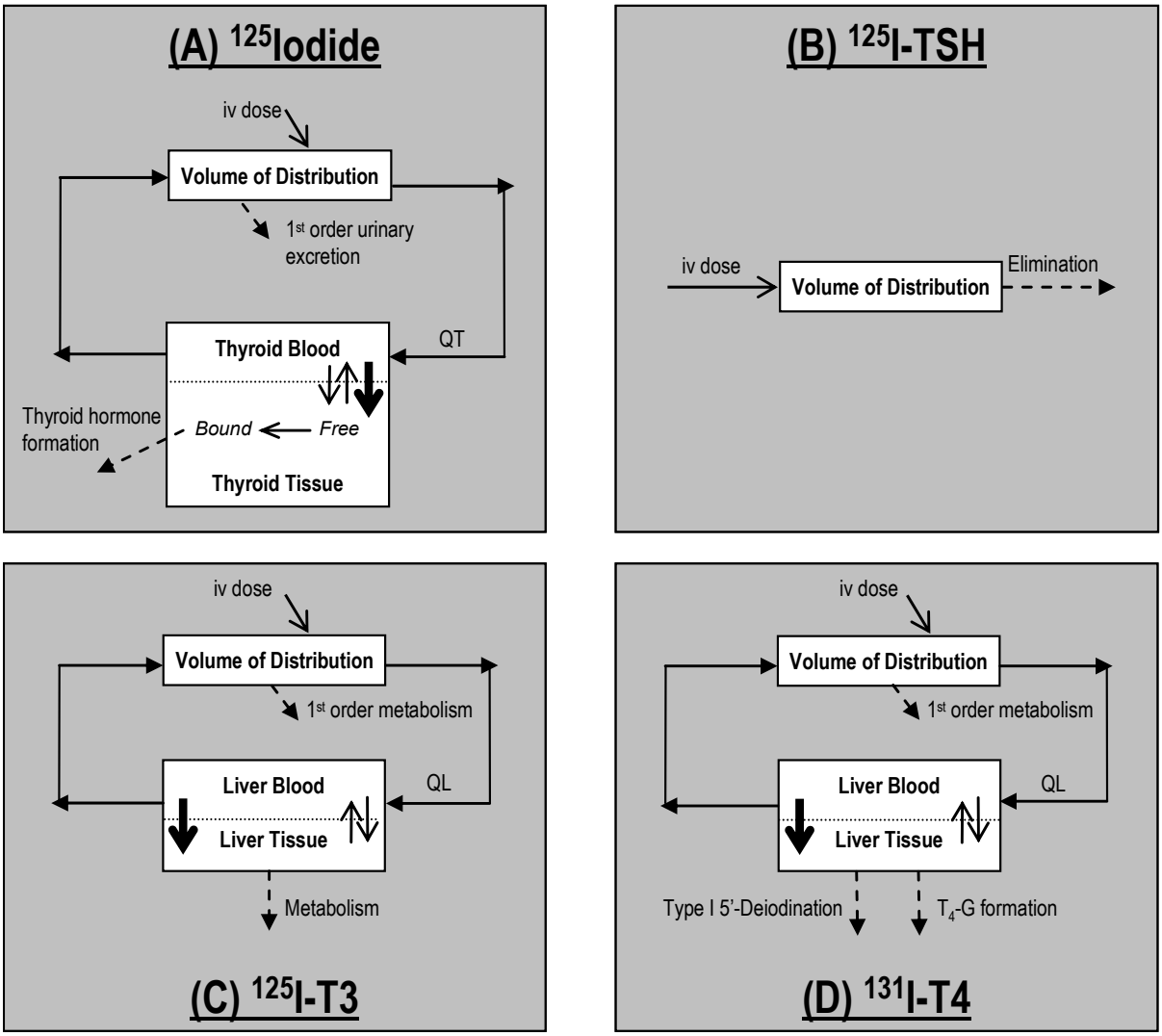
(A) 125Iodide
iv dose
Volume of Distribution
1st order urinary excretion
Thyroid Blood
QT
Thyroid hormone formation
Bound
Free
Thyroid Tissue
(B) 125I-TSH
iv dose
Volume of Distribution
Elimination
iv dose
Volume of Distribution
1st order metabolism
Liver Blood
QL
Liver Tissue
Metabolism
(C) 125I-T3
iv dose
Volume of Distribution
1st order metabolism
Liver Blood
QL
Liver Tissue
Type I 5'-Deiodination
T4-G formation
(D) 131I-T4

Figure 4.1.

Figure 4.2. BBDR-HPT axis model structure for the adult rat hypothalamic-pituitary-thyroid (HPT) axis, including sub-models (areas shaded in gray) for dietary iodide (^{127}I), TSH, T_4, and T_3. Solid arrows (⟶) represent blood flows, bold arrows (➔) within tissue compartments represent active uptake, solid arrows (⟶) within tissue compartments represent diffusion limitation, dashed arrows between models (- - ▸) represent metabolic links, while the dashed and dotted arrow (— · ▸) represents use of dietary iodide in thyroid hormone production, and the bold (➔) arrows connecting models processes controlled (stimulated or inhibited) by the compound. Specific details on the model links shown in the figure are as follows: ❶Formation of free iodide from T_3 metabolism in the Vd and liver; ❷Formation of free iodide from T_4 to T_3 metabolism in the Vd and liver; ❸Loss of bound thyroidal iodide secreted as thyroid hormones; ❹Metabolism of T_3 (30% into feces, 70% to free iodide); ❺Deiodination of T_4 in the liver to T_3 and free iodide; ❻Glucuronidation of T_4 (formation of T_4-glucuronide; T_4-G) and excretion into feces; ❼TSH stimulation NIS iodide uptake; ❽TSH stimulation of organification of iodide, forming thyroid hormone precursors; ❾TSH stimulation of thyroid hormone production; ❿T_4 negative feedback on TSH production.

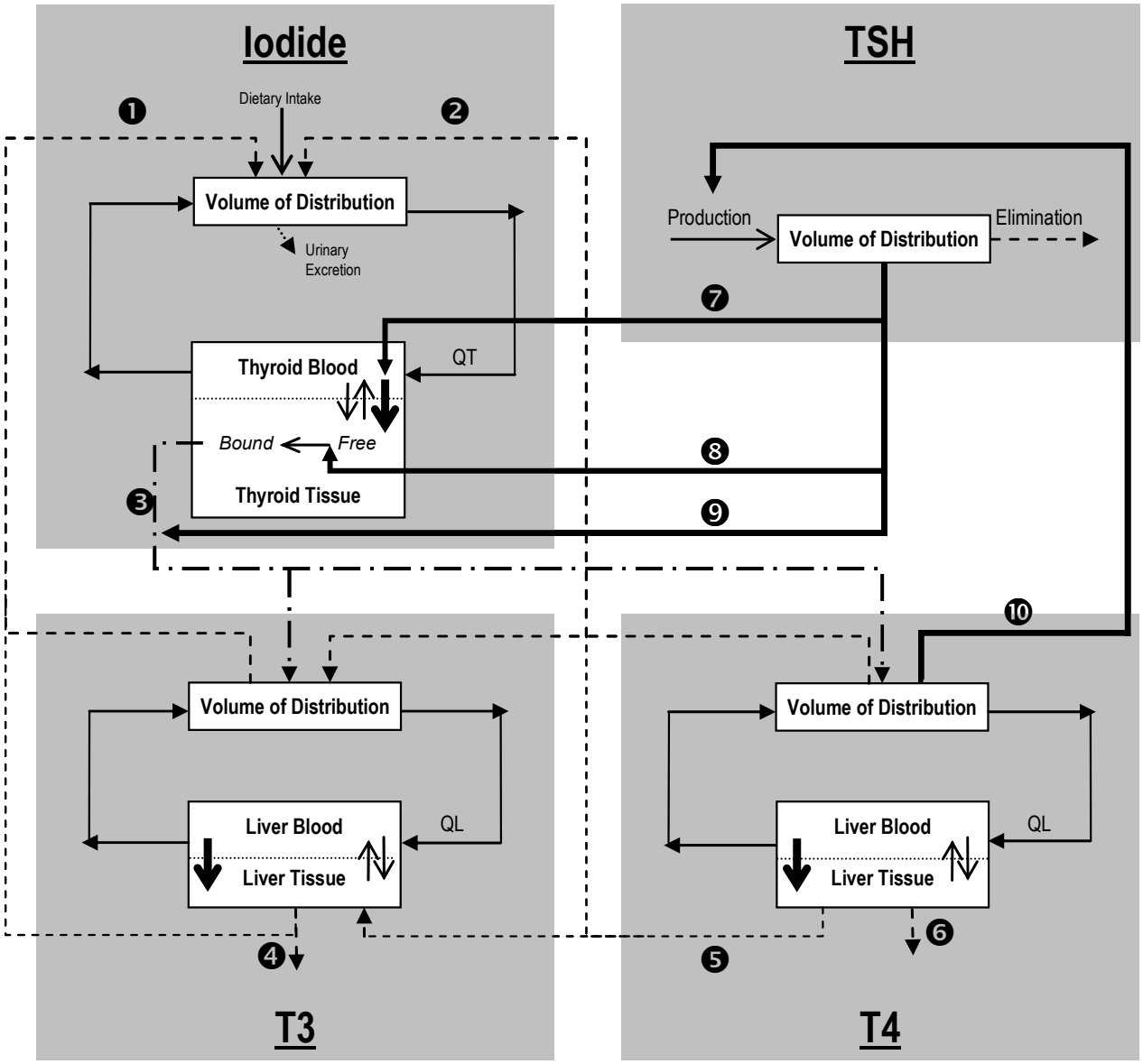
Iodide
TSH
Dietary Intake
Volume of Distribution
Urinary Excretion
Production
Volume of Distribution
Elimination
Thyroid Blood
QT
Bound
Free
Thyroid Tissue
Volume of Distribution
Liver Blood
QL
Liver Tissue
Volume of Distribution
Liver Blood
QL
Liver Tissue
T3
T4

Figure 4.2

Figure 4.3. Relationship between total amount of thyroidal iodide and fraction of total thyroid hormone production that is T_3. This relationship was used to fractionate the thyroid production rate of thyroid hormones as detailed in *Methods*. Data points adapted from Pedraza *et al.* (2006) are shown with best fit exponential line. The equation for the line is adapted for use in the model as shown in Equation 18.

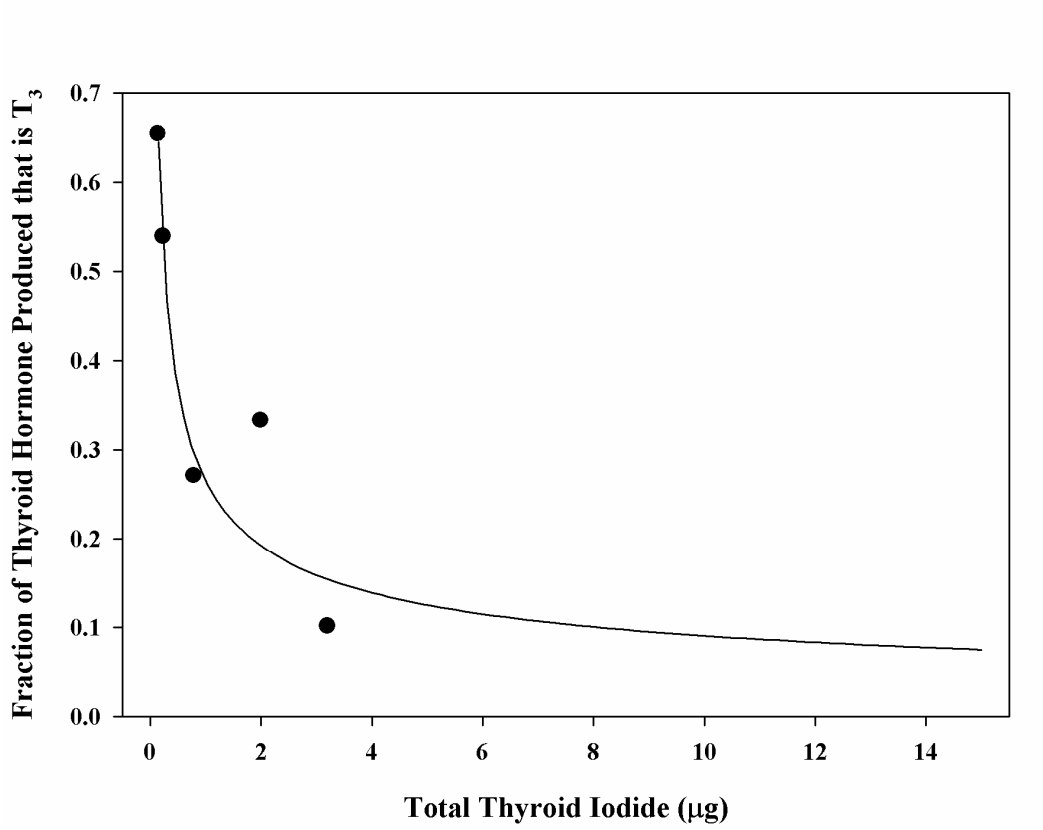
Fraction of Thyroid Hormone Produced that is T_3
0.7
0.6
0.5
0.4
0.3
0.2
0.1
0.0
0
2
4
6
8
10
12
14
Total Thyroid Iodide (μg)

Figure 4.3

Figure 4.4. Model simulations (lines) compared with literature data (points) for iv doses of radiolabeled compounds used in HPT axis model development. (A) Serum ^{125}Iodide (^{125}I, ——) and cumulative ^{125}I urinary excretion (– –) following a tail vein iv dose of 33μg ^{125}I/kg, data adapted from Yu *et al.* (2002) for serum (●) and urine (○); (B) Total (——) and bound (– –) ^{125}I in the thyroid after a tail vein iv dose of 33μg ^{125}I/kg, data provided by Dr. Yu (personal communication) for total (■) and bound (□) thyroid ^{125}I; (C) Serum (——) and liver (– –) ^{125}I-T_3 following iv injection of 0.83 ng ^{125}I-T_3, data adapted from DiStefano *et al.* (1993) for serum (●) and liver (▽); (D) Serum (——) and liver (– –) ^{131}I-T_4 following iv injection of 1.7 ng ^{131}I-T_4, data adapted from Schroder van der Elst *et al.* (1997) for serum (●) and liver (▽); and (E) Serum (——) ^{125}I-TSH following iv dose of 5 ng ^{125}I-TSH, serum data (●) adapted from Spira *et al.* (1979).

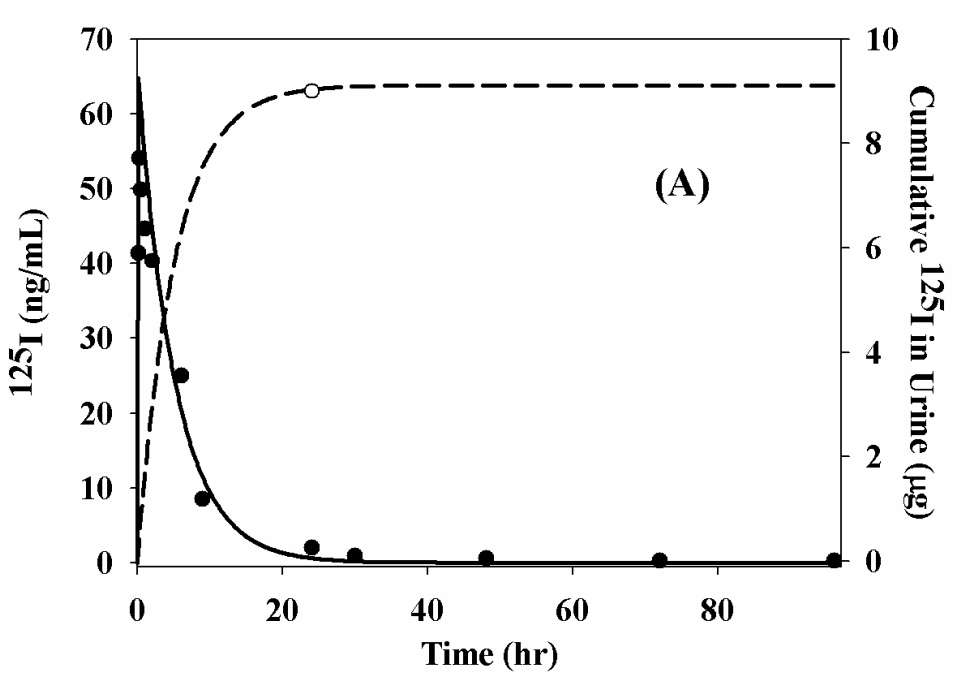

Figure 4.4A

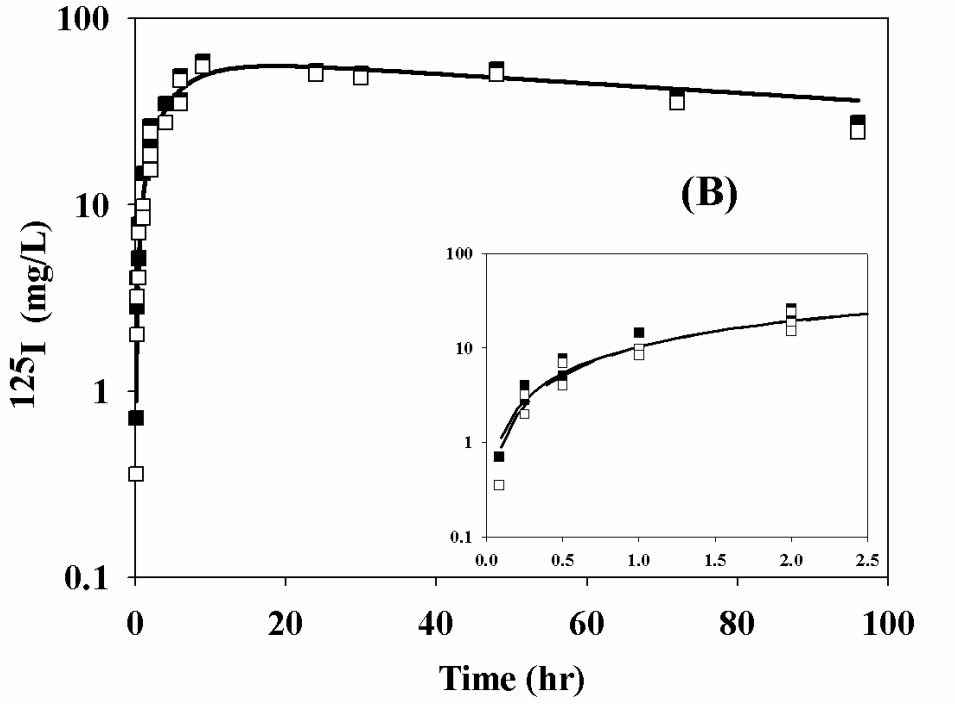

Figure 4.4B

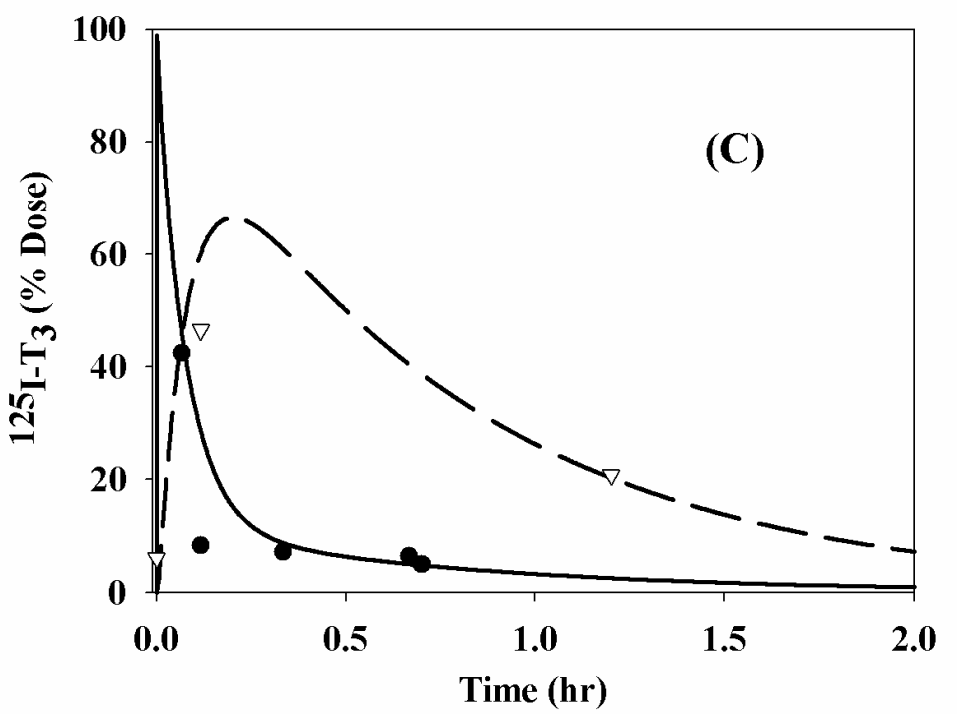

Figure 4.4C

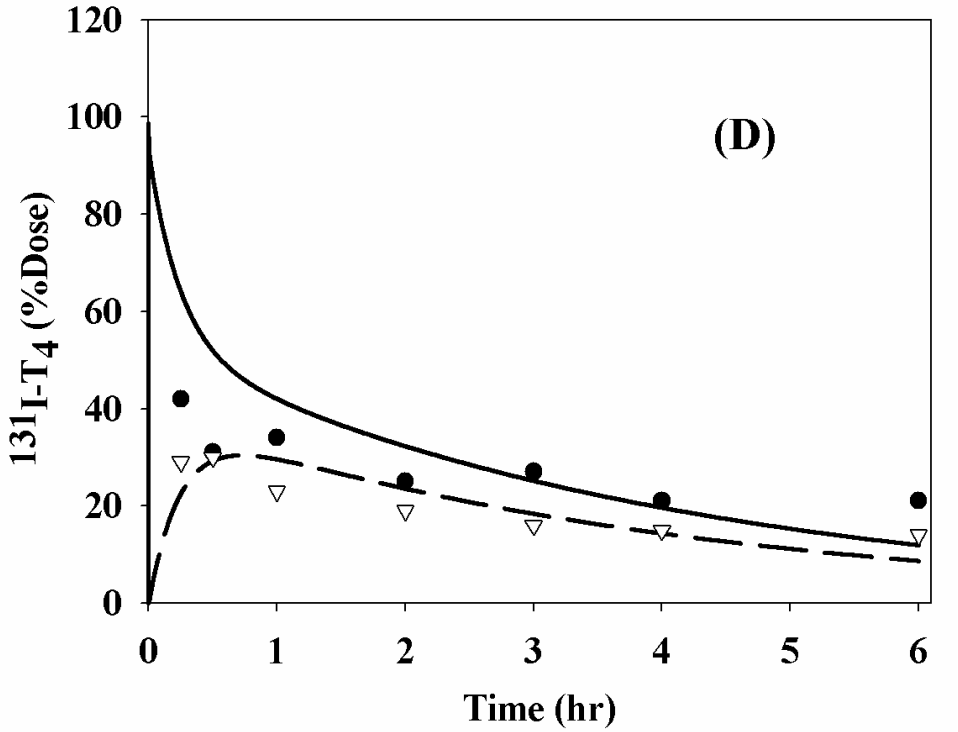

Figure 4.4D

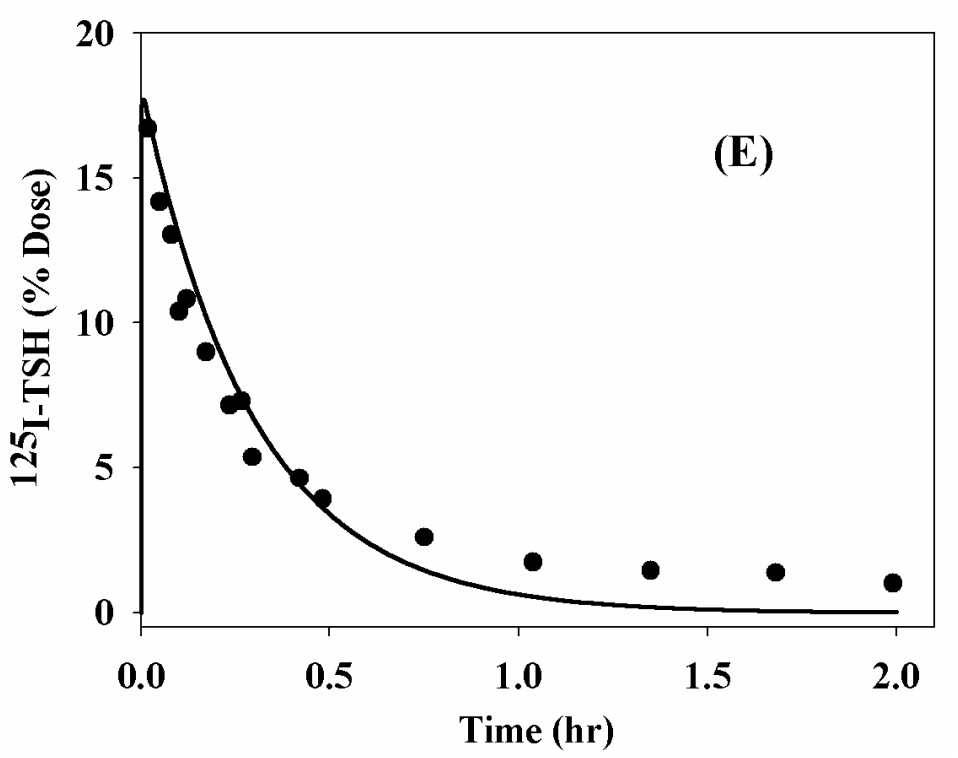

Figure 4.4E

Figure 4.5. Steady-state, iodide sufficient, model simulations (lines) shown with literature data (points) for HPT axis model calibration. (A) Total thyroid (— · —, μg) and free serum (——, μg/dL) iodide (^{127}I) model simulation, thyroid ^{127}I data (○ ± SD) from McLanahan *et al.* (2007) and serum (● ± SD) from Eng *et al.* (1999); (B) Serum TSH (——, ng/mL) model simulation, data (● ± SD) for McLanahan *et al.* (2007); (C) Serum (——) and liver (– –) T_4 model simulations, serum data (● ± SD) from McLanahan *et al.* (2007) and liver (▽) adapted from Morreale de Escobar *et al.* (1994); and (D) Serum (——) and liver (– –) T_3 model simulations, serum data (● ± SD) unpublished data from McLanahan *et al.* (2007) study and liver (▽) from Morreale de Escobar *et al.* (1994).

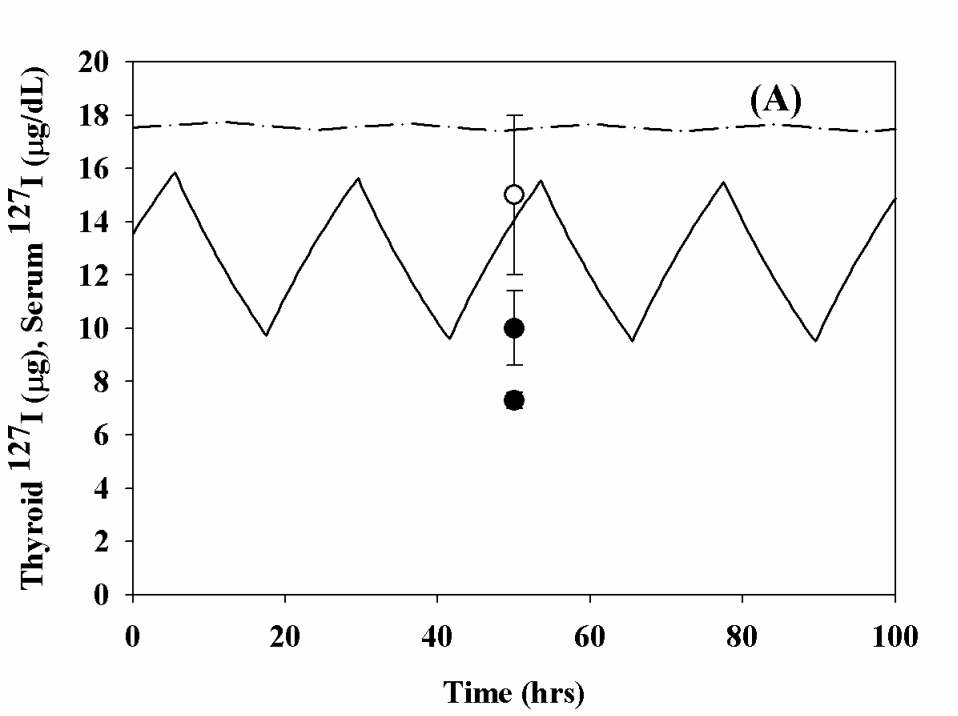

Figure 4.5A

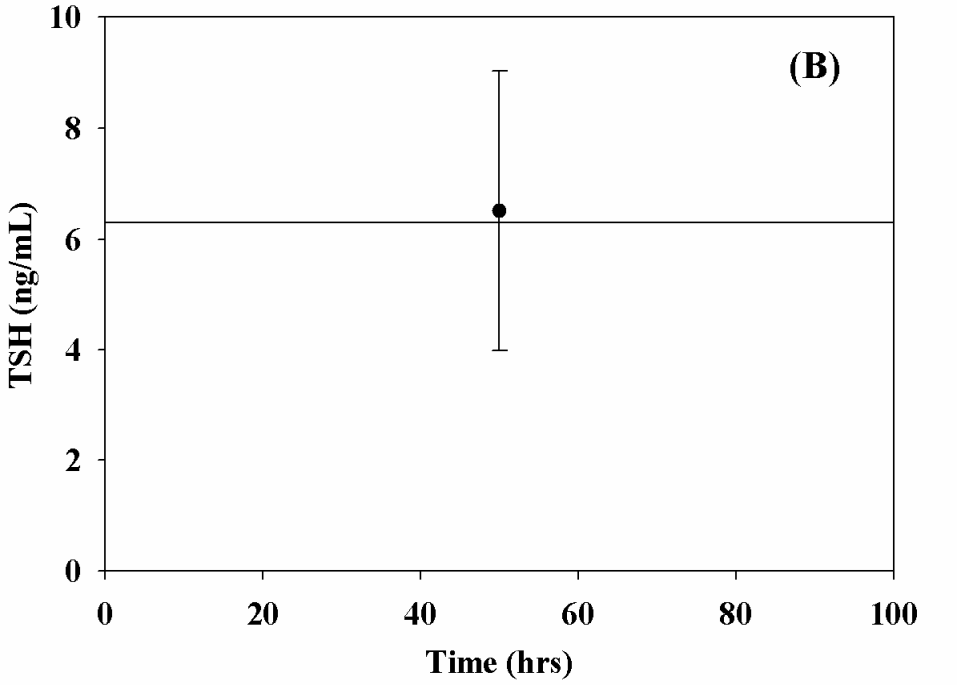

Figure 4.5B

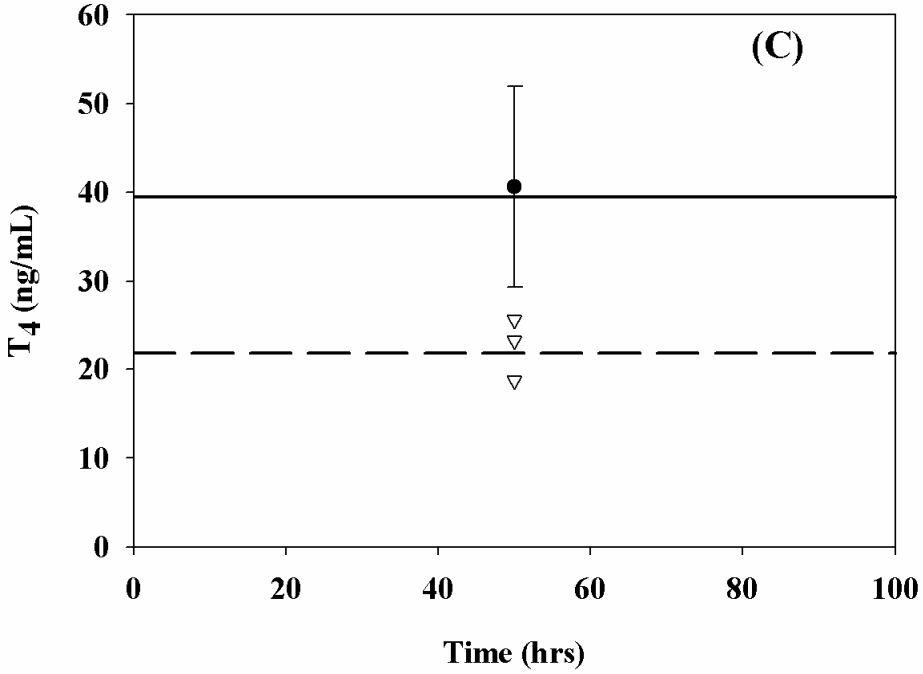

Figure 4.5C

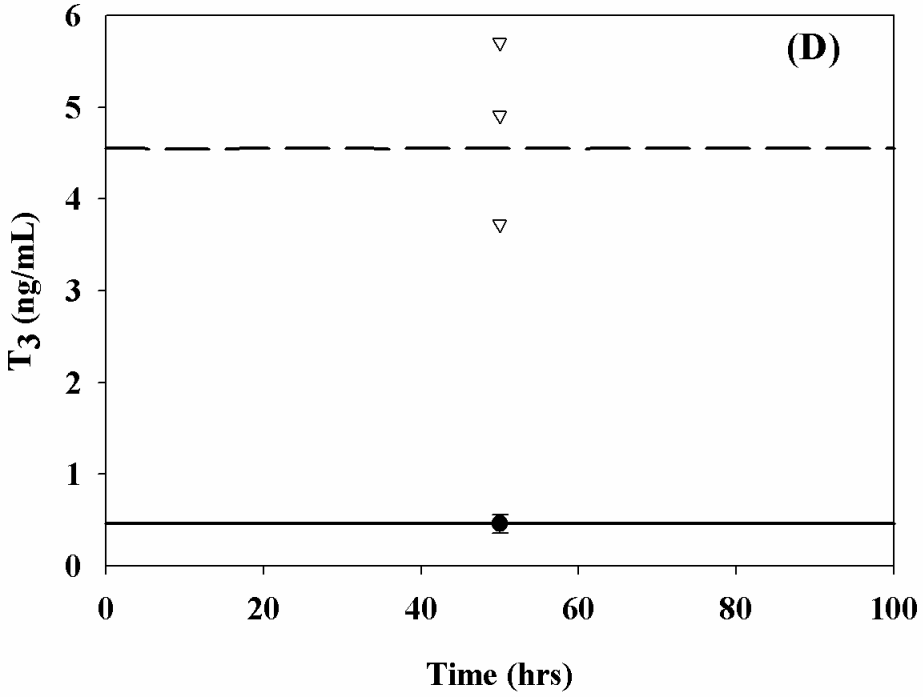

Figure 4.5D

Figure 4.6. Short term effects of LID (0.35μg I/day) on serum thyroid hormones and total thyroid iodide of adult male Holtzman Sprague-Dawley rats. On Day 0, rats began a LID of approximately 0.35 μg I/day and continued for 26 days (Riesco *et al.*, 1977). Model simulations are represented by lines for serum T_4 (———, ng/mL), T_3 (– – – –, ng/mL), TSH (— . —, fold change), and total thyroid ^{127}I (....., μg). LID data for serum T_4 (▼ ± SD), T_3 (■ ± SD), TSH (○), and total thyroid ^{127}I (● ± SD) was adapted from Riesco *et al.* (1977).

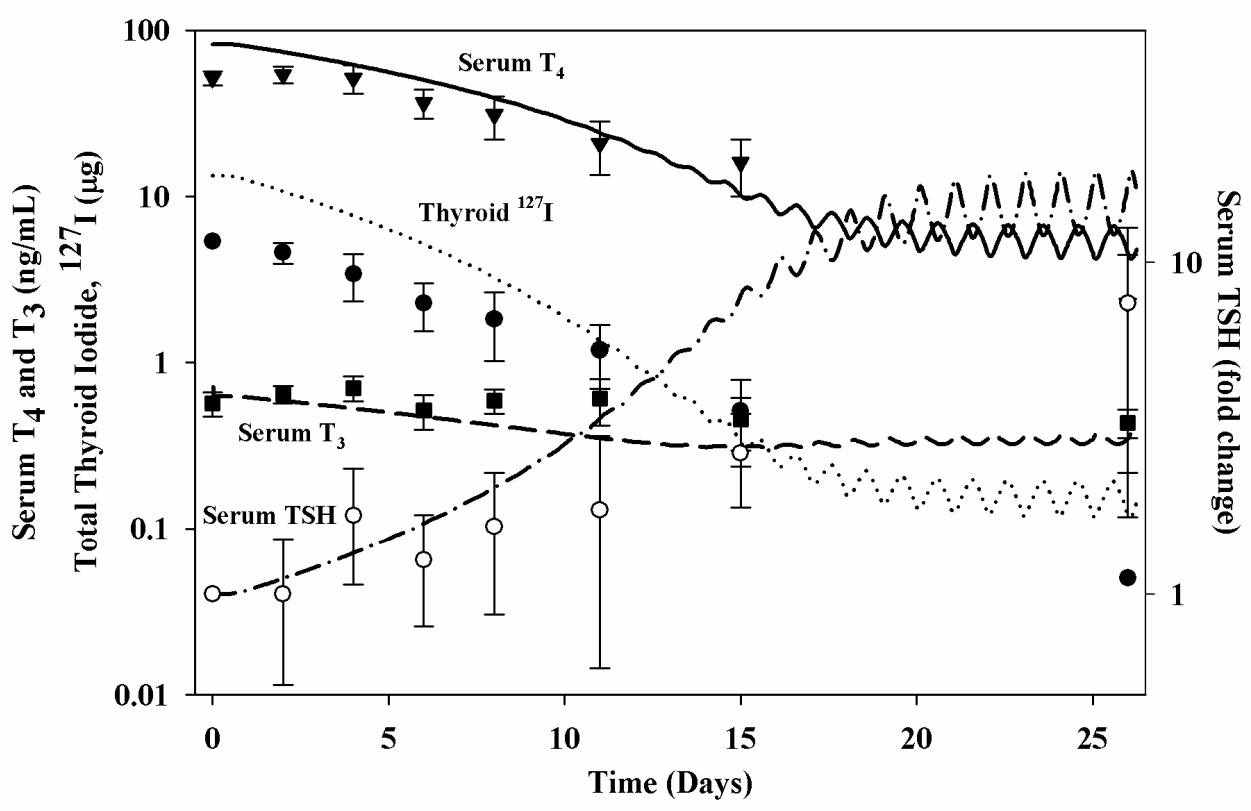
Serum T_4
Thyroid ^{127}I
Serum T_3
Serum TSH
Serum T_4 and T_3 (ng/mL)
Total Thyroid Iodide, ^{127}I (μg)
Serum TSH (fold change)
Time (Days)
100
10
1
0.1
0.01
0
5
10
15
20
25
10
1

Figure 4.6

Figure 4.7. Long term effects of LID (0.33μg I/day) on serum thyroid hormones and total thyroid iodide of adult male (A) Simonsen Albino and (B) Holtzman Sprague-Dawley rats. On Day 0, rats began a LID of approximately 0.33 μg I/day and continued for 84 days (Okamura *et al.* 1981a). Model simulations are represented by lines for serum T_4 (———, ng/mL), T_3 (– – – –, ng/mL), TSH (— · —, fold change), and total thyroid ^{127}I (....., μg). LID data for serum T_4 (▼ ± SD), T_3 (■ ± SD), TSH (○), and total thyroid ^{127}I (● ± SD) was adapted from Okamura *et al.* (1981a).

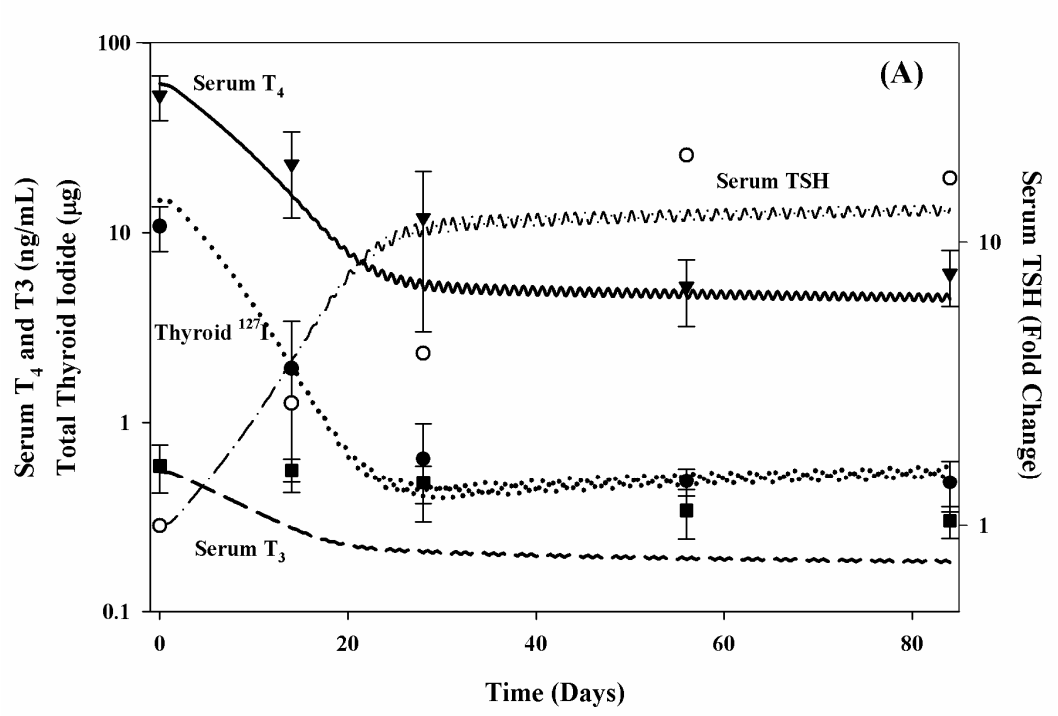

Figure 4.7A

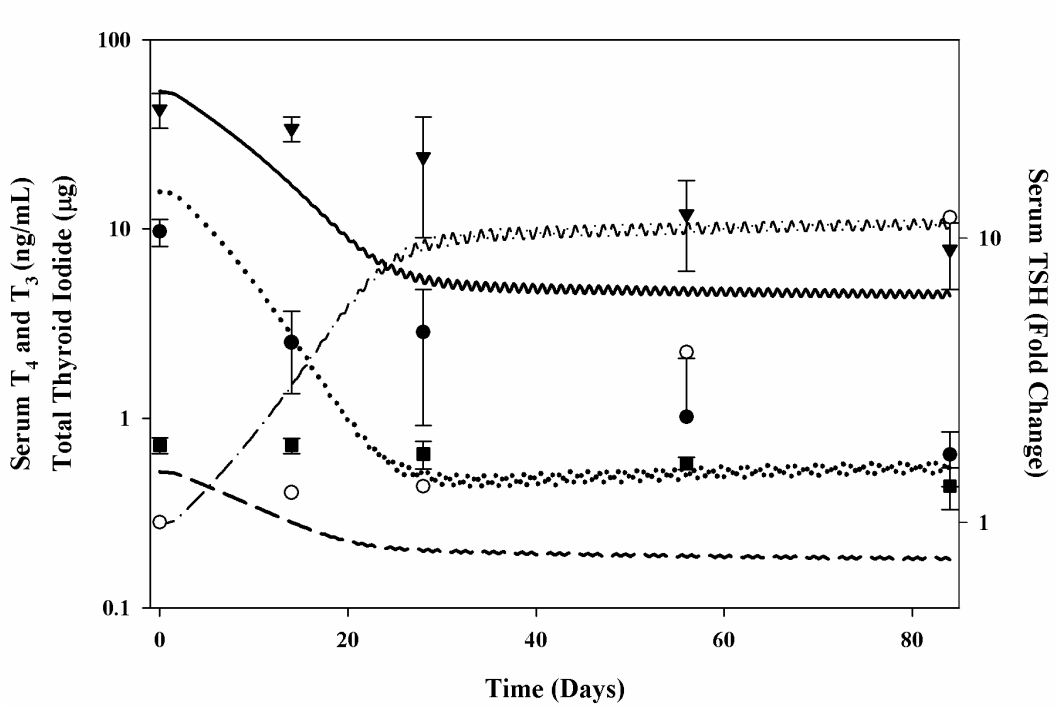

Figure 4.7B

Figure 4.8. Long term effects of LID (1.14 μg I/day) on serum thyroid hormones and total thyroid iodide of adult male Holtzman Sprague-Dawley rats. On Day 0, rats began a LID of 1.14 μg I/day and continued for 96 days (Okamura *et al.*, 1981b). Model simulations are represented by lines for serum T_4 (———, ng/mL), T_3 (– – – –, ng/mL), and total thyroid ^{127}I (....., μg). LID data for serum T_4 (▼ ± SD), T_3 (■ ± SD), and total thyroid ^{127}I (● ± SD) was adapted from Okamura *et al.* (1981b).

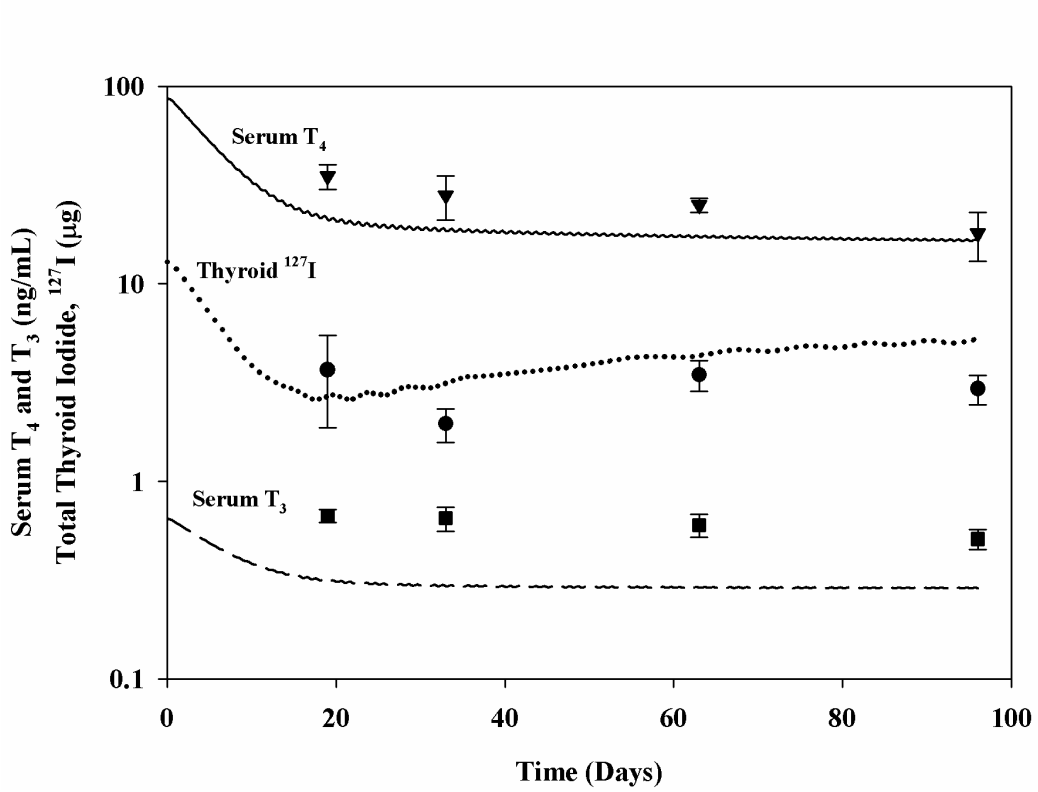
100
10
1
0.1
0
20
40
60
80
100
Serum T_4
Thyroid ^{127}I
Serum T_3
Serum T_4 and T_3 (ng/mL)
Total Thyroid Iodide, ^{127}I (μg)
Time (Days)

Figure 4.8

Figure 4.9. Recovery from ID in adult male Sprague-Dawley rats fed a LID for seven months. After seven months on a LID (0.6μg I/day), rats were supplemented with iodide to provide total intake of approximately 2.6 μg I/day (black) or 8.6 μg I/day (dark grey) beginning on Day 0 and continuing for 9 days (Fukuda *et al.*, 1975). Model simulations of serum T_4 (solid lines) and TSH (dashed lines) compared with recovery data modified from Fukuda *et al.* (1975) for serum T_4 (●, 2.6 μg I/day; ○, 8.6 μg I/day) and serum TSH (▼, 2.6 μg I/day; ▽, 8.6 μg I/day). Data expressed as percent of baseline recorded at Day 0.

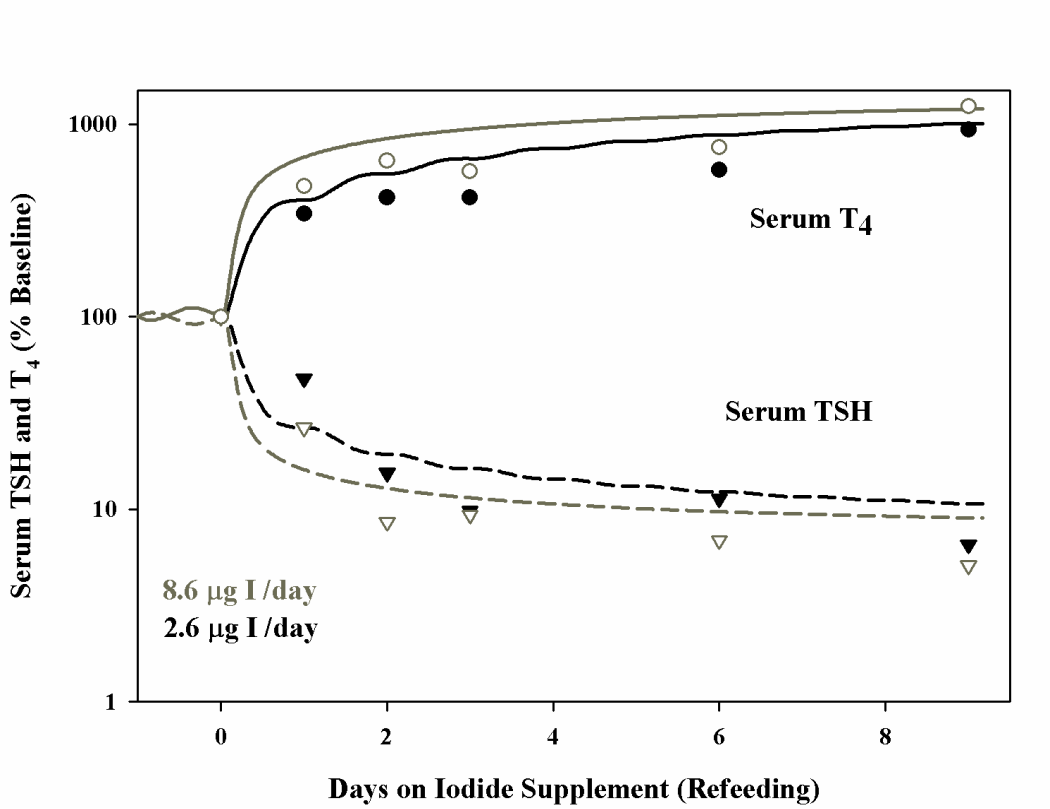
Serum TSH and T4 (% Baseline)
1000
100
10
1
0
2
4
6
8
Days on Iodide Supplement (Refeeding)
Serum T4
Serum TSH
8.6 µg I /day
2.6 µg I /day

Figure 4.9

Figure 4.10. Normalized sensitivity coefficient (NSC) graph for parameters that yielded a NSC of 0.90 or greater for at least one response (serum T_4, T_3, and TSH or total thyroid iodide) examined under iodide sufficient (20 μg/day) (left) and iodide deficient (1 μg/day) (right) steady-state conditions. Total amount of iodide in the thyroid is the most sensitive model response and followed by serum T_4 and T_3 concentrations, which were less sensitive than total thyroid iodide predictions to a one percent change in model parameters. Serum TSH was least sensitive to changes in model parameters.

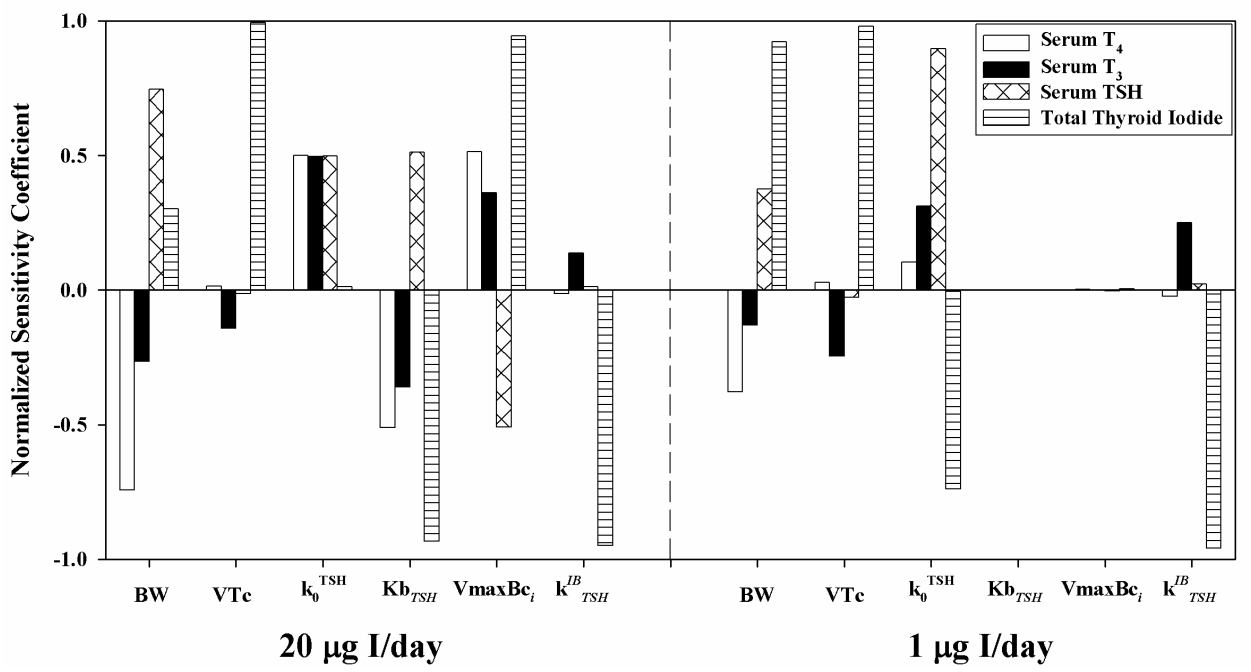
Normalized Sensitivity Coefficient
1.0
0.5
0.0
-0.5
-1.0
Serum T_4
Serum T_3
Serum TSH
Total Thyroid Iodide
BW
VTc
k_0^{TSH}
Kb_{TSH}
$VmaxBc_i$
k^{IB}_{TSH}
BW
VTc
k_0^{TSH}
Kb_{TSH}
$VmaxBc_i$
k^{IB}_{TSH}
20 μg I/day
1 μg I/day

Figure 4.10

Figure 4.11. Iodide dose-response plot for serum T_4 and TSH. BBDR-HPT axis model was used to determine steady-state serum T_4 and TSH concentrations over a wide range of iodide intakes, intakes ranged from insufficient (0-2 μg I/day) to sufficient (> 2 μg I/day).

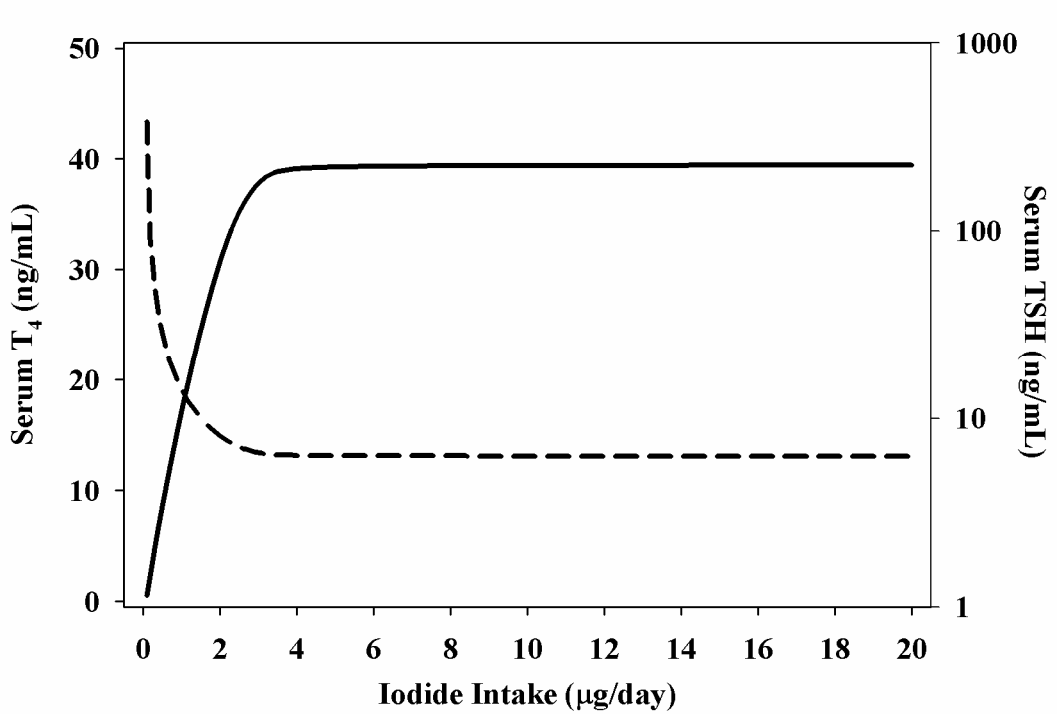
50
40
30
20
10
0
Serum T_4 (ng/mL)
1000
100
10
1
Serum TSH (ng/mL)
0
2
4
6
8
10
12
14
16
18
20
Iodide Intake (μg/day)

Figure 4.11

Supplementary Data

"A Biologically Based Dose-Response Model for Dietary Iodide and the Hypothalamic-Pituitary-Thyroid Axis in the Adult Rat: Evaluation of Iodide Deficiency"

Eva D. McLanahan, Melvin E. Andersen, and Jeffrey W. Fisher

The supplementary data includes a table of model parameters optimized for radiotracer sub-models and used to make plots shown in Figure 4.4. These model parameters were re-optimized to euthyroid, steady-state iodide sufficient conditions in the dietary iodide BBDR-HPT axis combined model that often resulting in minor changes in the parameter.

Table 4.1S. Compound-Specific Parameters for Radiotracer Sub-models

Parameter	Value	Source
Volume of distribution (% BW)		
Iodide, Vdc_i	50-VT	Visual Fit
TSH, Vdc_{TSH}	5.54	Connors *et al.*, 1984
T_4, Vdc_{T4}	15.6-VL	Kohn *et al.*, 1996
T_3, Vdc_{T3}	18.6-VL	DiStefano, 1986
Partition coefficients (unitless)		
T_4 – Liver:blood, PL_{T4}	1.27	Escobar-Morreale *et al.*, 1996
T_3 – Liver:blood, PL_{T3}	4.47	Escobar-Morreale *et al.*, 1996
Permeability area cross-products (L/hr/kg$^{0.75}$)		
T_4 – Liver blood to liver tissue, $PALc_{T4}$	0.04875	Optimized
T_3 – Liver blood to liver tissue, $PALc_{T3}$	0.0683	Optimized
Iodide – Thyroid blood to thyroid tissue, $PATc_i$	0.0001	Merrill *et al.*, 2003
Affinity constants (nmol/L)		
Iodide – Thyroid NIS, Km_i	31519	Merrill *et al.*, 2003; Gluzman and Niepomniszcze, 1983
TSH – Thyroid NIS, K^{NIS}_{TSH}	1.147	Optimized
Iodide – Iodide organification in thyroid, Kb_i	221.1	Optimized
TSH – Iodide organification in thyroid, Kb_{TSH}	1112.65	Optimized
T_4 – Liver Type I 5'-deiodinase, Km^{DI}_{T4}	2300	Leonard and Visser, 1986
T_4 – Liver glucuronidation, Km^{UGT}_{T4}	1×10^5	Visser *et al.*, 1993
T_4 – Liver uptake, Km^{LU}_{T4}	650	Blondeau *et al.*, 1988
Maximum velocities (nmol/hr/kg$^{0.75}$)		
Iodide – Thyroid NIS, $VmaxTc_i$	1119.396	Optimized
Iodide – Iodide organification in thyroid, $VmaxBc_i$	2243.598[a]	Optimized
T_4 – Liver Type I 5'-deiodinase, $Vmaxc^{DI}_{T4}$	15.105	Optimized
T_4 – Liver glucuronidation, $Vmaxc^{UGT}_{T4}$	1080.32	Optimized
T_4 – Liver uptake, $Vmaxc^{LU}_{T4}$	10552.8	Optimized
T_3 – 1st order Liver uptake, k^{LU}_{T3} (1/hr)	1.5	Optimized
Clearance values		
Iodide – Urinary excretion, $ClUc_i$ (L/hr/kg$^{0.25}$)	0.02	Optimized
TSH – Vd clearance, $kelc_{TSH}$ (/hr/kg$^{0.25}$)	1.8899	Lemarchand-Beraud and Berthier, 1981
T_4 – Vd metabolism, $kelc_{T4}$ (/hr/kg$^{0.25}$)	0.05[b]	Abrams and Larsen, 1973
T_3 – Vd metabolism, $Kelc_{T3}$ (/hr/kg$^{0.25}$)	0.12[b]	Abrams and Larsen, 1973
T_3 – Liver metabolism, $kmetLc_{T3}$ (/hr/kg$^{0.25}$)	1.15	Optimized
T_3 – fraction of liver T_3 metabolism excreted in feces, FT3feces (unitless)	0.30	Visually Fit
TSH / Thyroid hormone production parameters		
Thyroid hormone production constant, k^{IB}_{TSH} (L^2/nmol/hr)	5×10^{-7}	Optimized

[a] Scaled by dividing by BW$^{0.75}$. See footnote in *Materials and Methods*.
[b] Calculated from serum half-life using kel=ln2/$t_{1/2}$

CHAPTER 5

THE USE OF A BIOLOGICALLY BASED DOSE-RESPONSE MODEL OF THE HYPOTHALAMIC-PITUITARY-THYROID (HPT) AXIS TO EVALUATE PERCHLORATE INDUCED PERTURBATIONS OF THE HPT AXIS IN ADULT RATS[4]

[4] E.D. McLanahan, M.E. Andersen, J.L. Campbell, Jr., and J.W. Fisher. To be submitted to *Environmental Health Perspectives*

Abstract

The perchlorate anion (ClO_4^-) is an environmental contaminant known to disrupt the thyroid axis of many terrestrial and aquatic species. It is well known that ClO_4^- competitively inhibits iodide uptake into the thyroid at the sodium/iodide symporter (NIS), presumably leading to a decrease in available iodide for use in thyroid hormone production. A BBDR-HPT axis model for the adult male rat was combined with a PBPK model for ClO_4^- to describe perturbations in the thyroid axis resulting from ClO_4^- exposure in drinking water. First, the BBDR-HPT axis model was linked with a ClO_4^- PBPK model via competitive inhibition of thyroidal iodide uptake by ClO_4^-. However, model simulations were not able to predict the rapid decline in serum T_4 and rapid increase in serum TSH responses when laboratory rats were exposed to ClO_4^- in drinking water. Thus, a hypothesis that thyroidal ClO_4^- interferes with thyroid hormone synthesis was tested. When ClO_4^- interference with thyroid hormone production was included in the model, it adequately simulated adult male rat thyroid axis perturbations in serum T_4 and TSH reported in literature from exposures to ClO_4^- contaminated drinking water over a range of doses (1 mg ClO_4^-/kg-day to 15 mg ClO_4^-/kg-day). Perchlorate appears not only to affect iodide availability for thyroid hormone production, but also to interfere with production of thyroid hormones. TSH secretion in the presence of ClO_4^- also appeared to be more sensitive than in iodide deficient conditions as evidenced by a more rapid increase in TSH in the presence of ClO_4^- compared to changes under severe iodide deficiency. The integration of the ClO_4^- PBPK and BBDR-HPT axis modesl provide further biological insights into mode of action of ClO_4^- disruption of the thyroid axis and demonstrates the utility of a BBDR-HPT axis model.

Key Words: perchlorate, iodide, thyroid, rat, BBDR model, PBPK model, HPT axis

Introduction

The hypothalamic-pituitary-thyroid (HPT) axis is a dynamic system, composed of sophisticated feedback loops, often able to adapt to environmental and physiological insults that alter its function. The thyroid produces two major hormones, T_4 and a smaller quantity of the biologically active hormone, T_3. TSH is produced by the pituitary under normal conditions and synthesis increases in response to a decline in serum thyroid hormones. This is referred to as the T_4/TSH negative feedback loop. TSH stimulates the thyroid by binding to extracellular TSH receptors on the basolateral plasma membrane of thyroid follicular cells, which results in an intracellular cascade of secondary messenger events (Ferreira *et al.*, 2005; Riedel *et al.*, 2001). TSH upregulation of the thyroid can result in increased synthesis and activity of the NIS, increasing the rate of iodide sequestration by the thyroid, as well as events leading to increased rate of formation and secretion of thyroid hormones.

Environmental contaminants, such as perchlorate (ClO_4^-), may affect thyroid axis homeostasis. Competitive inhibition of NIS iodide transport is the most well-known and well-defined mode of action for ClO_4^- (Tonacchera *et al.*, 2004; Yu *et al.*, 2002; Wolff, 1998); although some have proposed that ClO_4^- may also affect the formation and secretion of thyroid hormones (Hildebrandt and Halmi, 1981; Wolff, 1998; and Yu *et al.*, 2002). The ClO_4^- anion has recently been classified as a ubiquitous environmental contaminant throughout the United States, with detectable concentrations in many drinking water supplies (Motzer, 2001), food and beverage products (e.g. milk, lettuce, grains) (El Aribi *et al.*, 2006), and also found as a contaminant in dietary supplements (Snyder *et al.*, 2006). The occurrence of ClO_4^- in the environment is most often attributed to anthropogenic uses of ClO_4^- salts as oxidizers in solid

rocket propellants and application of Chilean nitrate fertilizers (Motzer, 2001); however, ClO_4^- may also be formed naturally by atmospheric processes (Dasgupta *et al.*, 2005).

The inhibition of iodide uptake into the thyroid by ClO_4^- is thought to affect the thyroid axis by creating an iodide deficient (ID) condition within the thyroid, resulting in a decline in thyroid hormone production as reflected by decreased serum concentrations of thyroid hormones (Yu *et al.*, 2002; Siglin *et al.*, 2000). Under chronic exposures to ClO_4^- in rodents the upregulation of the thyroid gland by TSH may not be able to compensate for the lack of available iodide in the thyroid, leading to hypothyroidism. Alterations in the HPT axis by ClO_4^- have been observed in laboratory studies with rodents (inhibition of thyroidal uptake of radiolabeled iodide, decreased serum thyroid hormones and increased serum TSH) and clinical studies in humans (inhibition of thyroidal uptake of radiolabeled iodide). The human HPT axis is not as sensitive as rodents to ClO_4^- induced perutbrations and to date, only one human study suggests environmental levels of ClO_4^- may disrupt the HPT axis in women with low intake of iodide (Blount *et al.*, 2006). Thyroid hormones are essential for proper growth, development, reproduction, and metabolism. Transient changes in thyroid hormone economy during gestation and early development could result in life-long consequences, including irreversible neurological damage (Haddow *et al.*, 1999).

Several ClO_4^- physiologically based pharmacokinetic (PBPK) models have been developed for different life-stages of the rat and human (Clewell *et al.*, 2003a, 2003b; Merrill *et al.*, 2003, 2005). These models were combined with a radiolabeled iodide (^{125}I) PBPK model to predict inhibition of radiolabeled iodide uptake, which was determined to be the precursor to the critical effect used by the U.S. Environmental Protection Agency in development of the human RfD for ClO_4^- (U.S. EPA, 2005). While these rodent and human models adequately predicted

the inhibition of radiolabeled iodide uptake, they did not include the downstream consequences of thyroidal iodide deficiency, such as alterations in serum thyroid hormone concentrations. The adult rat model presented herein integrates the BBDR-HPT axis model developed by McLanahan et al. (submitted) with a modified PBPK model for ClO_4^- in the adult male rat (Merrill *et al.*, 2003). This integration of models is an example of how the BBDR-HPT axis model can be combined with PBPK models for environmental contaminants, via specific modes of action, to predict perturbations in thyroid hormone homeostasis. Depending on the mode of action of the chemical, the BBDR-HPT axis model may need to be modified. In addition, combining PBPK models of thyroid disrupting chemicals with the BBDR-HPT axis model provides a means to test hypotheses concerning mode of action of these chemicals on the HPT axis.

Materials and Methods

To analyze the dose-response relationship between ClO_4^- exposure and effects on the HPT axis, a physiologically-based pharmacokinetic (PBPK) model for ClO_4^- was developed and integrated with the BBDR-HPT axis model previously reported (McLanahan *et al.*, submitted) for the adult rat. Using these linked models provided a framework for evaluating the hypothesis that ClO_4^- indirectly decreases serum T_4 concentrations by inhibiting thyroidal iodide uptake, causing a lack of available iodide for thyroid hormone synthesis

Model Structure

The models were constructed in acslXtreme version 2.4.0.11 (AEgis Technologies, Huntsville, Alabama) and solved using the Gear algorithm for stiff systems. The BBDR-HPT axis model for dietary iodide and the thyroid axis was used as previously described (McLanahan *et al.*, submitted). Briefly, the BBDR-HPT axis model includes four sub-models: dietary iodide,

thyroid stimulating hormone TSH, T_4, and T_3. The models combine to form a simplified representation of the thyroid axis in the adult rat that includes TSH stimulation of thyroidal iodide uptake at the NIS, incorporation of iodide into thyroid hormone precursors within the thyroid, and secretion of thyroid hormones (T_4 and T_3) into the bloodstream. The TSH/T_4 negative feedback loop is described, along with metabolism of thyroid hormones and recycling of iodide. Several additions were made to the BBDR-HPT axis model to incorporate the mode of action for ClO_4^- perturbation of the thyroid axis. These modifications are detailed in the following sections.

Perchlorate PBPK Model Structure. A simple model structure for ClO_4^- was constructed consisting of three compartments: plasma, thyroid, and rest of body. Perchlorate is rapidly absorbed after oral administration and is distributed throughout the body, but excreted virtually unchanged through the urine (Wolff, 1998). Urinary excretion of ClO_4^- was described as a first order clearance from the plasma.

The thyroid is described with a blood and tissue compartment using a diffusion limited equation to describe bidirectional passive diffusion of iodide between the thyroid gland and blood and a Michaelis-Menten equation to describe active uptake of iodide into the thyroid via the NIS protein. Several studies have shown that ClO_4^- and $^{36}ClO_4^-$ are transported into the thyroid via the NIS and an increased uptake of this anion has been observed in rats administered TSH and in conditions where TSH serum levels are increased in response to ClO_4^- exposure (Anbar *et al.*, 1959; Chow *et al.*, 1969; Chow and Woodbury, 1970; Goldman and Stanbury, 1973; and Yu *et al.*, 2002).

Datasets Used for Perchlorate PBPK Model Development. The PBPK model for ClO_4^- was developed and tested using iv dosing study kinetics of $^{36}ClO_4^-$ from Yu *et al.* (2002). Adult

male Sprague-Dawley rats were administered 3.3 mg $^{36}ClO_4^-$/kg bw and serum and thyroid concentrations determined 0.5, 6, 12, 24, 32, and 48 hrs post injection. Cumulative urinary excretion of $^{36}ClO_4^-$ was reported 12 and 24 hrs post injection. In addition, the ClO_4^- serum and thyroid concentrations at 1, 5, and 14 days following administration of 1, 3, 10, and 30 mg ClO_4^- /kg bw in drinking water were simulated using the model (Yu *et al.*, 2002).

BBDR-HPT Axis and Perchlorate PBPK Model Integration. The PBPK model for ClO_4^- was integrated with the BBDR-HPT axis model for the adult male rat to test the hypothesis that ClO_4^- disruption of HPT axis homeostasis is due to its ability to competitively inhibit NIS thyroidal iodide transport. To test this hypothesis, competitive inhibition of ClO_4^- and iodide uptake at the thyroid NIS was described using the following equations:

$$\frac{dTNIS_i}{dt} = \frac{V\max T_i^{TSH} * Cvt_i}{Cvt_i + Km_i * (1 + \frac{Cvt_p}{Ki_p})} \quad [1]$$

$$V\max T_i^{TSH} = \frac{V\max T_i \times Ca_{TSH}}{K_{NIS}^{TSH} + Ca_{TSH}} \quad [2]$$

where Cvt_i is the free concentration of iodide in thyroid blood (nmol/L), Km_i is the affinity constant of iodide for the NIS (nmol/L), Ki_p is inhibition constant of ClO_4^- for iodide transport via the NIS (nmol/L), Cvt_p is the concentration of ClO_4^- in the thyroid blood (nmol/L), $VmaxT_i$ is the maximum rate of NIS iodide uptake (nmol/hr), Ca_{TSH} is the serum concentration of TSH (nmol/L), and K^{TSH}_{NIS} is the concentration of TSH that gives rise to half-maximal rate of NIS transport of iodide (nmol/L). A similar equation was used for the inhibition of iodide on the uptake of ClO_4^- via the NIS; however, the inhibition of ClO_4^- uptake is minimal because ClO_4^- has a much greater affinity for the NIS compared to iodide (1500 nmol ClO_4^-/L vs. 31519 nmol I/L).

Model Parameters

When possible, model parameters were derived from the published literature. Default allometric scaling assumptions were used. Blood flows (Q), maximum velocities (Vmax), and permeability area cross products were multiplied by $BW^{0.75}$ and clearance terms (Cl) were scaled by $1/BW^{0.25}$.

Physiological Parameters. Physiological parameters including tissue volumes (V) and blood flows (Q) were obtained from literature (Brown et al. 1997; Everett et al., 1956; Malendowicz and Bednarek, 1986; McLanahan et al. 2007) and are shown in Table 1.

Chemical-Specific Parameters. All parameter values for the BBDR-HPT axis model were identical to those previously detailed in McLanahan *et al.* (submitted) for the initial evaluation of the hypothesis that ClO_4^- disturbed the HPT axis by inhibition of active uptake of thyroidal iodide by the NIS. However, the model was modified to test the hypothesis that ClO_4^- also affects thyroid hormone synthesis. The parameters for ClO_4^-, iodide parameters, and the BBDR-HPT axis model parameters for the second hypothesis are shown in Tables 5.2 and 5.3. The affinity constant, Km_p, of ClO_4^- for the NIS was set equal to the inhibition constant (Ki_p) for the inhibition of iodide uptake by ClO_4^-, determined to be 1.5 μM by an *in vitro* study in Chinese Hamster Ovary cells (CHO-4J) by Kosugi and colleagues (1996). The tissue:blood partition coefficient ($PBody_p$, 0.416 unitless) for the rest of body compartment for ClO_4^- was first estimated by weighting the partition coefficients, based on tissue volume, used in the Merrill et al. (2003) adult male rat model. However to fit maximum serum $^{36}ClO_4^-$ concentrations following iv dose of 3.3 mg $^{36}ClO_4^-$/kg (Yu *et al.*, 2002), $PBody_p$ was optimized to a value of 0.36.

Datasets used for Simulation of Perchlorate HPT Axis Perturbations

Two studies on the time-course of ClO_4^- induced HPT axis perturbations were available. The first study conducted by Mannisto *et al.* (1979) examined the effect of a 15 mg ClO_4^-/kg-day drinking water exposure on adult male Sprague-Dawley (SD) rats. Serum T_4 and TSH concentrations were reported following 0, 2, 4, 6, 9, and 14 days of exposure. In the second study, Yu et al. (2002) administered 0, 1, 3, or 10 mg ClO_4^-/kg-day in drinking water to adult male SD rats. Serum total T_4, T_3, TSH, and ClO_4^- concentrations were determined after exposure for 1, 5, and 14 days.

Another study reported HPT axis perturbations after administration of ClO_4^- in drinking water for 14 days. Caldwell (1995) administered ClO_4^- in drinking water to adult male and female SD rats at dose rates of 0, 0.1, 0.4, 1, 2, 4, 11, or 22 mg/kg-day for 14 days. Serum T_4 and TSH were reported by Caldwell (1995). This dataset did not include time course data; responses were only measured at the end of the 14 day exposure period.

Results

Perchlorate PBPK Model Parameterization

Parameters for the PBPK model for ClO_4^- were derived from published literature when available. Several parameters were optimized (acslXtreme Parameter Estimation v 2.4.0.11) for the model as shown in Table 5.2. The 1st order urinary clearance constant ($Cluc_p$, 0.018 L/hr-kg) was optimized to fit the cumulative urinary excretion data from Yu *et al.* (2002) of $^{36}ClO_4^-$ following an iv injection of 3.3 mg $^{36}ClO_4^-$/kg to adult male rats. Several parameters for the movement of ClO_4^- into and out of the thyroid were optimized to the $^{36}ClO_4^-$ thyroid concentrations reported after the 3.3 mg $^{36}ClO_4^-$/kg bw iv dose reported by Yu *et al.* (2002).

These parameters included the maximum velocity for ClO_4^- NIS transport under TSH stimulation ($VmaxTc^{TSH}_p$, 177 nmol/hr-kg), concentration of serum TSH resulting in half-maximal rate of NIS transport (Kp^{TSH}_{NIS}, 0.949 nmol/L), and the permeability area cross-product for bidirectional diffusion of ClO_4^- across the thyroid membrane ($PATc_p$, 2.8×10^{-4} L/hr-kg). The simple PBPK model developed for ClO_4^- adequately predicted serum and thyroid $^{36}ClO_4^-$ concentrations as well as cumulative urinary excretion following an iv dose of 3.3 mg $^{36}ClO_4^-$/kg (Yu *et al.*, 2002) as seen in Figure 5.3.

Model Parameterization of Integrated Perchlorate PBPK and BBDR-HPT axis Models

After successfully simulating thyroid axis perturbations in iodide deficiency (McLanahan *et al.*, submitted), and evaluating previously published ClO_4^- and radiolabeled iodide models (Clewell *et al.*, 2003a, 2003b; Merrill *et al.*, 2003, 2005), we tested the ability of the model to predict HPT axis perturbations resulting from ClO_4^- competitive inhibition of NIS thyroidal iodide transport, the universally recognized mode of action for HPT axis effects following exposure to ClO_4^-. We then created model code to describe this mode of action for ClO_4^- (Equation 1) to predict ClO_4^- induced perturbations in the HPT axis. We speculated that the inhibition of thyroid iodide uptake by ClO_4^- would result in a lack of iodide available for thyroid hormone production, similar to decreased thyroid iodide seen after administration of low iodide diets to rodents.

Unexpectedly, using only the inhibition of iodide uptake via the NIS as the mode of action for ClO_4^- HPT axis perturbation (Equation 1), the model was unable to predict the rapid changes in serum T_4 and TSH following exposure to 1, 3, or 10 mg ClO_4^-/kg-day (Figure 5.4). In the ID BBDR-HPT axis model, thyroidal iodide stores were closely related to perturbations in the HPT axis. With ClO_4^- it was apparent that the HPT axis was disturbed before the thyroidal

iodide stores were predicted to be depleted. For ID, slow depletion of thyroidal iodide pools was governed by thyroidal iodide availability and the rate thyroid hormones were secreted and metabolized. As seen in Figure 5.4C, the model generated serum T_4 levels agreed favorably with the time course data only on day 14 for the 10 mg ClO_4^-/kg-day exposure; however, other HPT axis responses and time points were not predicted by the model.

To evaluate the role of the NIS in the discrepant behavior between prediction and observation the model was configured to assume the ClO_4^- caused complete inhibition of thyroidal iodide uptake. Simulations predicted a slower decline in serum T_4 concentrations than observed after administration of ClO_4^- in drinking water (data and simulation not shown). The rodent thyroid stores 10-15 µg iodide (McLanahan *et al.*, 2007), and uses about 1.4 µg/day in thyroid hormone production. After 5 days of complete inhibition of thyroidal NIS iodide transport, the model predicted a 30% decline in serum T_4 concentrations compared to controls and thyroid iodide stores were predicted to be about 8 µg (a decrease of 51%). With complete inhibition of NIS iodide transport, passive diffusion of iodide into the thyroid provided 0.14 µg I/day. However, after only one day of exposure to 10 mg ClO_4^-/kg-day in drinking water Yu *et al.* (2002) reported a 25% decline in serum T_4 concentrations relative to control animals.

Consequently, a new hypothesis was created which states that ClO_4^- affects the production and/or secretion of thyroid hormones in addition to the inhibition of NIS iodide transport. This idea that ClO_4^- may affect thyroid hormone synthesis has previously been discussed in the literature as a possibility (Hildebrandt and Halmi, 1981; Wolff, 1998; and Yu *et al.*, 2002). Although the exact mechanism for the rapid decline in serum T_4 due to ClO_4^- has yet to be elucidated; the use of a suppression constant, K_p (1.4×10^5 nmol ClO_4^-/L), for the effect of ClO_4^- on thyroid hormone production provided for a much better fit of literature data at the early

time points (Figure 5.5). Andersen *et al.* (1987) used inhibition constants to describe multiple mechanisms of substrate interaction for the metabolism of trichloroethylene and 1,1-dichloroethylene. A similar approach using suppression constants was employed by Vinegar et al. (1994), where a suppression constant was estimated for inhibition of the metabolism of HCFC-123 in rats.

A Hill coefficient (n_2=2) was also used in the equation to provide for a faster (steeper) slope for the rate of ClO_4^- inhibition of thyroid hormone synthesis. Hill coefficients have been used previously for describing gene induction (Andersen *et al.*, 1993, 1997 and Kohn *et al.*, 1993) resulting from exposure to dioxin. Using modified Hill equations allows dose-response curves to take on variable shapes, sigmoidal or logarithmic. The modified equation used for thyroid hormone production is:

$$\frac{dTH_{pr}}{dt} = k_{TSH}^{IB} \times Ca_{TSH} \times CT_{iB} \times \frac{\left(K_p\right)^{n_2}}{\left(Cvt_p\right)^{n_2} + \left(K_p\right)^{n_2}} \qquad [3]$$

where k^{IB}_{TSH} is the rate constant for thyroid hormone production (5×10^{-7}, L^2/nmol/hr), Ca_{TSH} is the model predicted serum concentration of TSH (nmol/L), CT_{IB} (nmol/L) is the concentration of iodide bound as thyroid hormone precursors in the thyroid, and Cvt_p (nmol/L) is the model predicted thyroid concentration of ClO_4^-.

Modifying the equation for thyroid hormone production resulted in better simulations for T_4, but still did not capture the rapid increase in serum TSH concentrations. Thus, the equation for TSH production used in the iodide deficiency BBDR-HPT axis model simulations was modified by adding a Hill coefficient (n_1=0.94) and the concentration of T_4 resulting in half-maximal TSH production (K^{inh}_{T4}) was increased to 0.3 nmol/L, compared to the 0.2 nmol/L used previously. The Hill coefficient for n_1 of 0.94 compared to 1 provided for a steeper dose

response for TSH production in low T_4 concentrations, less than K^{inh}_{T4}. Thus, the modified T_4/TSH negative feedback equation describing the rate of TSH production:

$$\frac{dTSH_{pr}}{dt} = \frac{k_0^{TSH} \times \left(K_{T4}^{inh}\right)^{n_1}}{\left(K_{T4}^{inh}\right)^{n_1} + \left(Ca_{T4}\right)^{n_1}} \qquad [4]$$

where k_0^{TSH} is the maximal rate of TSH production in the absence of T_4 (nmol/hr), K^{inh}_{T4} is the concentration of T_4 that results in half-maximal rate of TSH production (nmol/L), Ca_{T4} is the concentration of T_4 in the serum (nmol/L), and n_1 is a Hill coefficient (unitless).

The modified thyroid hormone (Equation 3) and TSH production (Equation 4) equations were used to visually fit the Hill coefficients (n_1=0.94 and n_2=2), serum T_4 control of TSH production (K^{inh}_{T4}=0.3 nmol/L), and the suppression of thyroid hormone production by ClO_4^- ($K_p=1.4\times10^5$ nmol/L) to the time course of perturbations resulting from ClO_4^- reported by Yu *et al.* (2002). Using this approach, along with ClO_4^- competitive inhibition of thyroidal iodide uptake, the model was able to predict the rapid changes in serum T_4 and TSH seen that were observed after one day of exposure to 1, 3, and 10 mg ClO_4^-/kg-day in drinking water (Figure 5.5). The model predicted only slight recovery over the 14 day period, but the predictions are in accordance with the literature reported data (Yu *et al.*, 2002). Inhibition of synthesis over the 14 day period does not lessen, according to model predictions. However, TSH stimulation of thyroidal processes is an apparent compensatory mechanism to prevent serum T_4 levels from dropping below 50% at the highest dose administered (10 mg ClO_4^-/kg-day). At this ClO_4^- dose rate, the model predicted TSH upregulation of thyroidal iodide uptake (2-fold), incorporation of the iodide in the thyroid into thyroid hormone precursors (2.5-fold), and the stimulation of hormone secretion (3-fold).

Simulated oscillations in T_4 and TSH concentrations result because the ClO_4^- concentrations in the thyroid are used to describe the inhibition of thyroid hormone synthesis (Equation 3) and are periodic relative to ClO_4^- consumption. Consumption of ClO_4^- (and dietary iodide) takes place over a 12-hr period, during the dark hours, thus over the 12-hr period when ClO_4^- is ingested serum and thyroid concentrations rise and are cleared during the period of non-ingestion (sleep). The periodicity of ClO_4^- concentrations in the serum and thyroid as predicted by the model are shown in Figures 5.6A and 5.6B, respectively. The model adequately predicts serum concentrations following exposure to 1, 3, and 10 mg ClO_4^-/kg-day in drinking water for 1-14 days. However, ClO_4^- thyroid concentrations are underpredicted by the model on day 5 of exposure to ClO_4^- for the 3 and 10 mg/kg-day dose groups. One possible explanation for this discrepancy is that at these doses changes in the thyroid gland begin to occur, leading to hypertrophy and increased thyroid weight. Perchlorate thyroid concentration in rats given an iv dose of 3.3 mg $^{36}ClO_4^-$/kg-day were adequately predicted (Figure 5.4).

Model Validation for the Adult Male Rat

The BBDR-HPT axis model integrated with the ClO_4^- PBPK model was tested for its ability to predict HPT axis disturbances observed in published literature ClO_4^- datasets not used for model calibration. The Yu *et al.* (2002) data, physiological parameters (Table 5.1), and compound specific parameters (Table 5.2) either derived from literature, optimized, or estimated, were used to obtain a calibrated model. The calibrated model was then used to simulate the data from Mannisto *et al.* (1979) and Caldwell (1995). Mannisto *et al.* (1979) administered 15 mg ClO_4^-/kg-day to adult male Sprague-Dawley rats (10-20 µg I /day) and measured serum T_4 and TSH concentrations after 2, 4, 6, 9, and 14 days of exposure. The model simulations were able to predict the temporal increase in TSH over the study period as well as decrease in T_4 (Figure

5.7). The TSH upregulation of the thyroid prevented the serum T_4 from decreasing more than 50% of control.

The model was tested over a wide range of concentrations to predict the adult rat T_4 and TSH dose-response following a 14 day exposure period to ClO_4^- in drinking water. Caldwell (1995) administered 0, 0.1, 0.4, 1, 2, 4, 11, or 22 mg ClO_4^-/kg-day to male and female rats. The dose-response curve generated by the model for serum T_4 and TSH is compared to the data reported by Caldwell (1995) in Figure 5.8. The model predicts the changes relative to control animals better for higher dose rates (>2 mg ClO_4^-/kg-day) of ClO_4^- in comparison to the under prediction of TSH and over prediction of T_4 at low dose rates (< 2 mg ClO_4^-/kg-day).

Discussion

A dietary iodide biologically based dose-response (BBDR) model of dietary iodide the hypothalamic-pituitary-thyroid (HPT) axis (BBDR-HPT axis model) was integrated with a physiologically-based pharmacokinetic (PBPK) model for perchlorate (ClO_4^-). Alone, the BBDR-HPT axis model was shown capable of predicting HPT axis perturbations resulting from iodide deficiency (McLanahan *et al.*, submitted). For many decades, ClO_4^- perturbations of the HPT axis were thought to arise because of a lack of available iodide within the thyroid for thyroid hormone production (Wyngaarden *et al.*, 1952; Yu *et al.*, 2002). We first tested the hypothesis that competitive inhibition of thyroidal iodide transport by ClO_4^- at the sodium/iodide symporter (NIS), causes an iodide deficient condition within the thyroid and subsequent decrease in serum T_4 and increase in serum TSH. The model failed to predict the rapid decline in serum T_4 and rapid compensatory rise in serum TSH (Figure 5.4) observed in adult rats (Yu *et al.*, 2002). We believe this failure occurred because the model predicted iodide stores within the

thyroid are not depleted within 24 hours of cessation of iodide intake or complete inhibition of NIS iodide transport.

When the BBDR-HPT axis model linked with the ClO_4^- PBPK model via inhibition of iodide uptake failed to predict the rapid changes in thyroid indices reported in literature, we hypothesized an additional mode of action for ClO_4^- induced perturbation of the HPT axis. The second hypothesis tested was that thyroidal ClO_4^- inhibits the production and secretion of thyroid hormones. By modifying the description of thyroid hormone production (Equation 3) by the including ClO_4^- suppression of the rate of hormone synthesis and secretion, coupled with the competitive inhibition of thyroidal iodide transport, we were able to adequately describe many changes in serum T_4 observed in literature (Figures 5.5, 5.7 and 5.8). It was also necessary to include Hill coefficients in the equation for TSH production (Equation 4) to describe a more sensitive negative feedback effect of T_4 on TSH production. The Hill coefficient (n_1=0.94) along with a slight increase in the set-point for TSH secretion (K^{inh}_{T4} = 0.3 nmol/L) provided for a more rapid TSH increase seen when ClO_4^- is administered, compared to changes seen in iodide deficient conditions.

With these modifications, the model predicted literature reported perturbations following exposure to 1-22 mg ClO_4^-/kg-day in drinking water (Caldwell, 1995; Mannisto *et al.*, 1979; and Yu *et al.*, 2002). However, the model was less successful at simulating low-dose exposures (<1 mg ClO_4^-/kg-day). The reason for this is unknown, but model parameters could be adjusted to account for this difference in future iterations and applications of the model. Noteworthy, there are many difficulties surrounding determination of HPT axis perturbations resulting from low-dose exposures to thyroid active compounds (McLanahan *et al.*, 2007). For example, the assay methods may not be sensitive enough to detect minor changes in the hormone levels; lack of

sensitivity of T_4 at low doses may also be due to the cyclic and diurnal secretion of thyroid hormones (McNabb *et al.*, 2004) and variability in time of sampling.

Several investigators have suggested that ClO_4^- could be acting on the thyroid via modes of action yet to be elucidated. Hildebrandt and Halmi (1981) suggested that ClO_4^- is capable of altering the processing and utilization of iodide within the thyroid as well as inhibiting NIS transport. In a review article, Wolff (1989) hypothesized that the anion effect, reduction in thyroid hormone secretion by anions themselves and not larger iodocompounds, resulting from excess iodide in the thyroid would be mimicked by similar anions that are related to iodide by hydration enthalpy, size, and accumulation in the thyroid. Iodide (I^-) and ClO_4^- are similar in ionic size, charge, and hydration enthalpy. The ClO_4^- anion has a hydration enthalpy of -238 and I^- anion of -295 kJ/mol; thus it is plausible that the anion effect could be seen with ClO_4^- resulting in a decrease in thyroid hormone production and secretion. Furthermore, due to the persistently low serum T_4 concentrations following ClO_4^- exposure, Yu *et al.* (2002) suggested that in addition to inhibition of thyroidal iodide uptake, ClO_4^- may also exert secondary effects on the thyroid. Although many researchers have suspected ClO_4^- of exerting effects in addition to inhibition of thyroidal iodide uptake, additional modes of action have yet to be confirmed in the laboratory.

We used the BBDR-HPT axis model combined with a PBPK model for ClO_4^- to test the hypothesis that ClO_4^- inhibits thyroid hormone synthesis and secretion. In order to fit the rapid decrease in serum T_4, the model predicted a 25-70% decrease in overall thyroid hormone production for the range of ClO_4^- doses examined (1-15 mg ClO_4^-/kg-day). The inhibition in thyroid hormone production does not appear to be alleviated by TSH, but does disappear when ClO_4^- is excreted. In this empirical description of thyroid hormone production and ClO_4^-

suppression, TSH appears to compensate for the decrease in T_4 by stimulating the thyroid but the effect of ClO_4^- on inhibition of thyroid hormone persists over the 14 day period. Possibly, TSH is able to help compensate for the inhibition of iodide transport and thyroid hormone production, but is unable to compensate to overcome the effect of perchlorate.

In summary, the use of a BBDR-HPT axis model coupled with a ClO_4^- PBPK model provided a mathematical framework for exploration of ClO_4^-induced perturbations of the HPT axis in adult rats. A simple link between the models using inhibition of NIS thyroidal iodide transport by ClO_4^- was unable to predict the rapid changes in serum T_4 and TSH reported in literature. Previously, the BBDR-HPT axis model successfully simulated changes in the HPT axis from differing degrees of iodide deficiency (McLanahan *et al.*, submitted); therefore, when the model failed to predict changes because of a lack of iodide in the thyroid due to ClO_4^- inhibition of uptake, we hypothesized that ClO_4^- also affected the synthesis and secretion of thyroid hormones. Modification of the thyroid hormone production rate with a suppression effect due to thyroidal ClO_4^- concentrations enabled the model to predict the ClO_4^- induced HPT axis perturbations reported in literature. Future laboratory experiments could confirm or reject this model generated hypothesis and more research is necessary to determine if this mode of action is applicable in humans, which exhibit less sensitivity to ClO_4^- perturbation than do rodents.

Acknowledgments

Funding provided by a U.S. EPA Science to Achieve Results research grant (RD83213401-0) and a U.S. EPA Science to Achieve Results Fellowship (FP-91679301-0 to EDM). Views expressed in this manuscript are those of the authors and do not represent official opinions of U.S. EPA.

References

Anbar, M., Guttmann, S., and Lewitus, Z. (1959). The Mode of Action of Perchlorate Ions on the Iodine Uptake of the Thyroid Gland. *Int. J. App. Radiat. Isotopes.* **7,** 87-96.

Andersen, M.E., Eklund, C.R., Mills, J.J., Barton, H.A., and Birnbaum, L.S. (1997). A Multicompartment Geometric Model of the Liver in Relation to Regional Induction of Cytochrome P450s. *Toxicol. Appl. Pharmacol.* **144,** 135-144.

Andersen, M.E., Gargas, M.L. Clewell, H.J., and Deveryn, K.M. (1987). Quantitative evaluation of the metabolic interactions between trichloroethylene and 1,1-dichloroethylene in vivo using gas uptake methods. *Toxicol. Appl. Pharmacol.* **89,** 149-157.

Andersen, M.E., Mills, J.J., Gargas, M.L., Kedderis, L., Birnbaum, L.S., Neubert, D., and Greenlee, W.F. (1993). Modeling receptor-mediated processes with dioxin: implications for pharmacokinetics and risk assessment. *Risk Anal.* **13,** 25-36.

Blount, B.C., Pirkle, J.L, Osterloh, J.D., Valentin-Blasini, L., and Caldwell, K.L. (2006). Urinary perchlorate and thyroid hormone levels in adolescent and adult men and women living in the United States. *Environ. Health Perspect.* **114**, 1865-1871.

Brown, R., Delp, M., Lindstedt, S., Rhombert, L., and Belies, R. (1997). Physiological Parameter Values for Physiologically Based Pharmacokinetic Models. *Toxicol. Ind. Health.* **13,** 407-484.

Caldwell, D.J., King, J.H., Kinkead, E.R, Wolfe, R.E., Narayanan, L., and Mattie, D.R. (1995). Results of a Fourteen Day Oral-Dosing Toxicity Study of Ammonium Perchlorate. Dayton, OH: Tri-Service Toxicology Consortium, Armstrong Laboratory, Wright-Patterson Air Force Base.

Chow, S.Y., Chang, L.R., and Yen, M.S. (1969). A Comparison between the Uptakes of Radioactive Perchlorate and Iodide by Rat and Guinea-Pig Thyroid Glands. *J. Endocrinol.* **45,** 1-8.

Chow, S.Y., and Woodbury, D.M. (1970). Kinetics of Distribution of Radioactive Perchlorate in Rat and Guinea-Pig Thyroid Glands. *J. Endocrinol.* **47,** 207-218.

Clewell, R.A., Merrill, E.A., Yu, K.O., Mahle, D.A., Sterner, T.R., Fisher, J.W., and Gearhart, J. M. (2003a). Predicting Neonatal Perchlorate Dose and Inhibition of Iodide Uptake in the Rat during Lactation Using Physiologically-Based Pharmacokinetic Modeling. *Toxicol. Sci.* **74,** 416-436.

Clewell, R.A., Merrill, E.A., Yu, K.O., Mahle, D.A., Sterner, T.R., Mattie, D., Robinson, P., and Fisher, J.W. (2003b). Predicting Fetal Perchlorate Dose and Inhibition of Iodide Kinetics during Gestation: A Physiologically-Based Pharmacokinetic Analysis of Perchlorate and Iodide Kinetics in the Rat. *Toxicol. Sci.* **73,** 235-255.

Dasgupta, P.K., Martinelango, P.K., Jackson, W.A., Anderson, T.A., Tian, K., Tock, R.W., and Rajagopalan, S. (2005). The Origin of Naturally Occurring Perchlorate: The Role of Atmospheric Processes. *Environ. Sci. Technol.* **39,** 1569-1575.

El Aribi, H., Le Blanc, Y.J.C., Antonsen, S., and Sakuma, T. (2006). Analysis of perchlorate in foods and beverages by ion chromatography coupled with tandem mass spectrometry (IC-ESI-MS/MS). *Anal. Chim. Acta.* **567,** 39-47.

Everett, N.B., Simmons, B., and Lasher, E.P. (1956). Distribution of Blood (Fe59) and Plasma (I131) Volumes of Rats Determined by Liquid Nitrogen Freezing. *Circ. Res.* **4,** 419-424.

Ferreira, A.C.F., Lima, L.P., Araujo, R.L, Muller, G., Rocha, R.P., Rosenthal, D., and Carvalho, D.P. (2005). Rapid regulation of thyroid sodium-iodide symporter activity by thyrotropin and iodine. *J. Endocrinol.* **184,** 69-76.

Goldman, S.J. and Stanbury, J.B. (1973). The Metabolism of Perchlorate in the Rat. *Endocrinol.* **92,** 1536-1538.

Haddow, J.E., Palomaki, G.E., Allan, W.C., Williams, J.R., Knight, G.J., Gagnon, J., O'Heir, C.E., Mitchell, M.L., Hermos, R.J., Waisbren, S.E., Faix, J.D., Klein, R.Z. (1999). Maternal Thyroid Deficiency During Pregnancy and Subsequent Neuropsychological Development of the Chlid. *N. Eng. J. Med.* **341,** 549-555.

Hildebrandt, J.D. and Halmi, N.S. (1981). Intrathyroidally Generated Iodide: The Role of Transport in Its Utilization. *Endocrinol.* **108,** 842-849.

Kohn, M.C., Lucier, G.W., Clark, G.C., Sewall, C., Tritscher, A.M., and Portier, C.J. (1993). A Mechanistic Model of Effects of Dioxin on Gene Expression in the Rat Liver. *Toxicol. Appl. Pharmacol.* **120,** 138-154.

Kosugi, S., Sasaki, N., Hai, N., Sugawa, H., Aoki, N., Shigemasa, C., Mori, T., and Yoshida, A. (1996). Establishment and Characterization of a Chinese Hamster Ovary Cell Line, CHO-4J, Stably Expressing a Number of Na^+/I^- Symporters. *Biochem. Biophys. Res. Commun.* **227,** 94-101.

Malendowicz, L.K, and Bednarek, J. (1986). Sex Dimorphism in the Thyroid Gland IV. Cytologic Aspects of Sex Dimorphism in the Rat Thyroid Gland. *Acta. Anat.* **127,** 115-118.

Männistö, P.T., Ranta, T., and Leppäluto, J. (1979). Effects of methylmercaptoimidazole (MMI), propylthiouracil (PTU), potassium perchlorate (KClO4) and potassium iodide (KI) on the serum concentrations of thyrotrophin (TSH) and thyroid hormones in the rat. *Acta. Endocrinol.* **91,** 271-281.

McLanahan, E.D., Andersen, M.E., and Fisher, J.W. (Submitted 10/02/2007). A Biologically Based Dose-Response Model for Dietary Iodide and the Hypothalamic-Pituitary-Thyroid Axis in the Adult Rat: Evaluation of Iodide Deficiency. *Toxicol. Sci.* Included as Chapter 4 of this Dissertation.

McLanahan, E.D., Campbell Jr., J.L., Ferguson, D.C., Harmon, B., Hedge, J.M., Crofton, K.M., Mattie, D.R., Braverman, L., Keys, D.A., Mumtaz, M., and Fisher, J.W. (2007). Low-Dose Effects of Ammonium Perchlorate on the Hypothalamic-Pituitary-Thyroid (HPT) Axis of Adult Male Rats Pretreated with PCB126. *Toxicol. Sci.* **97,** 308-317.

McNabb, F.M.A., Jang, D.A., and Larsen, C.T. (2004). Does thyroid function in developing birds adapt to sustained ammonium perchlorate exposure? *Toxicol. Sci.* **82,** 106-113.

Merrill, E.A., Clewell, R.A., Gearhart, J.M., Robinson, P.J., Sterner, T.R., Yu, K.O, Mattie, D.R., and Fisher, J.W. (2003). PBPK Predictions of Perchlorate Distribution and Its Effect on Thyroid Uptake of Radioiodide in the Male Rat. *Toxicol. Sci.* **73,** 256-269.

Merrill, E.A., Clewell, R.A., Sterner, T.R., and Fisher, J.W. (2005). PBPK Model for Radioactive Iodide and Perchlorate Kinetics and Perchlorate-Induced Inhibition of Iodide Uptake in Humans. *Toxicol. Sci.* **83,** 25-43.

Motzer, W.E. (2001). Perchlorate: Problems, Detection, and Solutions. *Environ. Foren.* **2,** 301-311.

Riedel, C., Levy, O., and Carrasco, N. (2001). Post-transcriptional Regulation of the Sodium/Iodide Symporter by Thyrotropin. *J. Biol. Chem.* **276,** 21458-21463.

Siglin, J.C., Mattie, D.R., Dodd, D.E., Hildebrandt, P.K., and Baker, W.H. (2000). A 90-Day Drinking Water Toxicity Study in Rats of the Environmental Contaminant Ammonium Perchlorate. *Toxicol. Sci.* **57,** 61-74.

Snyder, S.A., Pleus, R.C., Vanderford, B.J., and Holady, J.C. (2006). Perchlorate and chlorate in dietary supplements and flavor enhancing ingredients. *Anal. Chim. Acta.* **567,** 26-32.

Tonacchera, M., Pinchera, A., Dimida, A., Ferrarini, E., Agretti, P., Vitti, P., Santini, F., Crump, K., and Gibbs, J. (2004). Relative potencies and additivity of perchlorate, thiocyanate, nitrate, and iodide on the inhibition of radioactive iodide uptake by the human sodium iodide symporter. *Thyroid.* **14,** 1012-1019.

U.S. EPA (United States Environmental Protection Agency). (2005). Perchlorate and Perchlorate Salts. Office of Health and Environmental Assessment, Environmental Criteria and Assessment Office, Cincinnati, OH. http://www.epa.gov/iris/subst/1007.htm [18 June, 2007].

Vinegar, A., Williams, R.J., Fisher, J.W., and McDougal, J.N. (1994). Dose-Dependent Metabolism of 2,2-Dichloro-1,1,1-trifluoroethane: A Physiologically Based Pharmacokinetic Model in the Male Fischer 344 Rat. *Toxicol. Appl. Pharmacol.* **129,** 103-113.

Wolff, J. (1989). Excess iodide inhibits the thyroid by multiple mechanisms. *Adv. Exp. Med. Biol.* **261,** 211-244.

Wolff, J. (1998). Perchlorate and the Thyroid Gland. *Pharmacol. Rev.* **50,** 89-105.

Wyngaarden, J.B., Wright, B.M., and Ways, P. (1952). The Effect of Certain Anions Upon the Accumulation and Retention of Iodide by the Thyroid Gland. *Endocrinol.* **50,** 537-549.

Yu, K.O., Narayanan, L., Mattie, D.R., Godfrey, R.J., Todd, P.N., Sterner, T.R., Mahle, D.A.m Lumpkin, M.H., and Fisher, J.W. (2002). The pharmacokinetics of perchlorate and its effect on the hypothalamus-pituitary-thyroid axis in the male rat. *Toxicol. Appl. Pharmacol.* **182,** 148-159.

Table 5.1. Physiological Parameters for the Adult Rat

Parameter	Value	Source
Tissue volumes		
Body weight, BW (kg)	0.350	McLanahan *et al.*, 2007
Plasma (% BW)	4.44	Brown *et al*., 1997; Everett *et al.*, 1956
Thyroid, VTc (% BW)	0.005	McLanahan *et al.*, 2007
Thyroid blood, VTBc (% VT)	15.7	Malendowicz and Bednarek, 1986
Rest of body, VBody	BW-VT	
Blood flows		
Cardiac output, QCc (L/hr/kg$^{0.075}$)	14.0	Brown *et al.*, 1997
Thyroid, QTc (% QC)	1.6 [a]	Brown *et al.*, 1997
Rest of body, QBody	QC-QT	

[a] Human value.

Table 5.2. Perchlorate and Iodide Parameters

Parameter	Iodide	Perchlorate	Source
Partition coefficients (unitless)			
Body:blood, PB_p	NA	0.416	Optimized
Permeability area cross-product (L/hr/kg$^{0.75}$)			
Thyroid blood to thyroid tissue, $PATc_p$	1×10^{-4}	2.8×10^{-4}	Optimized
Affinity constants (nmol/L)			
Thyroid NIS transport – Km	31519	1500	Gluzman and Niepomniszcze, 1983; Kosugi *et al.*, 1996
Thyroid NIS TSH stimulation, K^{NIS}_{TSH}	0.949	0.949	Optimized
Maximum velocities (nmol/hr/kg$^{0.75}$)			
Iodide – Thyroid NIS, $VmaxTc_i$	4450	177	McLanahan *et al.*, submitted; Optimized
Clearance values (L/hr/kg$^{0.25}$)			
Urinary excretion, $ClUc_p$	0.0046	0.07	Optimized

Table 5.3. Thyroid Hormone and TSH Production Parameters

Parameter	Value	Units	Source
T_4 inhibition of TSH synthesis, K^{inh}_{T4}	0.3	nmol/L	Fitted
Thyroid hormone production, k^{TSH}_{IB}	5×10^{-7}	L^2/nmol/hr	McLanahan *et al.*, submitted.
Suppression of hormone production, K_p	1.4×10^5	nmol/L	Fitted
Hill coefficients			
TSH production, n_1	0.94	unitless	Fitted
Perchlorate suppression of hormone production, n_2	2	unitless	Fitted

Figure 5.1. Perchlorate PBPK model structure for the adult rat. Perchlorate (iv or oral drinking water dose) enters the plasma where it is excreted in urine or distributed to the thyroid or rest of the body. Thyroid is modeled with bidirectional diffusion and active uptake (bold arrow) into the thyroid via the Na+/I- symporter (NIS). The "Rest of the Body" compartment is a flow-limited compartment and includes all other body tissues into which ClO_4^- may distribute.

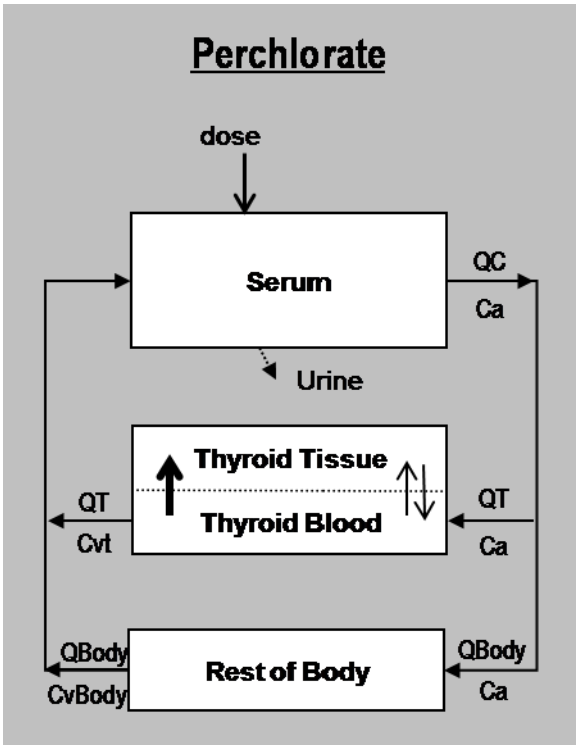
Perchlorate
dose
Serum
QC
Ca
Urine
Thyroid Tissue
Thyroid Blood
QT
Cvt
QT
Ca
QBody
CvBody
Rest of Body
QBody
Ca

Figure 5.1.

Figure 5.2. BBDR-HPT axis model structure as described previously (McLanahan *et al.*, submitted). Briefly, the model includes sub-models (areas shaded in gray) for dietary iodide (^{127}I), TSH, T_4, and T_3. Solid arrows (⟶) represent blood flows, bold arrows (➔) within tissue compartments represent active uptake, solid arrows (→) within tissue compartments represent diffusion limitation, dashed arrows between models (- - ▸) represent metabolic links, while the dashed and dotted arrow (— · ▸) represents use of dietary iodide in thyroid hormone production, and the bold (➔) arrows connecting models processes controlled (stimulated or inhibited) by the compound. Specific details on the model links shown in the figure (❶ - ❿) are described in Chapter 4 (Figure 4.2; McLanahan *et al.*, submitted).

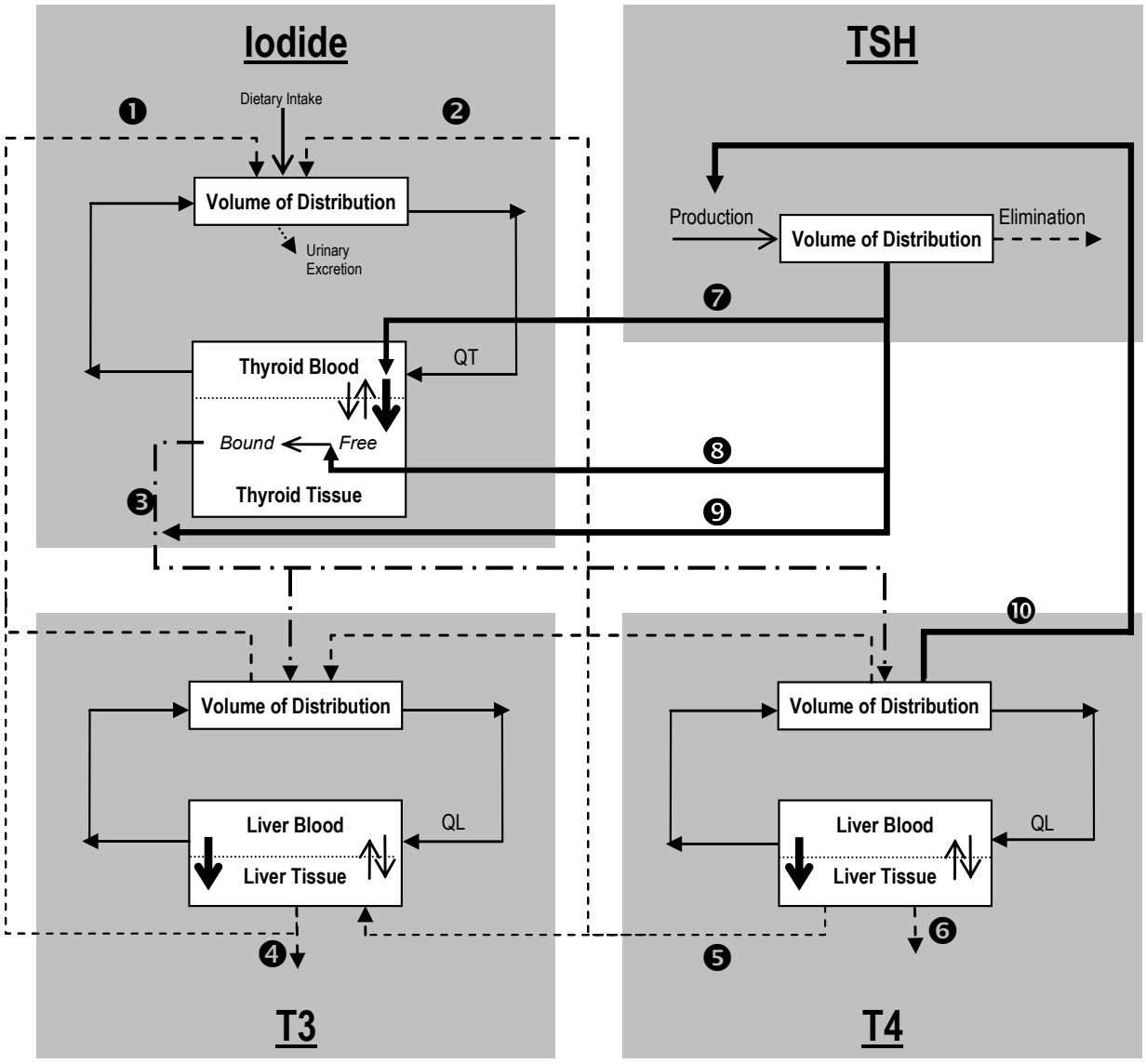
Iodide
TSH
Dietary Intake
Volume of Distribution
Urinary Excretion
Production
Volume of Distribution
Elimination
Thyroid Blood
QT
Bound
Free
Thyroid Tissue
Volume of Distribution
Liver Blood
QL
Liver Tissue
Volume of Distribution
Liver Blood
QL
Liver Tissue
T3
T4

Figure 5.2.

Figure 5.3. Model simulations (lines) of serum (——) and thyroid (– –) concentrations following 3.3 mg $^{36}ClO_4^-$/kg bw iv dose in adult male Sprague-Dawley rats compared with data (serum: ● ±SD and thyroid: ○ ± SD) from Yu *et al.*(2002). Cumulative urinary excretion model predictions of $^{36}ClO_4^-$ is shown (.....) with data (▼±SD).

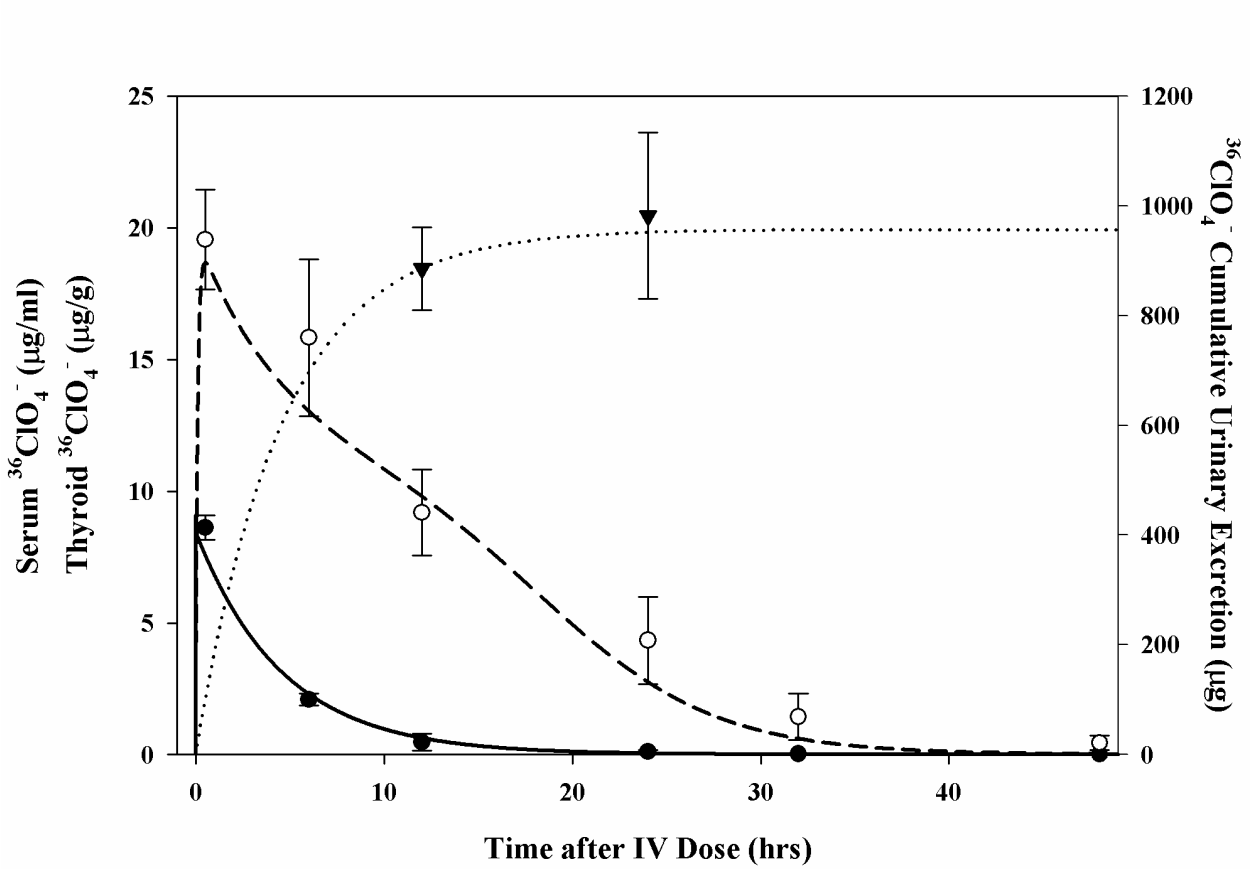
Serum $^{36}ClO_4^-$ (µg/ml)
Thyroid $^{36}ClO_4^-$ (µg/g)
$^{36}ClO_4^-$ Cumulative Urinary Excretion (µg)
Time after IV Dose (hrs)
0
5
10
15
20
25
0
200
400
600
800
1000
1200
0
10
20
30
40

Figure 5.3.

Figure 5.4. BBDR-HPT axis and ClO_4^- PBPK integrated model predictions with ClO_4^- inhibition of NIS thyroidal iodide transport. Serum T_4 and TSH model simulations following administration of (A) 1, (B) 3, or (C) 10 mg ClO_4^-/kg-day. Serum T_4 (——) and TSH (— . . —) are expressed as percent of control (100% represented by — —). Linking the BBDR-HPT axis and ClO_4^- PBPK models via ClO_4^- inhibition of iodide uptake (Equation 1) fails to produce model simulations that adequately predict the temporal or degree of changes in serum T_4 (●) and TSH (○) reported by Yu *et al.* (2002) in adult rats following exposure to ClO_4^- in drinking water.

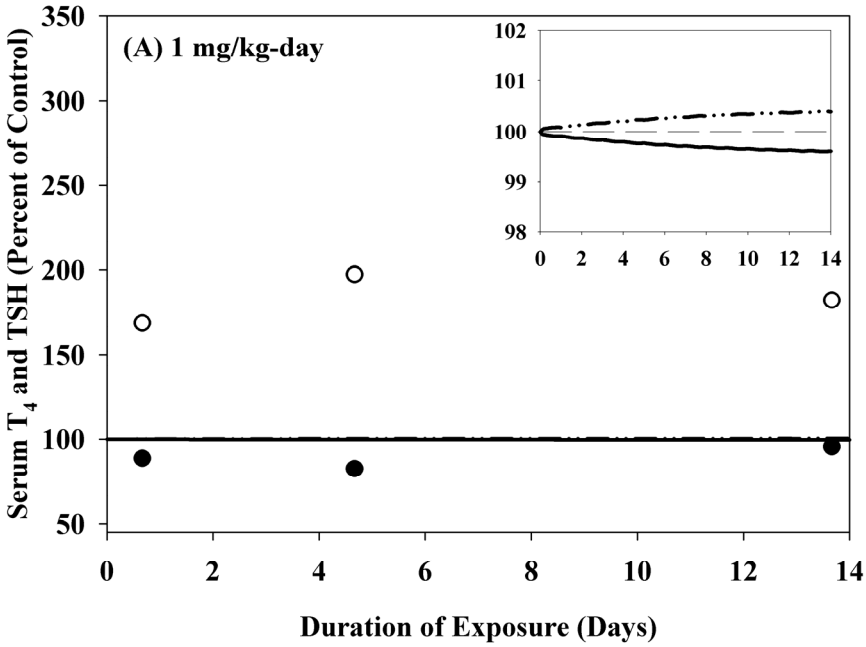

Figure 5.4A.

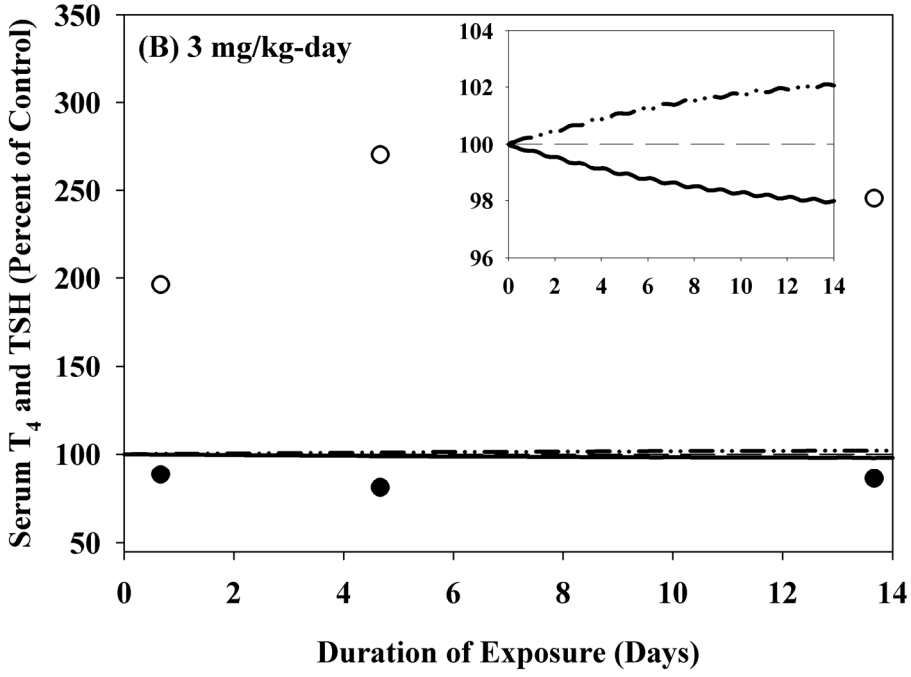

Figure 5.4B.

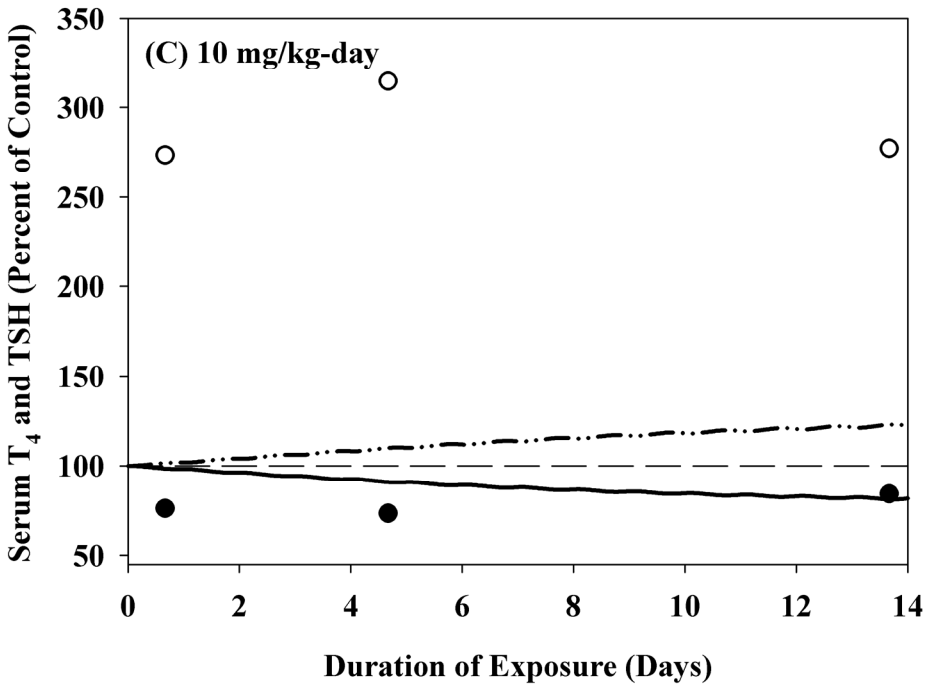
(C) 10 mg/kg-day
Serum T_4 and TSH (Percent of Control)
350
300
250
200
150
100
50
0
2
4
6
8
10
12
14
Duration of Exposure (Days)

Figure 5.4C.

Figure 5.5. BBDR-HPT axis model predictions following exposure to ClO_4^- in drinking water, including inhibition of thyroidal iodide uptake and suppression of thyroid hormone production by ClO_4^-. Serum T_4 and TSH model simulations following administration of (A) 1, (B) 3, or (C) 10 mg ClO_4^-/kg-day. Serum T_4 (——) and TSH (— . . —) are expressed as percent of control (100% represented by — —). Testing the hypothesis that thyroidal ClO_4^- also affects the synthesis and secretion of thyroid hormones provides for model simulations that adequately predict the rapid decrease in serum T_4 (●) and rise in TSH (○) reported by Yu *et al.* (2002) in adult rats following exposure to ClO_4^- in drinking water.

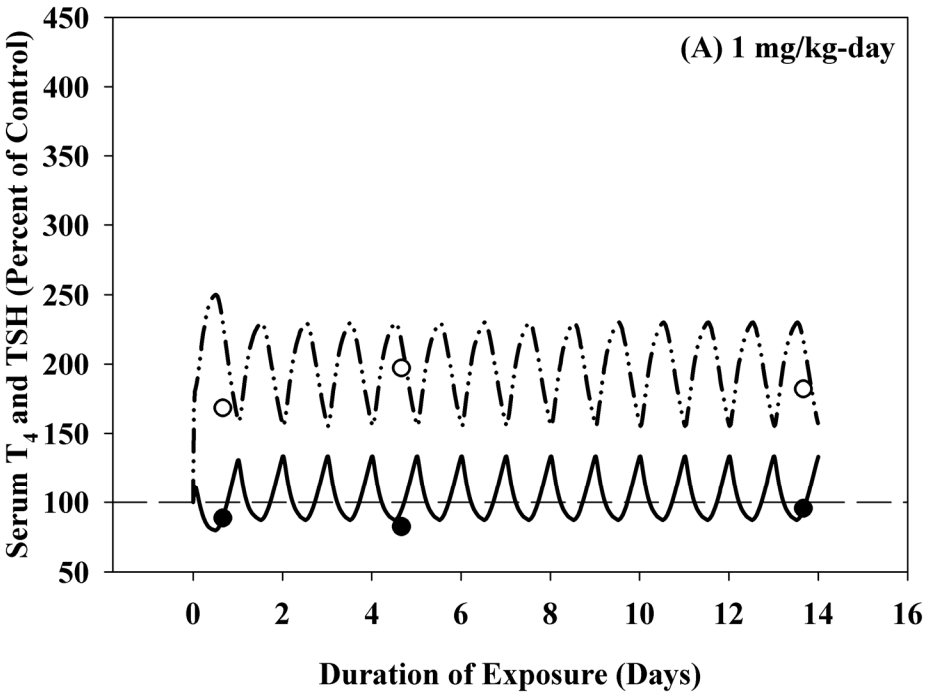

Figure 5.5A.

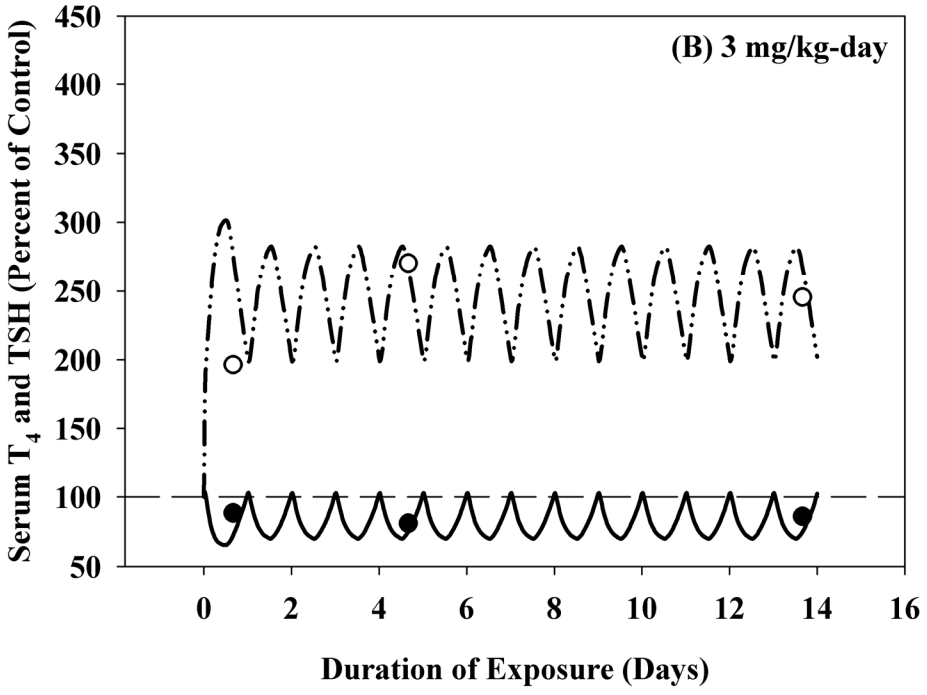

Figure 5.5B.

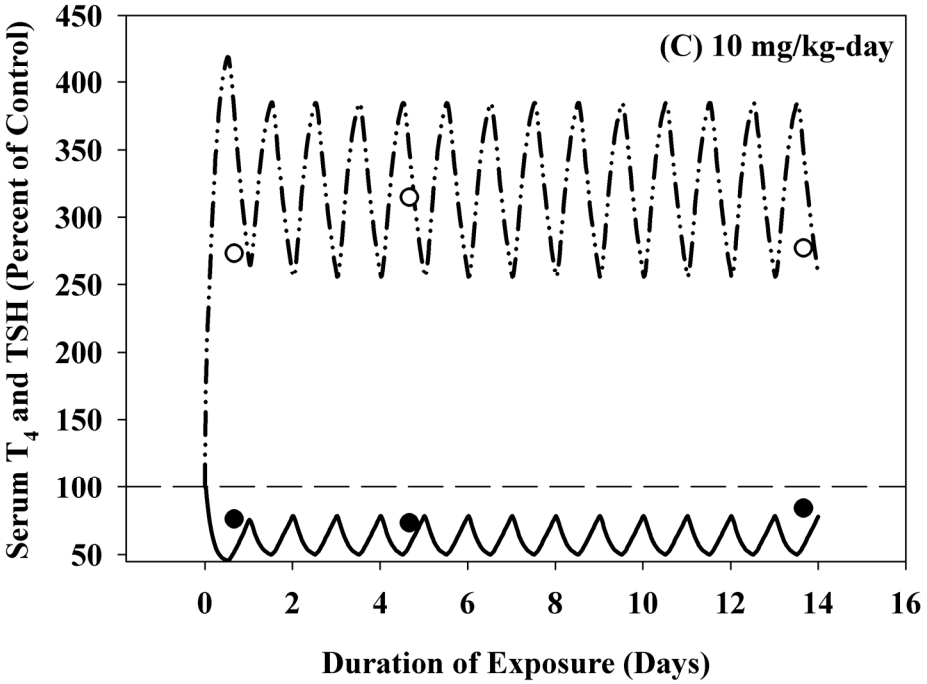
(C) 10 mg/kg-day
Serum T_4 and TSH (Percent of Control)
450
400
350
300
250
200
150
100
50
0
2
4
6
8
10
12
14
16
Duration of Exposure (Days)

Figure 5.5C.

Figure 5.6. Serum (A) and thyroid (B) concentrations of ClO_4^- in adult rats following exposure to ClO_4^- in drinking water. Model simulations (lines) are shown with data (points ± SD) from Yu *et al.* (2002). Perchlorate concentrations for 1 (——— and ●), 3 (- - - - - and ▽), and 10 (—·—·— and ■) mg ClO_4^-/kg-day.

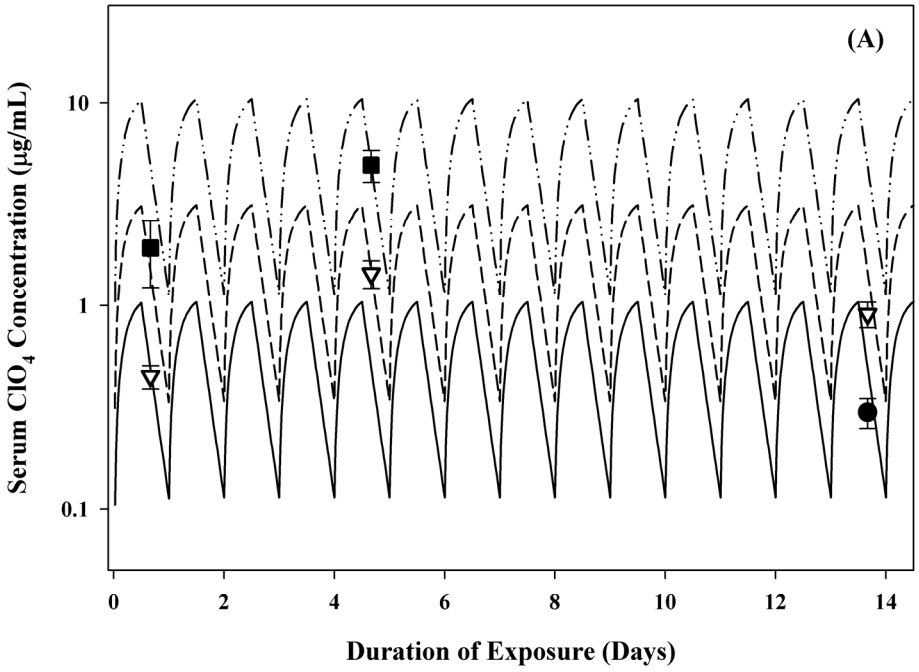

Figure 5.6A.

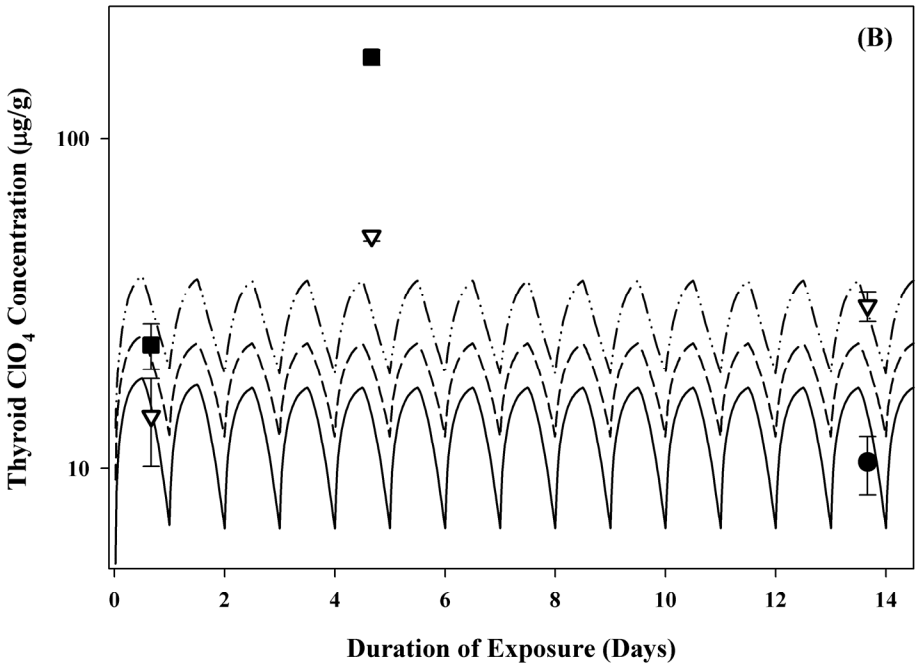

Figure 5.6B.

Figure 5.7. HPT axis perturbations in serum T_4 (——) and TSH (— . . —) following drinking water exposure to 15 mg ClO_4^-/kg-day in adult rats. Data expressed as percent of control (100%, — — —) for serum T4 (● ± SD) and TSH (○ ± SD) are adapted from Mannisto *et al.* (1979).

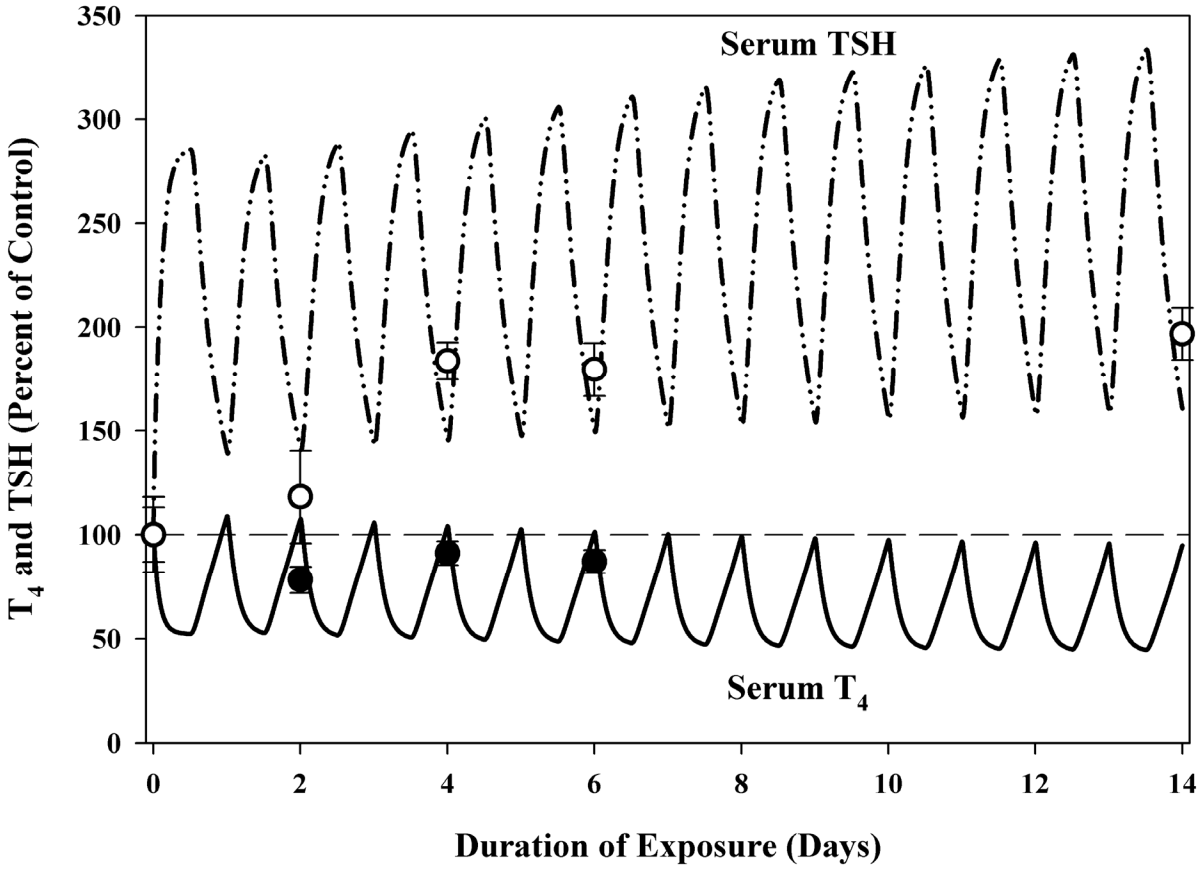
Serum TSH
Serum T_4
T_4 and TSH (Percent of Control)
Duration of Exposure (Days)
350
300
250
200
150
100
50
0
0
2
4
6
8
10
12
14

Figure 5.7.

Figure 5.8. Dose-response plot for serum T_4 and TSH after exposure to ClO_4^- in drinking water for 14 days. Model predictions of T_4 (solid line) and TSH (dashed line) are compared with adult rat data following exposure to 0, 0.1, 0.4, 1, 2, 4, 11, or 22 mg ClO_4^-/kg-day for 14 days adult rats (Caldwell, 1995). Data expressed as percent of control (100%) for serum T_4 (●) and TSH (○).

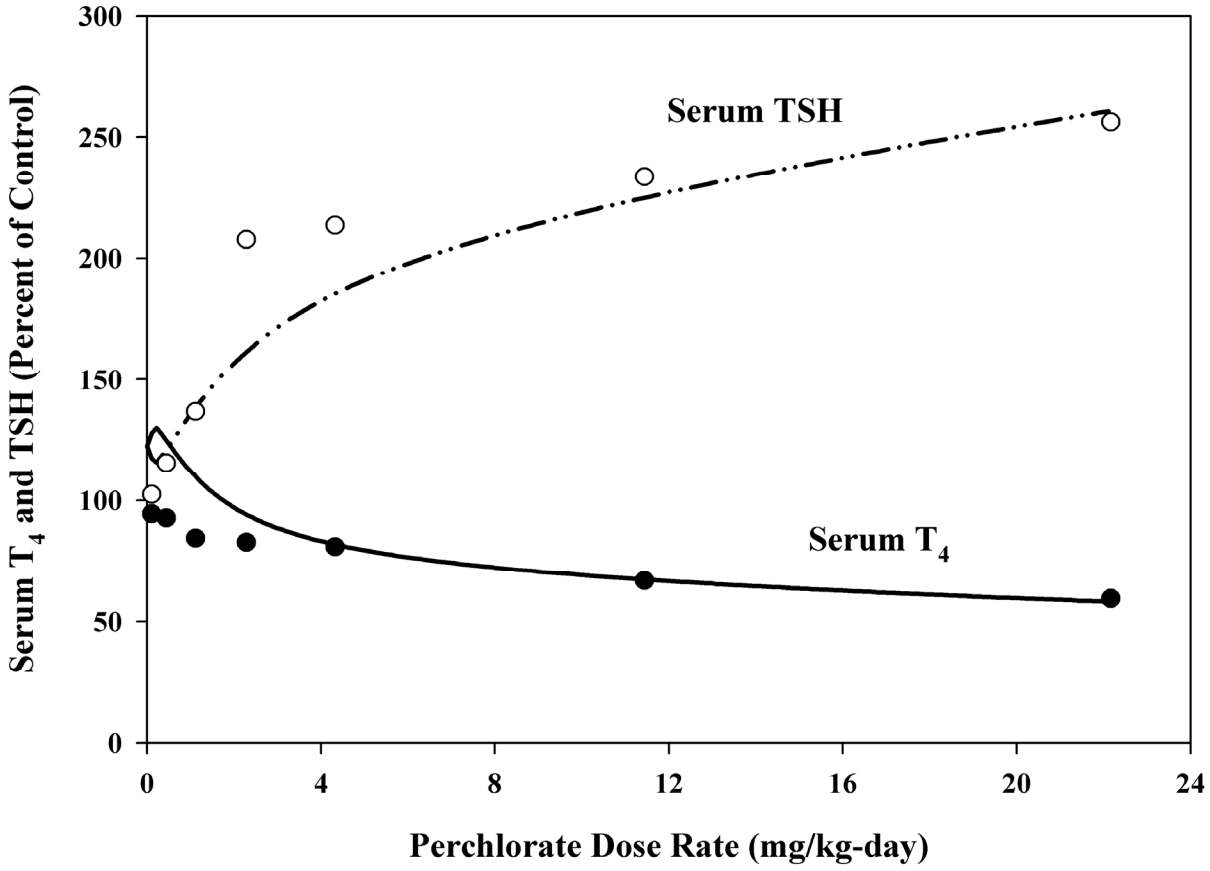
Serum TSH
Serum T_4
Serum T_4 and TSH (Percent of Control)
Perchlorate Dose Rate (mg/kg-day)
300
250
200
150
100
50
0
0
4
8
12
16
20
24

Figure 5.8.

CHAPTER 6

CONCLUSIONS

The hypothalamic-pituitary-thyroid (HPT) axis is an example of a very complex endocrine system, which is able to maintain homeostasis through a multitude of feedback loops and autoregulatory controls. An understanding of thyroid axis regulation is necessary in order to interpret perturbations, such as those in serum thyroxine (T_4) and thyroid stimulating hormone (TSH) caused by environmental pollutants determined in laboratory studies evaluating HPT axis indices. The conclusions from the research are derived using statistical approaches for the binary mixture of 3,3',4,4',5-pentachlorobiphenyl (PCB126) and perchlorate (ClO_4^-) and knowledge of HPT axis regulation and control mechanisms from published literature, as well as literature available on the mode of action for the thyroid active chemicals examined. Mathematical models are often used as tools to help us understand the kinetics of chemicals in the body, and this time we were able to couple our knowledge of the thyroid axis with existing information for ClO_4^- disturbances of the HPT and use the biologically based dose-response model of the HPT axis (BBDR-HPT model) as a dose-response analysis tool.

PCB126/Perchlorate Mixtures Study

Two large-scale laboratory experiments were conducted to determine the effects of ClO_4^- on the HPT axis of adult rats pretreated with PCB126. PCB126 has been shown to increase hepatic phase II metabolism of T_4 (increased rate in T_4-G formation), resulting in a decrease in serum T_4 concentrations and subsequent increase in TSH secretion and stimulation of the axis.

TSH stimulation of the axis results in a cascade of effects within the thyroid, one being the stimulation of sodium(Na^+)/iodide(I^-) symporter (NIS) protein production and expression. This is significant, in interpreting results from our studies, because the most well-defined mode of action for ClO_4^- is competitive inhibition of thyroidal iodide uptake.

Results from our studies suggest that in an upregulated or TSH stimulated thyroid system, ClO_4^- has less of a pronounced effect on serum thyroid hormone status. The ability of ClO_4^- to affect the axis is diminished and an apparent shift to the right of the ClO_4^- dose response curve occurs. This suggests that a greater dose of ClO_4^- is necessary to cause a similar magnitude of effect on serum T_4 and TSH. Our studies support this finding by a less than additive response in the HPT axis being observed when animals were pretreated with PCB126. Furthermore, our results did not indicate a synergistic response of the system by co-exposure to the compounds.

BBDR-HPT Axis Iodide Deficiency Model

The first generation dietary iodide BBDR-HPT axis model was constructed using simple model structure and empirical descriptions of the feedback loops. The simple model structures for the individual components were sufficient to describe radiolabeled tracer kinetic data for the individual components (^{125}I, ^{125}I-TSH, ^{131}I-T_4, and ^{125}I-T_3) modeled. When linked via negative feedback, TSH stimulation, and hormone metabolism the model structures effectively described the iodide sufficient and iodide deficient rat. The availability of thyroidal dietary iodide alone drove the endogenous model and resulted in decreases in serum T_4 and increases in serum TSH due to the lack of available iodide for thyroid hormone synthesis. Our model also was used to generate a dose-response plot for intake of dietary iodide and effects on serum T_4 and TSH. This plot showed a region of critical intake rate of iodide to be less than 2 μg /day.

BBDR-HPT Axis Model of Perchlorate Perturbation

The BBDR-HPT axis model developed and presented first in Chapter 4, was combined with a PBPK model for ClO_4^-, an ubiquitous environmental contaminant. Perchlorate has been shown to disrupt the HPT axis by inhibition of iodide uptake into the thyroid; however, the models linked via ClO_4^- competitive inhibition of thyroidal iodide uptake alone were unable to predict the rapid decrease in serum T_4 changes seen from ClO_4^- exposure. This was surprising, because we hypothesized that the blocking of iodide uptake by ClO_4^- resulted in an iodide deficient condition within the thyroid, and we expected the BBDR-HPT axis model to predict the changes in serum T_4 and TSH as it did under varying degrees of iodide deficiency. Furthermore, this led us to believe that ClO_4^- might be acting via an additional mode of action that has not been fully elucidated in laboratory studies.

We hypothesized that ClO_4^- also affected the synthesis and secretion of thyroid hormones and tested our hypothesis using the linked BBDR-HPT axis model and PBPK model for perchlorate. This hypothesis was tested and described using a suppression constant and Hill-type coefficients to inhibit thyroid hormone synthesis based upon the concentration of ClO_4^- in the thyroid tissue. This description accounted for the rapid decrease in serum T_4, but did not result in the rapid rate or degree of increase in serum TSH seen in several studies. So additionally, the T_4/TSH negative feedback describing TSH production was modified using Hill coefficients and the set point for half-maximal negative feedback by T_4 was increased slightly. Using this modification, serum T_4 and TSH were predicted following exposure to 1-22 mg ClO_4^-/kg-day in drinking water, suggesting that the sensitivity of TSH is altered in the presence of perchlorate. The mode of action of ClO_4^- should be further explored in the laboratory to confirm or reject the hypotheses suggested by this dose-response analysis using the mathematical models.

Future Applications of the BBDR-HPT Axis Model

The BBDR-HPT model developed can be linked to other PBPK models for thyroid active chemicals, via mode of action, to simulate and predict changes in thyroid hormones and TSH. For example, the BBDR-HPT axis model includes the phase II excretion of T_4 as T_4-glucornide (T_4-G) in the description of the liver compartment, and when combined with a PBPK model for PCB126, an increase in T_4-G formation is expected to result in the increased loss of T_4 from the body and subsequent rise in TSH to compensate. Linking the models together will provide for testing the hypothesis that PCB126 acts on the HPT axis via this single, well-defined mode of action. If the model is unable to predict changes in the HPT axis to the degree that is seen in experimental studies, then additional modes of action may be suggested and explored using the models (as demonstrated in Chapter 5). In addition, it is possible to link the BBDR-HPT axis model to multiple PBPK models to predict disturbances in the thyroid system from exposures to mixtures of compounds.

Finally, the development of this first-generation BBDR-HPT axis model will serve as a starting point for development of the maturing rat and human thyroid axis models. Other physiological compartments can be readily integrated into our model structure, such as the brain to correlate thyroid hormone levels in the brain to neurodevelopmental toxicity endpoints.

APPENDIX A

The acslXtreme (version 2.4.0.11) .csl file for BBDR-HPT axis radiolabeled model code (Chapter 4) is contained within this Appendix. Model code is structured as follows: First section contains physiological parameters and compound-specific constants. Second section includes scaled parameters and is followed by model code for the individual compounds, ^{125}I-TSH, ^{125}I, ^{131}I-T_4, and ^{125}I-T_3.

```
PROGRAM: Male Rat HPT Axis Model,RadioTracer studies

!-------------------------------------------------------------------------
!File name: Labelnogut.csl
!Units in nmol, L, hr, kg
!Created 02/11/2007 by Eva McLanahan
!Radiolabeled I, T4, T3, and TSH
!Last Revised 07/09/07 by Eva McLanahan

      INITIAL
            CONSTANT TSTOP=2            !Length of experiment
            CONSTANT CINT=0.001         !Communication interval

! ------------ Physiological Parameters------------------
CONSTANT   BW    =     0.350      !kg - Animal body weight
CONSTANT   QCC   =     14.0       !L/hr/kg - Total cardiac output  [Brown 1997]
CONSTANT   QLC   =     0.174      !%QC - Proportion cardiac output to the liver [Brown 1997]
CONSTANT   QTC   =     0.016      !%QC - Proportion cardiac output to the thyroid- human value
                                  (Brown 1997 & Merrill 2003)
CONSTANT   VLC   =     0.0366     !%BW liver tissue [Brown 1997 pg 416]
CONSTANT   VLBC  =     0.21       !%VL as liver blood [Brown 1997]
CONSTANT   VTC   =     0.00005    !%BW total thyroid tissue [My studies]
CONSTANT   VTBC  =     0.157      !%VT as thyroid blood [Malendowicz and Bednarek, 1986]

!-----------TSH Parameters--------------------------------
CONSTANT   MWTSH       =     28000      !g/mol - molecular weight TSH [chemfinder.com]
CONSTANT   Vd_TSHC     =     0.0554     !L/kg - VdTSH - Connors et al 1984
CONSTANT   KNIS_TSH    =     1.8        !nmol/L - Km TSH conc so Vmax of NIS I transport is 1/2 max
CONSTANT   KbTSH       =     1112.65    !nmol/L - Km TSH conc so I binding in thyroid is 1/2 max
CONSTANT   TSHc        =     0.232      !nmol/L-TSH concentration at steady-state in serum (calc
                                        from average of McLanahan et al 2007 studies 6.5ng/mL)
CONSTANT   Kel_TSHC    =     1.8899     !1/hr-kg - elimination rate constant for TSH from Vd
                                        (Lemarchand-Beraud and Berthier 1981)
```

```
!------------ I (Iodide) Parameters----------------------
CONSTANT   MWI         =     126.90447  !g/mol - molecular weight I [periodic table]
CONSTANT   Vd_ic       =     0.5        !L/kg - volume of distribution of iodide
CONSTANT   Km_i        =     31519      !nmol/L - affinity constant I for NIS
                                        (Gluzman and Niepomniszcze, 1983 and Merrill 2003)
CONSTANT   VmaxT_iC    =     1119.396   !nmol/hr-kg - maximal rate of NIS I uptake
CONSTANT   PAt_ic      =     0.0001     !L/hr - PA term thyroid [Merrill 2003]
CONSTANT   V0bindC     =     2243.598   !nmol/hr-kg - maximum rate of binding of iodide in thyroid
CONSTANT   Kmb_i       =     221.1      !nmol/L - Km of iodide binding
CONSTANT   ClU_iC      =     0.02       !L/hr-kg - urinary clearance of iodide

!------------ T4 (Thyroxine) Parameters------------------
CONSTANT   MWT4        =     776.8742   !g/mol - molecular weight T4 [calculated:C15H11I4NO4]
CONSTANT   MWT4G       =     952        !g/mol - m.w. T4-G [calc: T4(776)+GA(194)-H2O(18)=952]
CONSTANT   Vd_t4C      =     0.156      !%Vd of BW - Kohn 1996
CONSTANT   PL_t4       =     1.27       !unitless - PC for T4 liver (EscobearMorreale 1996)
CONSTANT   PAL_t4C     =     0.04875    !L/hr-kg - PA term T4 liver
CONSTANT   VMAXDIC     =     15.105     !nmol/hr-kgliver - fit - Vmax outer ring deiodinase
CONSTANT   KMDI        =     2300       !nmol/L - Km outer ring DI in liver (Leonard & Visser 1986)
CONSTANT   KEL_t4C     =     0.05       !1/hr-kg - rate of elim of T4 from body (vd)
                                        (Calc from Abrams and Larsen, 1973)
CONSTANT   KmUGT       =     100000     !nmol/L - (Km of UGT enzymes for T4 and T3) Visser 1993
CONSTANT   VmaxT4GC    =     1080.32    !nmol/hr - Vmax for T4-G formation in liver
CONSTANT   Vmaxt4luC   =     10552.8    !nmol/hr-kg - Vmax for active uptake of T4 into liver
CONSTANT   KmT4LU      =     650        !nmol/L - Km for T4 active uptake into liver
CONSTANT   FFT4        =     0.01       !fraction free for T4 uptake into liver

!------------ T3 (3,5,3'-Triiodothyronine) Parameters-----------------
CONSTANT   MWT3        =     650.97349  !g/mol - molecular weight T3 [calculated:C15H12I3NO4]
CONSTANT   Vd_T3C      =     0.186      !L/kg - Vd_T3 per kg bw [thyroid hormone metab pg 67]
CONSTANT   PL_t3       =     4.47       !unitless - liver T3 PC (EscobarMorreale1996)
CONSTANT   PAL_t3C     =     0.03       !L/hr/kg - PA term liver T3
CONSTANT   Kel_t3C     =     0.12       !1/hr/kg - rate of elim of T3 from body
                                        (Calc from Abrams and Larsen, 1973)
CONSTANT   Kmetl_t3C   =     1.15       !L/hr - metabolism of T3 in the liver
CONSTANT   KLUT3       =     1.1        !1/hr - liver 125I-T3 uptake rate
```

```
!---Thyroid hormone production parameters
CONSTANT   ktshcib    =     5e-7            !L2/nmol/hr- rate constant TH production
CONSTANT   ft3        =     0.20            !fraction of thyroid hormone production that is T3

!---T4 and T3 iodide equivalents
CONSTANT   I4CON      =     0.6534          !Fraction of t4 that is iodine
CONSTANT   I3CON      =     0.5848          !Fraction of T3 that is iodine

!IV dose parameters
CONSTANT   IVDOSEt4   =     0.0044     !131I-T4 IV Dose (ug)
CONSTANT   IVDOSEt3   =     0.00455    !125I-T3 IV Dose (ug)
CONSTANT   IVDOSEi    =     33         !125I IV Dose (ug/kg)
CONSTANT   IVDOSEtsh  =     5          !125I-TSH Dose (ng/rat)
CONSTANT   TINF       =     .01        !Length of IV infusion (hr)
CONSTANT   TINF3      =     0.001      !Length of IV infusion for T3 (hr)

           END ! INITIAL
     DYNAMIC
           ALGORITHM IALG = 2              !Gear method for stiff systems
DERIVATIVE

!--------------- Scaled Parameters--------------
QC    =     QCC*BW**0.75                !L/hr - Cardiac output
QL    =     QLC*QC                      !L/hr - blood flow to liver
QT    =     QTC*QC                      !L/hr - blood flow to thyroid

VL1   =     VLC*BW                      !L - liver volume with blood
VLB   =     VLBC*VL1                    !L - Volume of liver blood
VL    =     VL1-VLB                     !L - Liver tissue volume without blood
VT1   =     VTC*BW                      !L - total thyroid volume
VTB   =     VTBC*VT1                    !L - volume of thyroid blood
VT    =     VT1-VTB                     !L - volume of thyroid without blood


!TSH Scaled Parameters
Vd_TSH     =     Vd_TSHC*BW                !L - Vd for TSH
Kel_TSH    =     Kel_TSHC/BW**0.25         !1/hr - TSH elimination rate
```

```
!--T4 scaled parameters----
VMAXDI      =     VMAXDIC*BW**0.75      !nmol/hr - vmax T4 deiodination in liver
Vd_t4       =     Vd_T4c*BW - VL1       !L - Vd of T4
PAL_t4      =     PAL_t4C*BW**0.75      !L/hr - PA liver T4
Kel_t4      =     KEL_t4C/BW**0.25      !1/hr - T4 metabolism in Vd
Vmaxt4g     =     vmaxt4gc*BW**0.75     !nmol/hr - vmax T4-glucuronidation in liver
Vmaxt4lu    =     vmaxt4luc*BW**0.75    !nmol/hr - vmax T4 liver uptake

!--T3 scaled parameters--
PAL_t3      =     PAL_t3C*BW**0.75      !L/hr - PA liver T3
Vd_t3       =     Vd_t3C*BW - VL1       !L - Vd of T3
Kel_t3      =     Kel_t3C/BW**0.25      !1/hr - T3 metabolism in Vd
KmetL_t3    =     Kmetl_t3C/BW**0.25    !1/hr - T3 metabolism in liver

!--Iodide scaled parameters--
Vd_i        =     Vd_ic*BW - VT1        !L - volume of distribution of iodide
VmaxT_i     =     VmaxT_iC*BW**0.75     !nmol/hr - maximum rate of iodide uptake by NIS is thyroid
ClU_i       =     ClU_iC/BW**0.25       !L/hr - Urinary clearance of iodide
V0bind      =     V0bindC/BW**0.75      !nmol/hr - vmax binding of i in thyroid
PAT_i       =     PAT_ic*BW**0.75       !L/hr - pa term thyroid blood/tissue

!----MODEL CODE---TSH volume of distribution -----------------
!IV = IV TSH dose
IVDOSE_tsh=(IVDOSEtsh/MWTSH)
      iflag_tsh=pulse(0,tstop,tinf)
      IV_tsh=IVdose_tsh/TINF*iflag_tsh      !nmol/hr - rate of TSH iv infustion
      AIV_tsh=INTEG(IV_tsh,0.)              !nmol - amt of TSH iv infusioin

RClTSH=Kel_TSH*AVdTSH                       !nmol/hr - clearance of TSH from Vd
      AClTSH=INTEG(RClTSH,0.0)              !nmol - amt of TSH cleared from Vd

RAVdTSH=IV_tsh-RClTSH                       !nmol/hr - rate of change of TSH in Vd
      AVdTSH=INTEG(RAVdTSH,0.0)             !nmol - amt of TSH in Vd
      TSH=AVdTSH/Vd_TSH                     !nmol/L - Concentration TSH
      TSHngml=(TSH/1000) * MWTSH            !ng/mL (same as ug/L)- TSH concentration in Vd

TSHRPDP=((Avdtsh/(AIV_tsh+1e-6))*100)/(Vd_tsh*1000)    !%dose/ml - Total rad %dose/ml SERUM
```

```
!----MODEL CODE---Iodide, IV dose w/thyroid and Vd-----------
!----Iodide dosing----------iv dose radiolabeled-----------------------------
!IV = Intravenous infusion rate(nmol/hr)
    IVDOSE_i=(IVDOSEi*BW/MWI)*1000          !nmol amt ivdose
      iflag_i = pulse(0,tstop,tinf)         !iflag = pulse dose at time 0
        IV_i = IVDOSE_i/TINF*iflag_i        !nmol/hr - rate iodide iv infustion
       AIV_i = INTEG(IV_i,0.)               !nmol - amt of iv iodide dose

!------------THYROID IODIDE---------------------------
!ATIU= amount of free iodide actively transported into thyroid by NIS
RTNIS=((VmaxT_iTSH*Cvt_i)/(Km_i +Cvt_i))    !nmol/hr - rate of NIS uptake of iodide into thyroid
VmaxT_iTSH=(VmaxT_i*TSHc)/(KNIS_TSH+TSHc)
     ATIU=INTEG(RTNIS,0.0)                  !nmol - Amount of iodide uptake (active) into thyroid

!Atb_i=amount of free iodide in thyroid blood
RAtb_i=Qt*(CA_i-Cvt_i)+PAt_i*(Ctf_i-Cvt_i)-RTNIS      !nmol/hr - rate of change of I in thy blood
     Atb_i=INTEG(RAtb_i,0.0)                          !nmol - amount of iodide in thyroid blood
     Cvt_i=Atb_i/(VTB)                                !nmol/L - conc of iodide in thyroid blood

!At_i= amount of FREE iodide in thyroid tissue
RAt_iex1=(PAt_i*Ctf_i)                                !nmol/hr - rate of free I diff out of thy
     At_iex1=INTEG(RAt_iex1,0.0)                      !nmol - amount of free I diff out of thy
RAt_ien=RTNIS+(PAt_i*Cvt_i)                           !nmol/hr - rate of free I entering thy
     At_ien=INTEG(RAt_ien,0.0)
RAt_iex=(PAt_i*Ctf_i)+RIB       !nmol/hr - rate of loss of free I in thyroid tissue
                                (binding & diffusion out)
RAt_iex2=RAt_iex1+Rth           !nmol/hr - Total rate of iodide leaving thyroid
     At_iex2=INTEG(RAt_iex2,0.0)

!Rate of change of free iodide in thyroid tissue
RAtf_i=RTNIS+PAt_i*(Cvt_i-Ctf_i)-RIB        !nmol/hr - rate of change of free I in thyroid tissue
     dAtf_i=INTEG(RAtf_i,0.0)
     Atf_i=MAX(dAtf_i,0.0)                  !nmol - amount of free iodide in thyroid tissue
     Ctf_i=Atf_i/VT                         !nmol/L - amount of free iodide in thyroid tissue
     Ct_imgL=Ctf_i*MWI/10**6                !mg/L - amount of free iodide in thyroid tissue
```

```
!Rate of binding/storage of iodide in thyroid tissue
RIB=(Vmaxbt_i * Ctf_i)/(Kmb_i + Ctf_i)      !nmol/hr - rate of binding of iodide in thyroid
     Vmaxbt_i=(V0bind*TSHc)/(KbTSH+TSHc)    !nmol/hr - TSH stimulated Vmax of binding

     ARIB=INTEG(RIB,0.0)                    !nmol - amount of iodide bound in thyroid
     ARIBug=ARIB*MWI/1000                   !ug - amount of iodide bound in thyroid
     d_aribug=(ARIBug/((t+1e-6/24)))        !ug/d daily amt of iodide bound in thyroid

!Rate of change of BOUND iodide in thyroid tissue
RIB_i=RIB-Rth                           !nmol/hr - rate of change of bound iodide
     dAIB_i=INTEG(RIB_i,0.0)            !nmol - amount of iodide bound in thyroid tissue
     AIB_i=MIN(dAIB_i,160)
     CIB_i=AIB_i/VT                     !nmol/L    - concentration of bound iodide in thyroid tissue
     CIB_imgL=CIB_i*MWI/10**6           !mg/L - concentration of bound iodide in thyroid tissue

!Approach used in endogenous dietary model
RPR_th=ktshcib*TSHc*CIB_i               !nmol/hr - rate of thyroid hormone production
RPR_t3=ft3*RPR_th                       !nmol T3/hr - rate of T3 thyroidal production
RPR_t4=RPR_th-RPR_t3                    !nmol T4/hr - rate of T4 thyroidal production
Rth=(RPR_t4*I4CON)+(RPR_t3*I3CON)       !nmol/hr - Rate of thyroid hormone production from bound
     Ath=INTEG(Rth,0.0)                 !nmol - amount of iodide used in thyroid hormone production
     Athug=Ath*MWI/1000                 !ug - amt of iodide used in thyroid hormone production

!TTl_i=Total Iodide in thyroid tissue (nmol)
TAt_i=AIB_i+Atf_i                       !nmol - total iodide in thyroid tissue
TAt_img=TAt_i*MWI/10**6                 !mg - total iodide in thyroid tissue
TCt_imgL=TAt_img/VT                     !mg/L - total iodide in thyroid tissue

!----------Volume of Distribution Iodide--------
RAP_i=IV_i+QT*Cvt_i-QT*Ca_i-RU_i        !nmol/hr - rate of change of free iodide in Vd
     AP_i=INTEG(RAP_i,0.0)              !nmol - amount of free iodide in Vd
     CP_i=AP_i/VD_i                     !nmol/L - concentration of iodide in Vd
     Ca_i=CP_i
     CP_ing=CP_i*MWI                    !ng/L - concentration of iodide in Vd
     CP_ingml=CP_ing/1000               !ng/mL - concentration of iodide in Vd
     CP_imgl=(CP_ing/10**6)             !mg/L - concentration in Vd
```

```
RU_i=ClU_i*Ca_i                          !nmol/hr- rate of urinary clearance of iodide
     AU_i=INTEG(RU_i,0.0)                !nmol - amount of iodide cleared in urine
     AU_iug=AU_i*MWI/1000                !ug - amount of iodide cleared in urine


!---------MODEL CODE--- Total T4, IV dose with a Liver and Vd-----------
!----T4 dosing----------iv dose radiolabeled----------------
!IV = Intravenous infusion rate(nmol/hr)
    IVDOSE_t4=(IVDOSEt4/MWT4)*1000          !nmol 125I-T4 - amt ivdose
     iflag_t4 = pulse(0,tstop,tinf)         !iflag = pulse dose at time 0
       IV_t4 = IVDOSE_t4/TINF*iflag_t4      !nmol/hr - rate T4 iv infusion
      AIV_t4 = INTEG(IV_t4,0.)              !nmol 125I-T4 - Amount T4 iv dosed

!--------------SERUM T4 (Volume of distribution)------------------
RAP_t4=IV_t4+(QL*CVL_t4)-QL*Ca_t4-RVdel_t4  !nmol/hr - rate of change of T4 in Vd
     AP_t4=INTEG(RAP_t4,0.0)                !nmol - amount of T4 in Vd
     Ca_t4=AP_t4/Vd_t4                      !nmol/L - concentration of T4 in Vd
     Ca_t4ugdl=Ca_t4*(0.0001)*MWT4          !ug/dl - T4 in Vd
     Ca_t4ngg=(Ca_t4*MWT4)/1000             !ng/g - T4 in Vd
RVdel_t4=Kel_t4*Ap_t4                       !nmol/hr - rate of T4 elimination from Vd
     AVdel_t4=INTEG(RVdel_t4,0.0)           !nmol - amount of T4 eliminated from Vd

T4RPDT4VD=(AP_t4/(AIV_t4+1e-6))*100             !%dose T4 rad in Vd
T4RPDT4P=((AP_t4/(AIV_t4+1e-6))*100)/(Vd_t4*1000)   !%dose/ml - Total rad %dose/ml SERUM

!-------Liver T4-------------
RALb_t4=QL*(Ca_t4-Cvl_t4)+PAL_t4*(CL_t4-(Cvl_t4*FFT4))-RT4LU
                                        !nmol/hr - rate of change of T4 in the liver blood
     ALb_t4=INTEG(RALb_t4,0.0)          !nmol - amount of t4 in liver blood
     Cvl_t4=ALb_t4/(VLB*PL_t4)          !nmol/L - concentration of t4 in liver blood

RAL_t4=(PAL_t4*((Cvl_t4*FFT4)-Cl_t4))-RAGL-RADIL+RT4LU
                                        !nmol/hr - rate of change of T4 in liver tissue
     AL_t4=INTEG(RAL_t4,0.0)            !nmol - amount of T4 in liver tissue
     CL_t4=AL_t4/VL                     !nmol/L - concentration of t4 in liver blood
Cl_t4ngg=(CL_t4*MWT4/1000)/1.051        !ng/g - concentration of T4 in liver tissue
                                        (1.051=liver density, Obermoyer 1987)
```

```
RADIL=((VMAXDI*CVL_t4)/(CVL_t4+KMDI))       !nmol/hr - rate of T4 deiodination in liver (D1)
     ADIL=INTEG(RADIL,0.0)                  !nmol - Amount of T4 deiodinated (D1) in liver
     PC43L=(ADIL/(AIV_t4+1e-6))*100         !% T4 converted by Type I 5'-Deiodinase in liver

RAGL=(VmaxT4G * CVL_t4)/(KmUGT + CVL_t4)    !nmol T4/hr - rate of T4-glucuronidation in liver
     AGL=INTEG(RAGL,0.0)                    !nmol T4 lost/used to make T4-G
     RAGLT4G=(RAGL*(MWT4G/MWT4))            !nmol T4-G formed/hr

RT4LU=(VmaxT4LU*(CVl_t4*FFT4))/(KMT4LU+(CVL_t4*FFT4))       !nmol/hr - rate T4 active uptake

T4RPDL=(AL_t4/(AIV_t4+1e-6))*100                            !%dose T4 radioactivity in liver
T4RPDT4L=((AL_t4+ALb_T4)/(AIV_t4+1e-6))*100)/(VL*1000)      !%dose/ml - T4 rad %dose/ml liver
T4RPDDIL=(ADIL/(AIV_t4+1e-6))*100                           !%dose T4 deiodinated in liver
T4RPDGL=(AGL/(AIV_t4+1e-6))*100                             !%dose T4 glucuronidated in liver
PC43=((ADIL+AVdel_t4)/(AIV_t4+1e-6))*100                    !%dose T4 converted to T3 (whole body)

!--T4--Ratio amount in liver:blood in Wong paper should be around 1 up to 1hr post dose
LBAratio=AL_t4/(AP_t4+1e-6)      !Liver:blood amount ratio


!---------MODEL CODE--- Total t3, IV dose with a Liver and Vd-----------
!----t3 dosing----------iv dose radiolabeled----------------
      !IV = Intravenous infusion rate(nmol/hr)
    IVDOSE_t3=(IVDOSEt3/MWt3)*1000                !nmol amt ivdose
      iflag_t3 = pulse(0,tstop+1,tinf3)           !iflag = pulse dose at time 0
        IV_t3 = IVDOSE_t3/TINF3*iflag_t3          !rate t3 iv dosing(nmol/hr)
      AIV_t3 = INTEG(IV_t3,0.)                    !Amount t3 iv dosed(nmol)

!--------------SERUM t3 (Volume of distribution)------------------
RAP_t3=IV_t3+(QL*CVL_t3)-QL*Ca_t3-RVdel_t3             !nmol/hr - rate of change of T3 in Vd
     AP_t3=INTEG(RAP_t3,0.0)                           !nmol - amount of T3 in Vd
     Ca_t3=AP_t3/Vd_t3                                 !nmol/L - concentration of T3 in Vd
     Ca_t3ugdl=Ca_t3*(0.0001)*MWt3                     !ug/dL - T3 in Vd
     Ca_t3ngg=(Ca_t3*MWT3)/1000                        !ng/g - T3 in Vd

Rvdel_t3=Kel_t3*Ap_t3                                  !nmol/h - rate of t3 elimination from Vd
     AVdel_t3=INTEG(RVdel_t3,0.0)                      !nmol - amount of t3 eliminated from Vd
```

```
t3RPDP=(AP_t3/(AIV_t3+1e-6))*100                          !%dose T3 rad in Vd
t3RPDt3P=((AP_t3/(AIV_t3+1e-6))*100)/(Vd_t3*1000)         !%dose/ml - Total rad %dose/ml Vd

!-------Liver t3-------------
RALb_t3=QL*(CA_t3-Cvl_t3)+PAL_t3*(CL_t3-Cvl_t3)-RLt3U
                                                  !nmol/hr - rate of change in liver blood (t3)
     ALb_t3=INTEG(RALb_t3,0.0)                    !nmol - amount of t3 in liver blood
     Cvl_t3=ALb_t3/(VLB*PL_t3)                    !nmol/L - concentration of t3 in liver blood

RAL_t3=(PAL_t3*(Cvl_t3-Cl_t3))-RAMLt3+RLt3U       !nmol/hr - rate of change in liver tissue (t3)
     AL_t3=INTEG(RAL_t3,0.0)                      !nmol - amount of t3 in liver tissue
     CL_t3=AL_t3/VL                               !nmol/L - concentration of t3 in liver blood
     CL_t3ngg=(cl_t3*MWT3)/1000

RLT3U=KLUT3*cvl_t3                          !nmol/hr - 1st order rate of liver uptake of T3

RAMLt3=AL_t3*KmetL_t3                             !nmol T3/hr - rate of metabolism of T3 in liver
     AMLt3=INTEG(RAMLt3,0.0)                      !nmol T3 - amout of T3 metabolized in liver

RAT3feces=RAMLt3*0.30                             !nmol/hr - rate of T3 excreted in feces
     AT3_feces=INTEG(RAT3feces,0.0)               !nmol - amt of T3 excreted in feces
     t3RPDFE=(AT3_feces/(AIV_t3+1e-6))*100        !%dose in feces - DiStefano 1987 says 30%

t3RPDL=(AL_t3/(AIV_t3+1e-6))*100                  !%dose t3 radioactivity in liver
t3RPDt3L=((AL_t3+ALb_t3)/(AIV_t3+1e-6))*100)/(VL*1000)     !%dose/ml - t3 rad %dose/ml liver

!Blood flow limited liver - removed
!RAL_t3=QL*(Ca_t3-Cvl_t3)-RAMLt3
!AL_t3=INTEG(RAL_t3,0.0)
!Cl_t3=AL_t3/VL
!Cvl_t3=AL_t3/(VL*PL_t3)

!----------Mass balance T4---------------
TMASSt4=AP_t4+AL_t4+ADIL+Avdel_t4+AGL+Alb_t4
BALANCEt4=AIV_t4-TMASSt4
```

```
!----------Mass balance t3---------------
TMASSt3=AP_t3+AL_t3+Avdel_t3+AMLt3+Alb_t3
BALANCEt3=AIV_t3-TMASSt3

!----------Mass balance Iodide-----------
TMASSi=Atb_i+Atf_i+Ath+AIB_i+AP_i+AU_i
BALANCEi=AIV_i-TMASSi

!----------Mass balance of TSH-----------
TMASStsh=Avdtsh+Acltsh
BALANCEtsh=AIV_tsh-TMASStsh


END ! DERIVATIVE
           TERMT (T .GE. TSTOP, 'checked on communication interval: REACHED TSTOP')
      END ! DYNAMIC
      TERMINAL
                  END ! TERMINAL
END ! PROGRAM
```

APPENDIX B

The acslXtreme (version 2.4.0.11) .m file for BBDR-HPT axis radiolabeled model simulations (Chapter 4) is contained within this Appendix. The .m file was used to generate model simulations shown in Figure 4.4 for the radiotracer sub-models. The sequences used to generate all plots in Figure 4.4 are ordered in the .m file as follows: ^{125}I, ^{125}I-T_3, ^{131}I-T_4, and ^{125}I-TSH.

```
%Created 21 Aug 2006 by Eva McLanahan
%Last Modified: 21 August 2006
%Modified by: Eva McLanahan
%M file to plot 125I in serum and urine
%Figure 4.4A - Data from Yu et al 2002

%time(hrs), urine (ug)
RIIV33U    =     [     24    9     ];

%time (hrs), serum (ng/mL)
RIIV33SF2  =     [     0.083       41.41
                       0.25        54.03
                       0.5         49.82
                       1           44.63
                       2           40.32
                       6           24.97
                       9           8.49
                       24          1.95
                       30          0.86
                       48          0.52
                       72          0.26
                       96          0.19  ];

%Simulation commands
!!s ivdosei=33, tstop=96, cint=0.1, bw=0.300
!!prepare /All
!!start/nc

%Plotting Commands
plot(_t,_cp_ingml,RIIV33SF2(:,1),RIIV33SF2(:,2),_t,_au_iug,RIIV33U(:,1),RIIV33U(:,2),'urineplasma.
aps');
```

```
%Created 22 Aug 2006 by Eva McLanahan
%Last Modified: 22 Aug 2006
%Modified by: Eva McLanahan
%M file to plot thyroidal iodide
%Figure 4.4B - Data from WPAFB excel spreadsheets (not in Yu paper)
%time (hrs), 125I (%dose)
RIIV33TT1  =     [     0.25  2.84
                       1     14.68
                       2     20.31
                       4     34.89 ];

RIIV33TB1  =     [     0.25  2.01
                       1     9.87
                       2     15.36
                       4     27.55 ];

RIIV33TT2  =     [     0.5   7.85
                       2     19.73
                       6     36.26 ];

RIIV33TB2  =     [     0.5   7.03
                       2     18.50
                       6     34.71 ];

RIIV33TT3  =     [     0.083 0.714
                       0.25  4.05
                       0.5   5.157
                       1     9.674
                       2     26.277
                       6     48.948
                       9     58.685
                       24    51.965
                       30    50.315
                       48    53.118
                       72    37.654
                       96    27.476     ];
```

```
RIIV33TB3  =     [     0.083 0.36
                       0.25  3.202
                       0.5   4.06
                       1     8.505
                       2     24.371
                       6     46.482
                       9     54.947
                       24    49.834
                       30    48.012
                       48    50.095
                       72    35.252
                       96    24.611     ];

%Simulation commands
!!s ivdosei=33, tstop=96, cint=0.1, bw=0.300
!!prepare tct_imgl, cib_imgl, t, ct_imgl
!!start/nc

%Plotting Commands
plot(_t,_tct_imgl,RIIV33TT1(:,1),RIIV33TT1(:,2),RIIV33TT2(:,1),RIIV33TT2
(:,2),RIIV33TT3(:,1),RIIV33TT3(:,2),_t,_cib_imgl,RIIV33TB1(:,1),RIIV33TB1(:,2),RIIV33TB2(:,1),RIIV
33TB2(:,2),RIIV33TB3(:,1),RIIV33TB3(:,2),'thyroidbandt.aps');
```

```
%[125-I]-T3 data DiStefano1993
%Key for datasets in ThyroidDatasets.xls
%Units (%dose)
%Created 03/01/07
%Data from DiStefano et al 1993
%time (hrs), T3 (%dose)
RT3IVDP2   =     [     0.066666667      42.42424815
                       0.116666667      8.333342858
                       0.333333333      7.196996637
                       0.666666667      6.439436908
                       0.7              4.924302516      ];

RT3IVDL    =     [     0.01             6.060606562
                       0.116666667      46.59091824
                       1.2              20.83338672      ];

%Simulation commands
!!s ivdoset3=0.00083, tstop=2, cint=0.001, bw=0.375
!!prepare /All
!!start/nc

%Plotting Commands
plot(_t,_t3rpdp,_t,_t3rpdl,RT3IVDP2(:,1),RT3IVDP2(:,2),RT3IVDL(:,1),RT3IVDL(:,2),'t3plasmaliver_Di
stefano93.aps');
```

```
%Schroder-vanderElst 1997 131I-T4 distribution in vehicle control rats
%Created 07/09/07 by Eva McLanahan
%iv dose of 0.0017ug 131I-T4 to female wistar rats
%Figure 4.4C - T4 from Schroder van der Elst 1997

%Time (hrs), Blood (%dose), Liver (%dose)
RT4IVSVEB  =     [     0.25  42    29
                       0.5   31    30
                       1     34    23
                       2     25    19
                       3     27    16
                       4     21    15
                       6     21    14    ];

%Simulation commands
!!s ivdoset4=0.0017, bw=0.180, tstop=6, cint=0.001
!!prepare t, t4rpdt4vd, t4rpdl
!!start /nc

%Plotting Commands
plot(_t,_t4rpdt4vd,RT4IVSVEB(:,1),RT4IVSVEB(:,2),_t,_t4rpdl,RT4IVSVEB(:,1),RT4IVSVEB(:,3),'svet4.a
ps')
```

```
%IV dose of TSH
%Created 07/22/07 by Eva McLanahan
%Last edited 07/22/07 by Eva McLanahan
%Spira 1979 iv dose male rats with 5ngTSH/rat via tail vein
%Male Hebrew University rats 80-100g
%Data expressed as %Dose TSH/ml plasma/100g bw - assuming 100grat

%Time (hrs), 125I-TSH (%dose/ml)
SpiraTSHiv =     [     0.01949119      16.70926392
                       0.050148872     14.16756717
                       0.081021331     13.04201494
                       0.101155515     10.39869552
                       0.121987729     10.83116423
                       0.173316539     8.993441313
                       0.234900371     7.165413202
                       0.266041305     7.310211755
                       0.296323115     5.367511656
                       0.420296204     4.637900996
                       0.482041119     3.930251676
                       0.75038995      2.592929802
                       1.039517304     1.745539131
                       1.349906438     1.442738244
                       1.681396214     1.37651532
                       1.991516786     1.026596369     ];

%Simulation Commands
!!s bw=0.100, ivdosetsh=5, tstop=2
!!prepare t, tshrpdp
!!start/nc

%Plotting Commands
     plot (_t,_tshrpdp,SpiraTSHiv(:,1),SpiraTSHiv(:,2),'TSHiv.aps')
```

APPENDIX C

The acslXtreme (version 2.4.0.11) .csl file for BBDR-HPT axis iodide deficiency model code (Chapter 4) is contained within this Appendix. Model code with oral intake of iodide is structured as follows: First section contains physiological parameters and compound-specific constants. Second section includes scaled parameters and is followed by model code for TSH, dietary iodide, thyroxine (T_4), 3,5,3'-triiodothyronine (T_3), and ClO_4^-. Finally the mass balance equations for each chemical conclude the model code.

```
PROGRAM: Male Rat HPT Axis Model
!-----------------------------------------------------------------------
!File name:EHPTnogut.csl created 03/01/07 from EHPT_Imod_021407.csl
!Units in nmol, L, hr, kg
!Endogenous I, T4, T3, and TSH
!Blood binding of T4 99% bound - taken into account for liver uptake (0.01*cvl)
!Last Revised 08/08/07 by Eva McLanahan

      INITIAL
           CONSTANT   TSTOP=1416       !Length of experiment (1416=59 days)
           CONSTANT   CINT=0.5         !communication interval


! ------------ Physiological Parameters------------------
CONSTANT   QCC   =     14.0        !L/hr/kg - Total cardiac output  [Brown 1997
CONSTANT   QLC   =     0.174       !%QC - Proportion cardiac output to the liver [Brown 1997 p438]
CONSTANT   QTC   =     0.016       !%QC - Proportion cardiac output to the thyroid- human value
                                   (Brown 1997 & Merrill 2003)
CONSTANT   VLC   =     0.0366      !%BW liver tissue [Brown 1997 pg 416]
CONSTANT   VLBC  =     0.21        !%VL as liver blood [Brown 1997]
CONSTANT   VTC   =     0.00005     !%BW total thyroid tissue [McLanahan 2007]
CONSTANT   VTBC  =     0.157       !%VT as thyroid blood [Merrill et al 2003]

!------GROWTH EQUATION PARAMETERS---------
CONSTANT   BWC   =     0.320             !kg - body weight (a constant body weight)
CONSTANT   BWGon =     0                 !if BWGon=1 then BW growth equation on, else uses BWC
CONSTANT   BWs   =     170000            !mg - BW for start of study (must be given in lit.)
CONSTANT   BWt0  =     7314.70           !mg - initial BW at birth (Mirfazaelian 2007)
CONSTANT   KBW   =     63.21             !days - age at inflection point (Mirfazaelian 2007)
CONSTANT   BWtmax      =     521026.13   !mg - maximum body weight (Mirfazaelian 2007)
CONSTANT   gammaBW     =     2.01        !unitless - hill coeff for BW growth (Mirfazaelian 2007)

!------------ TSH Parameters-----------------------------
CONSTANT   MWTSH       =     28000       !g/mol - molecular weight TSH [chemfinder.com]
CONSTANT   Vd_TSHC     =     0.0554      !L/kg - VdTSH - (Connors et al 1984)
CONSTANT   K0TSHmaxC   =     6           !nmol/hr - Max prod of TSH (absence of T4) (Connors 1984)
CONSTANT   Kinh_T4     =     0.2         !nmol/L - Km of T4 such that prod of TSH is 1/2 maximal
```

```
CONSTANT   KNIS_TSH   =     0.949       !nmol/L - TSH conc so Vmax of NIS I transport is 1/2 max
CONSTANT   KbTSH      =     733.98      !nmol/L - Km TSH conc such that I binding/organification in
                                        thyroid is 1/2 maximal
CONSTANT   Kel_TSHC   =     1.8899      !1/hr-kg - elimination rate constant for TSH from Vd
                                        (Lemarchand-Beraud and Bertheir 1981)
CONSTANT   TSHb  =    5.08373           !ng/ml - TSH baseline to calc fold change. Set for each BW

!------------ I (Iodide) Parameters----------------------
CONSTANT   MWI        =     126.90447   !g/mol - molecular weight I [periodic table]
CONSTANT   Vd_iC      =     0.5         !L/kg - volume of distribution of iodide
CONSTANT   Km_i       =     31519       !nmol/L - affinity constant I for NIS (Gluzman and
                                        Niepomniszcze 1983 and Merrill 2003)
CONSTANT   VmaxT_iC   =     5738.267    !nmol/hr/kg - maximal rate of uptake
CONSTANT   PAt_iC     =     0.0001      !L/hr - PA term thyroid [Merrill 2003]
CONSTANT   V0bindC    =     1005.9      !nmol/hr-kg - maximum rate of binding of iodide in thyroid
CONSTANT   Kmb_i      =     244.59      !nmol/L - Km of iodide binding
CONSTANT   ClU_iC     =     0.0046      !L/hr-kg - urinary clearance of iodide

!-------Thyroid hormone production parameters--------------
CONSTANT   ktshcib    =     5e-7        !L2/nmol-hr - rate constant for thyroid hormone production

!------------ T4 (Thyroxine) Parameters------------------
CONSTANT   MWT4  =    776.8742         !g/mol - molecular weight T4 [calculated:C15H11I4NO4]
CONSTANT   MWT4G =    952              !g/mol - molecular weight T4-Glucuronide
                                        [calculated: T4(776)+GA(194)-H2O(18)=952]
CONSTANT   Vd_t4c     =     0.156       !L/kg bw - vd t4 (Kohn 1996)
CONSTANT   PL_t4      =     1.27        !Partition coefficient for T4 liver (EscobarMorreale 1996)
CONSTANT   PAL_t4C    =     0.0423      !nmol/hr/kg - from tracer - PA term for T4 liver
CONSTANT   VMAXDIC    =     19.89       !nmol/hr/kg - Vmax outer ring deiodinase
CONSTANT   KMDI       =     2300        !nmol/L - Km outer ring deiodinase in liver
                                        (Leonard and Visser 1986)
CONSTANT   KEL_t4C    =     0.05        !1/hr-kg - rate of elimination of T4 from body (Vd)
                                        (Abrams & Larsen 1973 t1/2 used for calculation)
CONSTANT   KmUGT      =     100000      !nmol/L - (Km of UGT enzymes for T4 and T3) (Visser 1993)
CONSTANT   VmaxT4GC   =     3435.89     !nmol/hr - max rate of T4-G formation in liver
CONSTANT   VMAXT4LUC  =     4384.73     !nmol/hr - Vmax for active uptake of T4 into liver
CONSTANT   KmT4LU     =     650         !nmol/L - Km for uptake in hepatocytes (Blondeau 1988)
```

```
CONSTANT   FFT4        =     0.01        !fraction of free t4 available for uptake to liver
CONSTANT   t4b         =     48.8846     !t4 baseline - to calc % control - diff for each BW

!------------ T3 (3,5,3'-Triiodothyronine) Parameters------------------
CONSTANT   MWT3        =     650.97349   !g/mol - molecular weight T3 [calculated:C15H12I3NO4]
CONSTANT   Vd_T3C      =     0.186       !L/kg - Vd_T3 per kg BW [thyroid hormone metab pg 67]
CONSTANT   PL_t3       =     4.47        !Partition coefficient for T3 liver (EscobarMorreale 1996)
CONSTANT   PAL_t3C     =     0.1699      !L/hr/kg - from tracer - PA term liver T3
CONSTANT   Kel_t3C     =     0.12        !1/hr-kg- rate of T3 elimination from body
                                         (Abrams and Larsen 1973 t1/2 used for calculation)
CONSTANT   KmetL_t3C   =     3.65        !1/hr-kg - fractional removal rate from liver
CONSTANT   KLUT3       =     1.25        !L/hr - 1st order liver uptake rate of T3
CONSTANT   t3b         =     0.556647    !t3 baseline - to calc % control - diff for each BW

!---T4 and T3 iodide equivalents
CONSTANT   I4CON       =     0.6534      !Fraction of t4 as iodine (4 Im.w./T4m.w.) T4 iodide equiv
CONSTANT   I3CON       =     0.5848      !Fraction of T3 as iodine (3 Im.w./T m.w.) T3 iodide equiv
CONSTANT   T43CON      =     0.8379      !T3/T4 molar equivalents (T3 m.w. / T4 m.w.)
CONSTANT   IFT4M       =     0.16335     !One I freed in T4 Metabolism (I mw./T4 m.w.)

!--IODIDE dosing parameters
!CONSTANT  pdose_i     =     20          !ug - oral dose of iodide (diet I intake for McLanahan 2007
                                         calculated to be 20ug/day)
!pdose1 and pdose2 used instead of pdose_i for changing iodide intake during studies
CONSTANT   pdose1      =     20          !ug - 1st half of study iodide intake
CONSTANT   pdose2      =     20          !ug - 2nd half of study iodide intake

!Compartment initial amounts from running EHPT model to steady state 2000hrs (1/27/07)
CONSTANT   initAvdTSH  =     0.          !nmol TSH - initial amt of TSH in Vd
CONSTANT   initAP_t4   =     0.          !nmol T4 - initial amt of T4 in Vd (blood)
CONSTANT   initAlb_t4  =     0.          !nmol T4 - initial amt of T4 in liver blood
CONSTANT   initAl_t4   =     0.          !nmol T4 - initial amt of T4 in liver tissue
CONSTANT   initAlb_t3  =     0.          !nmol T3 - initial amt of T3 in liver blood
CONSTANT   initAl_t3   =     0.          !nmol T3 - initial amt of T3 in liver tissue
CONSTANT   initAP_t3   =     0.          !nmol T3 - initial amt of T3 in Vd (blood)
CONSTANT   initAP_i    =     0.          !nmol I - initial amt of iodide in Vd (blood)
CONSTANT   initAtb_i   =     0.          !nmol I - initial amt of iodide in thyroid blood
```

```
CONSTANT   initdAT_i  =     0.          !nmol I - initial amt of free iodide in thyroid tissue
CONSTANT   initdAIB_i =     0.          !nmol I - initial amt of bound iodide in thyroid tissue

           END ! INITIAL
      DYNAMIC
           ALGORITHM IALG = 2               !Gear method for stiff systems

DERIVATIVE
if (BWGon.eq.1) then
BW=BWG
else
BW=BWC
end if

!------Growth equations------
BWG=(((BWt0*(KBW**gammaBW))+(BWtmax*(Age**gammaBW)))/((KBW**gammaBW)+(Age**gammaBW)))/10**6
                                                        !BW (kg) at a given Age (days)
Age=Age0+days                                           !Age (days)
Age0=KBW*(((BWs-BWt0)/(BWtmax-BWs))**(1/(gammaBW)))     !Age (days) at start of study if only
                                                        initial BWs (mg) is given

!--------------- Scaled Parameters--------------
QC    =     QCC*BW**0.75     !L/hr - Cardiac output
QL    =     QLC*QC           !L/hr - blood flow to liver
QT    =     QTC*QC           !L/hr - blood flow to thyroid

VL1   =     VLC*BW           !L - liver volume with blood
VLB   =     VLBC*VL1         !L - Volume of liver blood
VL    =     VL1-VLB          !L - Liver tissue volume without blood
VT1   =     VTC*BW           !L - total thyroid volume
VTB   =     VTBC*VT1         !L - volume of thyroid blood
VT    =     VT1-VTB          !L - volume of thyroid without blood

!--TSH scaled parameters---
Vd_TSH     =     Vd_TSHC*BW             !L - Vd for TSH
Kel_TSH    =     Kel_TSHC/BW**0.25      !1/hr - TSH elim rate
K0TSHmax   =     K0TSHmaxC*BW**0.75     !nmol/hr - max rate of TSH secretion (no T4)
```

```
!--T4 scaled parameters----
Vd_t4      =     Vd_t4c*BW - VL1            !L - Vd for T4
VMAXDI     =     VMAXDIC*BW**0.75           !nmol/hr - Vmax for type 1 5'd in liver for t4
PAL_t4     =     PAL_t4C*BW**0.75           !L/hr - PA term for liver t4
Kel_t4     =     KEL_t4C/BW**0.25           !1/hr - T4 elimination rate from body
VmaxT4G    =     VmaxT4GC*BW**0.75          !nmol/hr - Vmax for t4 glucuronidation in liver
VmaxT4LU   =     VmaxT4LUC*BW**0.75         !nmol/hr - Vmax for liver uptake of t4

!--T3 scaled parameters--
Vd_t3      =     Vd_t3C*BW - VL1            !L - Vd for T3
PAL_t3     =     PAL_t3C*BW**0.75           !L/hr - PA term for T3 in liver
Kel_t3     =     KEL_t3C/(BW**0.25)         !1/hr - T3 elimination rate from body
KmetL_t3   =     KmetL_t3C/(BW**0.25)       !1/hr - nonspecific T3 metabolism in liver

!--Iodide scaled parameters--
Vd_i       =     Vd_ic*BW - VT1             !L - volume of distribution of iodide
VmaxT_i    =     VmaxT_iC*BW**0.75          !nmol/hr - max rate of iodide uptake by NIS in thyroid
ClU_i =     ClU_iC/(BW**0.25)              !L/hr - Urinary clearance of iodide
     !Changed scaling from V0bindc*BW**0.75 to below on 7/18/07 based on initialconditions.xls
     showing total thyroid iodide in thyroid not dropping below 7 for 120-180g rats and not above
     20 for 400g rat
V0bind     =     V0bindC/(BW**0.75)         !nmol/hr - max rate of binding of iodide in thyroid
PAT_i      =     PAT_iC*BW**0.75            !L/hr - PA term for thyroidal iodide


!----MODEL CODE---TSH volume of distribution with feedback T4-----------------
RTSHPR=(K0TSHmax*Kinh_T4)/(Kinh_T4+Ca_t4)        !nmol/hr - Rate of TSH production
     ATSHPR=INTEG (RTSHPR,0.0)                   !nmol - Amount TSH produced
     ATSHPRug=ATSHPR*MWTSH/1000                  !ug - amount of TSH produced
     d_TSHPRugd=(ATSHPRug/(((t+1e-6)/24)))       !ug/d - TSH production
RClTSH=Kel_TSH*AVdTSH                            !nmol/hr - clearance of TSH from Vd
     AClTSH=INTEG(RClTSH,0.0)                    !nmol - amt of TSH cleared from Vd
RAVdTSH=RTSHPR-RClTSH                            !nmol/hr - rate of change of TSH in Vd
     AVdTSH=INTEG(RAVdTSH,initAVdTSH)            !nmol - amt of TSH in Vd
     TSH=AVdTSH/Vd_TSH                           !nmol/L - Concentration TSH
     TSHngml=(TSH/1000) * MWTSH                  !ng/mL (same as ug/L)- TSH concentration in Vd
!fold change tsh
```

```
TSHFOLD=(TSHngml/TSHb)                              !fold change TSH
TSHpercon=(TSHngml/TSHb)*100                        !TSH as % control

!----MODEL CODE---Iodide, IV dose w/thyroid and Vd -----------
!----Iodide dosing----------oral dose------------
!Change in iodide diet 1X - t=5040 for Fukuda Refeeding data
!pdose1 and pdose2 set in m file
      if (t.GT.5040) then
            pdose_i=pdose2
      else
            pdose_i=pdose1
      end if

!Normal Oral Dosing parameters for I
      dose_i    = (pdose_i*10**3)/MWI        !dietary intake amount (nmol)
      Rdose_i   = dose_i/12                  !dose rate for eating period (hrs) per day
!Food Consumption for a 12 hr period (light-dark cycle in rat)
      pflag=pulse(0.0,24.0,12)               !for one 12 hr eating period per day
      RMR_i = (Rdose_i * pflag)              !nmol/hr - dose rate for oral dose iodide
            AST_i = INTEG(RMR_i,0.0)         !nmol - amt of iodide received orally entering stomach
            d_AST_i=AST_i/(((t+1e-6)/24))    !nmol - daily amt of iodide received orally in stomach
            d_AST_iug=(d_AST_i*MWI)/(10**3)  !ug - daily amt of iodide received orally in stomach

!---Volume of Distribution of Free Iodide -----
RAP_i=RMR_i+QT*Cvt_i-QT*Ca_i+RAIFL_t4+RAIFL_t3+RAIFvd_t4+RAIFvd_t3-RU_i
                                             !nmol/hr - rate of change of free iodide in serum
AP_i=INTEG(RAP_i,initAP_i)                   !nmol - amount of free iodide in serum
      CP_i=AP_i/Vd_i                         !nmol/L - concentration of free iodide in serum
      Ca_i=CP_i
            CP_iugdl=(CP_i*MWI/10000)        !ug/dL - concentration of free iodide in serum
            CP_ingml=(CP_i*MWI/1000)
Ca_bi=(Ca_t4*I4CON)+(Ca_t3*I3CON)            !nmol/L - concentration of bound iodide in serum
      Ca_bingml=(Ca_bi*MWI)/1000             !ng/ml - concentration of bound iodide in serum
Ca_ti=Ca_i+Ca_bi                !nmol/L - concentration of total iodide (bound + free) in serum
      Ca_tiugdl=Ca_ti*MWI/10000 !ug/dl - total iodide
      Ca_tingml=Ca_ti*MWI/1000  !ng/ml - total iodide
RU_i=ClU_i*Ca_i                              !nmol/hr- rate of urinary clearance of iodide
```

```
      AU_i=INTEG(RU_i,0.0)                    !nmol - amount of iodide cleared in urine
      d_au_i=AU_i/((t+1e-6)/24)               !nmol/d - iodide cleared in urine
      AU_iug=AU_i*MWI/1000                    !ug - amount of iodide cleared in urine
      d_AUiug=AU_iug/((t+1e-6)/24)            !ug/d of iodide cleared in urine
      PINIEX=(d_AU_i/(d_AST_i+1e-6))*100      !% of daily intake of iodide excreted in urine

!---Rate of metabolism of TH in Vd -- freeing of iodide
RAIFvd_t4=Rvdel_t4*IFT4M                  !nmol/hr - rate of I freed from T4->T3 metabolism in Vd
      AIFVd_t4=INTEG(RAIFvd_t4,0.0)       !nmol - amount of I freed from T4->T3 metabolism in Vd
RAIFvd_t3=(Rvdel_t3*I3CON)                !nmol/hr - rate of I freed from T3 metabolism in Vd -
                                          assume all goes to T3, that T3 metab is rate limiting step
      AIFVd_t3=INTEG(RAIFvd_t3,0.0)       !nmol - amount of I freed from T3 metabolism in Vd

!-------Liver iodide metabolism of THs, added to Iodide Vd-------------
RAIFL_t4=RADIL*IFT4M                      !nmol/hr - rate of I freed in liver from T4 metab to T3
      AIFL_t4=INTEG(RAIFL_t4,0.0)         !nmol - amt of iodide released in liver from T4 metab to T3
RAIFL_t3=RAML_t3*0.70*I3CON               !nmol/hr - EST 70% of T3 metabolized into free I-
      AIFL_t3=INTEG(RAIFL_t3,0.0)         !nmol - amount of I freed in liver from T3 metabolism

!------------THYROID IODIDE---------------------------
!Rate of active iodide uptake into thyroid by the NIS
RTNIS=(VmaxT_iTSH*Cvt_i)/(Cvt_i+Km_i)              !nmol/hr - rate of I active uptake (NIS)
VmaxT_iTSH=((VmaxT_i*TSH)/(KNIS_TSH+TSH))          !nmol/hr - change in Vmax due to TSH stimulation
      ATIU=INTEG(RTNIS,0.0)                        !nmol - Amount of I uptake (active) into thyroid

!Rate of change of iodide in thyroid blood
RAtb_i=Qt*(CA_i-Cvt_i)+PAt_i*(Ctf_i-Cvt_i)-RTNIS       !nmol/hr - rate of change of I in thy blood
      Atb_i=INTEG(RAtb_i,initAtb_i)                    !nmol - amount of I in thyroid blood
      Cvt_i=Atb_i/VTB                                  !nmol/L - conc of I in thyroid blood

!Rate of change of FREE IODIDE IN THYROID
RAtf_i=RTNIS+PAt_i*(Cvt_i-Ctf_i)-RIB
      dAtf_i=INTEG(RAtf_i,initdAt_i)          !nmol - amount of free iodide in thyroid lumen was
      Atf_i=MAX(dAtf_i,0)
            Atf_iug=Atf_i*MWI/1000            !ug - amount of free iodide in thyroid lumen
      Ctf_i=Atf_i/VT                          !nmol/L - conc of free iodide in thyroid tissue
            Ctf_imgl=Ctf_i*MWI/10**6          !mg/L - concentration of free I in thyroid tissue
```

```
!Rate of incorporation (binding) of iodide in thyroid tissue
RIB=(Vmaxbt_i*Ctf_i)/(Kmb_i+Ctf_i)          !nmol/hr - rate of incorporation of iodide in thyroid
Vmaxbt_i=(V0bind*TSH)/(KbTSH+TSH)           !nmol/hr - vmax of binding change (stimulated by TSH
                                                  concentration in Vd
     ARIB=INTEG(RIB,0.0)                    !nmol - amount of iodide incorporated in thyroid
     ARIBug=ARIB*MWI/1000                   !ug - amount of iodide incorporated in thyroid
     d_aribug=(ARIBug/(((t+1e-6)/24)))      !ug - daily amt of iodide incorporated in thyroid

!Rate of change of BOUND iodide in thyroid tissue
RIB_i=RIB-Rth                           !nmol/hr - rate of change of bound iodide in thyroid
                                        (rate of binding - loss as secretion of thyroid hormone)
     dAIB_i=INTEG(RIB_i,initdAIB_i)
          AIB_iug=(AIB_i*MWI)/1000      !ug - amt iodide bound in thyroid
     CIB_i=AIB_i/VT                     !nmol/L - concentration of iodide bound in thyroid
          CIB_imgl=CIB_i*MWI/10**6      !mg/L - concentration of iodide bound in thyroid

!Set a maximum and minimum amt of iodide stores in thyroid - max is not really needed even for
iodide up to 500ug/day
if (dAIB_i.GT.160) then
AIB_i=160
else if (dAIB_i.LT.0)then
AIB_i=0
else
AIB_i=dAIB_i
end if

!Rate of utilization of bound I secreted as TH (rate of production of T4 and T3 in iodide equiv.)
Rth=(RPR_t4*I4CON)+(RPR_t3*I3CON)       !nmol I/hr - rate of utilization of thyroid I in TH prod
     Ath=INTEG(Rth,0.0)                 !nmol - amount of iodide used in TH prod
     d_ath=Ath/((t+1e-6)/24)            !nmol/day - daily amt of iodide used in TH prod
     Athug=Ath*MWI/1000                      !ug - amount of iodide used in TH prod
     d_athug=Athug/((t+1e-6)/24)             !ug/day - daily amount of iodide used in TH prod
     PINITHPR=(d_ath/(d_ast_i+1e-6))*100     !% of daily intake of iodide used in TH prod

!Rate of change of FREE iodide in thyroid tissue - allows you to look at the free entering and
leaving, also loss of free to binding
```

```
      RAt_ien=RTNIS+(PAt_i*Cvt_i)            !nmol/hr - rate of free iodide entering thyroid lumen
                                             (active uptake and diffusion)
           At_ien=INTEG(RAt_ien,0.0)         !nmol - total amt of I entering thyroid (NIS and diff)
      RAt_iex1=(PAt_i*Ctf_i)                 !nmol/hr - rate of free I diff out of thyroid tissue
           At_iex1=INTEG(RAt_iex1,0.0)       !nmol - amt of iodide diff out of thyroid
      RAt_iex2=RAt_iex1+Rth                  !nmol/hr - total loss of iodide from thyroid
                                             (diffusion and secretion as thyroid hormone)
           At_iex2=INTEG(RAt_iex2,0.0)       !nmol - total amt of iodide loss from thyroid
                                             (diffusion and secretion as thyroid hormone)

!Total Iodide in thyroid tissue (nmol)
TAt_i=AIB_i+Atf_i                 !nmol - total amount of iodide in thyroid (free and bound)
TAt_img=(TAt_i*MWI)/10**6         !mg - total amount of iodide in thyroid (free and bound)
TCt_imgL=TAt_img/VT               !mg/L - total concentration of iodide in thyroid (free and bound)
TAt_iug=TAt_i*MWI/1000            !ug (my data suggests should be between 10-18 ug)


!------------MODEL CODE-------Thyroid hormone production in the Thyroid------------
 !---Production of Total thyroid hormones--based on TSH and "bound" iodide pool----
RPR_th=ktshcib*TSH*CIB_i                          !nmol/hr - production rate of thyroid hormones

!Fractionation of thyroid hormone production
dFt3calc=0.2652*((TAT_iug)**(-0.4684))            !derived from Pedraza 2006
Ft3calc=MIN(dFT3calc,0.90)

RPR_t3=Ft3calc*RPR_th                             !nmol/h - rate of T3 production from thyroid
      APR_t3=INTEG(RPR_t3,0.0)                    !nmol - amt of T3 produced in thyroid
      APR_t3Tug=APR_t3*MWT3/1000                  !ug - amt of T3 produced in thyroid
      d_PRT3Tugd=(APR_t3Tug/(((t+1e-6)/24)))      !ug/day - daily production rate of T3 in thyroid

RPR_t4=RPR_th-RPR_t3                              !nmol/h - rate of T4 production from thyroid
      APR_t4=INTEG(RPR_t4,0.0)                    !nmol - amt of T4 produced in thyroid
      APR_t4ug=APR_t4*MWT4/1000                   !ug - amt of T4 produced
      d_PRT4ugd=(APR_t4ug/(((t+1e-6)/24)))        !ug/day - daily production rate of T4
      d_PRT4nmold=(APR_t4/(((t+1e-6)/24)))        !nmol/day - daily production rate of T4
!T3/T4 ratio
MR34T=APR_t3/(APR_t4+1e-6)                        !T3/T4 production ratio
```

```
!---------MODEL CODE--- Total T4 with a Liver and Vd-----------
!--------------SERUM T4 (Volume of distribution)------------------
!AP_t4= amount of total t4 in Vd
RAP_t4=RPR_t4+(QL*CVL_t4)-QL*Ca_t4-RVdel_t4      !nmol/hr - rate of change of T4 in serum
     AP_t4=INTEG(RAP_t4,initAP_t4)               !nmol - amount of T4 in SERUM
     Ca_t4=AP_t4/Vd_t4                           !nmol/L - concentration of T4 in SERUM
     Ca_t4ugdl=(Ca_t4*MWT4)/10000                !ug/dL - T4 in SERUM
     Ca_t4ngg=(Ca_t4*MWT4)/1000                  !ng/g or ng/mL - T4 in serum
     t4percon=(ca_t4ngg/t4b)*100                 !%control - serum T4

!AVdel_t4=amount of t4 cleared from vd - assumed to go to t3+free iodide
RVdel_t4=Kel_t4*Ap_t4                            !nmol/h - rate of T4 elimination from Vd
     AVdel_t4=INTEG(RVdel_t4,0.0)                !nmol - amount of T4 eliminated from Vd
     d_AVdel_t4=(AVdel_t4/(((t+1e-6)/24)))       !nmol/d - daily amount of T4 eliminated from Vd


!-------Liver T4-------------
!Diffusion limited liver with active uptake of free serum T4 (added 3.20.07)
!Cvl*FFT4 assumes only a fraction of the total blood concentration is available for diffusion or
active uptake into the liver
RALb_t4=QL*(Ca_t4-Cvl_t4)+PAL_t4*(CL_t4-(Cvl_t4*FFT4))-RLT4U
                                                 !nmol/hr - rate of change in liver blood (t4)
     ALb_t4=INTEG(RALb_t4,initAlb_t4)            !nmol - amount of t4 in liver blood
     Cvl_t4=ALb_t4/(VLB*PL_t4)                   !nmol/L - concentration of t4 in liver blood

RAL_t4=(PAL_t4*((Cvl_t4*FFT4)-Cl_t4))-RAGL-RADIL+RLT4U
                                                 !nmol/hr - rate of change in liver tissue (t4)
     AL_t4=INTEG(RAL_t4,initAl_t4)               !nmol - amount of T4 in liver tissue
     CL_t4=AL_t4/VL                              !nmol/L - concentration of t4 in liver tissue
     Cl_t4ngg=(CL_t4*MWT4/1000)/1.051            !ng/g - concentration of T4 in liver tissue
                                                 (1.051=liver density, Obermoyer 1987)

RLT4U=(VmaxT4LU*(Cvl_t4*FFT4))/(KmT4LU+(Cvl_t4*FFT4))  !nmol/hr - rate of liver T4 active
                                                       uptake (only FRACTION free available)
     ALT4U=INTEG(RLT4U,0.0)
```

```
!Metabolism of T4 in liver - via deiodination
RADIL=((VMAXDI*Cvl_t4)/(Cvl_t4+KMDI))       !nmol/hr - rate of T4 deiodination in liver (D1)
     ADIL=INTEG(RADIL,0.0)                  !(nmol) Amount of T4 deiodinated (D1) in liver
     d_ADIL_T4=(ADIL/(((t+1e-6)/24)))       !nmol/d - amount of T4 deiodinated in liver per day

     PC43L=(ADIL/(APR_t4+1e-6))*100         !% T4 converted by Type I 5'-D in liver

!Metabolism of T4 in the liver - via glucuronidation
RAGL=(VmaxT4G * Cvl_t4)/(KmUGT + Cvl_t4)    !nmol T4/hr - rate of T4-glucuronidation in liver
     AGL=INTEG(RAGL,0.0)                    !nmol T4 lost/used to make T4-G
RAGLT4G=(RAGL*(MWT4G/MWT4))                 !nmol T4-G formed/hr
     AGLT4G=INTEG(RAGLT4G,0.0)              !nmol T4-G formed
     RGLT4Gpmolhr=RAGLT4G*1000              !pmol T4-G formed/hr/liver

d_AT4_feces=(AGL/(((t+1e-6)/24)))           !nmol/d - amount of T4-G excreted in feces per day
PT4PRinfeces=(d_AT4_feces/(d_PRT4nmold+1e-6))*100     !% of T4 produced excreted in feces/day

! -- Overall T4 Metabolism --
!AWBT4Met=total amount of T4 metabolized (liver gluc + liver deiod + Vd metab)
RWBT4Met=RVdel_t4+RAGL+RADIL                !nmol/hr - whole body rate of T4 metabolism
     AWBT4Met=INTEG(RWBT4Met,0.0)           !nmol - amt of T4 metabolized (total - whole body)
     d_AWBT4Met=(AWBT4Met/(((t+1e-6)/24)))  !nmol/day - whole body loss of T4

AT4T3=Avdel_t4+Adil
FMWBT4=(AWBT4Met/(APR_t4+1e-6))*100         !% of produced T4 that is metab. Sum of all pathways
FMVdT4=(AVdel_t4/(APR_t4+1e-6))*100         !% of produced T4 that is metab in Vd
(FMGLT4=(AGL/(APR_t4+1e-6))*100             !% of produced T4 that is metab to T4-G in liver
FMDILT4=(ADIL/(APR_t4+1e-6))*100            !% of produced T4 that is metab to t3 in liver
FMT4T3=FMvdT4+FMDILT4                       !% of T4 converted to T3
```

```
!---------MODEL CODE--- Total t3, with a Liver and Vd-----------
!--------------SERUM t3 (Volume of distribution)-----------------
!----production of T3 in the Vd from T4 metabolism
!AT3FVd=amount of T3 formed in the Vd from T4 metabolism
RT3FVd=(RVdel_t4*T43CON)                    !nmol t3/hr - all T4 to T3+I
     AT3FVd=INTEG(RT3FVd,0.0)               !nmol - amt of T3 formed in Vd from T4 metabolism
     AT3FVdug=AT3FVd*MWT3/1000              !ug - amount of T3 produced from T4 metabolism in Vd

RAP_t3=(QL*CVL_t3)-QL*Ca_t3-RVdel_t3+RPR_t3+RT3FVd     !nmol/hr - rate of change of t3 in Vd
     AP_t3=INTEG(RAP_t3,initAP_t3)                     !nmol - amount of t3 in Vd
     Ca_t3=AP_t3/Vd_t3                                 !nmol/L - concentration of t3 in Vd
     Ca_t3ugdl=Ca_t3*(0.0001)*MWT3                     !ug/dL - t3 in Vd
     Ca_t3ngg=(Ca_t3*MWT3)/1000                        !ng/g - t3 in Vd
     t3percon=(ca_t3ngg/t3b)*100                       !%control - Vd T3

RVdel_t3=Kel_t3*Ap_t3                                  !nmol/h - rate of t3 elim from Vd
                                                       !assumed all metab to free I-
     AVdel_t3=INTEG(RVdel_t3,0.0)                      !nmol - amount of t3 elim from Vd

!-------Liver t3-------------
!----production of T3 in liver
RAT3FL=RADIL*T43CON             !nmol/hr - rate of T3 formed in liver from T4 deiod. in T3 equiv.
     AT3FL=INTEG(RAT3FL,0.0)    !nmol - amount of T3 formed in liver

!Diffusion limited liver
RALb_t3=QL*(CA_t3-Cvl_t3)+PAL_t3*(CL_t3-Cvl_t3)-RLt3U
                                                       !nmol/hr - rate of change in liver blood (t3)
     ALb_t3=INTEG(RALb_t3,initAlb_t3)                  !nmol - amount of t3 in liver blood
     Cvl_t3=ALb_t3/(VLB*PL_t3)                         !nmol/L - concentration of t3 in liver blood

RAL_t3=(PAL_t3*(Cvl_t3-Cl_t3))+RAT3FL-RAML_t3+RLt3U
                                                       !nmol/hr - rate of change in liver tissue (t3)
     AL_t3=INTEG(RAL_t3,initAl_t3)                     !nmol - amount of t3 in liver tissue
     CL_t3=AL_t3/VL                                    !nmol/L - concentration of t3 in liver tissue
     Cl_t3ngg=(CL_t3*MWT3/1000)/1.051                  !ng/g - concentration of T3 in liver tissue
                                                       (1.051=liver density, Obermoyer 1987)
RLT3U=Cvl_t3*KLUT3              !nmol/hr - 1st order rate of liver uptake of T3
```

```
      ALT3U=INTEG(RLT3U,0.0)      !nmol - amt of T3 actively transported into liver

RAML_t3=AL_t3*KmetL_t3            !nmol/hr - rate of T3 metabolism in liver (unspecified) - assume
                                  small portion excreted and rest forms free I-
      AML_t3=INTEG(RAML_t3,0.0)   !nmol - amount of T3 metabolized in liver
      RAT3feces=RAML_t3*0.30      !nmol/hr - rate of T3 excreted in feces
            AT3_feces=INTEG(RAT3feces,0.0)              !nmol - amt of T3 excreted in feces
            d_AT3_feces=(AT3_feces/(((t+1e-6)/24)))     !nmol/d - amt of T3 excreted in feces/day

!----Total production of t3
TAPR_t3=AT3FVd+AT3FL+APR_t3                       !nmol - total amount of T3 produced
TAPR_t3ug=TAPR_t3*MWT3/1000                       !ug - total amt of T3 produced
d_PRT3ugd=TAPR_t3ug/((t+1e-6)/24)                 !ug/d - whole body production of T3 per day
FAPR_t3Thy=(APR_t3Tug/(TAPR_t3ug+1e-6))*100       !% of total T3 prod that occurs in the thyroid

!---T3 Metabolism contribution of pathways
RWBT3Met=RAML_t3+RVdel_t3                         !nmol/hr - Rate of overall T3 metabolism
      AWBT3Met=INTEG(RWBT3Met,0.0)                !nmol - total amount of T3 metabolized
      d_AWBT3Met=(AWBT3Met/(((t+1e-6)/24)))       !nmol - total daily amount of T3 metabolized

FMWBT3=(AWBT3Met/(TAPR_t3+1e-6))*100        !% of produced T3 that is metab - sum of all pathways
FMVdT3=(AVdel_t3/(TAPR_t3+1e-6))*100        !% of produced T3 that is metabolized in the Vd
FMLT3=(AML_t3/(TAPR_t3+1e-6))*100           !% of produced T3 that is metabolize in the liver
FMFeT3=(AT3_feces/(TAPR_t3+1e-6))*100       !% of produced T3 that is excreted in Feces

!------END HPT AXIS MODEL-------------------------------------------------------
```

```
!----------MASS BALANCES-----------------
!----------Mass balance TSH---------------
TSHint=initAVdTSH                      !initial amts of TSH
TMASStsh=AClTSH+AvdTSH                 !total mass TSH
BALANCEtsh=TSHint+ATSHPR-TMASStsh      !mass balance TSH (initial amt + amt produced - total mass)

!----------Mass balance T4---------------
T4int=initAp_t4+initAlb_t4+initAl_t4             !initial amts of t4
tformt4=APR_t4                                   !total amt T4 produced in thyroid
TMASSt4=AP_t4+AL_t4+ADIL+Avdel_t4+AGL+Alb_t4     !total mass T4
BALANCEt4=T4int+tformt4-TMASSt4                  !mass balance t4

!----------Mass balance t3---------------
T3int=initAp_t3+initAlb_t3+initAl_t3             !initial amts of T3
tformt3=APR_t3+AT3FL+AT3FVd                      !total amount of T3 formed
TMASSt3=AP_t3+AL_t3+Alb_t3+Avdel_t3+AML_t3       !total mass of T3
BALANCEt3=T3int+tformt3-TMASSt3                  !mass balance t3

!----------Mass balance Iodide-----------
Iint=initAP_i+initAtb_i+initdAt_i+initdAIB_i     !initial amts of I
TMASSi=Atb_i+Atf_i+AIB_i+Ath+AP_i+AU_i           !total mass of I
tformi=AST_i+AIFL_t4+AIFL_t3+AIFVd_t4+AIFVd_t3   !dose I & I freed from metabolism of T4 and T3
BALANCEi=Iint+tformi-TMASSi                      !mass balance iodide

!Days
days=((t+1e-6)/24)                                          !days of model execution
END ! DERIVATIVE
            TERMT (T .GE. TSTOP, 'checked on communication interval: REACHED TSTOP')
      END ! DYNAMIC
      TERMINAL
      T4END=ca_t4ngg
      T3END=ca_t3ngg
      TSHEND=tshngml
      T4ENDPC=t4percon
      TSHENDPC=tshpercon
                     END ! TERMINAL
END ! PROGRAM
```

APPENDIX D

The acslXtreme (version 2.4.0.11) .m file for BBDR-HPT axis iodide sufficient and deficient model simulations (Chapter 4) is contained within this Appendix. The .m file is organized by the order the figures appear in the Chapter 4. Code to simulate steady-state iodide sufficiency plots (iodide, T_4, T_3, and TSH) are followed by the sequences used to generate the iodide deficiency simulations compared to literature data. Finally, the .m file used to generate the iodide dose response plot for T4 and TSH is included.

```
%Created 26 September 2007 by Eva McLanahan
%Last Modified: 26 September 2007
%Modified by: Eva McLanahan
%M file to plot Figures for BBDR-HPT axis LID model paper

%Figure 5A - Serum free iodide (ug/dL) and total amt in thyroid (ug)
%Male SD rats, 320g
%time(hrs), tat_iug(Yu2002-ug), and serum free iodide (Eng1999-ng/mL)
ISS   =     [     50    15    7.3
                  50    12    10
                  50    18    7
                  50    NaN   7.6
                  50    NaN   11.4
                  50    NaN   8.6];

!!s bwgon=0, ivdosep=0, pdose_p=0, pdose1=20, tstop=100
!!BW320
!!prepare t, tat_iug, cp_iugdl, ca_bingml
!!start/nc

plot (_t,_tat_iug,ISS(:,1),ISS(:,2),_t,_cp_iugdl,ISS(:,1),ISS(:,3),'Fig5A_LIDpaper.aps');

%Figure 5B - Serum TSH (ng/mL)
%time(hrs), serum tsh (McLanahan2007-ng/mL)
TSHSS =     [     50    6.5084
                  50    9.0293
                  50    3.9875];

!!s bwgon=0, pdose1=20, pdose_p=0, ivdosep=0, tstop=100
!!BW320
!!prepare t, tshngml
!!start/nc

plot (_t,_tshngml,TSHSS(:,1),TSHSS(:,2),'Fig5B_LIDpaper.aps');
```

```
%Figure 5C - Serum T4 (ng/g)and Liver T4 (ng/g)
%time(hrs), serum T4 (McLanahan2007-ng/g), liver T4 (MorrealdeEscobar1994-ng/g)
T4SS =     [     50    40.6145991 25.51
                 50    29.3301941 23.22
                 50    51.89900409     18.7];

!!s bwgon=0, pdose1=20, pdose_p=0, ivdosep=0, tstop=100
!!BW320
!!prepare t, ca_t4ngg, cl_t4ngg
!!start/nc

plot (_t,_ca_t4ngg,T4SS(:,1),T4SS(:,2),_t,_cl_t4ngg,T4SS(:,1),T4SS(:,3),'Fig5C_LIDpaper.aps');

%Figure 5D - Serum T3 (ng/g)and Liver T3 (ng/g)
%time(hrs), serum T3 (McLanahan2007-ng/g), liver T3 (MorrealdeEscobar1994-ng/g)
T3SS =     [     50    0.461260479     4.91
                 50    0.358993714     5.71
                 50    0.563527244     3.72];

!!s bwgon=0, pdose1=20, ivdosep=0, pdose_p=0, tstop=100
!!BW320
!!prepare t, ca_t3ngg, cl_t3ngg
!!start/nc

plot (_t,_ca_t3ngg,T3SS(:,1),T3SS(:,2),_t,_cl_t3ngg,T3SS(:,1),T3SS(:,3),'Fig5D_LIDpaper.aps');
```

```
%Created 26 September 2007 by Eva McLanahan
%Last Modified: 26 September 2007
%Modified by: Eva McLanahan
%M file to plot FIGURE 6 for LID paper (LID plots)
%Figure 6 - Riesco 1977 LID Diet
%0.35ugI/day HSD rats
%time(days),total thyroid iodide(ug),serum T4(ng/g),serum T3(ng/g),serum TSH(fold change)
LIDR77A    =    [     0     5.36332041 51.39660852     0.568138533     1
                      0     5.36332041 56.32452264     0.661482971     1
                      0     5.36332041 46.4686944 0.474794095     1
                      2     4.587266532     53.89146044     0.646783395     1.000001408
                      2     5.236509422     60.14695388     0.724539546     1.46666769
                      2     3.938023642     47.635967  0.569027244     0.533335126
                      4     3.414502333     51.46340794     0.703138094     1.733334979
                      4     4.485216854     61.29919394     0.823178757     2.400001024
                      4     2.343787812     41.62762194     0.583097431     1.066668934
                      6     2.275680693     36.50433073     0.51504231 1.266669585
                      6     3.005231253     43.66491697     0.635082974     1.733335764
                      6     1.546130133     29.34374449     0.395001646     0.800003406
                      8     1.831121078     30.95354164     0.589243891     1.600003094
                      8     2.645512921     39.90928406     0.686994446     2.333335574
                      8     1.016729235     21.99779922     0.491493336     0.866670614
                      11    1.189315295     20.8171726 0.605017283     1.80000344
                      11    1.685409814     28.19651748     0.791706048     3.000001902
                      11    0.693220776     13.43782772     0.418328518     0.600004978
                      15    0.512031337     15.96106834     0.455503371     2.666669297
                      15    0.788775688     21.99780294     0.615310738     3.500001435
                      15    0.235286986     9.924333739     0.295696004     1.833337159
                      26    0.05  2.28122021 0.434472206     7.533328393
                      26    0.05  4.444817479     0.518893137     12.73331992
                      26    0.05  0.117622941     0.350051275     2.333336868];
!!s bwc=0.120, bwgon=0, pdose_p=0, tstop=630, pdose1=0.35
!!BW120
!!prepare days, tat_iug, ca_t4ngg, ca_t3ngg, tshfold
!!start/nc
plot(_days,_tat_iug,LIDR77A(:,1),LIDR77A(:,2),_days,_ca_t4ngg,LIDR77A(:,1),LIDR77A(:,3),_days,_ca_
t3ngg,LIDR77A(:,1), LIDR77A(:,4),_days,_tshfold,LIDR77A(:,1),LIDR77A(:,5),'Fig6_LIDpaper.aps')
```

```
%Created 26 September 2007 by Eva McLanahan
%Last Modified: 26 September 2007
%Modified by: Eva McLanahan
%M file to plot FIGURE 7 for LID paper (LID plots)

%Figure 7A - Okamura 1981 Simonsen Albino rats
%0.45ugI/day (0.3-0.36?)
%time(days),total thyroid iodide(ug),serum T4(ng/g),serum T3(ng/g),serum TSH(fold change)

OK81SA     =     [     0     10.82592   53    0.59  1
                       0     13.68276   67    0.76  NaN
                       0     7.96908    39    0.42  NaN
                       14    1.925828   23    0.56  2.709677419
                       14    3.426841   34    0.64  NaN
                       14    0.424815   12    0.48  NaN
                       28    0.642369   12    0.48  4.0609319
                       28    0.98826    21    0.59  NaN
                       28    0.296478   3     0.37  NaN
                       56    0.4872     5.2   0.34  20.1827957
                       56    0.5684     7.2   0.44  NaN
                       56    0.406 3.2  0.24  NaN
                       84    0.478977   6.1   0.3   16.74910394
                       84    0.623784   8.1   0.357 NaN
                       84    0.33417    4.1   0.243 NaN];

!!s bwgon=0, tstop=2016, pdose1=0.30
!!BW270
!!prepare days, tat_iug, ca_t4ngg, ca_t3ngg, tshfold
!!start/nc

plot(_days,_tat_iug,OK81SA(:,1),OK81SA(:,2),_days,_ca_t4ngg,OK81SA(:,1),OK81SA(:,3),_days,_ca_t3ng
g,OK81SA (:,1),OK81SA (:,4),_days,_tshfold,OK81SA(:,1),OK81SA(:,5),'Fig7A_LIDpaper.aps')
```

```
%Figure 7B - Okamura 1981 Holtzman Sprague-Dawley rats
%0.45ugI/day (0.3-0.36?)
%time(days),total thyroid iodide(ug),serum T4(ng/g),serum T3(ng/g),serum TSH(fold change)

OK81HSD    =     [     0     9.68575    43    0.72  1
                       0     11.28105   52    0.789 NaN
                       0     8.09045    34    0.651 NaN
                       14    2.51784    34    0.72  1.272171254
                       14    3.67992    39    0.786 NaN
                       14    1.35576    29    0.654 NaN
                       28    2.854764   24    0.65  1.336391437
                       28    4.786776   39    0.76  NaN
                       28    0.922752   9     0.54  NaN
                       56    1.017093   12    0.58  3.972477064
                       56    2.082619   18    0.623 NaN
                       56    0     6     0.537 NaN
                       84    0.645216   7.8   0.44  11.82874618
                       84    0.852016   10.8  0.55  NaN
                       84    0.438416   4.8   0.33  NaN];

!!s bwgon=0, tstop=2016, pdose1=0.30
!!BW320
!!prepare days, tat_iug, ca_t4ngg, ca_t3ngg, tshfold
!!start/nc

plot(_days,_tat_iug,OK81HSD(:,1),OK81HSD(:,2),_days,_ca_t4ngg,OK81HSD(:,1),OK81HSD(:,3),_days,_ca_
t3ngg,OK81HSD(:,1),OK81HSD(:,4),_days,_tshfold,OK81HSD(:,1),OK81HSD(:,5),'Fig7B_LIDpaper.aps')
```

```
%Created 26 September 2007 by Eva McLanahan
%Last Modified: 26 September 2007
%Modified by: Eva McLanahan
%M file to plot FIGURE 8 for LID paper (LID plots)

%Figure 8 - Okamura 1981 Holtzman Sprague-Dawley rats
%1.14ugI/day, bw at end=0.391kg, at start=0.106kg
%time(days),total thyroid iodide(ug),serum T4(ng/g),serum T3(ng/g)

OK81BHSD   =     [     19    3.6656     35    0.67
                       19    1.8676     30    0.62
                       19    5.4636     40    0.72
                       33    1.950676   28    0.65
                       33    1.573476   21    0.56
                       33    2.327876   35    0.74
                       63    3.4572     25    0.6
                       63    2.8452     23    0.52
                       63    4.0692     27    0.68
                       96    2.934455   18    0.51
                       96    2.444655   13    0.45
                       96    3.424255   23    0.57];

!!BW110
!!s bws=110000, bwgon=1, pdose1=1.14, tstop=2304
!!prepare days, tat_iug, ca_t4ngg, ca_t3ngg
!!start/nc

plot(_days,_tat_iug,OK81BHSD(:,1),OK81BHSD(:,2),_days,_ca_t4ngg,OK81BHSD(:,1),OK81BHSD(:,3),_days,
_ca_t3ngg,OK81BHSD(:,1),OK81BHSD(:,4),'Fig8_LIDpaper.aps');
```

```
%Created 26 September 2007 by Eva McLanahan
%Last Modified: 26 September 2007
%Modified by: Eva McLanahan
%M file to plot FIGURE 9 for LID paper (LID plots)
%This data still has to be exported and percent baseline calculated to show in paper
%Figure 9 - Fukuda 1975 I Refeeding study adult male Sprague-Dawley rats
%Fed LID(0.6ug/day) for 7 months, then supplemented with iodide to provide total intake of
2.6ugI/day or 8.6ugI/day beginning on day 0 and continuing for 9 days
%time(days),serum T4 (ng/g), serum TSH (ng/ml)
FRF2p6     =     [     5040  4.516133379     154.4905452
                       5064  15.43012166     73.49038009
                       5088  18.81722635     23.78036763
                       5112  18.81723237     15.11962426
                       5184  25.96777454     17.5055683
                       5256  42              10.10610003     ];
FRF8p6     =     [     5040  4.892476996     140.8057019
                       5064  23.3333464      37.32329471
                       5088  31.61292306     12.0505026
                       5112  27.84948729     13.16990279
                       5184  36.88174628     9.685660734
                       5256  60.59140593     7.173635116     ];
!!BW400
!!s tstop=5260, bwgon=1, bws=400000, pdose1=0.2, pdose2=2.6, pdose_p=0
!!prepare t, ca_t4ngg, tshngml
!!start/nc
t4FRF2p6=_ca_t4ngg
tshFRF2p6=_tshngml

!!BW400
!!s tstop=5260, bwgon=1, bws=400000, pdose1=0.2, pdose2=8.6, pdose_p=0
!!prepare t, ca_t4ngg, tshngml
!!start/nc
t4FRF8p6=_ca_t4ngg
tshFRF8p6=_tshngml

plot(_t,t4FRF2p6(:,1),FRF2p6(:,1),FRF2p6(:,2),_t,tshFRF2p6(:,1),FRF2p6(:,1),FRF2p6(:,3),_t,t4FRF8p
6(:,1),FRF8p6(:,1),FRF8p6(:,2),_t,tshFRF8p6(:,1),FRF8p6(:,1),FRF8p6(:,3),'fFig9_LIDpaper.aps')
```

%M file to generate dose response plot for iodide. This is case sensitive.

```
!!prepare t, t4end, tshend
output @Clear
global PDOSE1
!!BW320
!!s tstop=1000
!!s pdose_p=0.01
pdose1=[0.1:0.1:20]
for x=[1:200]
PDOSE1=pdose1(x)
start @NoCallback
pdosei(x)=PDOSE1;
t4final(x)=T4END;
tshfinal(x)=TSHEND;
end
plot(pdosei,t4final,pdosei,tshfinal);
```

APPENDIX E

The procedure (PROCED) commands used in the BBDR-HPT axis model manuscript (Chapter 4) to set the initial values at each starting body weight are included in this Appendix Initial values were determined by running the model to steady-state (2000hrs) under iodide sufficienct (20 µg I/day) conditions. The PROCEDs were executed at the start of simulations for their corresponding body weight (see .m file code) to ensure steady-state conditions at the start of simulation.

```
!!PROCED BW500
s     bwc   =     0.5
s     t4b   =     28.2258
s     t3b   =     0.413853
s     tshb  =     8.7843
s     initavdtsh =     0.00869018
s     initap_t4  =     2.16906
s     initalb_t4 =     0.174259
s     inital_t4  =     0.304689
s     initalb_t3 =     0.00886592
s     inital_t3  =     0.074726
s     initap_t3  =     0.0474901
s     initap_i   =     285.104
s     initatb_i  =     0.00446223
s     initdat_i  =     10.3138
s     initdaib_i =     149.254
END
PROCED BW450
s     bwc   =     0.45
s     t4b   =     30.5456
s     t3b   =     0.42488
s     tshb  =     8.12055
s     initavdtsh =     0.00723019
s     initap_t4  =     2.11259
s     initalb_t4 =     0.169723
s     inital_t4  =     0.296861
s     initalb_t3 =     0.00807036
s     inital_t3  =     0.0731042
s     initap_t3  =     0.0438799
s     initap_i   =     250.898
s     initatb_i  =     0.00392517
s     initdat_i  =     8.52623
s     initdaib_i =     145.439
END
PROCED BW425
s     bwc   =     0.425
s     t4b   =     31.8826
s     t3b   =     0.431045
s     tshb  =     7.78168
s     initavdtsh =     0.00654356
s     initap_t4  =     2.08255
s     initalb_t4 =     0.167311
s     inital_t4  =     0.2927
s     initalb_t3 =     0.0076669
s     inital_t3  =     0.0722321
s     initap_t3  =     0.0420435
s     initap_i   =     234.154
s     initatb_i  =     0.00366229
s     initdat_i  =     7.68584
s     initdaib_i =     143.407
END
```

```
PROCED BW400
s     bwc   =     0.4
s     t4b   =     33.3644
s     t3b   =     0.437739
s     tshb  =     7.43768
s     initavdtsh =     0.00588639
s     initap_t4  =     2.05115
s     initalb_t4 =     0.164788
s     inital_t4  =     0.28835
s     initalb_t3 =     0.00725953
s     inital_t3  =     0.0713137
s     initap_t3  =     0.0401849
s     initap_i   =     217.565
s     initatb_i  =     0.00340184
s     initdat_i  =     6.879
s     initdaib_i =     141.28
END
PROCED BW390
s     bwc   =     0.39
s     t4b   =     34.0033
s     t3b   =     0.440585
s     tshb  =     7.29855
s     initavdtsh =     0.00563188
s     initap_t4  =     2.03817
s     initalb_t4 =     0.163745
s     inital_t4  =     0.286553
s     initalb_t3 =     0.00709545
s     inital_t3  =     0.0709321
s     initap_t3  =     0.039435
s     initap_i   =     210.992
s     initatb_i  =     0.00329865
s     initdat_i  =     6.56645
s     initdaib_i =     140.4
END
PROCED BW380
s     bwc   =     0.38
s     t4b   =     34.6715
s     t3b   =     0.443537
s     tshb  =     7.15852
s     initavdtsh =     0.00538218
s     initap_t4  =     2.02493
s     initalb_t4 =     0.162682
s     inital_t4  =     0.284721
s     initalb_t3 =     0.00693071
s     inital_t3  =     0.0705419
s     initap_t3  =     0.0386813
s     initap_i   =     204.454
s     initatb_i  =     0.00319601
s     initdat_i  =     6.25976
s     initdaib_i =     139.503
END
```

```
PROCED BW370
s     bwc   =     0.37
s     t4b   =     35.3712
s     t3b   =     0.446603
s     tshb  =     7.01754
s     initavdtsh =     0.00513734
s     initap_t4  =     2.01143
s     initalb_t4 =     0.161598
s     inital_t4  =     0.282852
s     initalb_t3 =     0.00676531
s     inital_t3  =     0.0701425
s     initap_t3  =     0.0379237
s     initap_i   =     197.952
s     initatb_i  =     0.00309393
s     initdat_i  =     5.95898
s     initdaib_i =     138.587
END
PROCED BW360
s     bwc   =     0.36
s     t4b   =     36.1047
s     t3b   =     0.449791
s     tshb  =     6.87558
s     initavdtsh =     0.00489738
s     initap_t4  =     1.99765
s     initalb_t4 =     0.160491
s     inital_t4  =     0.280945
s     initalb_t3 =     0.00659923
s     inital_t3  =     0.0697337
s     initap_t3  =     0.0371621
s     initap_i   =     191.485
s     initatb_i  =     0.00299241
s     initdat_i  =     5.66417
s     initdaib_i =     137.652
END
PROCED BW350
s     bwc   =     0.35
s     t4b   =     36.8746
s     t3b   =     0.45311
s     tshb  =     6.73262
s     initavdtsh =     0.00466234
s     initap_t4  =     1.98358
s     initalb_t4 =     0.159361
s     inital_t4  =     0.278998
s     initalb_t3 =     0.00643246
s     inital_t3  =     0.0693149
s     initap_t3  =     0.0363965
s     initap_i   =     185.056
s     initatb_i  =     0.00289148
s     initdat_i  =     5.37543
s     initdaib_i =     136.697
END
```

```
PROCED BW340
s     bwc   =     0.34
s     t4b   =     37.684
s     t3b   =     0.456571
s     tshb  =     6.58861
s     initavdtsh =     0.00443225
s     initap_t4  =     1.9692
s     initalb_t4 =     0.158206
s     inital_t4  =     0.277009
s     initalb_t3 =     0.006265
s     inital_t3  =     688855
s     initap_t3  =     0.0356266
s     initap_i   =     178.659
s     initatb_i  =     0.00279106
s     initdat_i  =     5.09266
s     initdaib_i =     135.72
END
PROCED BW330
s     bwc   =     0.33
s     t4b   =     38.536
s     t3b   =     0.460186
s     tshb  =     6.44352
s     initavdtsh =     0.00420716
s     initap_t4  =     1.9545
s     initalb_t4 =     0.157025
s     inital_t4  =     0.274976
s     initalb_t3 =     0.00609683
s     inital_t3  =     0.0684452
s     initap_t3  =     0.0348525
s     initap_i   =     172.288
s     initatb_i  =     0.00269105
s     initdat_i  =     4.81572
s     initdaib_i =     134.721
END
PROCED BW320
s     bwc   =     0.32
s     t4b   =     39.4344
s     t3b   =     0.463966
s     tshb  =     6.2973
s     initavdtsh =     0.00398709
s     initap_t4  =     1.93945
s     initalb_t4 =     0.155816
s     inital_t4  =     0.272896
s     initalb_t3 =     0.00592795
s     inital_t3  =     0.0679931
s     initap_t3  =     0.034074
s     initap_i   =     165.964
s     initatb_i  =     0.00259177
s     initdat_i  =     4.54528
s     initdaib_i =     133.699
END
```

```
PROCED BW310
s     bwc   =     0.31
s     t4b   =     40.3832
s     t3b   =     0.467927
s     tshb  =     6.14992
s     initavdtsh =     0.0037721
s     initap_t4  =     1.92405
s     initalb_t4 =     0.154579
s     inital_t4  =     0.270767
s     initalb_t3 =     0.00575833
s     inital_t3  =     0.0675287
s     initap_t3  =     0.033291
s     initap_i   =     159.672
s     initatb_i  =     0.002493
s     initdat_i  =     4.28098
s     initdaib_i =     132.652
END
PROCED BW300
s     bwc   =     0.3
s     t4b   =     41.387
s     t3b   =     0.472085
s     tshb  =     6.00132
s     initavdtsh =     0.00356221
s     initap_t4  =     1.90826
s     initalb_t4 =     0.153312
s     inital_t4  =     0.268586
s     initalb_t3 =     0.00558798
s     inital_t3  =     0.0670513
s     initap_t3  =     0.0325034
s     initap_i   =     153.421
s     initatb_i  =     0.00239488
s     initdat_i  =     4.02313
s     initdaib_i =     131.578
END
PROCED BW290
s     bwc   =     0.29
s     t4b   =     42.451
s     t3b   =     0.476457
s     tshb  =     5.85145
s     initavdtsh =     0.00335748
s     initap_t4  =     1.89208
s     initalb_t4 =     0.152011
s     inital_t4  =     0.26635
s     initalb_t3 =     0.00541687
s     inital_t3  =     0.06656
s     initap_t3  =     0.0317109
s     initap_i   =     147.207
s     initatb_i  =     0.00229735
s     initdat_i  =     3.77172
s     initdaib_i =     130.476
END
```

```
PROCED BW280
s     bwc   =     0.28
s     t4b   =     43.581
s     t3b   =     0.481064
s     tshb  =     5.70026
s     initavdtsh =     0.00315795
s     initap_t4  =     1.87547
s     initalb_t4 =     0.150677
s     inital_t4  =     0.264055
s     initalb_t3 =     0.00524499
s     inital_t3  =     0.066054
s     initap_t3  =     0.0309135
s     initap_i   =     141.04
s     initatb_i  =     0.00220056
s     initdat_i  =     3.52694
s     initdaib_i =     129.345
END
PROCED BW270
s     bwc   =     0.27
s     t4b   =     44.7838
s     t3b   =     0.485931
s     tshb  =     5.54769
s     initavdtsh =     0.00296366
s     initap_t4  =     1.8584
s     initalb_t4 =     0.149306
s     inital_t4  =     0.261699
s     initalb_t3 =     0.00507234
s     inital_t3  =     0.0655324
s     initap_t3  =     0.030111
s     initap_i   =     134.896
s     initatb_i  =     0.00210412
s     initdat_i  =     3.28835
s     initdaib_i =     128.182
END
PROCED BW260
s     bwc   =     0.26
s     t4b   =     46.067
s     t3b   =     0.491084
s     tshb  =     5.39368
s     initavdtsh =     0.00277466
s     initap_t4  =     1.84085
s     initalb_t4 =     0.147896
s     inital_t4  =     0.259277
s     initalb_t3 =     0.00489888
s     inital_t3  =     0.064994
s     initap_t3  =     0.0293033
s     initap_i   =     128.791
s     initatb_i  =     0.00200831
s     initdat_i  =     3.05644
s     initdaib_i =     126.986
END
```

```
PROCED BW250
s     bwc   =     0.25
s     t4b   =     47.4394
s     t3b   =     0.496553
s     tshb  =     5.23815
s     initavdtsh =     0.00259102
s     initap_t4  =     1.82278
s     initalb_t4 =     0.146445
s     inital_t4  =     0.256783
s     initalb_t3 =     0.00472462
s     inital_t3  =     0.0644378
s     initap_t3  =     0.02849
s     initap_i   =     122.701
s     initatb_i  =     0.00191272
s     initdat_i  =     2.83067
s     initdaib_i =     125.754
END
PROCED BW240
s     bwc   =     0.24
s     t4b   =     48.9112
s     t3b   =     0.502375
s     tshb  =     5.08104
s     initavdtsh =     0.00241277
s     initap_t4  =     1.80415
s     initalb_t4 =     0.144949
s     inital_t4  =     0.254215
s     initalb_t3 =     0.00454952
s     inital_t3  =     0.0638625
s     initap_t3  =     0.0276711
s     initap_i   =     116.67
s     initatb_i  =     0.00181807
s     initdat_i  =     2.61222
s     initdaib_i =     124.483
END
PROCED BW230
s     bwc   =     0.23
s     t4b   =     50.4941
s     t3b   =     0.508591
s     tshb  =     4.92225
s     initavdtsh =     0.00223997
s     initap_t4  =     1.78493
s     initalb_t4 =     0.143405
s     inital_t4  =     0.251565
s     initalb_t3 =     0.00437358
s     inital_t3  =     0.0632664
s     initap_t3  =     0.0268462
s     initap_i   =     110.647
s     initatb_i  =     0.00172356
s     initdat_i  =     2.3999
s     initdaib_i =     123.171
END
PROCED BW220
s     bwc   =     0.22
s     t4b   =     52.2018
s     t3b   =     0.515249
s     tshb  =     4.7617
s     initavdtsh =     0.0020727
s     initap_t4  =     1.76507
s     initalb_t4 =     0.14181
s     inital_t4  =     0.248828
s     initalb_t3 =     0.00419677
s     inital_t3  =     0.0626482
s     initap_t3  =     0.0260152
s     initap_i   =     104.656
s     initatb_i  =     0.00162955
s     initdat_i  =     2.19463
s     initdaib_i =     121.814
END
PROCED BW210
s     bwc   =     0.21
s     t4b   =     54.0507
s     t3b   =     0.522407
s     tshb  =     4.59928
s     initavdtsh =     0.001911
s     initap_t4  =     1.74451
s     initalb_t4 =     0.140159
s     inital_t4  =     0.245997
s     initalb_t3 =     0.00401907
s     inital_t3  =     0.0620057
s     initap_t3  =     0.0251777
s     initap_i   =     98.7042
s     initatb_i  =     0.00153614
s     initdat_i  =     1.99641
s     initdaib_i =     120.409
END
PROCED BW200
s     bwc   =     0.2
s     t4b   =     56.0599
s     t3b   =     0.530132
s     tshb  =     4.4349
s     initavdtsh =     0.00175495
s     initap_t4  =     1.7232
s     initalb_t4 =     0.138447
s     inital_t4  =     0.243063
s     initalb_t3 =     0.00384046
s     inital_t3  =     0.061337
s     initap_t3  =     0.0243333
s     initap_i   =     92.7534
s     initatb_i  =     0.00144277
s     initdat_i  =     1.80465
s     initdaib_i =     118.951
END
```

```
PROCED BW190
s     bwc   =     0.19
s     t4b   =     58.2524
s     t3b   =     0.538506
s     tshb  =     4.26842
s     initavdtsh =     0.00160462
s     initap_t4  =     1.70107
s     initalb_t4 =     0.13667
s     inital_t4  =     0.240017
s     initalb_t3 =     0.00366091
s     inital_t3  =     0.0606396
s     initap_t3  =     0.0234818
s     initap_i   =     86.8389
s     initatb_i  =     0.00134997
s     initdat_i  =     1.62027
s     initdaib_i =     117.436
END
PROCED BW180
s     bwc   =     0.18
s     t4b   =     60.6559
s     t3b   =     0.547625
s     tshb  =     4.09972
s     initavdtsh =     0.00146009
s     initap_t4  =     1.67803
s     initalb_t4 =     0.134819
s     inital_t4  =     0.236849
s     initalb_t3 =     0.00348039
s     inital_t3  =     0.0599106
s     initap_t3  =     0.0226226
s     initap_i   =     80.9273
s     initatb_i  =     0.00125722
s     initdat_i  =     1.44274
s     initdaib_i =     115.857
END
PROCED BW170
s     bwc   =     0.17
s     t4b   =     63.304
s     t3b   =     0.55761
s     tshb  =     3.92864
s     initavdtsh =     0.00132143
s     initap_t4  =     1.65399
s     initalb_t4 =     0.132889
s     inital_t4  =     0.233545
s     initalb_t3 =     0.00329887
s     inital_t3  =     0.519468
s     initap_t3  =     0.0217554
s     initap_i   =     75.0024
s     initatb_i  =     0.00116458
s     initdat_i  =     1.27234
s     initdaib_i =     114.208
END
PROCED BW160
s     bwc   =     0.16
s     t4b   =     66.238
s     t3b   =     0.568605
s     tshb  =     3.75504
s     initavdtsh =     0.00118874
s     initap_t4  =     1.62885
s     initalb_t4 =     0.130869
s     inital_t4  =     0.230092
s     initalb_t3 =     0.0031163
s     inital_t3  =     0.0583441
s     initap_t3  =     0.0208794
s     initap_i   =     69.1282
s     initatb_i  =     0.00107211
s     initdat_i  =     1.10938
s     initdaib_i =     112.48
END
PROCED BW150
s     bwc   =     0.15
s     t4b   =     69.5089
s     t3b   =     0.58079
s     tshb  =     3.57873
s     initavdtsh =     0.00106211
s     initap_t4  =     1.60245
s     initalb_t4 =     0.12875
s     inital_t4  =     0.226469
s     initalb_t3 =     0.00293264
s     inital_t3  =     0.0574976
s     initap_t3  =     0.0199939
s     initap_i   =     63.2203
s     initatb_i  =0.000979432
s     initdat_i  =     0.953656
s     initdaib_i =     110.662
END
PROCED BW140
s     bwc   =     0.14
s     t4b   =     73.1804
s     t3b   =     0.594391
s     tshb  =     3.39956
s     initavdtsh =0.000941678
s     initap_t4  =     1.57462
s     initalb_t4 =     0.126514
s     inital_t4  =     0.222652
s     initalb_t3 =     0.0027478
s     inital_t3  =     0.0566011
s     initap_t3  =     0.019098
s     initap_i   =     57.2967
s     initatb_i  =0.000886515
s     initdat_i  =     0.805462
s     initdaib_i =     108.74
END
```

```
PROCED BW130
s     bwc   =     0.13
s     t4b   =     77.3305
s     t3b   =     0.609676
s     tshb  =     3.21748
s     initavdtsh =0.000827583
s     initap_t4  =     1.54507
s     initalb_t4 =     0.124141
s     inital_t4  =     0.218601
s     initalb_t3 =     0.00256163
s     inital_t3  =     0.055645
s     initap_t3  =     0.0181899
s     initap_i   =     51.3558
s     initatb_i  =0.000793333
s     initdat_i  =     0.665139
s     initdaib_i =     106.684
END
PROCED BW120
s     bwc   =     0.12
s     t4b   =     82.0362
s     t3b   =     0.626885
s     tshb  =     3.03328
s     initavdtsh =0.000720188
s     initap_t4  =     1.513
s     initalb_t4 =     0.121566
s     inital_t4  =     0.214206
s     initalb_t3 =     0.00237349
s     inital_t3  =     0.0546065
s     initap_t3  =     0.172646
s     initap_i   =     45.376
s     initatb_i  =0.000699542
s     initdat_i  =     0.532868
s     initdaib_i =     104.406
END
PROCED BW110
s     bwc   =     0.11
s     t4b   =     87.0891
s     t3b   =     0.644923
s     tshb  =     2.85764
s     initavdtsh =0.000621944
s     initap_t4  =     1.47235
s     initalb_t4 =     0.1183
s     inital_t4  =     0.208594
s     initalb_t3 =     0.00217764
s     inital_t3  =     0.0533231
s     initap_t3  =     0.0162813
s     initap_i   =     39.3567
s     initatb_i  =0.000605082
s     initdat_i  =     0.410314
s     initdaib_i =     101.124
END
!!
```

APPENDIX F

The acslXtreme (version 2.4.0.11) .csl file for BBDR-HPT axis and ClO_4^- PBPK model code (Chapter 5) is contained within this Appendix. Model code is structured as follows: First section contains physiological parameters and compound-specific constants. Second section includes scaled model parameters. Last section includes model code for tbe BBDR-HPT axis (TSH, iodide, T4, and T3) and is followed by the ClO_4^- PBPK model code.

```
PROGRAM: Male Rat HPT Axis Model
!-------------------------------------------------------------------------
!File name:EHPTnogut.csl created 03/01/07 from EHPT_Imod_021407.csl
!Units in nmol, L, hr, kg
!Endogenous I, T4, T3, and TSH, and now combined with ClO4 PBPK model
!Blood binding of T4 99% bound - taken into account for liver uptake (0.01*cvl)
!Last Revised 10/12/07 by Eva McLanahan

      INITIAL
           CONSTANT   TSTOP=1416       !Length of experiment (1416=59 days)
           CONSTANT   CINT=0.5         !communication interval


! ------------ Physiological Parameters------------------
CONSTANT   QCC   =     14.0        !L/hr/kg - Total cardiac output  [Brown 1997
CONSTANT   QLC   =     0.174       !%QC - Proportion cardiac output to the liver [Brown 1997 p438]
CONSTANT   QTC   =     0.016       !%QC - Proportion cardiac output to the thyroid- human value
                                   (Brown 1997 & Merrill 2003)
CONSTANT   VLC   =     0.0366      !%BW liver tissue [Brown 1997 pg 416]
CONSTANT   VLBC  =     0.21        !%VL as liver blood [Brown 1997]
CONSTANT   VTC   =     0.00005     !%BW total thyroid tissue [McLanahan 2007]
CONSTANT   VTBC  =     0.157       !%VT as thyroid blood [Merrill et al 2003]

!------GROWTH EQUATION PARAMETERS---------
CONSTANT   BWC   =     0.320             !kg - body weight (a constant body weight)
CONSTANT   BWGon =     0                 !if BWGon=1 then BW growth equation on, else uses BWC
CONSTANT   BWs   =     170000            !mg - BW for start of study (must be given in lit.)
CONSTANT   BWt0  =     7314.70           !mg - initial BW at birth (Mirfazaelian 2007)
CONSTANT   KBW   =     63.21             !days - age at inflection point (Mirfazaelian 2007)
CONSTANT   BWtmax      =     521026.13   !mg - maximum body weight (Mirfazaelian 2007)
CONSTANT   gammaBW     =     2.01        !unitless - hill coeff for BW growth (Mirfazaelian 2007)

!------------ TSH Parameters-----------------------------
CONSTANT   MWTSH       =     28000       !g/mol - molecular weight TSH [chemfinder.com]
CONSTANT   Vd_TSHC     =     0.0554      !L/kg - VdTSH - (Connors et al 1984)
CONSTANT   K0TSHmaxC   =     6           !nmol/hr - Max prod of TSH (absence of T4) (Connors 1984)
!CONSTANT  Kinh_T4     =     0.2         !nmol/L - Km of T4 such that prod of TSH is 1/2 maximal
```

```
CONSTANT   Kinh_T4    =     0.3          !nmol/L - Km of T4 such that prod of TSH is 1/2 maximal
                                        (changed for Clo4 model)
CONSTANT   KNIS_TSH   =     0.949        !nmol/L - TSH conc so Vmax of NIS I transport is 1/2 max
CONSTANT   KbTSH      =     733.98       !nmol/L - Km TSH conc such that I binding/organification in
                                        thyroid is 1/2 maximal
CONSTANT   Kel_TSHC   =     1.8899       !1/hr-kg - elimination rate constant for TSH from Vd
                                        (Lemarchand-Beraud and Bertheir 1981)
CONSTANT   TSHb  =     5.08373          !ng/ml - TSH baseline to calc fold change. Set for each BW
CONSTANT   np    =     0.94             !unitless - Hill coefficient for production/feedback

!------------ I (Iodide) Parameters----------------------
CONSTANT   MWI        =     126.90447    !g/mol - molecular weight I [periodic table]
CONSTANT   Vd_iC      =     0.5          !L/kg - volume of distribution of iodide
CONSTANT   Km_i       =     31519        !nmol/L - affinity constant I for NIS (Gluzman and
                                        Niepomniszcze 1983 and Merrill 2003)
CONSTANT   VmaxT_iC   =     5738.267     !nmol/hr/kg - maximal rate of uptake
CONSTANT   PAt_iC     =     0.0001       !L/hr - PA term thyroid [Merrill 2003]
CONSTANT   V0bindC    =     1005.9       !nmol/hr-kg - maximum rate of binding of iodide in thyroid
CONSTANT   Kmb_i      =     244.59       !nmol/L - Km of iodide binding
CONSTANT   ClU_iC     =     0.0046       !L/hr-kg - urinary clearance of iodide

!-------Thyroid hormone production parameters--------------
CONSTANT   ktshcib    =     5e-7         !L2/nmol-hr - rate constant for thyroid hormone production
CONSTANT   np2        =     2            !unitless - Hill coefficient for TH production (clo4 supp.)

!------------ T4 (Thyroxine) Parameters------------------
CONSTANT   MWT4  =     776.8742         !g/mol - molecular weight T4 [calculated:C15H11I4NO4]
CONSTANT   MWT4G =     952              !g/mol - molecular weight T4-Glucuronide
                                        [calculated: T4(776)+GA(194)-H2O(18)=952]
CONSTANT   Vd_t4c     =     0.156        !L/kg bw - vd t4 (Kohn 1996)
CONSTANT   PL_t4      =     1.27         !Partition coefficient for T4 liver (EscobarMorreale 1996)
CONSTANT   PAL_t4C    =     0.0423       !nmol/hr/kg - from tracer - PA term for T4 liver
CONSTANT   VMAXDIC    =     19.89        !nmol/hr/kg - Vmax outer ring deiodinase
CONSTANT   KMDI       =     2300         !nmol/L - Km outer ring deiodinase in liver
                                        (Leonard and Visser 1986)
CONSTANT   KEL_t4C    =     0.05         !1/hr-kg - rate of elimination of T4 from body (Vd)
                                        (Abrams & Larsen 1973 t1/2 used for calculation)
```

```
CONSTANT   KmUGT       =     100000     !nmol/L - (Km of UGT enzymes for T4 and T3) (Visser 1993)
CONSTANT   VmaxT4GC    =     3435.89    !nmol/hr - max rate of T4-G formation in liver
CONSTANT   VMAXT4LUC   =     4384.73    !nmol/hr - Vmax for active uptake of T4 into liver
CONSTANT   KmT4LU      =     650        !nmol/L - Km for uptake in hepatocytes (Blondeau 1988)
CONSTANT   FFT4        =     0.01       !fraction of free t4 available for uptake to liver
CONSTANT   t4b         =     48.8846    !t4 baseline - to calc % control - diff for each BW

!------------ T3 (3,5,3'-Triiodothyronine) Parameters-----------------
CONSTANT   MWT3        =     650.97349  !g/mol - molecular weight T3 [calculated:C15H12I3NO4]
CONSTANT   Vd_T3C      =     0.186      !L/kg - Vd_T3 per kg BW [thyroid hormone metab pg 67]
CONSTANT   PL_t3       =     4.47       !Partition coefficient for T3 liver (EscobarMorreale 1996)
CONSTANT   PAL_t3C     =     0.1699     !L/hr/kg - from tracer - PA term liver T3
CONSTANT   Kel_t3C     =     0.12       !1/hr-kg- rate of T3 elimination from body
                                        (Abrams and Larsen 1973 t1/2 used for calculation)
CONSTANT   KmetL_t3C   =     3.65       !1/hr-kg - fractional removal rate from liver
CONSTANT   KLUT3       =     1.25       !L/hr - 1st order liver uptake rate of T3
CONSTANT   t3b         =     0.556647   !t3 baseline - to calc % control - diff for each BW

!---T4 and T3 iodide equivalents
CONSTANT   I4CON       =     0.6534     !Fraction of t4 as iodine (4 Im.w./T4m.w.) T4 iodide equiv
CONSTANT   I3CON       =     0.5848     !Fraction of T3 as iodine (3 Im.w./T m.w.) T3 iodide equiv
CONSTANT   T43CON      =     0.8379     !T3/T4 molar equivalents (T3 m.w. / T4 m.w.)
CONSTANT   IFT4M       =     0.16335    !One I freed in T4 Metabolism (I mw./T4 m.w.)

!--IODIDE dosing parameters
!CONSTANT  pdose_i     =     20         !ug - oral dose of iodide (diet I intake for McLanahan 2007
                                        calculated to be 20ug/day)
!pdose1 and pdose2 used instead of pdose_i for changing iodide intake during studies
CONSTANT   pdose1      =     20         !ug - 1st half of study iodide intake
CONSTANT   pdose2      =     20         !ug - 2nd half of study iodide intake

!---PERCHLORATE MODEL PARAMETERS-------------------------
CONSTANT   MWP   =     99.45            !g/mol - molecular weight of clo4 (chemfinder.com)
CONSTANT   PT_p  =     1                !unitless -
CONSTANT   PBody_p     =     0.36       !unitless - should be weighted (0.416 from Merrill)
CONSTANT   VmaxT_pC    =     177        !nmol/L/kg - opt - M.M Vmax for clo4 at thyroid NIS
```

```
CONSTANT   Km_p  =     1500            !nmol/L - Michaelis-Menten Km for clo4 at thyroid NIS
                                      (Kosugi et al 1996 - Ki value)
CONSTANT   Ki_p  =     1500            !nmol/L - Michaelis-Menten Km for clo4 at thyroid NIS
                                      (Kosugi et al 1996 - Ki value)
CONSTANT   PAT_pC      =     0.00028    !L/hr/kg - OPT - thyroid permeation coef-area cross product
CONSTANT   CLU_pC      =     0.018      !L/hr-kg - OPT - urinary clearance of perchlorate  0.025
CONSTANT   VmaxB_pC    =     6000       !nmol/hr/kg - Vmax binding perchlorate to serum proteins
CONSTANT   KmB_p =     225000          !nmol/L - Ka binding perchlorate to serum proteins
CONSTANT   Clunb_pC    =     0.032      !L/hr-kg - 1st order unbind of clo4 in serum (Merrill 2003)
CONSTANT   KNIS_TSHp   =     0.949      !nmol/L - OPT - TSH ½ max concentration for upreg of NIS
CONSTANT   pat_ip      =     0.0001     !just testing to see if diffusion out helps
     !Dosing Parameters for PERCHLORATE
          CONSTANT   PDOSE_p    =     0.    !mg/kg - Oral dose perchlorate
          CONSTANT   IVDOSEp    =     0.0       !mg/kg - iv dose clo4
          CONSTANT   tinf  =     0.001      !hr - length of iv infusion


!Compartment initial amounts from running EHPT model to steady state 2000hrs (1/27/07)
CONSTANT   initAvdTSH =     0.         !nmol TSH - initial amt of TSH in Vd
CONSTANT   initAP_t4  =     0.         !nmol T4 - initial amt of T4 in Vd (blood)
CONSTANT   initAlb_t4 =     0.         !nmol T4 - initial amt of T4 in liver blood
CONSTANT   initAl_t4  =     0.         !nmol T4 - initial amt of T4 in liver tissue
CONSTANT   initAlb_t3 =     0.         !nmol T3 - initial amt of T3 in liver blood
CONSTANT   initAl_t3  =     0.         !nmol T3 - initial amt of T3 in liver tissue
CONSTANT   initAP_t3  =     0.         !nmol T3 - initial amt of T3 in Vd (blood)
CONSTANT   initAP_i   =     0.         !nmol I - initial amt of iodide in Vd (blood)
CONSTANT   initAtb_i  =     0.         !nmol I - initial amt of iodide in thyroid blood
CONSTANT   initdAT_i  =     0.         !nmol I - initial amt of free iodide in thyroid tissue
CONSTANT   initdAIB_i =     0.         !nmol I - initial amt of bound iodide in thyroid tissue

          END ! INITIAL
     DYNAMIC
          ALGORITHM IALG = 2              !Gear method for stiff systems
```

```
DERIVATIVE
if (BWGon.eq.1) then
BW=BWG
else
BW=BWC
end if

!------Growth equations------
BWG=(((BWt0*(KBW**gammaBW))+(BWtmax*(Age**gammaBW)))/((KBW**gammaBW)+(Age**gammaBW)))/10**6
                                                        !BW (kg) at a given Age (days)
Age=Age0+days                                           !Age (days)
Age0=KBW*(((BWs-BWt0)/(BWtmax-BWs))**(1/(gammaBW)))     !Age (days) at start of study if only
                                                        initial BWs (mg) is given

!--------------- Scaled Parameters--------------
QC    =     QCC*BW**0.75     !L/hr - Cardiac output
QL    =     QLC*QC           !L/hr - blood flow to liver
QT    =     QTC*QC           !L/hr - blood flow to thyroid

VL1   =     VLC*BW           !L - liver volume with blood
VLB   =     VLBC*VL1         !L - Volume of liver blood
VL    =     VL1-VLB          !L - Liver tissue volume without blood
VT1   =     VTC*BW           !L - total thyroid volume
VTB   =     VTBC*VT1         !L - volume of thyroid blood
VT    =     VT1-VTB          !L - volume of thyroid without blood

!--TSH scaled parameters---
Vd_TSH      =     Vd_TSHC*BW             !L - Vd for TSH
Kel_TSH     =     Kel_TSHC/BW**0.25      !1/hr - TSH elim rate
K0TSHmax    =     K0TSHmaxC*BW**0.75     !nmol/hr - max rate of TSH secretion (no T4)
```

```
!--T4 scaled parameters----
Vd_t4      =     Vd_t4c*BW - VL1            !L - Vd for T4
VMAXDI     =     VMAXDIC*BW**0.75           !nmol/hr - Vmax for type 1 5'd in liver for t4
PAL_t4     =     PAL_t4C*BW**0.75           !L/hr - PA term for liver t4
Kel_t4     =     KEL_t4C/BW**0.25           !1/hr - T4 elimination rate from body
VmaxT4G    =     VmaxT4GC*BW**0.75          !nmol/hr - Vmax for t4 glucuronidation in liver
VmaxT4LU   =     VmaxT4LUC*BW**0.75         !nmol/hr - Vmax for liver uptake of t4

!--T3 scaled parameters--
Vd_t3      =     Vd_t3C*BW - VL1            !L - Vd for T3
PAL_t3     =     PAL_t3C*BW**0.75           !L/hr - PA term for T3 in liver
Kel_t3     =     KEL_t3C/(BW**0.25)         !1/hr - T3 elimination rate from body
KmetL_t3   =     KmetL_t3C/(BW**0.25)       !1/hr - nonspecific T3 metabolism in liver

!--Iodide scaled parameters--
Vd_i       =     Vd_ic*BW - VT1             !L - volume of distribution of iodide
VmaxT_i    =     VmaxT_iC*BW**0.75          !nmol/hr - max rate of iodide uptake by NIS in thyroid
ClU_i =    ClU_iC/(BW**0.25)                !L/hr - Urinary clearance of iodide
     !Changed scaling from V0bindc*BW**0.75 to below on 7/18/07 based on initialconditions.xls
     showing total thyroid iodide in thyroid not dropping below 7 for 120-180g rats and not above
     20 for 400g rat
V0bind     =     V0bindC/(BW**0.75)         !nmol/hr - max rate of binding of iodide in thyroid
PAT_i      =     PAT_iC*BW**0.75            !L/hr - PA term for thyroidal iodide

!--Perchlorate scaled parameters--
VBody_p    =     BW-VT-VTB-VPlas       !L - volume of "rest of body" for clo4 distribution
VPlas      =     VPLC*BW               !L - volume of plasma
QBody_p    =     QC-QT                 !L/hr - blood flow to rest of body for clo4 distribution
ClU_p      =     CLU_pC/(BW**0.25)     !L/hr - urinary clearance of clo4 (from rest of body)
VmaxT_p    =     VmaxT_pC*BW**0.75     !nmol/hr - vmax for perchlorate uptake into thyroid
PAT_p      =     PAT_pC*BW**0.75       !L/hr - PAterm for clo4 diffusion into thyroid
VmaxB_p    =     VmaxB_pC*BW**0.75     !nmol/hr - Vmax binding perchlorate to serum proteins
Clunb_p    =     Clunb_pC/(BW**0.25)   !L/hr - unbinding of clo4 to serum proteins
```

```
!----MODEL CODE---TSH volume of distribution with feedback T4-----------------
!RTSHPR=(K0TSHmax*Kinh_T4)/(Kinh_T4+Ca_t4)       !nmol/hr - Rate of TSH production
RTSHPR=(K0TSHmax*Kinh_T4**np)/(Kinh_T4**np+Ca_t4**np))
     ATSHPR=INTEG (RTSHPR,0.0)                   !nmol - Amount TSH produced
     ATSHPRug=ATSHPR*MWTSH/1000                  !ug - amount of TSH produced
     d_TSHPRugd=(ATSHPRug/(((t+1e-6)/24)))       !ug/d - TSH production
RClTSH=Kel_TSH*AVdTSH                            !nmol/hr - clearance of TSH from Vd
     AClTSH=INTEG(RClTSH,0.0)                    !nmol - amt of TSH cleared from Vd
RAVdTSH=RTSHPR-RClTSH                            !nmol/hr - rate of change of TSH in Vd
     AVdTSH=INTEG(RAVdTSH,initAVdTSH)            !nmol - amt of TSH in Vd
     TSH=AVdTSH/Vd_TSH                           !nmol/L - Concentration TSH
     TSHngml=(TSH/1000) * MWTSH                  !ng/mL (same as ug/L)- TSH concentration in Vd
!fold change tsh
TSHFOLD=(TSHngml/TSHb)                           !fold change TSH
TSHpercon=(TSHngml/TSHb)*100                     !TSH as % control

!----MODEL CODE---Iodide, IV dose w/thyroid and Vd -----------
!----Iodide dosing----------oral dose------------
!Change in iodide diet 1X - t=5040 for Fukuda Refeeding data
!pdose1 and pdose2 set in m file
     if (t.GT.5040) then
          pdose_i=pdose2
     else
          pdose_i=pdose1
     end if

!Normal Oral Dosing parameters for I
     dose_i    = (pdose_i*10**3)/MWI        !dietary intake amount (nmol)
     Rdose_i   = dose_i/12                  !dose rate for eating period (hrs) per day
!Food Consumption for a 12 hr period (light-dark cycle in rat)
     pflag=pulse(0.0,24.0,12)               !for one 12 hr eating period per day
     RMR_i = (Rdose_i * pflag)              !nmol/hr - dose rate for oral dose iodide
          AST_i = INTEG(RMR_i,0.0)          !nmol - amt of iodide received orally entering stomach
          d_AST_i=AST_i/(((t+1e-6)/24))     !nmol - daily amt of iodide received orally in stomach
          d_AST_iug=(d_AST_i*MWI)/(10**3)   !ug - daily amt of iodide received orally in stomach
```

```
!---Volume of Distribution of Free Iodide -----
RAP_i=RMR_i+QT*Cvt_i-QT*Ca_i+RAIFL_t4+RAIFL_t3+RAIFvd_t4+RAIFvd_t3-RU_i
                                        !nmol/hr - rate of change of free iodide in serum
AP_i=INTEG(RAP_i,initAP_i)              !nmol - amount of free iodide in serum
     CP_i=AP_i/Vd_i                     !nmol/L - concentration of free iodide in serum
     Ca_i=CP_i
          CP_iugdl=(CP_i*MWI/10000)     !ug/dL - concentration of free iodide in serum
          CP_ingml=(CP_i*MWI/1000)
Ca_bi=(Ca_t4*I4CON)+(Ca_t3*I3CON)       !nmol/L - concentration of bound iodide in serum
     Ca_bingml=(Ca_bi*MWI)/1000         !ng/ml - concentration of bound iodide in serum
Ca_ti=Ca_i+Ca_bi                !nmol/L - concentration of total iodide (bound + free) in serum
     Ca_tiugdl=Ca_ti*MWI/10000  !ug/dl - total iodide
     Ca_tingml=Ca_ti*MWI/1000   !ng/ml - total iodide
RU_i=ClU_i*Ca_i                         !nmol/hr- rate of urinary clearance of iodide
     AU_i=INTEG(RU_i,0.0)               !nmol - amount of iodide cleared in urine
     d_au_i=AU_i/((t+1e-6)/24)          !nmol/d - iodide cleared in urine
     AU_iug=AU_i*MWI/1000               !ug - amount of iodide cleared in urine
     d_AUiug=AU_iug/((t+1e-6)/24)       !ug/d of iodide cleared in urine
     PINIEX=(d_AU_i/(d_AST_i+1e-6))*100 !% of daily intake of iodide excreted in urine

!---Rate of metabolism of TH in Vd -- freeing of iodide
RAIFvd_t4=Rvdel_t4*IFT4M                !nmol/hr - rate of I freed from T4->T3 metabolism in Vd
     AIFVd_t4=INTEG(RAIFvd_t4,0.0)      !nmol - amount of I freed from T4->T3 metabolism in Vd
RAIFvd_t3=(Rvdel_t3*I3CON)              !nmol/hr - rate of I freed from T3 metabolism in Vd -
                                        assume all goes to T3, that T3 metab is rate limiting step
     AIFVd_t3=INTEG(RAIFvd_t3,0.0)      !nmol - amount of I freed from T3 metabolism in Vd

!-------Liver iodide metabolism of THs, added to Iodide Vd-------------
RAIFL_t4=RADIL*IFT4M                    !nmol/hr - rate of I freed in liver from T4 metab to T3
     AIFL_t4=INTEG(RAIFL_t4,0.0)        !nmol - amt of iodide released in liver from T4 metab to T3
RAIFL_t3=RAML_t3*0.70*I3CON             !nmol/hr - EST 70% of T3 metabolized into free I-
     AIFL_t3=INTEG(RAIFL_t3,0.0)        !nmol - amount of I freed in liver from T3 metabolism

!------------THYROID IODIDE---------------------------
!Rate of active iodide uptake into thyroid by the NIS
!RTNIS=(VmaxT_iTSH*Cvt_i)/(Cvt_i+Km_i)          !nmol/hr - rate of I active uptake (NIS)-no clo4
RTNIS=((VmaxT_iTSH*Cvt_i)/(Cvt_i+Km_i*(1+(Cvt_p/Ki_p))))
```

```
                    !nmol/hr - rate of active uptake (NIS) and inhibition by perchlorate
!RTNIS=0.0001                                   !very very low NIS to see effects
VmaxT_iTSH=((VmaxT_i*TSH)/(KNIS_TSH+TSH))       !nmol/hr - change in Vmax due to TSH stimulation
     ATIU=INTEG(RTNIS,0.0)                      !nmol - Amount of I uptake (active) into thyroid

!Rate of change of iodide in thyroid blood
RAtb_i=Qt*(CA_i-Cvt_i)+PAt_i*(Ctf_i-Cvt_i)-RTNIS     !nmol/hr - rate of change of I in thy blood
     Atb_i=INTEG(RAtb_i,initAtb_i)                   !nmol - amount of I in thyroid blood
     Cvt_i=Atb_i/VTB                                 !nmol/L - conc of I in thyroid blood

!Rate of change of FREE IODIDE IN THYROID
RAtf_i=RTNIS+PAt_i*(Cvt_i-Ctf_i)-RIB
     dAtf_i=INTEG(RAtf_i,initdAt_i)         !nmol - amount of free iodide in thyroid lumen was
     Atf_i=MAX(dAtf_i,0)
          Atf_iug=Atf_i*MWI/1000            !ug - amount of free iodide in thyroid lumen
     Ctf_i=Atf_i/VT                         !nmol/L - conc of free iodide in thyroid tissue
          Ctf_imgl=Ctf_i*MWI/10**6          !mg/L - concentration of free I in thyroid tissue

!Rate of incorporation (binding) of iodide in thyroid tissue
RIB=(Vmaxbt_i*Ctf_i)/(Kmb_i+Ctf_i)          !nmol/hr - rate of incorporation of iodide in thyroid
Vmaxbt_i=(V0bind*TSH)/(KbTSH+TSH)           !nmol/hr - vmax of binding change (stimulated by TSH
                                                 concentration in Vd
     ARIB=INTEG(RIB,0.0)                    !nmol - amount of iodide incorporated in thyroid
     ARIBug=ARIB*MWI/1000                   !ug - amount of iodide incorporated in thyroid
     d_aribug=(ARIBug/(((t+1e-6)/24)))      !ug - daily amt of iodide incorporated in thyroid

!Rate of change of BOUND iodide in thyroid tissue
RIB_i=RIB-Rth                           !nmol/hr - rate of change of bound iodide in thyroid
                                        (rate of binding - loss as secretion of thyroid hormone)
     dAIB_i=INTEG(RIB_i,initdAIB_i)
          AIB_iug=(AIB_i*MWI)/1000      !ug - amt iodide bound in thyroid
     CIB_i=AIB_i/VT                     !nmol/L - concentration of iodide bound in thyroid
          CIB_imgl=CIB_i*MWI/10**6      !mg/L - concentration of iodide bound in thyroid

!Set a maximum and minimum amt of iodide stores in thyroid - max is not really needed even for
iodide up to 500ug/day
if (dAIB_i.GT.160) then
```

```
AIB_i=160
else if (dAIB_i.LT.0)then
AIB_i=0
else
AIB_i=dAIB_i
end if

!Rate of utilization of bound I secreted as TH (rate of production of T4 and T3 in iodide equiv.)
Rth=(RPR_t4*I4CON)+(RPR_t3*I3CON)     !nmol I/hr - rate of utilization of thyroid I in TH prod
     Ath=INTEG(Rth,0.0)                      !nmol - amount of iodide used in TH prod
     d_ath=Ath/((t+1e-6)/24)                 !nmol/day - daily amt of iodide used in TH prod
     Athug=Ath*MWI/1000                      !ug - amount of iodide used in TH prod
     d_athug=Athug/((t+1e-6)/24)             !ug/day - daily amount of iodide used in TH prod
     PINITHPR=(d_ath/(d_ast_i+1e-6))*100     !% of daily intake of iodide used in TH prod

!Rate of change of FREE iodide in thyroid tissue - allows you to look at the free entering and
leaving, also loss of free to binding
     RAt_ien=RTNIS+(PAt_i*Cvt_i)             !nmol/hr - rate of free iodide entering thyroid lumen
                                             (active uptake and diffusion)
          At_ien=INTEG(RAt_ien,0.0)          !nmol - total amt of I entering thyroid (NIS and diff)
     RAt_iex1=(PAt_i*Ctf_i)                  !nmol/hr - rate of free I diff out of thyroid tissue
          At_iex1=INTEG(RAt_iex1,0.0)        !nmol - amt of iodide diff out of thyroid
     RAt_iex2=RAt_iex1+Rth                   !nmol/hr - total loss of iodide from thyroid
                                             (diffusion and secretion as thyroid hormone)
          At_iex2=INTEG(RAt_iex2,0.0)        !nmol - total amt of iodide loss from thyroid
                                             (diffusion and secretion as thyroid hormone)

!Total Iodide in thyroid tissue (nmol)
TAt_i=AIB_i+Atf_i                !nmol - total amount of iodide in thyroid (free and bound)
TAt_img=(TAt_i*MWI)/10**6        !mg - total amount of iodide in thyroid (free and bound)
TCt_imgL=TAt_img/VT              !mg/L - total concentration of iodide in thyroid (free and bound)
TAt_iug=TAt_i*MWI/1000           !ug (my data suggests should be between 10-18 ug)
```

```
!------------MODEL CODE-------Thyroid hormone production in the Thyroid------------
 !---Production of Total thyroid hormones--based on TSH and "bound" iodide pool----
!RPR_th=ktshcib*TSH*CIB_i              !nmol/hr - production rate of thyroid hormones (used in ID)
RPR_th1=ktshcib*TSH*CIB_i                   !nmol/hr - production rate of thyroid hormones
PTHS=((Kp**np3)/(Kp**np3+(Ct_p**np3)))      !unitless-inhibition of th production
Rpr_th=Rpr_th1*PTHS                         !nmol/hr - final rate of thyroid hormone production
!RPR_th=0.001                               !test shut off of thyroid hormone production

!Fractionation of thyroid hormone production
dFt3calc=0.2652*((TAT_iug)**(-0.4684))           !derived from Pedraza 2006
Ft3calc=MIN(dFT3calc,0.90)

RPR_t3=Ft3calc*RPR_th                            !nmol/h - rate of T3 production from thyroid
     APR_t3=INTEG(RPR_t3,0.0)                    !nmol - amt of T3 produced in thyroid
     APR_t3Tug=APR_t3*MWT3/1000                  !ug - amt of T3 produced in thyroid
     d_PRT3Tugd=(APR_t3Tug/(((t+1e-6)/24)))      !ug/day - daily production rate of T3 in thyroid

RPR_t4=RPR_th-RPR_t3                             !nmol/h - rate of T4 production from thyroid
     APR_t4=INTEG(RPR_t4,0.0)                    !nmol - amt of T4 produced in thyroid
     APR_t4ug=APR_t4*MWT4/1000                   !ug - amt of T4 produced
     d_PRT4ugd=(APR_t4ug/(((t+1e-6)/24)))        !ug/day - daily production rate of T4
     d_PRT4nmold=(APR_t4/(((t+1e-6)/24)))        !nmol/day - daily production rate of T4
!T3/T4 ratio
MR34T=APR_t3/(APR_t4+1e-6)                       !T3/T4 production ratio


!---------MODEL CODE--- Total T4 with a Liver and Vd-----------
!--------------SERUM T4 (Volume of distribution)-----------------
!AP_t4= amount of total t4 in Vd
RAP_t4=RPR_t4+(QL*CVL_t4)-QL*Ca_t4-RVdel_t4      !nmol/hr - rate of change of T4 in serum
     AP_t4=INTEG(RAP_t4,initAP_t4)               !nmol - amount of T4 in SERUM
     Ca_t4=AP_t4/Vd_t4                           !nmol/L - concentration of T4 in SERUM
     Ca_t4ugdl=(Ca_t4*MWT4)/10000                !ug/dL - T4 in SERUM
     Ca_t4ngg=(Ca_t4*MWT4)/1000                  !ng/g or ng/mL - T4 in serum
     t4percon=(ca_t4ngg/t4b)*100                 !%control - serum T4
```

```
!AVdel_t4=amount of t4 cleared from vd - assumed to go to t3+free iodide
RVdel_t4=Kel_t4*Ap_t4                              !nmol/h - rate of T4 elimination from Vd
     AVdel_t4=INTEG(RVdel_t4,0.0)                  !nmol - amount of T4 eliminated from Vd
     d_AVdel_t4=(AVdel_t4/(((t+1e-6)/24)))         !nmol/d - daily amount of T4 eliminated from Vd


!-------Liver T4-------------
!Diffusion limited liver with active uptake of free serum T4 (added 3.20.07)
!Cvl*FFT4 assumes only a fraction of the total blood concentration is available for diffusion or
active uptake into the liver
RALb_t4=QL*(Ca_t4-Cvl_t4)+PAL_t4*(CL_t4-(Cvl_t4*FFT4))-RLT4U
                                                   !nmol/hr - rate of change in liver blood (t4)
     ALb_t4=INTEG(RALb_t4,initAlb_t4)              !nmol - amount of t4 in liver blood
     Cvl_t4=ALb_t4/(VLB*PL_t4)                     !nmol/L - concentration of t4 in liver blood

RAL_t4=(PAL_t4*((Cvl_t4*FFT4)-Cl_t4))-RAGL-RADIL+RLT4U
                                                   !nmol/hr - rate of change in liver tissue (t4)
     AL_t4=INTEG(RAL_t4,initAl_t4)                 !nmol - amount of T4 in liver tissue
     CL_t4=AL_t4/VL                                !nmol/L - concentration of t4 in liver tissue
     Cl_t4ngg=(CL_t4*MWT4/1000)/1.051              !ng/g - concentration of T4 in liver tissue
                                                   (1.051=liver density, Obermoyer 1987)

RLT4U=(VmaxT4LU*(Cvl_t4*FFT4))/(KmT4LU+(Cvl_t4*FFT4))  !nmol/hr - rate of liver T4 active
                                                       uptake (only FRACTION free available)
     ALT4U=INTEG(RLT4U,0.0)


!Metabolism of T4 in liver - via deiodination
RADIL=((VMAXDI*Cvl_t4)/(Cvl_t4+KMDI))        !nmol/hr - rate of T4 deiodination in liver (D1)
     ADIL=INTEG(RADIL,0.0)                   !(nmol) Amount of T4 deiodinated (D1) in liver
     d_ADIL_T4=(ADIL/(((t+1e-6)/24)))        !nmol/d - amount of T4 deiodinated in liver per day

     PC43L=(ADIL/(APR_t4+1e-6))*100          !% T4 converted by Type I 5'-D in liver

!Metabolism of T4 in the liver - via glucuronidation
RAGL=(VmaxT4G * Cvl_t4)/(KmUGT + Cvl_t4)     !nmol T4/hr - rate of T4-glucuronidation in liver
     AGL=INTEG(RAGL,0.0)                     !nmol T4 lost/used to make T4-G
```

```
RAGLT4G=(RAGL*(MWT4G/MWT4))                  !nmol T4-G formed/hr
     AGLT4G=INTEG(RAGLT4G,0.0)               !nmol T4-G formed
     RGLT4Gpmolhr=RAGLT4G*1000               !pmol T4-G formed/hr/liver

d_AT4_feces=(AGL/(((t+1e-6)/24)))            !nmol/d - amount of T4-G excreted in feces per day
PT4PRinfeces=(d_AT4_feces/(d_PRT4nmold+1e-6))*100     !% of T4 produced excreted in feces/day

! -- Overall T4 Metabolism --
!AWBT4Met=total amount of T4 metabolized (liver gluc + liver deiod + Vd metab)
RWBT4Met=RVdel_t4+RAGL+RADIL                 !nmol/hr - whole body rate of T4 metabolism
     AWBT4Met=INTEG(RWBT4Met,0.0)            !nmol - amt of T4 metabolized (total - whole body)
     d_AWBT4Met=(AWBT4Met/(((t+1e-6)/24)))   !nmol/day - whole body loss of T4

AT4T3=Avdel_t4+Adil
FMWBT4=(AWBT4Met/(APR_t4+1e-6))*100          !% of produced T4 that is metab. Sum of all pathways
FMVdT4=(AVdel_t4/(APR_t4+1e-6))*100          !% of produced T4 that is metab in Vd
(FMGLT4=(AGL/(APR_t4+1e-6))*100              !% of produced T4 that is metab to T4-G in liver
FMDILT4=(ADIL/(APR_t4+1e-6))*100             !% of produced T4 that is metab to t3 in liver
FMT4T3=FMvdT4+FMDILT4                        !% of T4 converted to T3


!---------MODEL CODE--- Total t3, with a Liver and Vd-----------
!--------------SERUM t3 (Volume of distribution)------------------
!----production of T3 in the Vd from T4 metabolism
!AT3FVd=amount of T3 formed in the Vd from T4 metabolism
RT3FVd=(RVdel_t4*T43CON)                     !nmol t3/hr - all T4 to T3+I
     AT3FVd=INTEG(RT3FVd,0.0)                !nmol - amt of T3 formed in Vd from T4 metabolism
     AT3FVdug=AT3FVd*MWT3/1000               !ug - amount of T3 produced from T4 metabolism in Vd

RAP_t3=(QL*CVL_t3)-QL*Ca_t3-RVdel_t3+RPR_t3+RT3FVd     !nmol/hr - rate of change of t3 in Vd
     AP_t3=INTEG(RAP_t3,initAP_t3)                     !nmol - amount of t3 in Vd
     Ca_t3=AP_t3/Vd_t3                                 !nmol/L - concentration of t3 in Vd
     Ca_t3ugdl=Ca_t3*(0.0001)*MWT3                     !ug/dL - t3 in Vd
     Ca_t3ngg=(Ca_t3*MWT3)/1000                        !ng/g - t3 in Vd
     t3percon=(ca_t3ngg/t3b)*100                       !%control - Vd T3
```

```
RVdel_t3=Kel_t3*Ap_t3                                   !nmol/h - rate of t3 elim from Vd
                                                        !assumed all metab to free I-
     AVdel_t3=INTEG(RVdel_t3,0.0)                       !nmol - amount of t3 elim from Vd

!-------Liver t3-------------
!----production of T3 in liver
RAT3FL=RADIL*T43CON             !nmol/hr - rate of T3 formed in liver from T4 deiod. in T3 equiv.
     AT3FL=INTEG(RAT3FL,0.0)    !nmol - amount of T3 formed in liver

!Diffusion limited liver
RALb_t3=QL*(CA_t3-Cvl_t3)+PAL_t3*(CL_t3-Cvl_t3)-RLt3U
                                                        !nmol/hr - rate of change in liver blood (t3)
     ALb_t3=INTEG(RALb_t3,initAlb_t3)                   !nmol - amount of t3 in liver blood
     Cvl_t3=ALb_t3/(VLB*PL_t3)                          !nmol/L - concentration of t3 in liver blood

RAL_t3=(PAL_t3*(Cvl_t3-Cl_t3))+RAT3FL-RAML_t3+RLt3U
                                                        !nmol/hr - rate of change in liver tissue (t3)
     AL_t3=INTEG(RAL_t3,initAl_t3)                      !nmol - amount of t3 in liver tissue
     CL_t3=AL_t3/VL                                     !nmol/L - concentration of t3 in liver tissue
     Cl_t3ngg=(CL_t3*MWT3/1000)/1.051                   !ng/g - concentration of T3 in liver tissue
                                                        (1.051=liver density, Obermoyer 1987)

RLT3U=Cvl_t3*KLUT3                                      !nmol/hr - 1st order rate of liver uptake of T3
     ALT3U=INTEG(RLT3U,0.0)     !nmol - amt of T3 actively transported into liver

RAML_t3=AL_t3*KmetL_t3          !nmol/hr - rate of T3 metabolism in liver (unspecified) - assume
                                small portion excreted and rest forms free I-
     AML_t3=INTEG(RAML_t3,0.0)  !nmol - amount of T3 metabolized in liver
     RAT3feces=RAML_t3*0.30     !nmol/hr - rate of T3 excreted in feces
          AT3_feces=INTEG(RAT3feces,0.0)                !nmol - amt of T3 excreted in feces
          d_AT3_feces=(AT3_feces/(((t+1e-6)/24)))       !nmol/d - amt of T3 excreted in feces/day

!----Total production of t3
TAPR_t3=AT3FVd+AT3FL+APR_t3                             !nmol - total amount of T3 produced
TAPR_t3ug=TAPR_t3*MWT3/1000                             !ug - total amt of T3 produced
d_PRT3ugd=TAPR_t3ug/((t+1e-6)/24)                       !ug/d - whole body production of T3 per day
FAPR_t3Thy=(APR_t3Tug/(TAPR_t3ug+1e-6))*100             !% of total T3 prod that occurs in the thyroid
```

```
!---T3 Metabolism contribution of pathways
RWBT3Met=RAML_t3+RVdel_t3                          !nmol/hr - Rate of overall T3 metabolism
     AWBT3Met=INTEG(RWBT3Met,0.0)                  !nmol - total amount of T3 metabolized
     d_AWBT3Met=(AWBT3Met/(((t+1e-6)/24)))         !nmol - total daily amount of T3 metabolized

FMWBT3=(AWBT3Met/(TAPR_t3+1e-6))*100          !% of produced T3 that is metab - sum of all pathways
FMVdT3=(AVdel_t3/(TAPR_t3+1e-6))*100          !% of produced T3 that is metabolized in the Vd
FMLT3=(AML_t3/(TAPR_t3+1e-6))*100             !% of produced T3 that is metabolize in the liver
FMFeT3=(AT3_feces/(TAPR_t3+1e-6))*100         !% of produced T3 that is excreted in Feces

!------END HPT AXIS MODEL-----------------------------------------------------

!------BEGIN PBPK MODELS FOR CHEMICALS-----------------------------------
!-------ClO4 model-----iv and drinking water-----------------------------
!Oral Dosing (water consumption) parameters for perchlorate
     dose_p    = (pdose_p1*BW*10**6)/MWP          !nmol - administered amount of clo4 in d.w
     Rdose_p=dose_p/12                            !nmol/hr - dose rate for drinking avg over 12 hr
     pflag_p=pulse(0.0,24.0,12)                   !pulse command for perchlorate dosing -
     RMR_p=(Rdose_p*pflag_p)                      !nmol/hr - dose rate of clo4 in drinking water
          AST_p=INTEG(RMR_p,0.0)                  !nmol - total amt of clo4 dosed/administered
          d_AST_p=AST_p/(((t+1e-6)/24))           !nmol - daily amt of clo4 rec. orally in stomach

!IV Dosing parameters for perchlorate
    IVDOSE_p=(IVDOSEp*(10**6)*BW)/(MWP)           !nmol amt ivdose
     iflag_p=pulse(0,tstop,tinf)                  !iflag = pulse -->dose at time 0
     RIV_p=(IVDOSE_p/TINF)*iflag_p                !nmol/hr - rate iodide iv dosing
          AIV_p=INTEG(RIV_p,0.)                   !nmol - Amount iodide iv dosed

!----Plasma compartment for perchlorate-----
Ca_p=Cv_p
RAb_p=RMR_p+RIV_p+(QT*Cvt_p)+(Qbody_p*Cvbody_p)-(QC*Ca_p)-RU_p!-RBB_p
                                          !nmol/hr - rate of change of free clo4 in plasma
     Ab_p=INTEG(RAb_p,0.0)                !nmol - free amount clo4 in plasma
     Cv_p=Ab_p/VPlas                      !nmol/L - free amount of clo4 in plasma

!Binding of perchlorate to serum proteins. Approach used by Merrill and Clewel. Determined not
sensitive, so not used in this model.
```

```
!RBB_p=((VmaxB_p*Ca_p)/(KmB_p+Ca_p))-(Clunb_p*Cabnd_p)
           !nmol/hr - rate of change in amt of clo4 bound in plasma (binding rate - unbinding)
!     Abbnd_p=INTEG(RBB_p,0.0)                !nmol - amt of clo4 bound in plasma
!     Cabnd_p=Abbnd_p/Vplas                   !nmol/L - concentration of clo4 bound in plasma
!PERB_p=Cabnd_p/(Catot_p+1e-6)                !Percent bound in blood

CaTot_p=Cv_p          !+Cabnd_p              !nmol - total clo4 in plasma (bound + free)
Ca_pugml=CaTot_p*MWp/10**6                   !ug/mL - concentration of perchlorate in plasma

RU_p=ClU_p*Cv_p                              !nmol/hr - rate of urinary clo4 excretion
     AU_p=INTEG(RU_p,0.0)                    !nmol - amt of clo4 excreted in urine
     AU_pug=AU_p*MWP/1000                    !ug - amt of clo4 excreted in urine

!------THYROID PERCHLORATE------
RTNIS_p=(VmaxT_pTSH*Cvt_p)/(Cvt_p+Km_p*(1+(Cvt_i/Km_i)))
                      !nmol/hr - rate of NIS uptake of clo4 into thyroid (no iodide competition)
     VmaxT_pTSH=((VmaxT_p*TSH)/(KNIS_TSHp+TSH))
                      !nmol/hr - Vmax for clo4 uptake into thyroid stimulated by TSH
     ATNIS=INTEG(RTNIS_p,0.0)                    !nmol - amt of clo4 taken up into thyroid via NIS

RATB_p=QT*(Ca_p-Cvt_p)+PAt_p*(Ct_p-Cvt_p)-RTNIS_p
                      !nmol/hr - rate of change in thyroid blood of clo4
     Atb_p=INTEG(RATB_p,0.0)                 !nmol - amt of clo4 in thyroid blood
     Cvt_p=Atb_p/VTB                         !nmol/L - conc of clo4 in thyroid blood

RAT_p=RTNIS_p+PAT_p*(Cvt_p-Ct_p)             !nmol/hr - rate of change of clo4 in thyroid tissue
     At_p=INTEG(RAT_p,0.0)                   !nmol - amt of clo4 in thyroid tissue
     Ct_p=At_p/(VT*PT_p)

Ct_pugg=(At_p/VT)*MWp/10**6                  !ug/g - conc of clo4 in thyroid tissue

!To look at rates in and out of thyroid for perchlorate
RATp_in=RTNIS_p+(PAt_p*Cvt_p)
RATp_out=PAT_p*Ct_p
```

```
!-------Rest of Body Perchlorate----------
RABody_p=Qbody_p*(Ca_p-Cvbody_p)            !nmol/hr - rate of change of clo4 in 'rest of body'
     ABody_p=INTEG(RABody_p,0.0)            !nmol - amt of clo4 in 'rest of body'
     Cvbody_p=ABody_p/(VBody_p*PBody_p)     !nmol/L - clo4 in venous blood leaving 'rest of body'
     Cbody_p=ABody_p/VBody_p                !nmol/L - concentration of clo4 in 'rest of body'

!----------MASS BALANCES-----------------
!----------Mass balance TSH--------------
TSHint=initAVdTSH                       !initial amts of TSH
TMASStsh=AClTSH+AvdTSH                  !total mass TSH
BALANCEtsh=TSHint+ATSHPR-TMASStsh       !mass balance TSH (initial amt + amt produced - total mass)

!----------Mass balance T4---------------
T4int=initAp_t4+initAlb_t4+initAl_t4            !initial amts of t4
tformt4=APR_t4                                  !total amt T4 produced in thyroid
TMASSt4=AP_t4+AL_t4+ADIL+Avdel_t4+AGL+Alb_t4    !total mass T4
BALANCEt4=T4int+tformt4-TMASSt4                 !mass balance t4

!----------Mass balance t3---------------
T3int=initAp_t3+initAlb_t3+initAl_t3            !initial amts of T3
tformt3=APR_t3+AT3FL+AT3FVd                     !total amount of T3 formed
TMASSt3=AP_t3+AL_t3+Alb_t3+Avdel_t3+AML_t3      !total mass of T3
BALANCEt3=T3int+tformt3-TMASSt3                 !mass balance t3

!----------Mass balance Iodide-----------
Iint=initAP_i+initAtb_i+initdAt_i+initdAIB_i    !initial amts of I
TMASSi=Atb_i+Atf_i+AIB_i+Ath+AP_i+AU_i          !total mass of I
tformi=AST_i+AIFL_t4+AIFL_t3+AIFVd_t4+AIFVd_t3  !dose I & I freed from metabolism of T4 and T3
BALANCEi=Iint+tformi-TMASSi                     !mass balance iodide

!----------Mass Balance Perchlorate------
TMASSp=Atb_p+AU_p+ABody_p+Ab_p+At_p        !total amount of perchlorate
TDosep=AST_p+AIV_p                                      !total dose of perchlorate
balancep=TDosep-TMASSp                                  !mass balance perchlorate

!Days
days=((t+1e-6)/24)                                      !days of model execution
```

```
END ! DERIVATIVE
          TERMT (T .GE. TSTOP, 'checked on communication interval: REACHED TSTOP')
     END ! DYNAMIC
     TERMINAL
     T4END=ca_t4ngg
     T3END=ca_t3ngg
     TSHEND=tshngml
     T4ENDPC=t4percon
     TSHENDPC=tshpercon
                    END ! TERMINAL
    END ! PROGRAM
```

APPENDIX G

The acslXtreme (version 2.4.0.11) .m files for BBDR-HPT axis and ClO_4^- PBPK model simulations (Chapter 5) is contained within this Appendix. Each .m file includes the data plotted, simulation commands, and plotting commands.s

```
%Serum and Thyroid Perchlorate concentrations in adult male SD rats (Yu et al 2002) following IV
dose of hot clo4 3.3mg/kg
%File: HPERIVYU.m Created 04/13/07 by Eva McLanahan
%File name change on 7/25/07 - Yu2002_iv_36ClO4.m
%Last modified 07/25/07 by Eva McLanahan
%.M file for creating FIGURE 5.3
%Data from Yu et al 2002 36-ClO4 tail vein IV injection (3.3mg/kg) - cl-36 data in male rat.xls
%time:serum clo4 (ug/g): thyroid clo4 (ug/g): urine clo4 (ug)
HPERIVYU   =     [     0.5   8.62  19.55 NaN
                       0.5   8.16  17.66 NaN
                       0.5   9.07  21.45 NaN
                       6     2.09  15.83 NaN
                       6     1.87  12.85 NaN
                       6     2.31  18.81 NaN
                       12    0.47  9.19  885.502971
                       12    0.16  7.55  810.51
                       12    0.78  10.83 960.49
                       24    0.11  4.34  981.7950263
                       24    0.05  2.68  830.48
                       24    0.17  5.99  1133.12
                       32    0.03  1.43  NaN
                       32    0.01  0.55  NaN
                       32    0.05  2.30  NaN
                       48    0.01  0.45  NaN
                       48    0.00  0.18  NaN
                       48    0.01  0.72  NaN   ];
%3.3 mg/kg of clo4 tail vein IV dose - Yu et al 2002)
!!s tstop=50, pdose_p=0, ivdosep=3.3, pdose1=20, cint=0.01, np=1
!!BW290
!!s bw=0.294, bwgon=0
!!prepare t, ca_pugml, ct_pugg, au_pug, ca_t4ngg, ca_t3ngg, tshngml, tat_iug
!!start/nc

Plot(_t,_ca_pugml,HPERIVYU(:,1),HPERIVYU(:,2),_t,_ct_pugg,HPERIVYU(:,1),HPERIVYU(:,3),_t,_au_pug,H
PERIVYU(:,1),HPERIVYU(:,4),'HPERIVYU.aps')
```

```
%YuPerCON.m
%M file for plotting T4 and TSH from Yu 2002 clo4 drinking water study as percent of control (T4)
and fold change (TSH)
%Created 07/20/2007 by Eva McLanahan
%.M file for creating FIGURE 5.4 and 5.5
%Yu 2002 TSh Data as fold change (time, 0.1, 1, 3, 10 mg/kg-day clo4 dose)
YuTSH=[    16    1.616182573      1.684647303      1.962655602      2.734439834
           112   1.347921225      1.971553611      2.704595186      3.146608315
           328   1.24009324       1.820512821      2.454545455      2.771561772      ];
%Yu 2002 T4 Data as percent of control change (time, 0.1, 1, 3, 10 mg/kg-day clo4 dose)
YuT4 = [   16    94.47674419      88.6627907       88.37209302      76.1627907
           112   99.6969697       82.42424242      80.90909091      73.33333333
           328   97.25            95.5             86          84.25];

%Estimated parameters from visual fits
!!s np=0.94, np3=2, kp=140000, kinh_t4=0.3

%Thyroid Hormone Effects (THE) following 1 mg/kg of clo4 in drinking water 14 days - Yu et al
2002)
!!s tstop=336, ivdosep=0, pdose_p=1, pdose1=20, bwgon=0
!!BW330
!!prepare t, tshfold, t4percon, tat_iug
!!start/nc
yut4percon1=_t4percon
yutshfold1=_tshfold
yutat1=_tat_iug


%Thyroid Hormone Effects (THE) following 3 mg/kg of clo4 in drinking water 14 days - Yu et al
2002)
!!s tstop=336, ivdosep=0, pdose_p=3, pdose1=20, bwgon=0
!!BW330
!!prepare t, tshfold, t4percon, tat_iug
!!start/nc
yut4percon3=_t4percon
yutshfold3=_tshfold
yutat3=_tat_iug
```

```
%Thyroid Hormone Effects (THE) following 10 mg/kg of clo4 in drinking water 14 days - Yu et al
2002)
!!s tstop=336, ivdosep=0, pdose_p=10, pdose1=20, bwgon=0
!!BW330
!!prepare t, tshfold, t4percon, tat_iug
!!start/nc
yut4percon10=_t4percon
yutshfold10=_tshfold
yutat10=_tat_iug


plot(_t,yut4percon1(:,1),_t,yut4percon3(:,1),_t,yut4percon10(:,1),YuT4(:,1),YuT4(:,3),YuT4(:,1),Yu
T4(:,4),YuT4(:,1),YuT4(:,5),'YuT4percon.aps')

plot(_t,yutshfold1(:,1),_t,yutshfold3(:,1),_t,yutshfold10(:,1),YuTSH(:,1),YuTSH(:,3),YuTSH(:,1),Yu
TSH(:,4),YuTSH(:,1),YuTSH(:,5),'YuTSHfold.aps')

plot (_t,yutat1(:,1),_t,yutat3(:,1),_t,yutat10(:,1),'YuTATstores.aps')
```

```
%Yu2002.m file
%Created 04/01/07 by Eva McLanahan
%Serum and Thyroid data from drinking water studies Yu et al 2002
%04/02/07- Added 12hrs to each time point to account for time of sacrifice compared to water
intake (drink at night - sac in morning)
%Last Modified 04/02/07 by Eva McLanahan
%.M file for creating FIGURE 5.6
%Data plotted in Merrill et al 2003 from email from Jeff
%time (hrs), serum total perchlorate (ug/mL), thyroid perchlorate (ug/mL)
dw1   =     [     0     0          0
                  328   0.000025   8.36
                  328   0.3        10.44
                  328   0.35       12.52 ];


dw3   =     [     0     0     0
                  16    0.39  10.14
                  16    0.45  14.43
                  16    0.51  18.72
                  112   1.22  48.65
                  112   1.44  50.4
                  112   1.66  52.15
                  328   0.78  27.78
                  328   0.91  30.98
                  328   1.04  34.18 ];


dw10  =     [     0     0     0
                  16    1.23  20
                  16    1.92  23.68
                  16    2.61  27.36
                  112   4.05  166.29
                  112   4.93  175.71
                  112   5.81  185.13     ];
```

```
%Low dose (1mg/kg of ClO4 in drinking water 1, 4, 14 days - Yu et al 2002)
!!s tstop=350, ivdosep=0, pdose_p=1, pdose1=20, bwgon=0, cint=0.5
!!BW330
!!prepare t, ca_pugml, ct_pugg
!!start/nc
ca_p1=_ca_pugml
ct_p1=_ct_pugg


%Mid dose (3mg/kg of ClO4 in drinking water 1, 4, 14 days - Yu et al 2002)
!!s tstop=350, ivdosep=0, pdose_p=3, pdose1=20, bwgon=0, cint=0.5
!!BW330
!!prepare t, ca_pugml, ct_pugg
!!start/nc
ca_p3=_ca_pugml
ct_p3=_ct_pugg


%High dose (10mg/kg of ClO4 in drinking water 1, 4, 14 days - Yu et al 2002)
!!s tstop=350, ivdosep=0, pdose_p=10, pdose1=20, bwgon=0, cint=0.5
!!BW330
!!prepare t, ca_pugml, ct_pugg
!!start/nc
ca_p10=_ca_pugml
ct_p10=_ct_pugg


plot(_t,ca_p1(:,1),_t,ca_p3(:,1),_t,ca_p10(:,1),dw10(:,1),dw10(:,2),dw3(:,1),dw3(:,2),dw1(:,1),dw1
(:,2),'YuDWCA.aps')

plot(_t,ct_p1(:,1),_t,ct_p3(:,1),_t,ct_p10(:,1)dw10(:,1),dw10(:,3),dw3(:,1),dw3(:,3),dw1(:,1),dw1(
:,3),'YuDWCT.aps')
```

```
%Mannisto 1979 ClO4 in drinking water
%15mg ClO4/kg-day, iodide intake 10-20ug/day (0.5-1.0mgI/kg chow), adult male SD 180-220g
%Created 8/5/2007 by Eva Mclanahan
%.M file for creating FIGURE 5.7
%Mannisto 1979 ClO4 in drinking water
%15mg ClO4/kg-day, iodide intake 10-20ug/day, adult male SD 180-220g

%Time (hrs), Serum T4 (%con), Serum T3 (%con), Serum TSH (%con)
MANN79_ClO4dw_percon= [     0     100             100             100
                            0     113.0518234     105             118.0327869
                            0     86.94817658     95              81.96721311
                            48    78.3109405      105             118.0327869
                            48    84.68348952     112.6190476     140.2550091
                            48    71.93839148     97.38095238     95.81056466
                            96    91.17082534     80              183.6065574
                            96    96.85503586     86.875          192.5351288
                            96    85.48661481     73.125          174.6779859
                            144   87.14011516     80              179.5081967
                            144   92.64672309     83.75           192.2935848
                            144   81.63350723     76.25           166.7228086
                            336   NaN             NaN             196.7213115
                            336   NaN             NaN             209.2213115
                            336   NaN             NaN             184.2213115     ];


%Estimated parameters from visual fits to Yu 2002 data
!!s np=0.94, np3=2, kp=140000, kinh_t4=0.3

%iodide intake tested 10-20 does not make a difference in model simulations
!!BW200
!!s tstop=336, pdose1=10, pdose_p=15
!!prepare t, t4percon, tshpercon
!!start/nc

plot(_t,_t4percon,MANN79_ClO4dw_percon(:,1),MANN79_ClO4dw_percon(:,2),_t,_tshpercon,MANN79_ClO4dw_
percon(:,1),MANN79_ClO4dw_percon(:,4),'Mannisto1979_clo4dw_percon.aps')
```

```
%Caldwell 1995 14-d Perchlorate Exposure (dose mg/kg-day)
%Male Rat Data. Digitized in Caldwell1995_CLO4.xls
%.M file for creating FIGURE 5.8
%Body weight and I diet not reported
%Caldwell 1995 14-d Perchlorate Exposure (dose mg/kg-day)
%Dose-Response plot data format
%clo4 dose (mg/kg-day), serum t3 (percent of control), serum t4 (% control), serum tsh (%control)
Cald95dr=[ 0.11       93.26088322     94.43432826     102.3669782
           0.44       79.56524137     92.67576932     115.3847389
           1.11       67.7717714      84.49084828     136.686509
           2.28       57.11960464     82.69511045     207.6923824
           4.32       53.31525974     80.90123157     213.6095383
           11.44      49.89134977     66.92756484     233.7278661
           22.16      49.51091586     59.33936349     256.213055 ];
%Estimated parameters from visual fits from Yu 2002 data
!!s np=0.94, np3=2, kp=140000, kinh_t4=0.3
!!prepare t, t4end, tshend, t3end, tat_iug
output @Clear
global PDOSE_P
%Calculate and store T4, T3, and TSH for each dose then plot in one DR graph the final value at
14d
!!BW350
!!s bwgon=0, pdose1=20, tstop=336, pdose_p=0.11

pdose_p=[0:0.11:22.22]
for x=[1:202]
PDOSE_P=pdose_p(x)
start @NoCallback
pdosep(x)=PDOSE_P;
t4finalpc(x)=T4ENDPC;
tshfinalpc(x)=TSHENDPC;
tat_iug(x)=TAT_IUG;
end

plot(pdosep,t4finalpc, Cald95dr(:,1), Cald95dr(:,3),'caldwell95t4pc.aps')
plot(pdosep,tshfinalpc, Cald95dr(:,1), Cald95dr(:,4),'caldwell95tshpc.aps')
%plot(pdosep,tat_iug,'cald95_tatiug.aps'
```